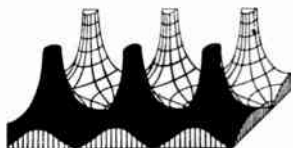


Proceedings of the IRE



Poles and Zeros



Roses To Ye Editors. An important adjunct of electronic and IRE communications, not too generally appreciated, is the

local IRE Section publication. Now the products of 47 Sections or almost half of all, these magazines have come fully of age as a means of passing Section, Professional Group Chapter, and national news to IRE members. From the six or eight-page publication of the small Section to the 32 to 40-page output of the large, they all provide a means of informing the members of Section and PG Chapter meetings and programs, and many publish abstracts of past programs for those members who unfortunately missed the most recent meeting.

With total meetings mounting into the range of 12 to 20 in some Sections, augmented by special symposia, technical lecture series, or by Regional activities, the superiority of the Section magazine over smoke signals, carrier pigeons, post cards, or any earlier technique need not be argued. What has not been so apparent is the excellent editorial work being done by our volunteer Section editors. The addition of editorials, Section personnel and business news, ladies' columns (to placate the wife for those IRE nights out), student branch or local engineering college news, even prize contests, has made what could have been dusty dissertations into praiseworthy prose.

These editors have also learned well that basic rule of local journalism—"names and pictures of local faces, will put the paper through its daily paces," and embellish their columns with pictures of authors, local Fellow awardees, Section officers and other personalities of local interest. This often also permits noncommercial bows to the supporters of it all, the local and national advertisers, and disseminates from their printed pages the feeling that the Section is a very well integrated technical and social family.

Much originality has gone into the titles of these papers, and we cite a few as "The Missile" (Alamogordo-Holloman), "Crosstalk" (Detroit), "The Long Island Pulse," or the "Kansas City Local Oscillator." If Albuquerque-Los Alamos did not already possess a good title in "The Blast" we might suggest "The Q Point," and we feel that the Washington Section overlooked one in the possibilities in "The DC Amplifier." In fact, always desiring to be helpful, this Editor offers free and with no rights reserved, the following titles to a few Sections not yet having publications. Why do we not have: "The Rochester Radiator," "The Beaumont Beeper," the Buffalo "BISONic News," "The Twin Cities Stereo," or "Phoenix Phonics?"

Pills and Pulses. As you scan the photographs and biographies of the new IRE Fellows in this issue, you will not want to miss an historic first—Dr. Lee Lusted who is the first medical doctor to be elected an IRE Fellow. This gives formal and significant recognition to the growing bond between the physician, the physiologist, the biologist, and the electronic engineer or the physical scientist.

Many of us at present may think of this relationship as somewhat of a one-way street in which electronic measuring or recording techniques are used to obtain medical information. However, this may soon be replaced with a two-lane boulevard in which knowledge from medicine and physiology will return to aid us in the solution of future problems. Especially is this true in the areas of communication, memory, and navigation, where knowledge of the human brain, our sensory organs, and the navigation methods of birds, bats, and fish may be needed before we become really sophisticated in those areas. Needless to say, our Professional Group on Medical Electronics in which Dr. Lusted has been active, is a strong motivating force in this exchange of knowledge.

It should also be mentioned that another new Fellow, Herman P. Schwan, is the third biophysicist to be so honored, and that Dr. Alfred Goldsmith, our Editor Emeritus, has long been a member of several noted medical societies. Thus do the barriers between fields of science continue to fall.

A Reminder. Those of you not attending the March Convention may have missed the announcement that IRE Convention Record parts will no longer be distributed free to PG members. After study by the Editorial Board, the PG committee, and the Board of Directors, this action was taken to encourage broader publication of selected Convention papers by the PG Transactions—which are then available to the PG member. The move also permits a drastic reduction in price for those completing their files by purchase. Convention Record orders must be placed with Headquarters before April 30. Information on how to order and prices for the various parts appear on page 20A of this issue.

This And That. Attention should be turned to a letter in this month's Correspondence Section (p. 584) from Mr. Floyd W. Hough, chairman of an American Geophysical Union committee for Study of the Metric System in the United States. He asks for expressions of interest in a proposal to adopt the metric system in the United States through a phased procedure covering 33 years, or a generation. With the MKS system already well established in our area, we might then be able to forget that a meter is 39.37 inches, that 32 ounces made up a quart but 16 ounces make a pound—or that sometimes there are five quarts in a gallon.—J.D.R.



Bernard M. Oliver

Director, 1959–1961

Bernard M. Oliver (A'40–M'46–SM'53–F'54) was born on May 27, 1916, in Santa Cruz, California. He was graduated from Stanford University, Stanford, Calif., with the B.A. degree in electrical engineering in 1935, and in 1936 received the M.S. degree from The California Institute of Technology in Pasadena. The next year he studied in Germany as an exchange student under the auspices of the Institute of International Education. At the age of twenty-three he received the Ph.D. degree, magna cum laude, in electrical engineering from the California Institute of Technology.

Dr. Oliver was with the Bell Telephone Laboratories in New York from 1940 to 1952, where he worked on the de-

velopment of automatic tracking radar, television, information theory, and high efficiency systems. In 1952 he joined the Hewlett-Packard Co., Palo Alto, Calif., as director of research, and in 1957 became vice-president in charge of research and development there. For the past several years he has also been a lecturer in electrical engineering at Stanford University.

Dr. Oliver holds twenty-seven U. S. patents in the field of electronics; others are pending. He has also contributed several papers to the PROCEEDINGS of the IRE.

He has served as Chairman of the IRE San Francisco Section, and for several years was Vice-Chairman of WESCON

Scanning the Issue

A New Concept in Computing (Wigington, p. 516)—The late John Von Neumann, who contributed so much to so many fields, is especially renowned for the leading role he played in the birth of the modern electronic computing machine. One of his last major contributions was contained in a patent submitted in 1954 and granted posthumously only 16 months ago. This paper presents a description and explanation of the new computing scheme disclosed in that patent. In it Von Neumann proposed that digital information be represented by the *phase* of a sine wave. He suggested that this could be done by using a nonlinear reactance device as a subharmonic generator to produce oscillations at one- n th the pumping frequency. It can be shown that the subharmonic wave will have a choice of n instants during the period of each cycle when it can start off in phase with the pumping wave. In other words, the subharmonic wave will lock into any of n phases. The choice of phase can be controlled by the phase of an input signal at the subharmonic frequency. This can be thought of as a mechanism for producing n logic states. When several subharmonic generators are connected in a circuit, the output of one will change the state (phase) of another, producing an n -ary logic system. This idea is closely related to the parametron, which was independently developed in Japan and which has aroused so much interest in the past couple of years. The parametron uses nonlinear oscillators operating in the one-megacycle range. However, it is the possibility of applying this scheme to microwave frequencies that makes it of such outstanding importance, because microwaves would greatly increase the operating speed of computers. This work will be of great importance not only to computer engineers but also to all those who are interested in parametric amplifiers.

Stored Charge Method of Transistor Base Transit Analysis (Varnerin, p. 523)—The operating frequency of a transistor can be increased by reducing the base transit time, presumably either by increasing the velocity of the carrier flow or by reducing the base width. Velocities can be increased by grading the base impurity densities to produce built-in aiding electric fields. This principle has been widely used in recent high-frequency designs since the advent of diffusion techniques for fabricating transistors. Base transit time, as presently defined, is primarily a mathematical concept; that is, it is expressed in terms which have mathematical validity but which do not all have a direct physical interpretation. In this paper, the author re-expresses base transit time in terms of stored charge per unit emitter current—terms which are conceptually much simpler to deal with and which greatly facilitate the understanding of high-frequency performance. Using this fresh viewpoint, the author readily shows that base thickness is more important than the built-in field in determining base transit time. In fact, this gives rise to a seeming paradox: shorter transit times are possible with retarding than with aiding fields, because they permit a narrower base width. Both the new method of analysis and the results will be of wide interest to the considerable body of engineers interested in high-frequency transistor design.

The Hall Effect Circulator—A Passive Transmission Device (Grubbs, p. 528)—One of the notable features of the 1950's has been the variety of devices that have been developed which exhibit nonreciprocal transmission characteristics. These developments have led not only to new components and improved systems but to new methods of network analysis as well. The development of ferrites has provided nonreciprocal devices for the microwave range, while the exploitation of the Hall effect in semiconductors is leading to devices with similar functions for use at the lower "wire" frequencies. Hall effect gyrators and isolators have already been investigated for use in wire circuits. This paper describes

an important addition to the nonreciprocal device family, a Hall effect circulator.

Theory of the Crestatron: A Forward-Wave Amplifier (Rowe, p. 536)—Past experimental data have indicated that gain can occur in a traveling-wave tube even though the voltage is so high that a growing wave cannot exist, but the phenomenon has not heretofore been understood. The author has now developed a theory which satisfactorily explains the previous data. To verify his work, he has built a tube which utilizes this new mode of operation. The tube proves to have moderate gain, good efficiency and, perhaps the most significant feature, a very short length, which suggests the interesting possibility that the device might operate with little or no magnetic focusing field.

Theory and Experiments on Shot Noise in Silicon P-N Junction Diodes and Transistors (Schneider and Strutt, p. 546)—It has been found that the theory which describes the noise performance of germanium diodes and transistors does not hold true for silicon devices. This is not surprising since the electrical characteristics of silicon devices differ to some extent from those of the corresponding germanium types. In fact, it was not until a year and a half ago that this difference in the characteristics of silicon junctions was adequately explained. Armed with this information, the authors have succeeded in deriving new noise expressions which are valid for silicon devices operating at low current densities. This paper is of great interest in understanding the noise behavior of silicon devices—indeed, it is the first paper to tackle the problem.

A Constant-Temperature-Operation Hot-Wire Anemometer (Janssen, *et al.*, p. 555)—This paper discusses a type of instrument that is very useful in studying turbulent air flow. When a small, electrically heated wire is placed in the air flow, turbulence will cause variations in the cooling effect of the air stream on the heated wire. These temperature changes, in turn, cause the resistance of the wire to vary. By incorporating the heated wire in an appropriate circuit—in this case, a dc bridge and a dc differential amplifier—air velocity fluctuations containing frequencies of several tens of kilocycles can be measured electrically. While the instrument is not new, the application of a chopper stabilized amplifier described here is novel, as is the use of signal flow graphs in an analysis of this sort.

IRE Standards on Waveguide and Waveguide Component Measurements (p. 568)—This standard provides very useful and important information on the proper methods of measuring some two dozen major quantities which characterize waveguides, waveguide components, and the associated electromagnetic fields.

IRE Award Winners (p. 593)—Last month at the annual IRE Convention banquet in New York, over 1000 persons crowded into the Grand Ballroom of the Waldorf-Astoria Hotel to witness what in many respects is the climactic event of the year. On that occasion the leading contributors to the progress of our profession were singled out for recognition by the IRE—seven by means of IRE's highest awards and 76 by elevation to Fellow grade. The photographs and award citations of this distinguished group are presented in a special section of this issue.

IRE TRANSACTIONS Index (follows p. 628)—During 1958 the Professional Groups of the IRE published 81 issues of TRANSACTIONS, comprising more than 800 papers and letters. So substantial has the TRANSACTIONS activity become that it now represents half of the total technical publication output of the IRE. This wealth of material has been catalogued by tables of contents, by authors, and by subjects in the 1958 index which appears toward the rear of this issue.

Scanning the Transactions appears on page 604.

A New Concept in Computing*

R. L. WIGINGTON†, MEMBER, IRE

Summary—A new computing scheme was proposed by von Neumann in a patent¹ submitted in 1954 and granted posthumously last December. This paper is an explanatory statement of those ideas. The concept of using the phase of a sine-wave signal as an information-bearing medium which together with majority logic permits the realization of logic operations is described in detail. Simple logical aggregates are given as examples.

INTRODUCTION

VON NEUMANN recognized the limitations of computing speeds inherent in the existing technology due to device operation times, signal propagation delays, and transmission distortion of information video pulses. Of course, we cannot reconstruct the thinking that led him to the proposed solution, but the attractiveness of large bandwidths which could be obtained at microwave frequencies and of representation of digital information by distinct phases of an RF signal (neither of which had been exploited in computer technology) no doubt seemed fertile ground for investigation. Whatever the prompting force was, von Neumann proposed a computing scheme using RF techniques which is potentially faster if employed at microwave frequencies than present conventional methods. The same methods will also work at lower frequencies.

The availability of an element of the following nature was assumed:

- a) An element is available that has both L and C , one of which is nonlinear.
- b) The dissipation in the element is not great in comparison to the nonlinearity. This dissipation may be resistive loss or a hysteresis.
- c) The element has approximately linear operation for small signals having a resonant frequency (which later is referred to as f_0).

NONLINEAR REACTANCE ANALYSIS

To see that such an element can exist, consider the nonlinear capacitor that has no loss and no hysteresis² and is mounted in multiply-tuned circuits. The bare outline of the analysis will be presented. Full discussion of it has been published by Manley and Rowe.³ As pointed out in that reference, consideration of nonlinear

reactances as elements to transfer power from one frequency to another is not a new subject, having been discussed by Hartley in 1916.

Consider the circuit in Fig. 1.

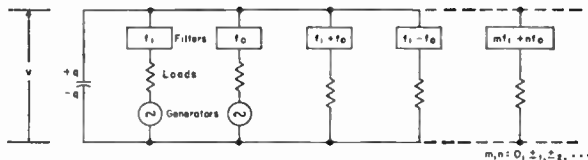


Fig. 1—Generalized nonlinear reactance circuit.

$v=f(q)$ is an arbitrary, single-valued function, being in general nonlinear.

The filters have zero impedance at the labeled frequency and infinite impedance otherwise.

Such a circuit might be a number of tuned circuits in parallel with the nonlinear reactance (which also may be inductance rather than capacitance). Two of the tuned circuits contain RF generators.

The charge on the capacitor, the current into it, and the voltage across it may all be expressed as double Fourier series in the frequencies $mf_1 + nf_0$ for $m, n = 0, \pm 1, \pm 2, \dots$. By manipulation of these expressions⁴ one may derive others giving the summation of real power at all frequencies into the nonlinear element in terms of double integrals over complete cycles of f_1 and f_0 wherein the integrand is $v=f(q)$.

The variable q , hence $f(q)$, is periodic in f_1 and f_0 and thus for an element without hysteresis these double integrals are identically zero. From this are obtained the Manley-Rowe conditions, namely:

$$\sum_{m=0}^{\infty} \sum_{n=-\infty}^{\infty} \frac{mW_{m,n}}{mf_1 + nf_0} = 0 \quad m, n = \text{integers}$$

$$\sum_{m=-\infty}^{\infty} \sum_{n=0}^{\infty} \frac{nW_{m,n}}{mf_1 + nf_0} = 0$$

where $W_{m,n}$ is the real power at frequency $mf_1 + nf_0$ into the nonlinear reactance.

Of course, a reactance without hysteresis, whether linear or nonlinear, can dissipate no energy. Therefore, as must be true and as can be obtained from the above conditions, the summation of energy at all frequencies into the reactance is zero, and power supplied from one source at a given frequency will show up in another branch of the circuit at another frequency. The exact manner in which this takes place is controlled by the above conditions.

* Complete discussion is given in Manley and Rowe, *ibid.*

* Original manuscript received by the IRE, October 15, 1958; revised manuscript received, December 31, 1958.

† National Security Agency, Dept. of Defense, Ft. Meade, Md.
¹ J. von Neumann, "Non-linear Capacitance or Inductance Switching, Amplifying, and Memory Organs," U. S. Patent No. 2,815,488, issued December 3, 1957, assigned to the IBM Corporation.

² These restrictions may be relaxed somewhat in the practical case, but are assumed here to make explanation simpler.

³ J. M. Manley and R. E. Rowe, "Some general properties of nonlinear elements—Part I. General energy relations," *Proc. IRE*, vol. 44, pp. 904-913; July, 1956.

The circuit initially pictured was a general circuit; variations of it may lead to modulators, demodulators, amplifiers, oscillators, or combinations of them. Of interest to this discussion is a subharmonic generator, as shown in the circuit of Fig. 2. V_G is an RF generator, essentially an ac power supply. The f_1 filter and R_G correspond to the resonant tank of the RF generator. The f_0 filter and R_L are the load tank at the subharmonic frequency desired. The filters at all other frequencies are terminated in pure reactances, X , which for simplicity may be open or short circuits. There will be no power loss at these other frequencies.

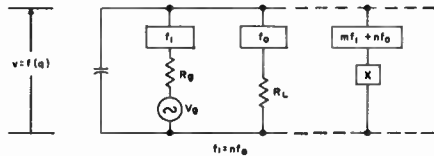


Fig. 2—Generalized subharmonic generator.

The only terms of interest in the Mauley-Rowe conditions are for $(m, n) = (0, 1)$ and $(0, n)$. The rest of the $W_{m,n}$ are zero. This gives

$$\frac{W'_{0,1}}{f_0} + \frac{nW'_{0,n}}{nf_0} = 0$$

or simply

$$W'_{0,1} = -W'_{0,n}$$

The minus sign indicates that all the energy put into the nonlinear reactance at the $f_1 = nf_0$ frequency is transferred to the load tuned to the f_0 frequency. This is a harmonic generator with an ideal efficiency of 100 per cent, assuming no losses in the reactive termination of the other frequencies. Of course, with real elements some losses, and resultant reduction of efficiency, will occur, but the basic (sub)harmonic generation process, unlike that of Class C multipliers or crystal multipliers, is not limited in efficiency.

NATURE OF NONLINEARITY REQUIRED

It remains to show that an element with a threshold of subharmonic generation is possible. The transfer function for such an element is shown in Fig. 3.

The reactance function shown in Fig. 4 is, of course, idealized. In the actual case only a smoothly varying reactance would be obtainable which could be approximated by the lines in Fig. 4. At V_c , the nonlinearity is great enough to produce sufficient negative resistance at the subharmonic frequency to overcome passive circuit losses. At this level of the RF power supply, the circuit would break into oscillation at the subharmonic frequency and the threshold action be obtained. For $V_{in} > V_c$, the amount of signal $V_{in} - V_c$ will be effective in producing subharmonic voltage. Whether this is a straight-line function or one that saturates will depend on other amplitude nonlinearities in the circuit.

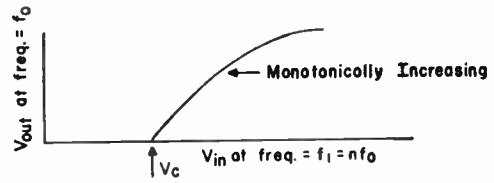


Fig. 3—Transfer function for subharmonic generator with threshold.

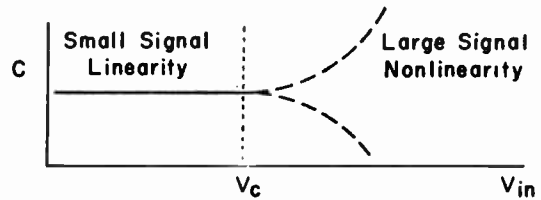


Fig. 4—Reactance variation to give threshold action.

DEVICES

Various solid-state elements have been proposed to perform the function of the nonlinear reactance.⁵ An equivalent circuit for a nonlinear capacitance, as realized with a semiconductor diode, is shown in Fig. 5.

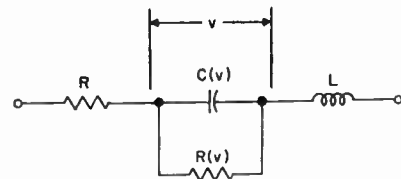


Fig. 5—Equivalent circuit for nonrectifying region of a semiconductor diode.

- v = barrier voltage
- R = bulk resistance
- $R(v)$ = barrier resistance (which may be nonlinear)
- L = lead inductance
- $C(v)$ = barrier capacity (nonlinear).

The barrier capacity is the primary nonlinearity of the device. Among these components the following relationships are assumed:

$$\left. \begin{aligned} R(v) \gg R \\ R_0 = \sqrt{L/C_s} \gg R, \end{aligned} \right\} \text{(The element has a reasonable } Q.)$$

C_s = small signal $C(v)$

$$f_0 = 1/(2\pi\sqrt{LC_s})$$

(Tuned to the subharmonic frequency desired.)

⁵ A. Uhler, Jr., "Two-terminal *p-n* junction devices for frequency conversion and computation," Proc. IRE, vol. 44, pp. 1183-1191; September, 1956.
 H. Suhl, "The theory of the ferromagnetic microwave amplifier," *J. Appl. Phys.*, pp. 1225-1236; November, 1957.
 F. Dill, Jr. and L. Depian, "Semiconductor capacitance amplifier," 1956 IRE CONVENTION RECORD, pt. 3, pp. 172-174.
 A. E. Bakenowski, "Small-Signal Measurements on Planar *P-N* Junction Diodes," "Task 8 Report on Crystal Rectifiers," Bell Tel. Labs., April 15, 1955.
 A. Uhler, "Frequency Conversion in *P-N* Junction Devices," "Task 8 Report on Crystal Rectifiers," Bell Tel. Labs., January 15, 1955.

This equivalent circuit as drawn includes both linear and nonlinear reactances. These may be physically separated in real devices. Research is being done at many laboratories on other practical means of achieving subharmonic response.

INFORMATION IN TERMS OF PHASE

The phase of the f_0 signal is determined by the phase of the f_1 signal. Qualitatively, this may be understood by observing that the oscillations in the f_0 circuit are not like the oscillations in an ordinary negative resistance oscillator, in which the power supply is dc and the phase of the oscillation is determined by noise when the oscillator is turned on. The nonlinear-reactance subharmonic generator is more akin to a crystal harmonic generator in which power is transferred from one frequency to another by a nonlinear element. This is true even though the action of the nonlinear-reactance device in general may be explained in terms of the apparent negative resistance reflected into each appropriate branch of the circuit.

Eliminating any constant phase shift between the fundamental and the n th harmonic, the phase relationships are examined more closely in Fig. 6.

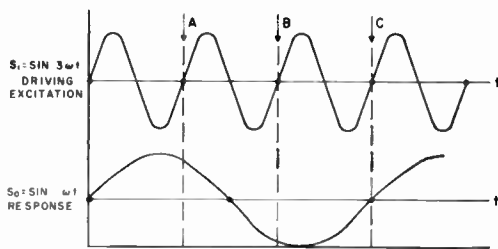


Fig. 6—Demonstration of three indeterminate phase relationships for the case $n=3$.

In the example in which $n=3$, the two signals are assumed in phase at $t=0$. (The $n=3$ example is chosen deliberately to point out important relationships and to avoid the $n=2$ case, in which simplicity may cause some essential points to be overlooked.) One full cycle of S_1 later, at point A, S_1 is the same as it was at $t=0$, but S_0 has a relative phase shift of $2\pi/3$. Similarly, at point B, S_1 is the same again, but S_0 now has a phase shift of $4\pi/3$. At point C, S_0 has a phase shift of $6\pi/3=2\pi$ or, like S_1 , the same relative phase as when $t=0$. Thus there are, for $n=3$, three indeterminate phase relationships between S_0 and S_1 , because in the continuous wave, S_1 , one cycle is just like another. In the general case there are n such indeterminate relationships between the RF power supply (S_1) and the induced subharmonic response (S_0), each of which can represent a logical state.

PHASE SELECTION AND CONTROL

If the power supply (S_1) is increased from zero amplitude past the critical amplitude, V_c , a subharmonic response S_0 will appear when the amplitude of S_1 is V_c .

Since which of the n possible phases of S_0 will result is indeterminate, noise, or—indifferently—a small S_0 signal from another element, will dictate which phase will appear. Once the harmonic response has started, however, no external signal of less magnitude than $|S_0|$ can change the phase of the response. A simple cycle can be diagrammed (Fig. 7), plotting envelope amplitudes only. The S_0' signal would have no effect if present at any other time than when $|S_1| = V_c$ and is increasing. Note that

- $|S_0| > S_0'$ (Amplification)
- Duration of $S_0 >$ Duration of S_0' (Memory)
- Phase of $S_0 =$ Phase of S_0' (Control or Toggle Action).

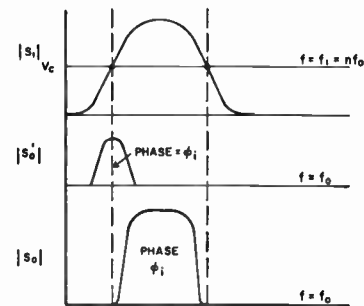


Fig. 7—Excitation, S_0' , and response, S_0 , during one cycle of pump modulation, S_1 .

For practical realization of any computing scheme the electrical process must have natural or built-in margins. Noise, stray signal pickup, slight misadjustment of circuits, component changes with age, all can cause a certain malfunction of the equipment, if the parameters which determine the action of the machine must have precise values to cause action. For action must occur if the appropriate parameter falls within a certain region or margin, about the ideal value.

The controlling signal, S_0' , has up to now been assumed to coincide exactly with one of the n possible phases, Φ_{i1} , of the response, S_0 , and to cause S_0 to respond with that phase, Φ_{i1} .

In Fig. 8, the phase of S_0' is shown as being closer to the phase Φ_0 than either Φ_{i1} or Φ_{i2} . The system will stabilize with S_0 at phase Φ_0 , since this requires the minimum amount of energy in the presence of the S_0' signal to respond at the Φ_0 phase as compared with the other possible phases. The figure is not intended to illustrate the exact duration (in terms of number of cycles) of the transient condition, but is only a qualitative picture. The duration of the transient will depend on the rate of build-up of the S_1 envelope and the ratio of the response S_0 to the control S_0' during and after the start of the response. The magnitude of $\Delta\Phi$ and the effective damping constant of the transient condition will also be important.

One may conclude from this that the phase-locking property of the subharmonic generator has natural margins, and hence is a practical method.

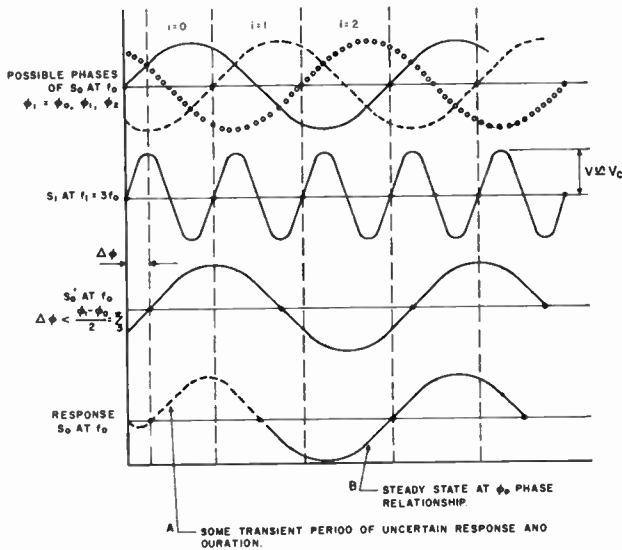


Fig. 8—Illustration of the natural margins of the phase locking mechanism.

AGGREGATES OF ELEMENTS

In order to control the flow of information in a logical machine, ways must be devised to establish an order of control. For example, if information is to flow from *A* to *B*, then *A* must control *B* but *B* must not control *A*. Ordinarily this is no problem, because the nonreciprocal devices normally used in a logical circuit to provide gain or gating perform this function automatically, but in this case one must consider the control problem separately.

It is now necessary to devise a diagrammatic model of devices and their interconnection (see Fig. 9). The following symbolism and nomenclature will be used:

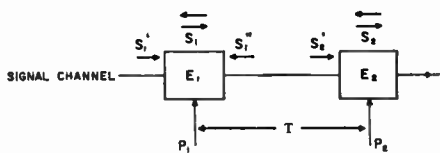


Fig. 9—Diagrammatic model of devices and their interconnection.

- E_1, E_2 are elements such as have been described.
- P_1, P_2 are amplitude-modulated AC power supplies.
- S_1, S_2 are the output signals of E_1, E_2 , respectively.
- S_1', S_2' are the controlling signals for E_1, E_2 , respectively.
- S_1'', S_2'' are the signals reaching E_1, E_2 from E_2, E_1 , respectively.

The signal channel is an electromagnetic propagation path which permits propagation in either direction. The response S_1 , from E_1 travels in both directions on the signal channel. The problem is to make E_1 control E_2 and not the reverse. Let T be the time delay of the signal between elements E_1 and E_2 . Consider next the timing sequence in Fig. 10.

With the timing cycle as pictured, E_1 can control E_2 but E_2 cannot control E_1 . If the relative timing (*i.e.*, the

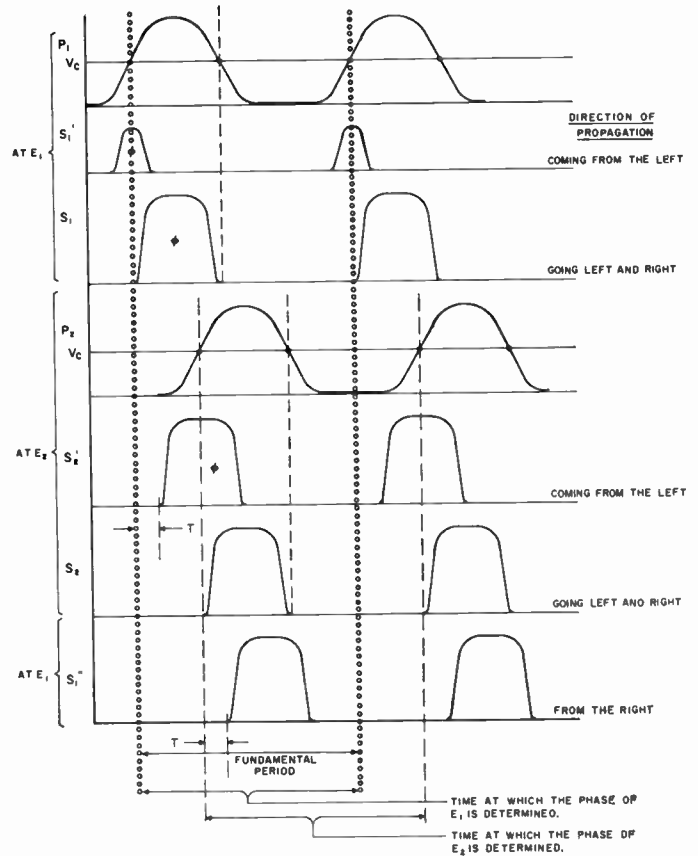


Fig. 10—Asymmetry of control between two adjacent elements.

order of occurrence) of the P_1 and P_2 modulation is reversed, the direction of control is reversed.

To prevent signals other than those from next neighbors from forcing synchronization with the wrong phase an attenuator is placed in the signal path between each element. Stray signals will have had to pass through at least two attenuators, instead of only one, so that unwanted signals will not have a major influence in determining the phase of the subharmonic response. The natural margins of the process enable this to work properly.

With the simple combination of elements described above, not much can be done. If, however, three classes of elements are used as shown in Fig. 11, and the timing principles discussed above are employed, all logical operations can be realized. Classes of elements are defined by the timing of the modulation of the ac power supply, as shown in the figure.

The elements of classes *A, B* and *C* are shown interconnected by signal paths. Their respective power supplies have modulation as illustrated. The delay between elements is assumed to be negligible with respect to the power-supply modulation period. *Recalling that the phase of the response is determined by the phase of signals from other elements present when the power supply passes the critical level (the heavy dots in the diagram), observe at each dot which other element is ON.* For example at \odot in the diagram P_a is passing the critical level, element *B* is off, and element *C* is on. Therefore, *C* controls *A*.

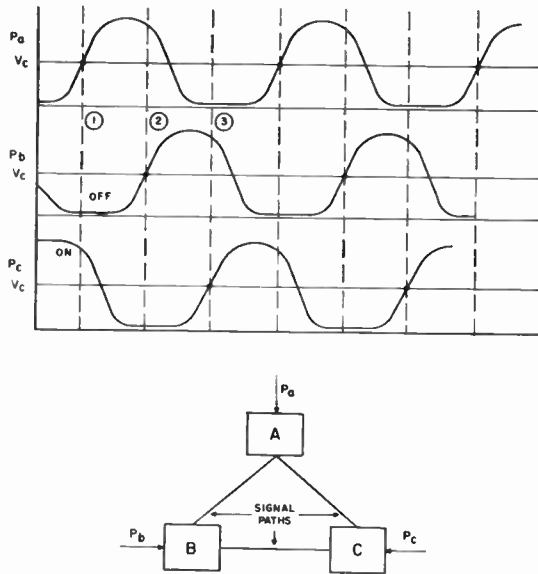


Fig. 11—Three elements classes as determined by the power supply modulation of each.

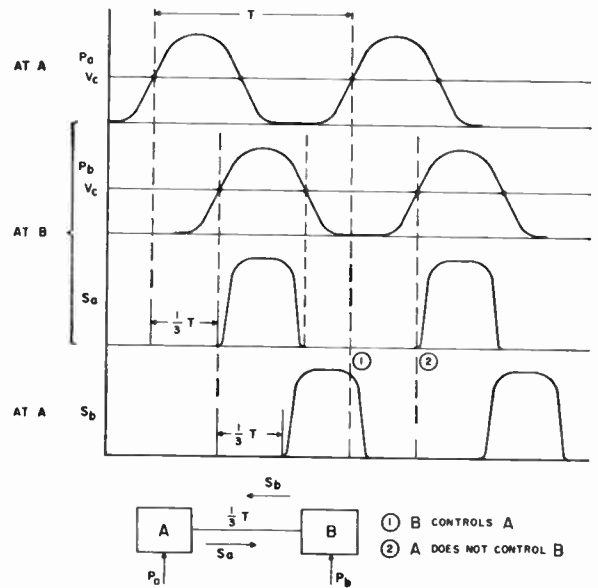


Fig. 12—Inversion of order of control.

Similarly, at ②, *A* controls *B*, and at ③, *B* controls *C*. Putting a delay between elements equal to one-third of the period of the power-supply modulation, as in Fig. 12, inverts the order of control. The exact fraction of a cycle needed to do this is related to the number of different types of elements (*i.e.*, *A*, *B*, *C*, . . .). Three is the minimum number of types required, and results in the simplest hierarchy of control. This order of control is independent of which phase is induced in the controlled element by the controlling element. Similarly the number of classes of elements is independent of the number of possible phase states.

The delays referred to above are in terms of *group velocity* with respect to the power-supply modulation period. This period has been assumed to be long compared to the period of the sinusoidal signals involved, so that adjustments of delay to fractional cycles of the sinusoidal voltage in the signal channel will not affect appreciably the delays previously discussed. Consider now the *phase velocity* of the signal channel. The phase induced in the controlled element will depend on the phase delay between it and its controlling element. A phase Φ_i in the controlling element after a phase delay K would put the controlled element into phase state $\Phi_i + K$. For the binary case, the phase shift K would be either an even or an odd multiple of π .

Up to this point all discussion has admitted the possibility of n phase states, or equivalently that $f_1 = n f_0$, where n is an integer. The elements can thus be used to implement n -state logic. At this point complete generality will be dropped, and we shall proceed to illustrate how these principles can be applied to built up binary logic with $n = 2$. With minor changes in the illustrations an n -state logic can also be realized.

Collecting nomenclature and graphical conventions which have been used, a lexicon of terminology for $n = 2$ is shown in Fig. 13.

MAJORITY LOGIC

The chief value of the aggregates of subharmonic generators is that they can be used to perform majority logic. By definition, a majority organ is a device or circuit which has multiple inputs and a single output. The value of the output is the value of the majority of the inputs. To avoid the indeterminate case, there must be an odd number of inputs.

In Fig. 14 the linear addition of signals from three *A* elements is applied to a *B* element.

Let

$$S_{a1} = E \cos (\omega_0 t + \Phi_1)$$

$$S_{a2} = E \cos (\omega_0 t + \Phi_2)$$

$$S_{a3} = E \cos (\omega_0 t + \Phi_3)$$

where $\Phi_1, \Phi_2, \Phi_3 = 0, \pi$, depending on the state of each *A* element, and $\omega_0 = 2\pi f_0$, the angular frequency of the subharmonic response. Possible results for S_a are:

$$E \cos (\omega_0 t + 0) \quad \text{two } \Phi_i = 0, \text{ one } \Phi_i = \pi$$

$$E \cos (\omega_0 t + \pi) \quad \text{two } \Phi_i = \pi, \text{ one } \Phi_i = 0$$

$$3E \cos (\omega_0 t + 0) \quad \Phi_1 = \Phi_2 = \Phi_3 = 0$$

$$3E \cos (\omega_0 t + \pi) \quad \Phi_1 = \Phi_2 = \Phi_3 = \pi.$$

Since the information is carried in the phase, S_a' has either 0 or π phase depending on the majority of the phases of S_{a1}, S_{a2} , and S_{a3} , and since the phase of S_b is determined by the phase of S_a' then $B = \text{Maj}(A_1, A_2, A_3)$. The amplitude variation has no importance. The truth table and equivalent logical expression are as in Fig. 15, arbitrarily letting $\Phi = 0$ be state "0" and $\Phi = \pi$ be state "1."

The majority organ and a negation operation (as shown in Fig. 13) are sufficient to build all logic.

The only thing lacking at this point is a method for putting information into such a system. Permanent

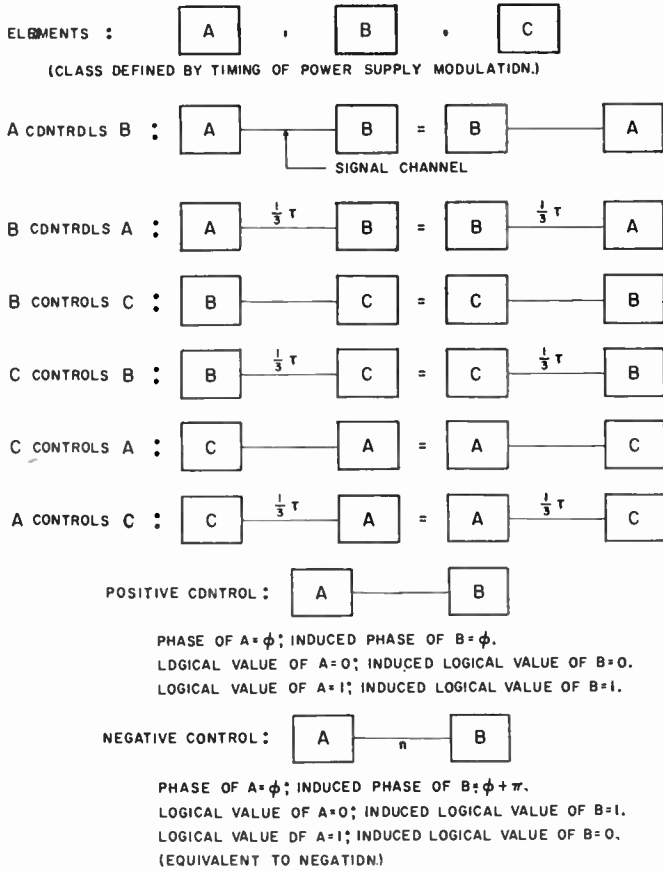


Fig. 13—Nomenclature and graphical conventions.

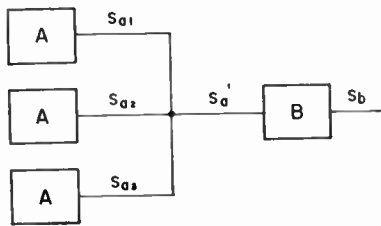


Fig. 14—Majority organ.

sources at the f_0 frequency which are gated on when desired by external controls, fill this need. A permanent source can control any class (A, B, C) of element. There are two possible types of permanent sources as illustrated in Fig. 16. The reference permanent source p is assumed to have state "1."

By using majority organs, negation, and permanent sources, the elementary logical operations shown in Fig. 17 can be performed. (At this point the separate designation of S_a as being a response of an element, A , will be dropped. The logical state represented by S_a will be called simply the *state* or *binary value* of A .)

The use of the majority organ also allows realization of other nonelementary logical functions. One of its great values is that a single organ can be used to realize many logical operations by what might be called logical biasing. This is shown in Fig. 18.

Fig. 18 may be generalized in an obvious way to n

A_1	A_2	A_3	B
0	0	0	0
0	0	1	0
0	1	0	0
0	1	1	1
1	0	0	0
1	0	1	1
1	1	0	1
1	1	1	1

$$B = A_1 \cdot A_2 \cdot A_3 + (A_1 \cdot A_2 + A_1 \cdot A_3 + A_2 \cdot A_3)$$

WHERE "•" IS INTERSECTION,
 AND "+" IS CONJUNCTION.

Fig. 15—Truth table for majority organ.

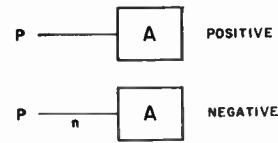


Fig. 16—Permanent sources.

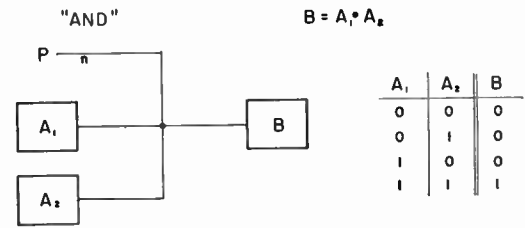
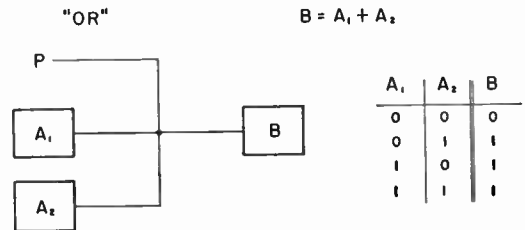


Fig. 17—Elementary logic operations.

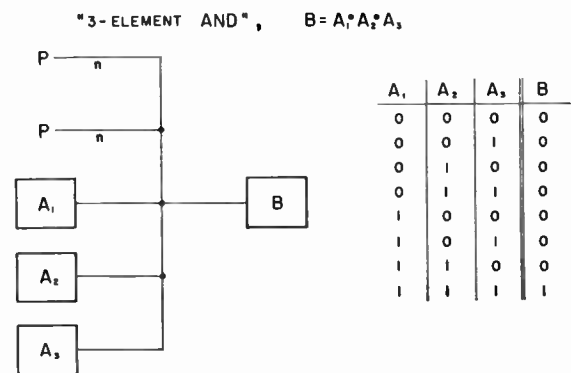
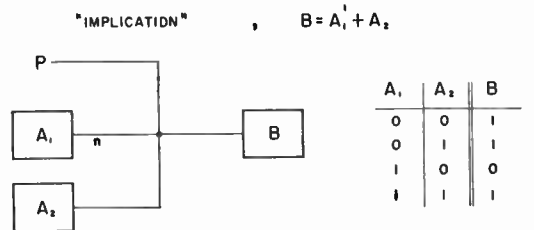


Fig. 18—Examples of nonelementary logic operations.

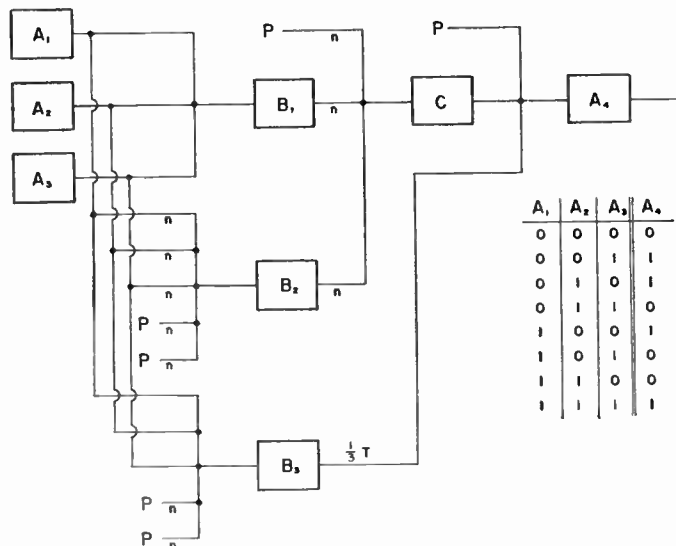


Fig. 19—Parity circuit.

elements. Also, an n -element “or” circuit differs from the “and” circuit only in having a positive rather than a negative relationship for the permanent sources. One other important aggregate is the “parity” circuit (Fig. 19).

$$\begin{aligned}
 B_1 &= \text{Maj}(A_1, A_2, A_3) & C &= B_1' \cdot B_2' \\
 B_2 &= A_1' \cdot A_2' \cdot A_3' & A_4 &= B_3 + C \\
 B_3 &= A_1 \cdot A_2 \cdot A_3 \\
 A_4 &= A_1 \cdot A_2 \cdot A_3 + \{ [\text{Maj}(A_1, A_2, A_3)]' \cdot (A_1' \cdot A_2' \cdot A_3') \}' \\
 &= A_1 \cdot A_2 \cdot A_3 + [(A_1 \cdot A_2 \cdot A_3) \cdot (A_1' \cdot A_2' \cdot A_3')] + (A_1 \cdot A_2) \\
 &\quad + (A_2 \cdot A_3) + (A_1 \cdot A_3) \}'
 \end{aligned}$$

As an example of the performance of a specific non-elementary logical operation, we show the majority organ and the parity circuit combined to make one stage of an adder (Fig. 20).

Reviewing what has been discussed: after establishing that the phase of the subharmonic response of a “tuned” nonlinear reactance can be used to represent logical states, the processes of negation and majority were shown to arise naturally. From these two operations the basic logical elements “and” and “or” were shown to be possible, along with other more complex logical functions from which can be built all logical operation. The entire discussion was in terms of binary computation, although it can be generalized to n -valued logic. An added attraction of majority logic is that the function of an aggregate of elements can be changed by processes implicit in the programming. For example, an “or” circuit becomes an “and” circuit by shifting the phase of the permanent source or, equally, by biasing the specific majority circuit with the output of another element involved in the computation. This provides great flexibility.

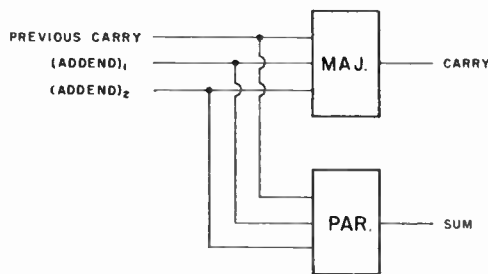


Fig. 20—One stage of an adder.

SOME PRACTICAL CONSIDERATIONS

A typical sequence of events in a signal channel is illustrated in Fig. 21. This shows a peculiar type of AM-phase-modulated sine wave. Information is represented by phase states Φ_1 and Φ_2 , which may be the same or different. The AM has no purpose in the logical processing, and so may be used to monitor the operation of the machine and, in servo-control circuits, to maintain signal levels at the proper average. The phase reference of the entire machine is the phase of the master oscillator supplying or controlling the power-supply signals for each element. The modulation of the power supply determines the basic logical time-cycle.

The modulation envelope of the power supply has been assumed to have time variations that are slow compared to the periods of both f_0 and f_1 . To give a numerical example, let the period of the power supply modulation be 50 cycles of f_1 (25 cycles of f_0) in a binary circuit. Reasonable values of f_1 and f_0 are 20 kmc and 10 kmc, respectively. The basic computing cycle has, therefore, a period of 2.5 μsec or a clock rate of 400 mc. The envelope of the modulation of both frequencies is not sinusoidal, but good rectangular pulses are not required. Three harmonics would be sufficient. Thus the modulation envelope would involve frequencies of 400–1200 mc.

To achieve a computing period of 1 μsec (a “clock rate” of 1000 mc) with the above time ratios would require $f_0 = 25$ kmc and $f_1 = 50$ kmc. The modulation envelopes would contain frequency components between 1000 and 3000 mc. For an absolute bandwidth of 2000 mc, this would be 4 per cent and 8 per cent relative bandwidth at f_1 and f_0 , respectively.

Hardware realization of this scheme may well seem outrageous to computer-systems engineers who now are in the transistor age. And it would truly be outrageous in size, cost, and power, with conventional waveguide components at X-band (8.6–12.4 kmc) and below. The techniques worked out with these conventional, readily available components can be applied to more practical geometries at a wide range of microwave frequencies. The higher frequencies of course have bad characteristics, such as high transmission attenuation, extreme precision requirements, and the lack, at present, of a complete line of components. These are things that must be overcome to push the speed of computation to the ultimate.

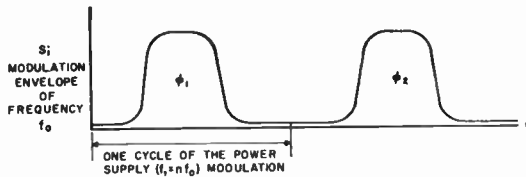


Fig. 21—Representation of PM-AM wave in the signal channel.

Von Neumann who played the leading role in the birth of the modern electronic computing machine, has, in these ideas, made another great contribution to the field. Whether this contribution will have as much importance as his original efforts can be decided only after the technology for implementing the subharmonic response scheme has been more fully worked out. At this point the prospects look good.

The above estimates of the number of cycles of the power supply and signal oscillations required for each computing cycle were made by von Neumann. Experiments using analog computer simulation of the subharmonic oscillators and LF (1–10 mc) lumped circuit models have shown that these estimates are realistic although they may be somewhat conservative. Circuits using that number of oscillation cycles per computation cycle would certainly work, and a reduction by a factor of 2.5 to 10 cycles of the signal and 20 cycles of the power supply appears to be possible. The chance of re-

ducing the required number of cycles very much beyond this is doubtful.

Note: The Japanese have developed a subharmonic oscillator computer based on nonlinear inductance which uses the same phase script for information representation and majority logic schemes as represented in the von Neumann ideas described in this paper.^{6–13} The basic circuit, called the Parametron, uses RF frequencies of 1 and 2 mc and has a computing rate of 10 kc. These two efforts are almost identical in concept, although far different in the speed of the suggested implementation, and, from available records, they seem to have been proposed in the same year, namely 1954. However, there is no direct connection between them known to this author.

⁶ S. Muroga, "Elementary principle of Parametron and its application to digital computers," *Datamation*, vol. 4, No. 5, pp. 31–34; September/October, 1958.

⁷ E. Goto, "On the application of parametrically excited nonlinear resonators," *Denki Tsushin Gakkai-shi*; October, 1955.

⁸ E. Goto, "New Parametron circuit element using nonlinear reactance," *KDD Kenkyu Shiryo*; November, 1954.

⁹ S. Oshima, "Introduction to Parametron," *Denshi Kogyo*, vol. 4, No. 11, p. 4; December, 1955.

¹⁰ S. Oshima, "General remarks on a Parametron circuit," *Denshi Kogyo*, special volume.

¹¹ H. Takahashi, "The Parametron," *Tsugakkai Shi*, vol. 39, No. 6, p. 56; June, 1956.

¹² H. Yamada, "A Parametron circuit examined from the point of mathematical logic," *Denshi Kogyo*, special volume.

¹³ Ohima, Enemoto, and Watanabe, "Oscillation theory of Parametron and method of measuring nonlinear elements," *KDD Kenkyu Shiryo*; November, 1955.

Stored Charge Method of Transistor Base Transit Analysis*

L. J. VARNERIN†, SENIOR MEMBER, IRE

Summary—A base layer transit time analysis has been made for high-frequency transistor base donor distributions. Transit time is defined as stored charge per unit emitter current. The emphasis on the stored charge/current ratio is particularly pertinent to high-frequency performance and facilitates qualitative analyses. The analysis applies to a *p-n-p* transistor in which the base donor density at the emitter (which specifies emitter breakdown voltage and emitter capacity for an alloyed emitter) and total number of donors per unit area of the base (which determines base resistance and emitter to collector punch-through voltage) are specified. It is shown that shorter transit times result with retarding fields since smaller base thicknesses are possible. It is thus shown that a built-in field is of lesser importance in determining transit time than is base thickness.

INTRODUCTION

THE USE of diffusion techniques in transistor fabrication¹ has resulted in transistor designs with cut-off frequencies in the range of 1000 mc.² In such transistors, basic design limitations³ seriously intrude upon freedom of design. For this reason it becomes increasingly important that each limitation be

¹ C. A. Lee, "A high frequency diffused base germanium transistor," *Bell Sys. Tech. J.*, vol. 35, pp. 23–34; January, 1956.

² C. H. Knowles and E. A. Temple, "Diffused base transistors," *Electronic Design*, vol. 6, pp. 12–15; July 9, 1958.

³ J. M. Early, "Design theory of junction transistors," *Bell Sys. Tech. J.*, vol. 32, pp. 1271–1312; November, 1953. Also "Structure-determined gain-band product of junction triode transistors," *Proc. IRE*, vol. 110, pp. 1924–1927; December, 1958.

* Original manuscript received by the IRE, October 29, 1958.

† Bell Telephone Labs., Inc., Murray Hill, N. J.

examined carefully in the approach to optimum designs. This paper considers the factors affecting base transit time τ of injected carriers in a diffused base junction transistor with an alloyed emitter. For convenience, p - n - p transistors are considered.

In the analysis presented in this paper, base transit time is defined as the ratio of stored or injected base charge to emitter current. In this sense it is more properly described as the base transit time constant. This stored charge/current ratio is important because it is directly related to high-frequency transistor performance. Recognition of the identity between stored charge and transit time allows a simple physical understanding of the qualitative features of base impurity distributions.

The base charge control concept of transistor operation is a particularly powerful one and is not generally appreciated. The first explicit exposition of this method in the literature was given by Beaufoy and Sparkes,⁴ who point out that the junction transistor is fundamentally a base charge-controlled device rather than a current controlled device. While the dc characteristics can be described in terms of current control, the ac or transient characteristics are determined by the requirement for changing the charge distribution.

Reductions in base transit time^{5,6} in a transistor with a given base width w can be obtained with aiding electric fields resulting from the grading of base impurity densities. This principle has been widely used^{1,2,7} with the advent of diffusion techniques. The limitations imposed in the highest frequency designs employing alloyed emitters do not permit advantage to be taken of this phenomenon, and shorter transit times are possible with retarding fields. This seemingly paradoxical result is made understandable by demonstrating that requirements for adequate emitter breakdown and emitter to collector punch-through voltages, and for minimum emitter junction capacity and base resistance, lead to narrower base widths and lower transit times if retarding fields are accepted.

BASE TRANSIT TIME

The concept of base transit time is useful in analyzing high-frequency performance of transistors. While it sheds no light directly on the broadening of an input signal as do the ac solutions of carrier flow of Kromer,⁵ it is particularly valuable in approximate and comparative analyses because of its conceptual simplicity.

On closer examination this simplicity has not always

been apparent. Signal transmission cannot be thought of rigorously as a time of flight phenomenon. This is inherent in the diffusion mechanism and mathematically is a consequence of the diffusion equation which possesses no traveling-wave solutions. Moll and Ross⁶ calculated transit time by defining a velocity v associated with the carrier flow through the relation

$$J = qp v$$

where J is current density, q electronic charge, and p hole density. While this yields a correct result, the procedure is essentially mathematical because v is not a real velocity having a direct physical interpretation.

The conceptual difficulties are eliminated, however, by defining transit time as the ratio of stored or injected charge Q_s to emitter current I_e

$$\tau = \frac{Q_s}{I_e}$$

or more generally

$$\tau = q \int_0^w \frac{p dx}{J}, \quad (1)$$

where w is base width and J is emitter current density. It will be noted that the ratio of stored charge to current is the average time spent per carrier in the base and this is the principal reason for defining it as transit time. While this procedure is formally equivalent to that of Moll and Ross, the point of view differs because it focuses attention on the stored-charge/current ratio as the important physical concept.

The importance of this point of view can be demonstrated by showing that the ratio of high-frequency base current I_{b1} to emitter current I_{e1} is directly proportional to the stored charge/current ratio. In a transistor having unity dc α , the base stored charge can change only through base current flow. This is related to Q_{s1} , the ac component of stored charge, $I_{b1} = j\omega Q_{s1}$, giving

$$\begin{aligned} \frac{I_{b1}}{I_{e1}} &= j\omega \frac{Q_{s1}}{I_{e1}} \\ &= j\omega \tau. \end{aligned}$$

This current ratio, which is proportional to the charge/current ratio or transit time constant τ , should be minimized for the most favorable high-frequency performance. We have used the familiar low-frequency approximation ($\omega < 1/\tau$) of a modulated dc hole distribution for which the ratios of ac quantities are equal to the ratios of the corresponding dc quantities.

As demonstrated in the analyses to follow, consideration of stored charge can often simplify problems by substituting physical reasoning and intuition for detailed calculations. The effects of complicated variations of donor distributions on transit time are analyzed in this way.

⁴ R. Beaufoy and J. J. Sparkes, "The junction transistor as a charge-controlled device," *ATE J.*, vol. 13, no. 4, pp. 310-327; 1957.

⁵ H. Kromer, "Zur theorie des diffusions- und des drift transistors," *Arch. elek. Übertragung*, vol. 8, pp. 223-228, 363-369, 499-504; May, August, November, 1954.

⁶ J. L. Moll and I. M. Ross, "The dependence of transistor parameters on the distribution of base layer resistivity," *Proc. IRE*, vol. 44, pp. 72-78; January, 1956.

⁷ H. Kromer, "Der Drifttransistor," *Naturwiss.*, vol. 40, pp. 578-579; November, 1953.

SOLUTIONS FOR CARRIER FLOW

Eq. (1) requires knowledge of base hole distribution for calculation of transit time. The general solutions for carrier transport through a base region from $x=0$ at the emitter to $x=w$ at the edge of the collector depletion layer have been given by Moll and Ross.⁶ Eqs. (2) through (5) have been taken from their paper.

The hole current density is given by

$$J = q\mu_p p E - qD_p \frac{dp}{dx}, \quad (2)$$

where μ_p and D_p are mobility and diffusion coefficients for holes in the base and p is hole density. Recombination in the base has been neglected. The built-in field is given by

$$E = -\frac{kT}{q} (1/N) dN/dx, \quad (3)$$

where N is donor density. Solution of (1) and (2) gives the hole density

$$p = (J/qD_p)(1/N(x)) \int_x^w N dx. \quad (4)$$

The lower limit $x=0$ defines the hole density at the emitter p_0

$$\begin{aligned} p_0 &= (J/qD_p N_0) \int_0^w N dx \\ &= (J/qD_p N_0) N_T, \end{aligned} \quad (5)$$

where N_0 is the donor density at the emitter ($x=0$) and N_T , given by

$$N_T = \int_0^w N dx, \quad (6)$$

is the total number of donors per unit area of the base.

CONDITIONS IMPOSED ON HIGH-FREQUENCY TRANSIT TIME ANALYSIS

Freedom to choose base layer distribution of impurities is more severely limited in high-frequency designs than in low-frequency designs. In addition to the usual requirement for a high emitter doping relative to base doping, several specifically high-frequency conditions are encountered. For convenience, a p - n - p transistor will be considered.

If the base doping level does not change appreciably in the emitter space charge region, the usual case, the emitter breakdown voltage⁸ and the junction capacity C_{TE} ,⁹ are specified by the base doping level at the emitter. Since the current which flows in C_{TE} is not part of

of the injected base current, C_{TE} must be limited in order to have adequate high-frequency current gain. These considerations lead to a specification in the subsequent analysis of a maximum doping level at the emitter N_0 .

The total number of impurities per cm^2 of the base, N_T , introduced in the preceding section, specifies both the transverse base resistance and the punch-through voltage. The base resistance directly affects the high-frequency figure of merit.³ This requirement as well as the necessity for an adequate punch-through voltage lead to a specified value N_T for the total number of impurities per cm^2 in the base.

With the specification of N_0 and N_T the problem then is how to distribute the donors to minimize base transit time. How this is done will determine base thickness w . Note from (5) that the hole density at the emitter p_0 is expressed in terms of J , N_0 , and N_T . Thus if J is assigned a fixed value, any two of the three parameters, p_0 , N_0 , and N_T can be selected to have specified values.

QUALITATIVE HIGH-FREQUENCY TRANSIT TIME ANALYSIS

In this section a qualitative analysis is made of the effect of different types of donor distributions on transit time. It relies solely on a consideration of stored charge.

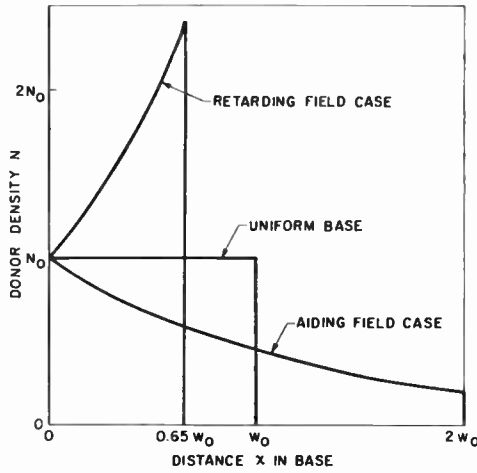
Three donor distributions for which N_0 and N_T are the same are shown in Fig. 1(a). The uniform distribution has width w_0 while the two simple exponential distributions giving rise to a retarding and to an aiding field have, as required, smaller and larger values of w , respectively. The corresponding solutions to p of Fig. 1(b) for equal values of emitter current J can be sketched without recourse to calculation. The solution for the uniform distribution is known to be linear. Each distribution has the same value p_0 at $x=0$ for equal current density J as noted in the previous section. Equal values for J require equal slope for each curve at $x=w$ ($p=0$) from (2). With this information the curves of Fig. 1(b) follow.

The area under each curve of Fig. 1(b) is the stored charge and is proportional to transit time. Thus, the narrower retarding field distribution gives the smallest value of transit time, and the wider aiding field distribution gives rise to the greatest.

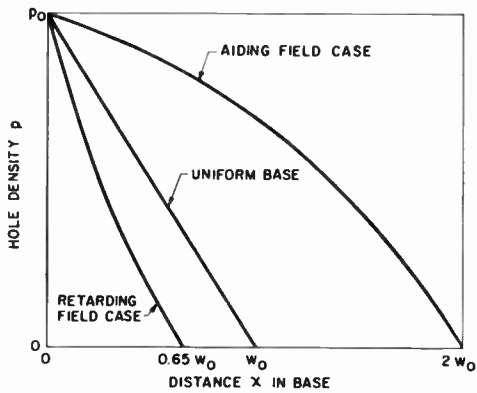
This qualitative procedure can be applied to more complicated cases. The retarding field case (A) just discussed will be compared in Fig. 2(a) with a distribution (B) having simultaneously both aiding and retarding fields while still having equal values for N_0 and N_T . The B distribution is more nearly a physically realizable distribution which might result from the out-diffusion of an initially high concentration very close to the surface. The discontinuity at $x=w$ corresponds to the edge of the collector space charge depletion layer. At $x=x_m$, the maximum of the donor curve, there is no built-in

⁸ S. L. Miller, "Avalanche breakdown in germanium," *Phys. Rev.*, vol. 99, pp. 1234-1241; August 15, 1955.

⁹ W. Shockley, "The theory of p - n junctions in semiconductors and p - n junction transistors," *Bell Sys. Tech. J.*, vol. 28, pp. 435-489; July, 1949.

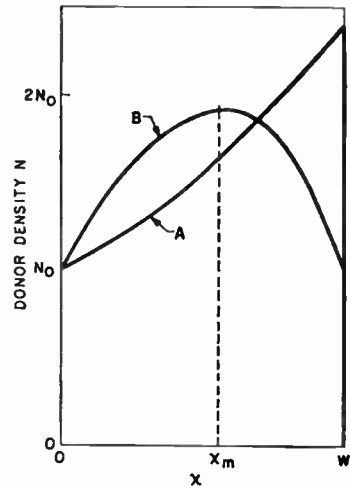


(a)

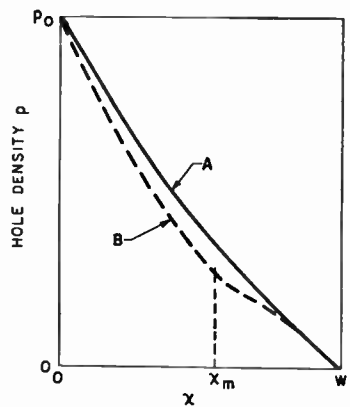


(b)

Fig. 1—(a) Comparison of donor distributions for uniform base, retarding and aiding field cases. (b) Comparison of hole distributions for uniform base, retarding and aiding field cases.



(a)



(b)

Fig. 2—(a) Comparison of A and B donor distributions. (b) Comparison of hole distributions for A and B donor distributions.

field while a retarding field exists for $x < x_m$ and an aiding field for $x > x_m$.

The qualitative features of the density curve for holes p can be readily seen for each of these distributions. The curve for the simple retarding exponential A distribution is taken from Fig. 1(b). For the same reason as in the comparisons made in Fig. 1 and as discussed above, the slopes of the curves at $x = w$ and the values for p_0 must be identical for the A and B distributions. In addition, the slope for the B distribution at $x = x_m$ (the zero field point) must be the same as at $x = w$. The slope in the range $x_m < x < w$ (for which $E > 0$) must be less than at $x = w$, as can be seen from the aiding field case discussed in connection with Fig. 1(b). The hole curve for this B distribution is now readily constructed, starting at $x = w$. The slope here is identical with the A curve, but decreases initially as x approaches x_m because of the aiding field. The slope then increases again so that the slope at $x = x_m$ is the same as at $x = w$. For $x < x_m$ the slope increases smoothly as the curve approaches p_0 at $x = 0$. Thus it is seen that the area under the hole density curve or stored charge corresponding to the B distribution and consequently the transit time is less than for the A distribution.

QUANTITATIVE ANALYSIS FOR EXPONENTIAL DISTRIBUTIONS

The qualitative results for the exponential distribution of donors will be demonstrated analytically. The base donor distribution is given by

$$N = N_0 \exp(-\beta x). \tag{7}$$

From (2) the field is given by $E = \beta(kT/q)$, showing that $\beta > 0$ and $\beta < 0$ correspond to aiding and retarding fields, respectively. Distributions of this type were given in Fig. 1(a).

The condition for a specified value of N_T (6) leads to a relation between w and β ,

$$\frac{w}{w_0} = \frac{\ln(1/(1 - \beta w_0))}{\beta w_0}, \tag{8}$$

where w_0 is the width corresponding to uniform doping.

From (4) the hole density is given by

$$p = \frac{J}{qD_p\beta} [1 - \exp(\beta(x - w))]. \tag{9}$$

From (1) the transit time is given by

$$\tau = \frac{w_0^2}{2D_p} f, \tag{10}$$

which is the product of the transit time for a uniform base times a base transit time factor f given by

$$f = 2 \frac{w/w_0 - 1}{\beta w_0}. \tag{11}$$

It will be recalled that this solution applies, as described earlier, to donor distributions with specified values of N_0 (donor density at the emitter) and N_T (total number of donors per unit area).

Because of the transcendental character of (8), it is not possible to express βw_0 , and hence τ and f , as a function of w/w_0 . However, this function is presented graphically in Fig. 3. As expected, f is unity for $w/w_0 = 1.0$ ($\tau = w_0^2/2D_p$ for a uniform base).

It is interesting to note that the base transit time factor f is given approximately by

$$f \cong (w/w_0)^{4/3} \tag{12}$$

to within a few per cent for $0.1 \leq w/w_0 \leq 6$. Expansion of f in powers of $(w/w_0) - 1$ shows that the first and second derivatives of f are identical with those for the $4/3$ power law and the third derivative is very nearly the same.¹⁰ The effect of built-in fields can be appreciated by comparing this with

$$f = (w/w_0)^2$$

for a uniform base with no built-in fields and no restriction on N_T .

So far, variation of diffusion coefficient with doping level has not been taken into account. For $N \geq 10^{16}$, the diffusion coefficient¹¹ in germanium varies roughly as $N^{-1/3}$. In a crude way the average donor density varies as w_0/w , so that D_p varies as

$$D_p \cong D_{p0}(w/w_0)^{1/3}$$

where D_{p0} is the diffusion coefficient applicable to the uniformly doped base. Thus the base transit time is given roughly by

$$\tau \cong \frac{w_0^2}{2D_{p0}} (w/w_0). \tag{13}$$

Eqs. (12) and (13) show that considerable advantage in reducing transit time can be obtained by making base thickness less than w_0 even though retarding fields result.

CONCLUSION

An analysis has been made of the effects on transit time required by high-frequency designs. This has been

¹⁰ The author is indebted to F. W. Terman for analyzing the equations.

¹¹ M. B. Prince, "Drift mobilities in semiconductors. I. Germanium," *Phys. Rev.*, vol. 92, pp. 681-687; November 1, 1953.

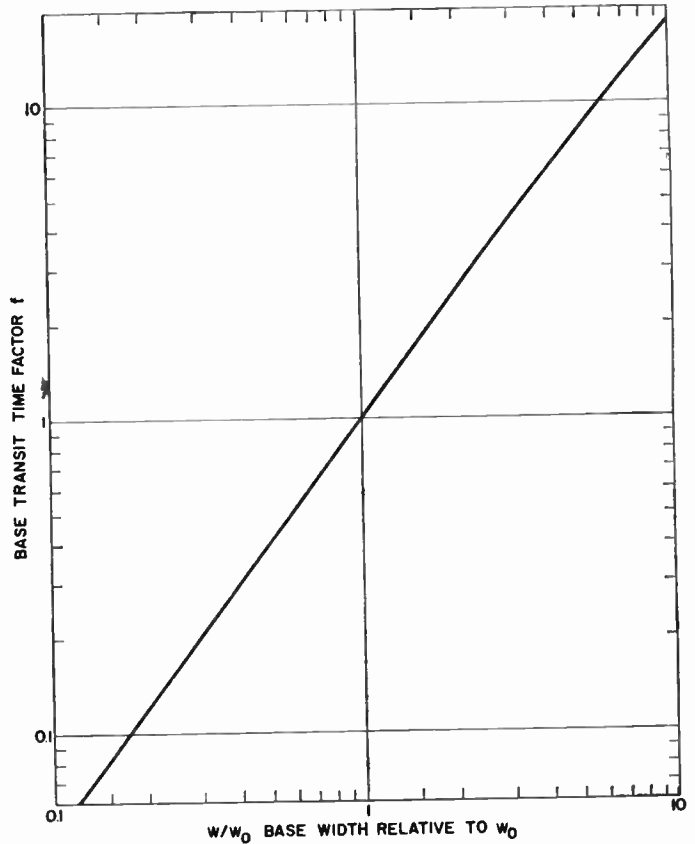


Fig. 3—Base transit time factor as a function of base thickness.

done by defining base transit time as the ratio of stored base charge to emitter current. In this way it can be interpreted as the average time spent per carrier in the base. Simple physical reasoning applied to this stored charge point of view provides considerable insight into the factors affecting transit time.

This method of analysis has been applied to the design of base layer impurity distributions of high-frequency transistors. By requiring that the base donor density at the emitter (which determines breakdown voltage and emitter capacity with alloyed emitters) and the total number of donors per unit area of the base (which determines base resistance and emitter to collector punch-through voltage) be specified, it is shown that distributions having retarding fields yield shorter transit times than do those with aiding fields. This result stems from the narrower base thickness possible with retarding fields for these boundary conditions. Thus it can be concluded that the effects of built-in fields are minor compared to the actual value of base thickness and that in high-frequency designs the actual value should be reduced even though retarding fields result.

ACKNOWLEDGMENT

The author wishes to thank J. M. Early for many stimulating discussions and helpful suggestions during the course of this work. He also wishes to thank I. M. Ross for helpful comments on the manuscript.

The Hall Effect Circulator—a Passive Transmission Device*

W. J. GRUBBS†

Summary—Three-port nonreciprocal Hall effect devices have been made which circulate dc and ac signals either in a clockwise or counterclockwise sense. Forward losses of 17 db and reverse losses of 61 db have been obtained, giving a transmission ratio of 44 db. With the aid of simple six-resistor networks (or even simpler three-resistor networks) the nine short circuit admittance parameters of the circulator can be adjusted in a calculable manner. These networks permit asymmetrical circulators to appear symmetrical, to operate over a wide range of impedance levels, to operate with any value of magnetic field, and to introduce no loss—or even gain—if negative resistances are used. An analysis of the circulator, with and without the parallel networks, is included. It is shown that the minimum possible forward loss for a Hall effect circulator is 8.4 db.

INTRODUCTION

MOST of the passive transmission devices one normally encounters are reciprocal in nature; that is, they exhibit the same transfer characteristic whether a signal is applied at some point A and is removed at point B , or vice versa. A list of such devices might include transformers, filters, equalizers, transmission lines, etc. Some passive transmission devices, however, are not reciprocal. In these devices, the nature of the transfer characteristic depends on whether the signal goes through from A to B or from B to A . Gytrators, isolators, and circulators are in the category of nonreciprocal devices and have been made for use in waveguides for several years.

In 1953, it was reported that Hall effect gytrators and isolators could be made for use in wire circuits.¹ These latter devices function throughout the frequency range from dc to some upper limit which depends theoretically only on the dielectric relaxation time of the material used. The purpose of this paper is to describe and analyze the Hall effect circulator, which has a similar frequency range. This device was originally conceived by Semmelman² of Bell Laboratories.

THE HALL EFFECT CIRCULATOR

A circulator is a three-port (six-terminal) nonreciprocal passive device which circulates signals essentially in one direction only—clockwise, for example, as shown in Fig. 1. Thus, an input signal on terminals 1-1' is transmitted to terminals 2-2', but no signal appears at 3-3'. The same clockwise circulation occurs when a sig-

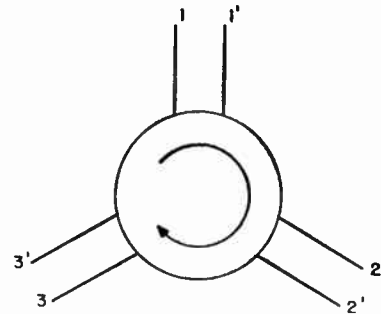


Fig. 1—Symbol for three-port circulator.

nal is applied to any of the three terminal pairs.

If a magnetic field is applied perpendicular to a current flow (see Fig. 2), the current carriers are deflected sidewise and a transverse electric field (perpendicular to both the magnetic field and the longitudinal current flow) is built up between the sides of the conductor. Thus the net electric field in the sample makes some angle θ with the direction of current flow. This angle is known as the Hall angle and, to a first approximation, its tangent is given by the product of the magnetic field and the Hall mobility of the majority carriers in the sample when the product of the majority carrier density and mobility is much greater than the same product for minority carriers. Hall effect devices use semiconductors rather than metals because most metals have much lower mobilities.

If six equally-spaced contacts are made to the edge of a slice of semiconductor, as shown in Fig. 3, and a constant magnetic field is applied perpendicular to the plane of the slice, the slice becomes a Hall effect circulator for the proper value of magnetic field. That is, θ must be such that the net electric field produces no voltage between terminals 3 and 3'.

As soon as a load is attached to terminals 2-2' so that a current can flow, an additional Hall field (not shown here) is produced which has the effect of decreasing the effective Hall angle in the sample. Consequently, a stronger magnetic field is required to balance the circulator. The value of the magnetic field required for a matching load impedance will be called B_0 . Thus, the circulator can be made to operate properly with a range of load resistances by adjusting the magnetic flux density.

ANALYSIS OF CIRCULATOR

Most n -port circuits or devices can be completely described and characterized by n^2 parameters. These parameters may be either open-circuit impedances or short-

* Original manuscript received by the IRE, October 29, 1958; revised manuscript received, December 22, 1958.

† Bell Telephone Laboratories, Inc., Murray Hill, N. J.

¹ W. P. Mason, W. H. Hewitt, and R. F. Wick, "Hall effect modulators and gytrators' employing magnetic field independent orientations in germanium," *J. Appl. Phys.*, vol. 24, pp. 166-175; February, 1953.

² C. L. Semmelman, "Nonreciprocal Transmitting Devices," U. S. Pat. 2,774,890; December 18, 1956.

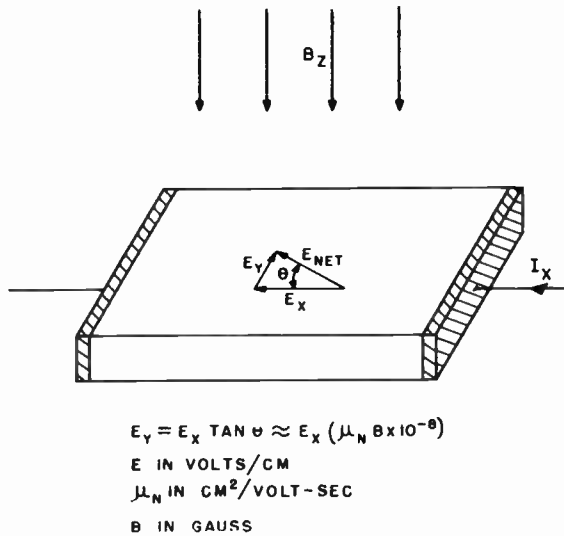


Fig. 2—Illustration of the Hall effect.

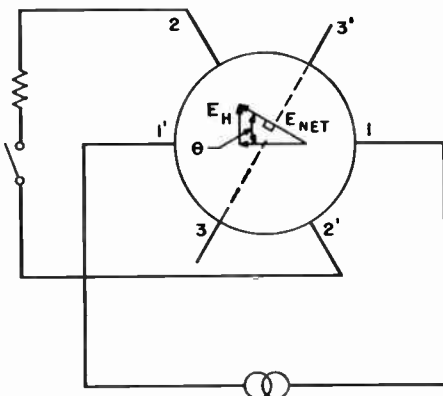


Fig. 3—Diagram showing qualitatively how the Hall field (E_H) causes 3 and 3' to be on the same equipotential line with a signal applied between 1 and 1'.

circuit admittances. Although impedances are more easily measured, in the circulator it is preferable to work with the short-circuit admittances. In practice, admittances are computed from measured impedances.

These admittances are defined as:

$$y_{mn} = \frac{i_m}{v_n} \Big|_{\text{all } v_s=0 \text{ except } v_n}$$

The set of three equations relating v 's, i 's, and y 's are

$$i_m = \sum_{n=1}^3 y_{mn} v_n; \quad m = 1, 2, 3. \quad (1)$$

One form of equivalent circuit which incorporates these admittances is shown in Fig. 4. In the case of a symmetrical circulator, the three self-admittances are equal ($y_{11} = y_{22} = y_{33} = y_S$); and three forward transfer admittances are equal ($y_{13} = y_{32} = y_{21} = y_F$); and the three reverse transfer admittances are equal ($y_{12} = y_{23} = y_{31} = y_R$).

The input admittance is given by

$$y_{IN} = y_S \left[1 + \frac{U_F^3 + U_R^3 - 2U_R U_F (1 + U_L)}{(1 + U_L)^2 - U_R U_F} \right], \quad (2)$$

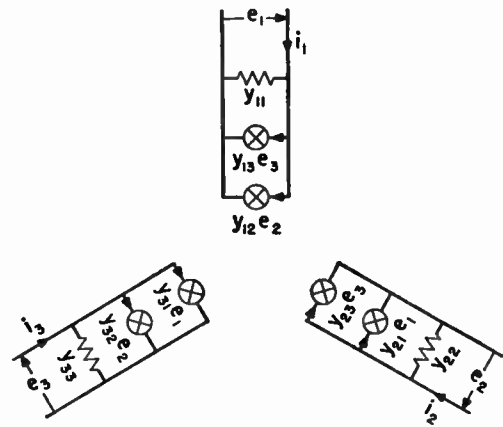


Fig. 4—Equivalent circuit of Hall effect circulator.

where the admittances have been normalized with respect to y_S , such that $U_F = y_F/y_S$, $U_R = y_R/y_S$, and $U_L = y_L/y_S$. y_L is the load admittance and is assumed to be the same at each terminal pair. These normalized admittances are useful for analysis because they will be the same for any Hall effect circulator in which θ has the same value.

The forward voltage transmission ratio (from 1-1' to 2-2', or from 2-2' to 3-3', etc.) is

$$\frac{V_F}{V_{IN}} = \frac{U_R^2 - U_F(1 + U_L)}{(1 + U_L)^2 - U_R U_F}. \quad (3)$$

The reverse voltage ratio (that is, for a signal transmitted in the counterclockwise direction) is

$$\frac{V_R}{V_{IN}} = \frac{U_F^2 - U_R(1 + U_L)}{(1 + U_L)^2 - U_R U_F}. \quad (4)$$

In a circulator V_R must be zero. Thus, the condition for circulation may be stated as

$$U_F^2 - U_R(1 + U_L) = 0. \quad (5)$$

Fig. 5 shows how the admittances vary in an n -type Ge circulator with the magnetic field, B . At $B=0$, $y_R = y_F$; in other words, with no magnetic field, the device is reciprocal and cannot distinguish the clockwise from the counterclockwise direction. When B has some finite value, $y_R \neq y_F$, and the device is nonreciprocal. As B increases, the device becomes more and more nonreciprocal. At any flux density greater than about 10 kilogauss, the condition for circulation can be met by proper choice of y_L . At $B=10$ kg, y_L must be zero; i.e., the load terminals must be open-circuited. As B is increased, y_L must increase to satisfy (5). At the value of flux density called B_0 , about 14.5 kg for n -type Ge, $y_L = y_{IN}$. Therefore, this is the logical value of field to use, because this is the field at which the load matches the admittance seen looking back into the circulator.

Using (3) and the admittance values at $B = B_0$, we can calculate the forward loss to be 17 db. The measured forward losses ranged from 16 to 18 db on the various n -type Ge circulators which were fabricated. The for-

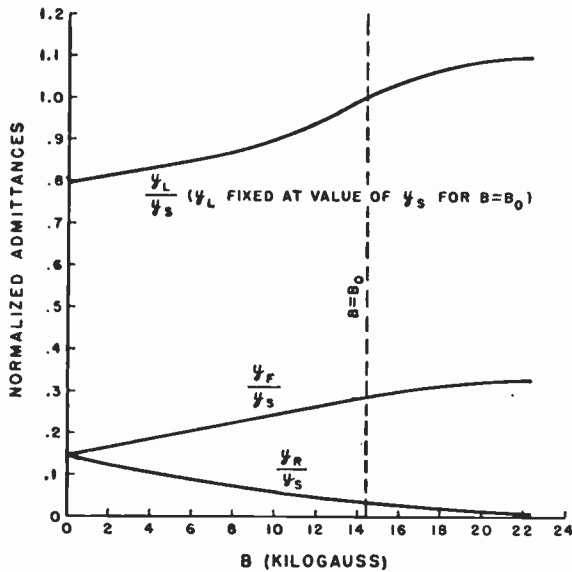


Fig. 5—Variation of short-circuit admittances with magnetic field.

ward loss will be the same for any Hall effect circulator, even for a larger or smaller sample made of a different material. The preceding statement is based on the assumptions that there are no surface effects and no asymmetrical bulk effects, in which case the Hall angle θ must always have the same value. With the same θ , the normalized forward and reverse transfer admittances will have the same value. Therefore, v_F/v_{LN} will be unchanged, assuming, of course, that U_L is given a value of one.

Because of the relatively high forward loss (17 db), reflections are severely attenuated, so that the input admittance is very nearly constant. In fact, it can be shown from (2) that $Y_{LN} = y_s \pm 0.5$ per cent for any symmetrical load admittance from short circuit to open circuit.

USE OF PARALLEL NETWORKS

Hall effect circulators have been made which are quite symmetrical. The best circulator made to date has an average reverse loss of 61 db and an average forward loss of 17 db, giving an average transmission ratio of 44 db. Any two pairs of terminals on such a circulator would act as an isolator with 17 db loss in the forward direction. However, the symmetry depends primarily on having a regular 60° angular spacing between the six edge contacts. This is not impossible, but it is difficult, to say the least. Furthermore, it is almost impossible to obtain a specific input admittance (or operating impedance level) because, to a good approximation, this is directly proportional to the material's conductivity and the reciprocal of the sample thickness. In a null transmission device such as a circulator, impedance matching is essential.

With the aid of a resistance network connected in

parallel with the circulator, imperfections can be effectively removed and several other interesting features are made available. For instance, the forward loss may be decreased by using a larger magnetic field ($B > B_0$). On the other hand, if one can tolerate greater forward loss, one can use a smaller magnet ($B < B_0$). The main requirement for circulation is that the reverse loss be theoretically infinite. This requirement can be met for the limiting case of $B = 0$, but the forward loss also becomes infinite.

With any fixed B , circulation is obtainable with any load admittance from about ten times the normal admittance down to zero—*i.e.*, open-circuit. However, the admittance of the circulator with the network changes only slightly over this range, so that the forward loss becomes quite high when a widely different load admittance is used, due simply to the admittance mismatch. Furthermore, the resistance networks can provide circulation when an essentially symmetrical circulator is used with a different load conductance on each of the three terminal pairs.

If one were willing to use negative resistances in the network, one could eliminate the forward loss (which is normally about 17 db) without decreasing the maximum reverse loss in the balanced condition. In fact, one could obtain negative loss, or gain.

The six-terminal (three-port) resistance network can be represented by

$$i_m' = \sum_{n=1}^3 y_{mn}' v_n'; \quad m = 1, 2, 3. \quad (6)$$

If we connect the resistance network in parallel with the circulator by connecting terminals 1 and 1' of the one to 1 and 1' of the other, etc., then the three equations describing the combined network are

$$I_m = \sum_{n=1}^3 Y_{mn} V_n; \quad m = 1, 2, 3,$$

where [see (1)]

$$I_m = i_m + i_m' \quad (7)$$

$$Y_{mn} = y_{mn} + y_{mn}', \quad (8)$$

$$V_n = v_n = v_n'. \quad (9)$$

The resistance network admittances (y_{mn}') for an asymmetrical network become so bulky that they are practically useless. However, if one assumes symmetry, they are (for network C_p shown in Fig. 6).

$$y_F' = y_R' = -\frac{1}{2R}$$

$$y_S' = \frac{1}{R}. \quad (10a)$$

For the network shown in Fig. 7 (C_S), the admittances are

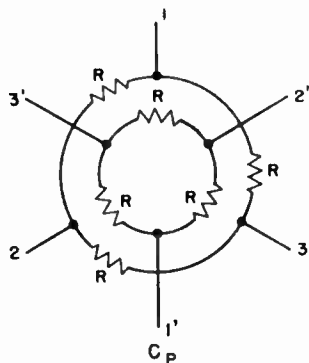


Fig. 6—Network C_p .

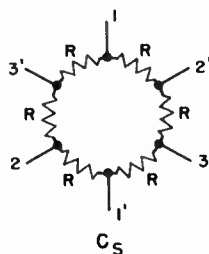


Fig. 7—Network C_s .

$$\begin{aligned}
 Y_F^S &= y_F + \frac{1}{2R} \\
 Y_R^S &= y_R + \frac{1}{2R} \\
 Y_S^S &= y_S + \frac{1}{R}
 \end{aligned}
 \tag{12}$$

The requirements for circulation (when C_p is used) may be written as

$$(Y_F^P)^2 - Y_R^P(Y_S^P + y_L) = 0,$$

or

$$\begin{aligned}
 \left(y_F - \frac{1}{2R}\right)^2 \\
 - \left(y_R - \frac{1}{2R}\right)\left(y_S + y_L + \frac{1}{R}\right) = 0.
 \end{aligned}
 \tag{13}$$

If we define $R=1/ky_S$, we can use normalized admittances in (13):

$$\left(U_F - \frac{k}{2}\right)^2 - \left(U_R - \frac{k}{2}\right)(1 + U_L + k) = 0.
 \tag{14}$$

Solving (14) for k yields

$$\frac{3}{2}k = U_F + U_R - \frac{1}{2}(1 + U_L) + \sqrt{[-U_F - U_R + \frac{1}{2}(1 + U_L)]^2 - 3[U_F^2 - U_R(1 + U_L)]}.
 \tag{15}$$

Eq. (15) is of the form

$$\frac{3}{2}k = -a + \sqrt{a^2 - 3b}.$$

It may be noted that, when $B=B_0$, $b=0$, and $k=0$. In other words, the parallel resistance network must be removed for the circulator to work properly. Examination of (15) and the curves of Fig. 5 shows that k is real, positive and finite only when $0 \leq B < B_0$.

The requirement for circulation (when C_s is used) is

$$\left(y_F + \frac{1}{2R}\right)^2 - \left(y_R + \frac{1}{2R}\right)\left(y_S + y_L + \frac{1}{R}\right) = 0,$$

which, using normalized admittances, is

$$\left(U_F + \frac{k}{2}\right)^2 - \left(U_R + \frac{k}{2}\right)(1 + U_L + k) = 0.
 \tag{16}$$

Solving (16) for k yields

$$\frac{k}{2} = U_F - U_R - \frac{1}{2}(1 + U_L) + \sqrt{[-U_F + U_R + \frac{1}{2}(1 + U_L)]^2 + [U_F^2 - U_R(1 + U_L)]}.
 \tag{17}$$

$$\begin{aligned}
 y_F'' &= y_R'' = + \frac{1}{2R} \\
 y_S'' &= \frac{1}{R}.
 \end{aligned}
 \tag{10b}$$

In both cases, R is the value of the individual resistors.

Thus, by the simple addition indicated in (8), we arrive at the effective admittances of the parallel combination of circulator and resistance network C_p :

$$\begin{aligned}
 Y_F^P &= y_F + y_F' = y_F - \frac{1}{2R} \\
 Y_R^P &= y_R - \frac{1}{2R} \\
 Y_S^P &= y_S + \frac{1}{R}.
 \end{aligned}
 \tag{11}$$

Similarly, the effective admittances when the resistance network is C_s are:

Eq. (17) is of the form

$$\frac{k}{2} = -c + \sqrt{c^2 + b}$$

Again, when $B = B_0$, $b = 0$, and $k = 0$. Studying (17) and Fig. 5 shows that k is real, positive and finite only when $B > B_0$. For completeness, the expressions for forward and reverse voltage ratios are given below for combined networks using C_P and C_S . The symbols have the same meanings as before.

With network C_P

$$\frac{e_F}{e_{IN}} = \frac{\left(U_R - \frac{k}{2}\right)^2 - \left(U_F - \frac{k}{2}\right)(1 + U_L + k)}{(1 + U_L + k)^2 - \left(U_R - \frac{k}{2}\right)\left(U_F - \frac{k}{2}\right)} \quad (18)$$

$$\frac{e_R}{e_{IN}} = \frac{\left(U_F - \frac{k}{2}\right)^2 - \left(U_R - \frac{k}{2}\right)(1 + U_L + k)}{(1 + U_L + k)^2 - \left(U_R - \frac{k}{2}\right)\left(U_F - \frac{k}{2}\right)} \quad (19)$$

with network C_S

$$\frac{e_F}{e_{IN}} = \frac{\left(U_R + \frac{k}{2}\right)^2 - \left(U_F + \frac{k}{2}\right)(1 + U_L + k)}{(1 + U_L + k)^2 - \left(U_R + \frac{k}{2}\right)\left(U_F + \frac{k}{2}\right)} \quad (20)$$

$$\frac{e_R}{e_{IN}} = \frac{\left(U_F + \frac{k}{2}\right)^2 - \left(U_R + \frac{k}{2}\right)(1 + U_L + k)}{(1 + U_L + k)^2 - \left(U_R + \frac{k}{2}\right)\left(U_F + \frac{k}{2}\right)} \quad (21)$$

It is possible to use simpler forms of these resistance networks. The simplified networks (which will be called $C_{P'}$ and $C_{S'}$) consist of only three resistors instead of six. See Figs. 8 and 9. Either of the forms of $C_{S'}$ are usable. However, the one on the right has the advantage of being symmetrical. Furthermore, the symmetrical $C_{S'}$ is the only one of the three which can be analyzed by the method used on the six-resistor networks, and it is the only one of the three which permits the terminal pairs to be balanced-to-ground.

A major advantage of $C_{P'}$ and $C_{S'}$ (aside from the obvious one that they use only half as many resistors) is that they are much easier to adjust. For any particular desired circuit condition, there is only one set of three resistance values which will operate properly; also, if the resistance values are nearly right, the isolation between any two terminal pairs is controlled almost entirely by one particular resistor. With the six-resistor networks there is an infinity of sets of six resistance values which will cause the circuit to operate in a desired fashion. In this latter case, the resistors work in

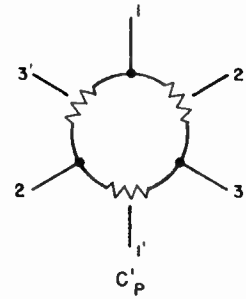


Fig. 8—Network $C_{P'}$.

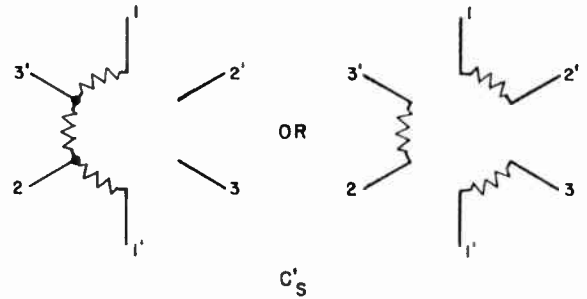


Fig. 9—Two possible forms of network $C_{S'}$.

pairs and each interacts strongly with one another. Thus, each of the three pairs of resistors can take on an infinite number of paired values.

If negative resistances are used in the resistance networks, calculations indicate that the forward loss can be reduced to zero while the infinite reverse loss is maintained.

Thus it is possible to cause a circulator to operate with any value of B field from zero to as high a field as is attainable. This has been demonstrated with an n -type Ge circulator which, with $B = B_0$, requires a load impedance $z_L = 220 \Omega$. So $y_L = 1/220 = 4.55$ millimhos. The measured admittances plotted in Fig. 5 were used in (15) and (17) to calculate values of k . These k values, along with the experimentally determined k 's, are plotted in Fig. 10 as the k_6 curve. Considering the amount of numerical calculation involved, the agreement is quite close. The solid k_3 curve was calculated in a similar manner for the symmetrical $C_{S'}$. The expression is

$$k = \frac{3[U_F^2 - U_R(1 + U_L)]}{U_R + U_L - 2U_F + 1} \quad (22)$$

The square points for magnetic fields of less than B_0 give measured values of k_3 in $C_{P'}$. The solid L_F curve was calculated from (18) for $B < B_0$, and (20) for $B > B_0$. The points represent experimentally determined values. B_0 is the field at which this n -type Ge circulator operates with no parallel network (14.5 kg in this instance).

(See the Appendix for a calculation of a lower bound on the forward loss.) The preceding analysis has dealt with the case of constant load admittance and varying B field. Likewise, the circulator can be made to operate with either increased or decreased load admittance and

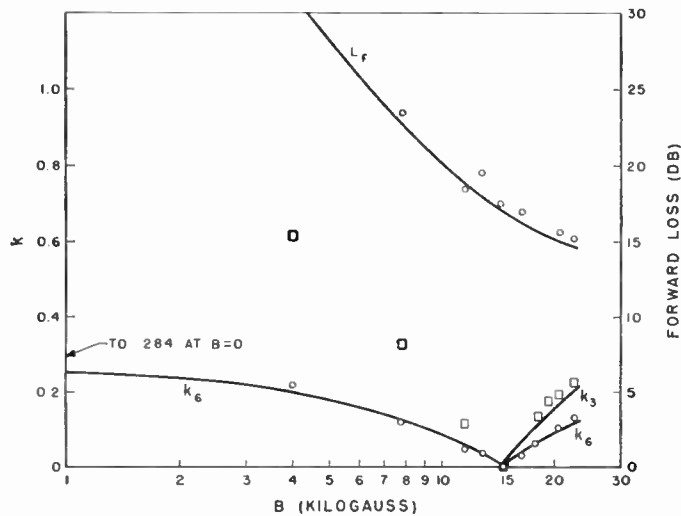


Fig. 10—Variation of L_F (forward loss) and k_3 and k_6 (normalized admittances of three-resistor and six-resistor network elements, respectively) with magnetic field; reverse loss is maintained theoretically at infinity.

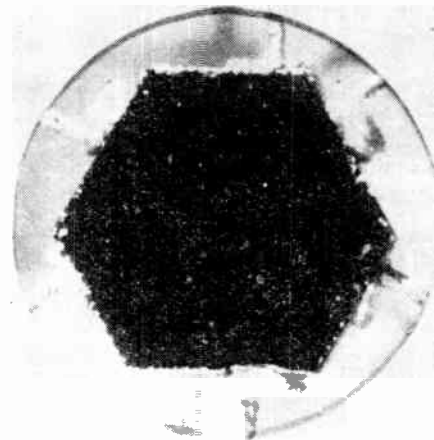
the same B field; e.g., $B = B_0$. This is accomplished by varying the value of k . However, the impedance at the terminals is nearly constant in this case. Therefore, although the loads are such as to allow the circulator to function properly, there is considerable power loss due to the admittance mismatch. Nevertheless, this is a desirable method of "tuning" the admittance level of the device. If y_L is not very different from y_S , the increased forward loss will be negligible. This procedure is immensely more practical than attempting to maintain accurate control over the thickness and resistivity of the sample. Furthermore, the use of a parallel network removes the need for accurate placement of terminals.

This last sentence refers to the fact that asymmetrical circulators can be made symmetrical with the addition of a resistance network. Likewise, an essentially symmetrical circulator can be made to appear asymmetrical in some desired manner to permit the use of different load admittances at the three terminal pairs. It will be remembered that additional loss is experienced when this is done, but it might still be desirable in some instances.

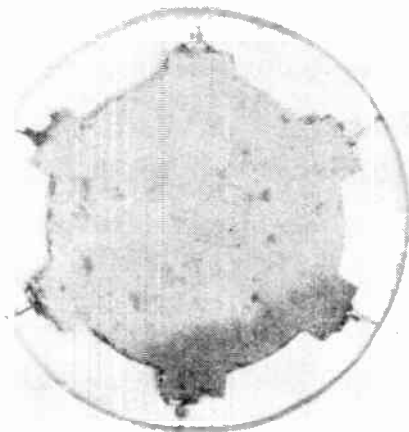
METHOD OF CONSTRUCTION

The degree of balance which a circulator will afford is dependent almost exclusively on the geometric placement of the six terminals. Therefore, considerable effort has been devoted to finding a "foolproof" method of achieving a regular 60° angular spacing between adjacent terminal centers.

The circulators made to date have been made from a single ingot of n -type Ge ($\rho = 6$ to 7 ohm-cm). The sample thicknesses have been 20 to 40 mils, and they have been oriented so that the magnetic field is perpendicular to the (100) plane. Sample diameters have been about 0.125 inch.



(a)



(b)

Fig. 11—Examples of poor (a) and excellent (b) germanium circulator samples, with bonded gold wires.

The first sample was made by thermo-compression bonding³ a gold wire to each of the six faces of an approximately hexagonal slab. The spacing of the terminals was so irregular that the results were very poor, with no parallel network.

Subsequent circulators were made from samples cut with an ultrasonic cutter. These samples have six projections which lend themselves to being electroplated with antimony-doped gold without getting any plating on any of the rest of the surface. This plating was then alloyed into the pips and small balled gold wires were thermo-compression bonded to the centers of the plated surfaces. This technique produced quite symmetrical circulators.

The results of using these two different methods are shown in Fig. 11.

Most of the experimental work has been done in a four-inch Varian electromagnet, but the device will

³ O. L. Anderson, H. Christensen, and P. Andreach, "Technique for connecting electrical leads to semiconductors," *J. Appl. Phys.*, vol. 28, p. 923; August, 1957.

ultimately be used with a relatively small permanent magnet.

PRACTICAL LIMITATIONS

Assuming external stray reactances can be made negligibly small if proper care is taken in the design and use of the device, the speed of response will be limited only by the properties of the semiconductor material. That is, all the circulator admittances are pure conductances; consequently, the loads should also be pure conductances. This accounts for the fact that, theoretically, the circulator should function properly over the entire frequency range from dc up to the dielectric relaxation frequency of the material, which is of the order of a few kmc in the Ge used in these experiments. Unfortunately, the sample geometry requires that all leads be fairly close to one another, so radiation and pickup will undoubtedly place a lower practical limit on the usable frequency range. Skin effect will probably become important at high frequencies, also. These practical limitations have not yet been determined.

If the Hall effect circulator is used in an atmosphere whose temperature is not kept constant, both μ_n (the electron mobility) and B , (and thus θ_H), will depend somewhat on temperature. It is hoped that the following condition can be obtained:

$$\frac{\partial \mu_n}{\partial T} \approx - \frac{\partial B}{\partial T} \quad (23)$$

so that

$$\frac{\partial \theta}{\partial T} \approx \frac{\partial(\mu_n B)}{\partial T} \approx 0 \quad (24)$$

where T is temperature.

Impedance levels from 200 to 600 ohms have been attained on various samples, and it should be fairly simple to extend this range to 10 to 5000 ohms, still using only *n*-type Ge. With InAs and InSb, the low end of this range could be brought down to about 0.05 ohm. Of course, to be usable such a circulator would require extremely low resistance contacts. The use of high-mobility materials (*e.g.*, InSb, InAs, HgSe) would permit one to operate with smaller permanent magnets; however, circulators made of such materials would have extremely low impedance levels (perhaps on the order of the one-ohm) and would not be useful in most circuits.

One tremendous advantage this device has over most semiconductor devices is that it has no junctions. Because of this, its lifetime will probably depend only on the stability of the permanent magnet used. It requires no special atmosphere for good operation. If extremely thin samples were used, surface effects would play a more important role and special housings might be necessary.

The contacts, of course, must be ohmic. If not, their resistance will vary with current level, and so will the admittance of the device. As a consequence, the circu-

lator would be balanced only for one particular signal level.

CONCLUDING REMARKS

It is possible to make three-port nonreciprocal Hall effect devices which will circulate dc and ac signals either in a clockwise or counterclockwise sense. With the aid of simple six-resistor networks (or even simpler three-resistor networks) the nine short-circuit admittance parameters of the circulator can be adjusted in a calculable manner. Incidentally, the corresponding parameters of any six-terminal circuit or black box could be adjusted in a similar manner without changing anything inside the three-port box. Modified forms of the parallel circuits might prove useful in conjunction with circuits with more or less than three ports. It should be remembered that the admittance equations would be equally valid for the case of complex admittances. In Hall effect circulators, an almost unlimited number of tricks must be possible. We have seen that such circulators can be made to operate at any desired impedance level, can be made to operate with any desired magnetic field, and can be made to introduce no loss—or even gain—if one uses negative resistances.

Circulators could be used in place of the hybrid coils in two-way, two-wire amplifiers. However, the 17 db forward loss will undoubtedly prevent them from being used in this way except, possibly, at frequencies above and below the usable frequency range of hybrid coils.

A circulator permits a transmitter and receiver to use a common antenna simultaneously if the circulator's losses are acceptable.

A circulator's sensitivity to variations in load impedance suggests its possible use as an impedance measuring device. In this case, it would measure the power reflected from a load, giving an indication of amount of impedance mismatch.

Probably the most important applications of circulators have yet to be devised. They have not made themselves evident previously because of the absence of circulators for "wire" frequencies. Whoever discovers such an application must not be discouraged by the circulator's high forward loss and its possible sensitivity to ambient temperature variations, and he must take advantage of the circulator's unique property: nonreciprocity.

APPENDIX

A LOWER BOUND ON FORWARD LOSS

At $B = B_0$, L_F is about 17.5 db. As the flux density is increased beyond B_0 , L_F is decreased and asymptotically approaches a value corresponding to the maximum Hall angle which is theoretically possible.

To evaluate this minimum L_F , it will be advantageous to start with the open-circuit impedances (rather than the short-circuit admittances). When a voltage is applied to one of the three-terminal pairs with the other terminals open-circuited, the magnitudes of the two out-

put voltages will approach (but not exceed) the input voltage as $B \rightarrow \infty$. Thus, let us assume

$$\lim_{B \rightarrow \infty} |z_R| = \lim_{B \rightarrow \infty} |z_F| = \lim_{B \rightarrow \infty} |z_S| = z_\infty \quad (25)$$

where z_R , z_F , and z_S are the three open-circuit impedances (defined in a manner analogous to that used for y_R , y_F , and y_S) of a symmetrical circulator. Measured values of these impedances are plotted against B for an n -type Ge circulator in Fig. 12. It can be seen from this figure that, in the limit of very large B , (25) leads to the result that

$$z_R = -z_F = z_\infty. \quad (26)$$

With these impedance values, a simple calculation yields the following admittances:

$$y_S = y_F = \frac{1}{2z_\infty} \quad (27)$$

$$y_R = 0$$

which, when normalized, yield

$$U_S = \frac{y_S}{y_S} = U_F = 1$$

$$U_R = 0. \quad (28)$$

Substituting (27) and (28) in (17) gives for the condition for circulator action

$$k = 1 - U_L + \sqrt{(1 - U_L)^2 + 4}. \quad (29)$$

Requiring that the load admittance equal the input admittance gives

$$U_L = 1 + k + \frac{\left(1 + \frac{k}{2}\right)^3 + \left(\frac{k}{2}\right)^3 - k\left(1 + \frac{k}{2}\right)(1 + k + U_L)}{(1 + k + U_L)^2 - \frac{k}{2}\left(1 + \frac{k}{2}\right)}. \quad (30)$$

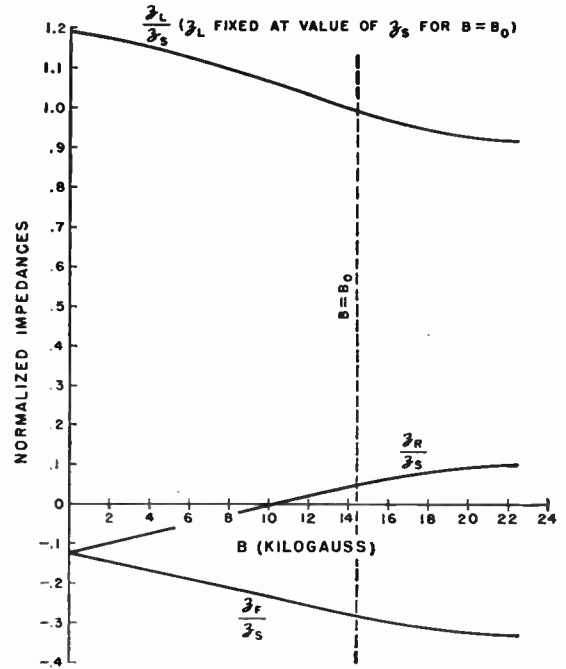


Fig. 12—Variation of open-circuit impedances with magnetic field.

Solving (29) and (30) simultaneously tells one that

$$U_L = 2.00$$

and

$$k = 1.24. \quad (31)$$

Using the values given in (28) and (31), one calculates the lowest possible forward loss for this type circulator to be 8.4 db.

ACKNOWLEDGMENT

The author wishes to express his appreciation for W. A. Taylor's assistance in preparing samples and making measurements.

Theory of the Crestatron: A Forward-Wave Amplifier*

J. E. ROWE†, MEMBER, IRE

Summary—In the past a considerable amount of experimental evidence presented by various workers has indicated that gain apparently occurs in a traveling-wave type device even though the voltage may be so high that growing waves cease to exist. This means, in terms of Pierce's traveling-wave tube theory, that the growth constant of the growing wave x_1 is zero in this regime of operation. A theory explaining this phenomenon has been worked out and both small-signal and large-signal calculations have been carried out to investigate the characteristics of this type of operation. The gain occurs in this region due to a beating effect produced between the three small-signal forward waves described in traveling-wave tube theory as they travel along the RF structure. The maximum achievable gain is determined by the injection velocity and not by the length of the tube as in the normal case. Based on the above theory a device named the *Crestatron*, which utilizes this new mode of operation, has been built and tested to verify the theory, and it has been found that moderate gain (10–20 db) and high operating efficiency coupled with a very short length (4–6 wavelengths) characterize this mode of operation.

LIST OF SYMBOLS

- $b = u_0 - v_0 / C v_0$ = injection velocity parameter
 C = gain parameter
 d = loss parameter
 F = helix impedance reduction factor
 f = frequency
 I_0 = dc stream current
 \bar{i} = RF convection current in the beam
 K_s = sheath-helix impedance
 K_s' = normalized sheath-helix impedance
 N = structure length in wavelengths
 QC = space-charge parameter
 u_0 = stream velocity
 V = input RF voltage amplitude
 V_{ci} = circuit component of wave amplitude
 V_i = wave-voltage amplitude
 V_0 = dc stream voltage
 \bar{v} = RF velocity in the beam
 v_0 = circuit characteristic wave-phase velocity
 z = distance measured from the input
 $\beta = \omega / v$ = wave-phase constant
 $\beta_c = \omega / u_0$ = stream-phase constant
 Γ = wave-propagation constant in the presence of the beam
 $\delta_i = x_i + jy_i$ = wave-incremental propagation constant
 η = charge-to-mass ratio of the electron
 η_s = saturation efficiency
 $\theta = 2\pi CN$ = radian length of the tube
 λ_0 = guide wavelength
 λ_s = stream wavelength
 ω = angular frequency.

INTRODUCTION

IT IS well known that the operation of backward-wave devices, both O-type and M-type, depends on an interference phenomenon resulting from the beating between waves propagating along an RF structure. It can also be shown that in forward-wave devices, such as the traveling-wave amplifier, gain can occur due to the beating of waves traveling on the RF structure, providing the length is correct. The maximum achievable gain for any given set of circuit and operating parameters is determined by the relative injection velocity b rather than by the length of the tube as in the case of the conventional traveling-wave amplifier.

In order to clarify the principles and verify the theory proposed, a device, called the Crestatron, was designed and built to operate on the beating-wave principle. Measurements of gain on short-length tubes have indicated a substantial agreement with the theory. Theoretical calculations have also been correlated with measurements taken at other laboratories and very excellent agreement is obtained.

A voltage gain is produced in the Crestatron by a beating between the three forward waves propagating on the slow-wave structure. The device is operated with a beam velocity such that $b > b_{x_1=0}$ and, hence, there are no growing waves. The gain is achieved by adjusting the tube length to the proper value such that all the waves, one of which is out of phase with the others at the input, add together to give an RF voltage greater than that at the input. Hence there is not voltage gain in the sense of that produced by growing waves, but there is gain if the tube is considered to be a two-port network. The amount of gain is determined by the value of b and decreases as the beam velocity is raised above that at which growing waves cease to exist. The gain characteristics of the Crestatron can be calculated from the small-signal theory and these calculations also give information on the CN bandwidth ($\theta = 2\pi CN$) achievable in the device.

The large-signal theory of traveling-wave amplifiers¹ has been used to evaluate the nonlinear performance of the phenomenon as represented by the Crestatron in terms of the achievable gain and the expected operating efficiency.

Ample experimental evidence² has already been offered in this and other laboratories to verify the theory and indicate that high efficiency is obtained with short-

* Original manuscript received by the IRE, October 31, 1958. Revised manuscript received, December 22, 1958. The work was supported by the Rome Air Dev. Center, Griffiss Air Force Base, Rome, N. Y., under Contract No. AF 30(602)-1596 and AF 30(602)-1845.

† Dept. of Elec. Eng., University of Michigan, Ann Arbor, Mich.

¹ J. E. Rowe, "A large-signal analysis of the traveling-wave amplifier: theory and general results," IRE TRANS. ON ELECTRON DEVICES, vol. ED-3, pp. 39–56; January, 1956.

² J. J. Caldwell and O. L. Hoch, "Large-signal behavior of high power traveling-wave amplifiers," IRE TRANS. ON ELECTRON DEVICES, vol. ED-3, pp. 6–18; January, 1956.

length and moderate gains. During the course of this work it was learned that Mourier and Sugai had shown that a similar type of operation is possible with the forward-wave magnetron amplifier.³ They treated the special case of small C , no space-charge and zero-circuit loss. These conditions in the magnetron amplifier give rise to two forward-traveling waves which under certain conditions can beat with one another to produce gain.

DERIVATION OF THE GAIN EQUATION

The three forward waves propagating on a traveling-wave tube RF structure are known to vary in the following manner:⁴

$$e^{-\Gamma z} = e^{-j\beta z} \cdot e^{\beta C \delta z}, \tag{1}$$

where β is the wave phase constant and is equal to β_c at synchronism. The normalized voltage V_z/V at any point along the RF structure may be written in terms of the amplitudes of the three waves, neglecting space charge, as

$$\frac{V_z}{V} = e^{-j(\theta/C)} \left[\frac{V_1}{V} e^{\delta_1 \theta} + \frac{V_2}{V} e^{\delta_2 \theta} + \frac{V_3}{V} e^{\delta_3 \theta} \right] \tag{2}$$

where

- $\delta_i = x_i + jy_i, i = 1, 2, 3,$
- $V_i/V =$ normalized voltage amplitude of each wave,
- $\theta = \Delta\beta Cz = 2\pi CN,$
- $N =$ structure length in wavelengths, and
- $C =$ gain parameter.

From the small-signal theory of the traveling-wave tube, the following expressions for the RF convection current and velocity are obtained by retaining terms proportional to C :

$$\frac{(1 + jC\delta_1)}{\delta_1} V_1 + \frac{(1 + jC\delta_2)}{\delta_2} V_2 + \frac{(1 + jC\delta_3)}{\delta_3} V_3 = \left(\frac{j u_0 C}{\eta} \right) \bar{v} \tag{3}$$

and

$$\frac{(1 + jC\delta_1)}{\delta_1^2} V_1 + \frac{(1 + jC\delta_2)}{\delta_2^2} V_2 + \frac{(1 + jC\delta_3)}{\delta_3^2} V_3 = \left(\frac{-2V_0 C^2}{I_0} \right) \bar{i}, \tag{4}$$

where

- $\eta = e/m,$ charge-to-mass ratio of the electron,
- $\bar{v} =$ RF velocity in the stream,
- $\bar{i} =$ RF convection current in the stream,
- $V_0 =$ dc stream voltage, and
- $I_0 =$ dc stream current.

If an unmodulated stream is injected at $z=0$ and an RF signal level V is applied to the RF structure at that point, the boundary conditions require that the right-hand sides of (3) and (4) be zero and that

$$V = V_1 + V_2 + V_3. \tag{5}$$

Eqs. (3), (4) and (5) may be solved simultaneously to give the normalized amplitudes of the individual waves. The general result is

$$\frac{V_i}{V} = \left[1 + \frac{1 + jC\delta_i}{1 + jC\delta_{i+1}} \left(\frac{\delta_{i+1}}{\delta_i} \right)^2 \frac{\delta_{i+2} - \delta_i}{\delta_{i+1} - \delta_{i+2}} + \frac{1 + jC\delta_i}{1 + jC\delta_{i+2}} \left(\frac{\delta_{i+2}}{\delta_i} \right)^2 \frac{\delta_i - \delta_{i+1}}{\delta_{i+1} - \delta_{i+2}} \right]^{-1}, \tag{6}$$

where $\delta_i \equiv \delta_{i+3}$. Eq. (6) gives the total voltage associated with each wave and in the absence of space charge also gives the circuit voltage. The effect of passive modes or space charge is to reduce the circuit voltage from the value predicted by (6). The ratio of the circuit voltage to the total voltage is found from the ratio of the second term on the right-hand side of the following familiar quartic determinantal equation to the total right-hand side⁵ of (6):

$$\delta^2 = \frac{(1 + jC\delta)^2 [1 + C(b - jd)]}{\left[-b + jd + j\delta + C \left(jbd - \frac{b^2}{2} + \frac{d^2}{2} - \frac{\delta^2}{2} \right) \right] - 4QC(1 + jC\delta)^2}. \tag{7}$$

The general result for the circuit component of voltage is

$$\frac{V_{ci}}{V_i} = 1 + 4QC \frac{(1 + jC\delta_i)^2}{\delta_i^2}. \tag{8}$$

Eqs. (6) and (8) have been obtained by Brewer and Birdsall.⁶

Thus the voltage along the RF structure, including the effects of finite C and space charge QC , generally may be written as

$$\frac{V_z}{V} = e^{-j(\theta/C)} \sum_{i=1}^3 \left(\frac{V_i}{V} \right) \left(\frac{V_{ci}}{V_i} \right) e^{\delta_i \theta}, \tag{9}$$

where $\delta_i \equiv \delta_{i+3}$. When C is small and the effect of passive modes or space charge is negligible, (6) and (8) reduce to the following familiar form:

$$\frac{V_i}{V} = \frac{\delta_i^2}{(\delta_i - \delta_{i+1})(\delta_i - \delta_{i+2})} \tag{10}$$

and

$$\frac{V_{ci}}{V_i} = 1. \tag{11}$$

⁵ *Ibid.*, p. 113, eq. (7.13) with corrections.

⁶ G. R. Brewer and C. K. Birdsall, "Normalized Propagation Constants for a Traveling-Wave Tube for Finite Values of C ," Tech. Memo. No. 331, Hughes Res. and Dev. Labs., Culver City, Calif.; October, 1953.

³ G. Mourier and I. Sugai, private communication.

⁴ J. R. Pierce, "Traveling-Wave Tubes," D. Van Nostrand Co., Inc., New York, N. Y.; 1950.

The voltage gain is written as

$$G_{\text{db}} = 10 \log \left(\frac{V_z V_z^*}{V V^*} \right) = 10 \log \left| \left(\frac{V_z}{V} \right)^2 \right|. \quad (12)$$

It is important to note that, unlike conventional standing waves on a transmission line, each wave sees the RF structure characteristic impedance at all points along the line.

The gain that occurs when the velocity parameter b is greater than that for which the growth constant of the growing wave is zero is, as mentioned before, due to a beating effect between the three small-signal waves which are set up at the input and propagate along the RF structure. The energy taken from the stream in this type of operation goes into setting up the three forward-circuit waves at the input, and then these waves propagate with different velocities and constant amplitude along the RF structure. The gain occurs due to the eventual adding in phase of the two larger waves. The interaction is primarily between the circuit wave and the slow space-charge wave. It will be seen later that the fast space-charge wave is excited to a negligible extent. This is the same basic mode of operation as in the backward-wave device of both the traveling-wave tube and crossed-field types. As the three waves travel along the structure, the phase relationship between the RF current in the beam and the RF field on the circuit changes, and at certain points along the circuit the phase is such that energy is transferred to the circuit. At the same time there are certain regions along the tube where the phase relationship between the beam current and the circuit field is such that energy is fed from the circuit back to the beam. The realizable gain in this mode of operation depends upon the relative injection velocity b for any given set of tube parameters rather than on the length as in the case of the conventional traveling-wave tube.

A forward-wave embodiment of the beating phenomenon, such as the Crestatron, is inherently more efficient than the backward-wave devices which operate on the same beating principle because the modulation in the stream and the field on the circuit producing the modulation travel in the same direction, whereas in the backward-wave device the modulation in the beam and the circuit field travel in opposite directions. In the backward-wave device the circuit field is strongest where the modulation is weakest and vice versa.

Mathematically speaking, all the energy is abstracted from the beam at the input since in satisfying the boundary conditions energy is put into setting up the three circuit waves. Then the circuit length is simply adjusted so that at the end of the tube the wave energies all add in phase. It should be recalled that in this region of operation the propagation constants are purely imaginary, giving rise to real voltage amplitudes, and at the input one voltage component is 180° out of phase with the other two.

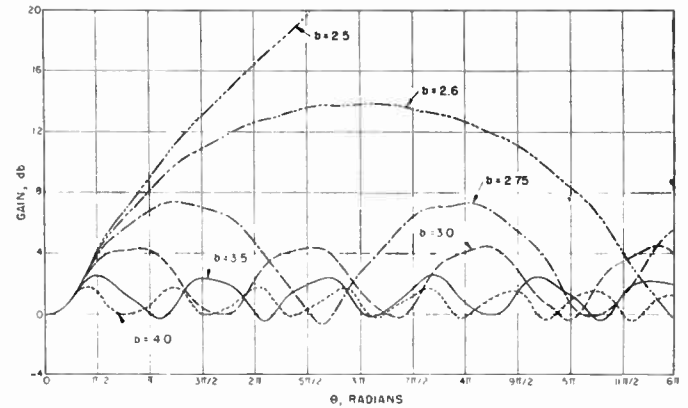


Fig. 1—Gain vs length ($C=0.1$, $QC=0.25$, $d=0$, $b_{x_1=0}=2.57$).

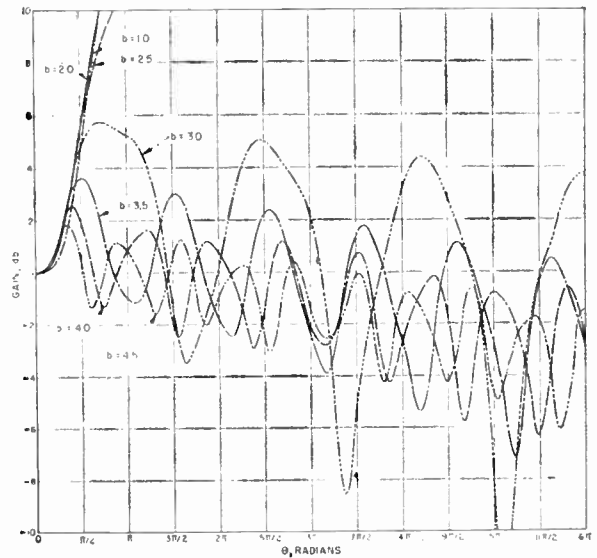


Fig. 2—Gain vs length ($C=0.2$, $QC=0.125$, $d=0.025$, $b_{x_1=0}>3.0$).

SMALL-SIGNAL GAIN

It was pointed out above that the normalized voltage amplitudes are purely real since the propagation constants are purely imaginary when $b > b_{x_1=0}$. For fixed values of C , QC , and d the gain may be calculated from (9) and (12) as a function of θ for particular values of b . Typical gain curves are shown in Figs. 1 and 2. The above gain equations are valid for all values of b , and it is seen from the figures that the normal exponential gain is obtained when $x_1 \neq 0$. The gain curves were plotted over a range of 6π radians to indicate their repetitive nature. In Fig. 2 it is seen that the effect of circuit loss is to reduce the gain, particularly for large θ .

The results plotted in Fig. 2 do not show the large negative dip in the gain curve for $b=0$ that Brewer and Birdsall⁷ found. The fact that they assumed a $QC=0.25$ whereas the above data are for $QC=0.125$ is of little consequence to this discrepancy. It is believed that their results are incorrect, since to compute gain they used the

⁷ G. R. Brewer and C. K. Birdsall, "Traveling-wave tube propagation constants," IRE TRANS. ON ELECTRON DEVICES, vol. ED-4, pp. 140-144; April, 1957 (Fig. 2).

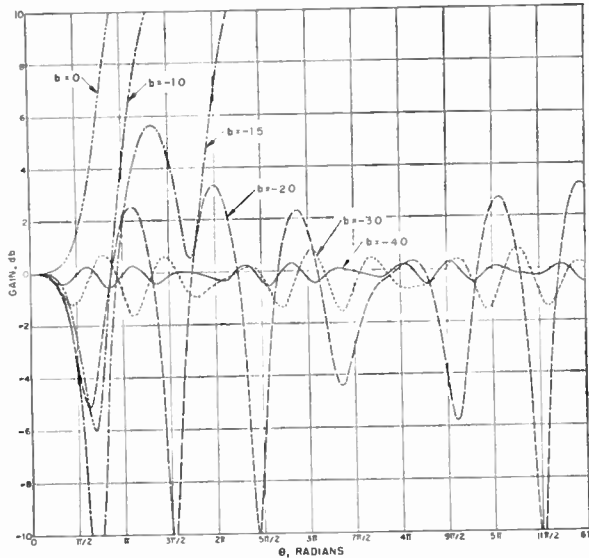


Fig. 3—Gain vs length ($C=0.1$, $QC=0.125$, $d=0$, $b_{x1=0}=2.34$).

small- C equations, which are not valid when $C=0.2$ and $QC=0.25$. It should be pointed out, as is predicted here, that only very small dips in the gain curves were noted in the large-signal calculations. Large negative dips in the gain seem to occur at $b = -1$ for most values of C and QC and for positive values of b when d is large.

The gain curves of Fig. 3 show that gain is also achieved for negative values of b such that $x_1=0$. Negative values of b correspond to operating voltages less than the synchronous voltage, and the resulting gains are less than those obtained with large values of b .

When the loss parameter is zero all maxima of the gain curve are approximately equal (the slight variations and lack of periodicity will be explained later), but when $d \neq 0$ the first maximum will be highest and subsequent peaks will generally be lower. This merely emphasizes the fact that when circuit loss is significant the tube length should be chosen so as to operate on the first maximum of the gain curve. Because of the relatively low gain of the Crestatron a large attenuator like those used in ordinary traveling-wave amplifiers is not necessary.

It is seen from the gain curves that for fixed b and variable θ the curves are nonperiodic within the interval 6π and exhibit periodic undulations in amplitude. The explanation of this phenomenon for voltage amplitude vs distance is contained in (9). The lack of periodicity with 2π and the undulating peak amplitudes are a result of the product of $\exp(-j\theta/C)$ and $\exp(\delta_i\theta)$, where each represents a vector rotating about the origin as a function of θ . The rate of rotation of the first vector is related to $1/C$, which is typically between 5 and 20, and the rate of rotation of the second is determined by δ_i , which varies between 1 and 3. The first, then, perturbs the second as a modulation, and the fact that δ_i is non-integral in general means that it is not periodic with 2π . It may be that θ must travel through $2m\pi$ radians with

m very large before a periodicity is apparent, if ever.

The above phenomenon indicates that there is something more than a simple beating effect occurring between the waves. In fact there is a continual slipping of one wave with respect to the others along the RF structure. This process accounts for the fact that there is or may be a net interchange of energy between the beam and the circuit in a device of infinite length. It is interesting to examine the condition necessary for the gain curve to be periodic with period $2m\pi$ and also the condition required for the peak amplitudes to be constant. In fact these two conditions would result in a gain curve that is exactly reproduced every 2π radians.

For V_z/V in (9) when b is held fixed, the phase condition is determined by the product

$$e^{-j(\theta/C)} \cdot e^{\delta_i\theta} = e^{j\theta(y_i-1/C)}, \tag{13}$$

since $x_1=0$. Thus in order for the phase to be periodic with $2m\pi$,

$$n\left(y_i - \frac{1}{C}\right) = 2m\pi. \tag{14}$$

Solving for y_i gives

$$y_i = \frac{2m\pi}{n} + \frac{1}{C}, \tag{15}$$

where n and m are independent integers. Thus for phase periodicity the value of y_i must be equal to a constant plus some integral or subintegral multiple of 2π . When $C \rightarrow 0$, $y_i = 1/C$ and all the waves travel at approximately the same rate, they maintain the same relative phase positions with respect to one another. This results in a constant-amplitude vector rotating about the origin with a period of 2π radians. Thus the gain curve will be periodic in amplitude also.

Under very restricted conditions a simplified expression for the gain of the tube may be obtained from (9). When $C \rightarrow 0$, $QC=0$, $d=0$, and b is sufficiently large that the propagation constants are purely imaginary, it can be determined that the δ_i 's are given approximately by

$$\delta_1 \approx -j/b^{1/2},$$

$$\delta_2 \approx -jb,$$

and

$$\delta_3 \approx j/b^{1/2}. \tag{16}$$

Substitution of (16) into (9) yields for the gain, after some simplification,

$$\left|\frac{V_z}{V}\right|^2 = \left(\frac{1}{1-b^3}\right)^2 \left[1 + b^6 + (b^3 - 1) \sin^2 \frac{\theta}{b^{1/2}} - 2b^3 \left\{ \cos \theta b \cos \frac{\theta}{b^{1/2}} + b^{3/2} \sin \theta b \sin \frac{\theta}{b^{1/2}} \right\} \right]. \tag{17}$$

Since b is usually greater than 2.5, (17) can be simplified further to

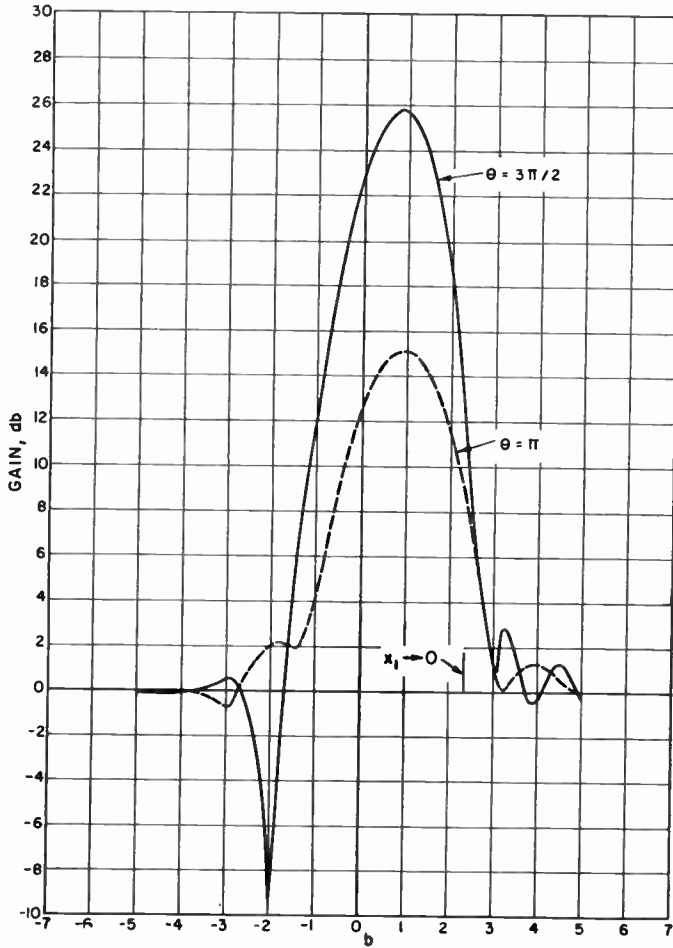


Fig. 4—Gain vs injection velocity for fixed tube length ($C=0.1, QC=0.125, d=0$).

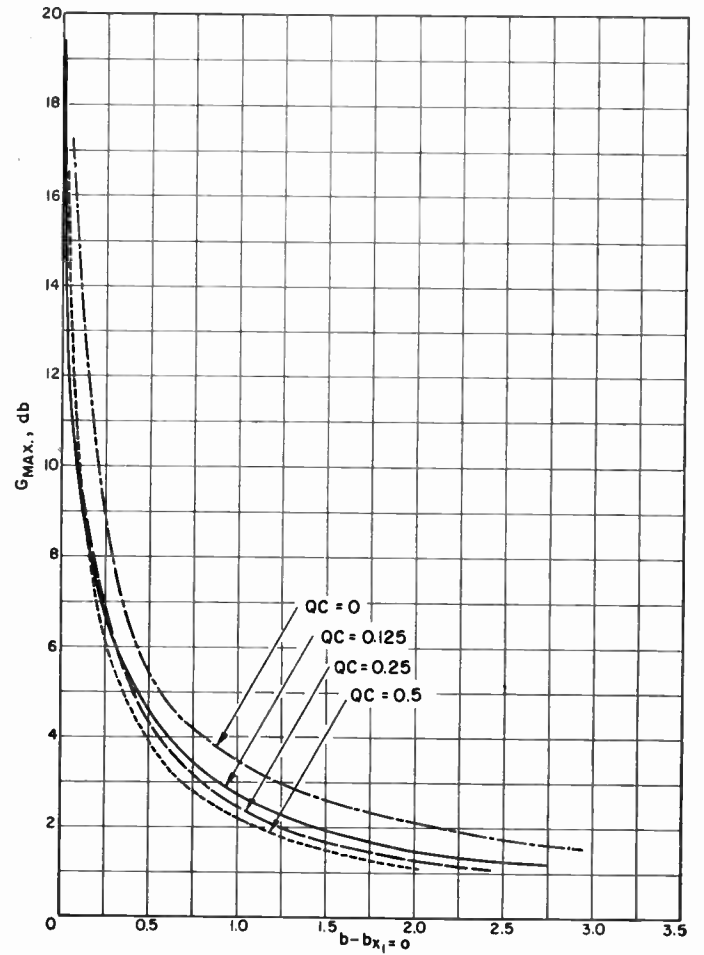


Fig. 5—Maximum gain vs $b - b_{x_1=0}$ with space charge as the parameter ($C=0.1, d=0$).

$$\left| \frac{V_z}{V} \right|^2 = 1 + \frac{1}{b^3} \left[\sin^2 \frac{\theta}{b^{1/2}} - 2 \cos \theta b \cos \frac{\theta}{b^{1/2}} + b^{3/2} \sin \theta b \sin \frac{\theta}{b^{1/2}} \right]. \quad (18)$$

A useful expression for predicting the value of CN at the first maximum of the gain curve may be obtained by differentiating (17) with respect to θ and setting the result equal to zero. In this way

$$\sin \frac{\theta}{b^{1/2}} \left[\cos \frac{\theta}{b^{1/2}} - b^3 \cos \theta b \right] = 0. \quad (19)$$

Thus maxima and minima in the gain occur for

$$\sin \frac{\theta}{b^{1/2}} = 0$$

or

$$CN = \frac{nb^{1/2}}{2} \quad n = 0, 1, 2, \dots \quad (20)$$

The other condition is

$$\cos \theta b = \frac{\cos \frac{\theta}{b^{1/2}}}{b^3} \approx 0 \text{ for large } b$$

or

$$CN = \frac{2n + 1}{4b}, \quad n = 0, 1, 2, \dots \quad (21)$$

Eq. (21) predicts quite accurately the distance to the first maximum in the gain curve when $n=1$. Thus

$$CN \text{ to first maximum} = \frac{0.75}{b}. \quad (22)$$

Eqs. (20) and (21) coupled with information on the second derivative of the gain curve may be used to determine subsequent maxima in the gain vs θ curve.

In addition to gain vs length curves for fixed b , a set of gain curves may be obtained for fixed tube length with variable voltage or b . Typical curves of this type are shown in Fig. 4. The main hump in the gain curve vs b is of course due to exponential gain, and the other lower peaks correspond to gain through beating waves. When $C \rightarrow 0, QC=0$ and $d=0$ the gain vs b curve will

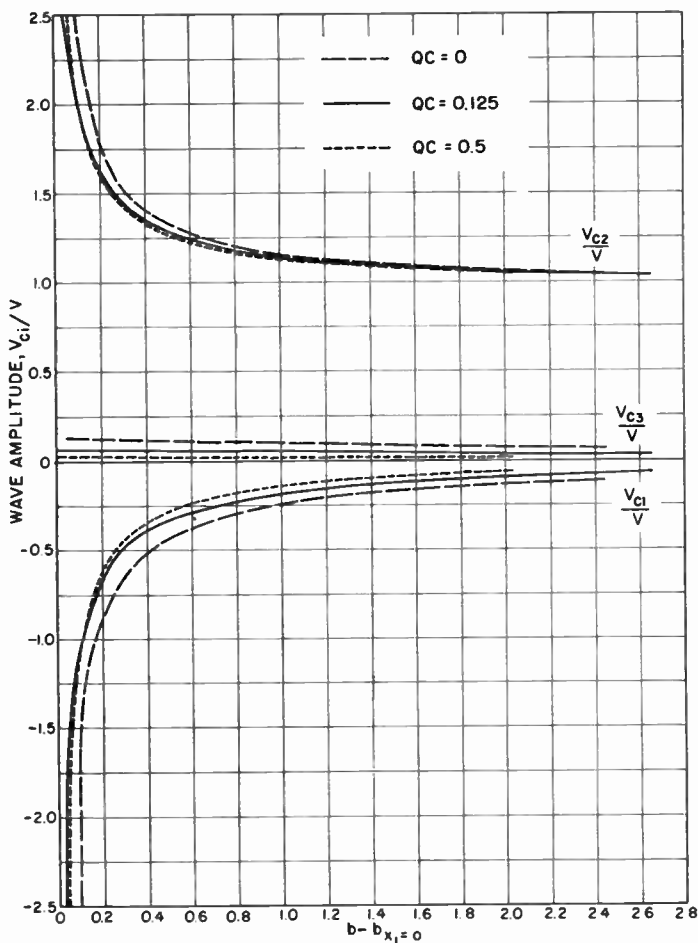


Fig. 6—Normalized amplitudes of the wave voltages vs injection velocity ($C=0.1, d=0$).

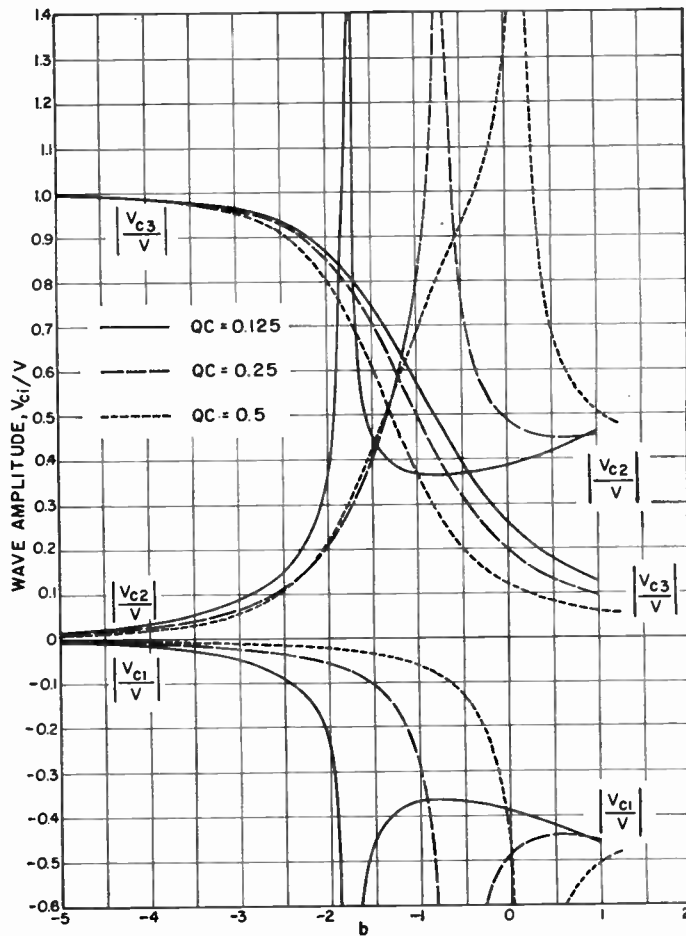


Fig. 7—Normalized amplitudes of the wave voltages vs injection velocity ($C=0.1, d=0$).

be symmetrical with respect to b since maximum exponential gain occurs at synchronism.

BANDWIDTH

The bandwidth of a device operating on the beating-wave principle may be determined from the gain curves shown in Figs. 1 and 2. The CN bandwidth ($\theta = 2\pi CN$) can be as large as ± 50 per cent between 3-db points on the gain curve. If the impedance of the structure remained constant over this range, then the device would have a frequency bandwidth of 3:1. In general, impedance variations will limit this figure to some lower value. Experimental Crestatrons have been built with nearly an octave bandwidth at 3 kmc.

MAXIMUM GAIN VS C AND QC

It was pointed out earlier that the voltages are purely real for $b > b_{x_1=0}$, and at the input one voltage is 180° out of phase with the other two. Thus the maximum gain will occur when the three waves all add in phase. The value of b for which $x_1=0$ can be computed from the quartic determinantal equation. When $d \neq 0$, x_1 is not exactly zero anywhere but does drop to less than one per cent of its maximum value for large b .

Maximum-gain curves for various values of QC when

$C=0.1$ are shown in Fig. 5. The gain decreases with increasing voltage and for very high voltage approaches zero asymptotically. As would be expected the gain increases with C and decreases as QC is increased. The effect of loss on the circuit also reduces the gain. The greatest gain occurs for a b which is equal to that for which growing waves cease to exist. There is a smooth transition from the region of exponentially growing waves to the region in which the gain is a result of the beating of the three waves.

The gain for large positive values of b is a result of the combining of V_{c1}/V and V_{c2}/V , since V_{c3}/V is usually negligible. The magnitudes of these normalized voltages for a typical range of parameters are shown in Fig. 6. For large values of b , it is seen from Fig. 6 that V_{c1}/V approaches zero and V_{c3}/V is still small, so that almost all the energy is in the second wave (circuit wave) V_{c2}/V . On the other hand, for negative values of b (voltage below synchronism), the third wave (fast space-charge wave) V_{c3}/V predominates, as shown in Fig. 7.

A typical plot of the distance to the first maximum of the gain curve is shown in Fig. 8 for several values of space charge. The theoretical relation (22) is also shown.

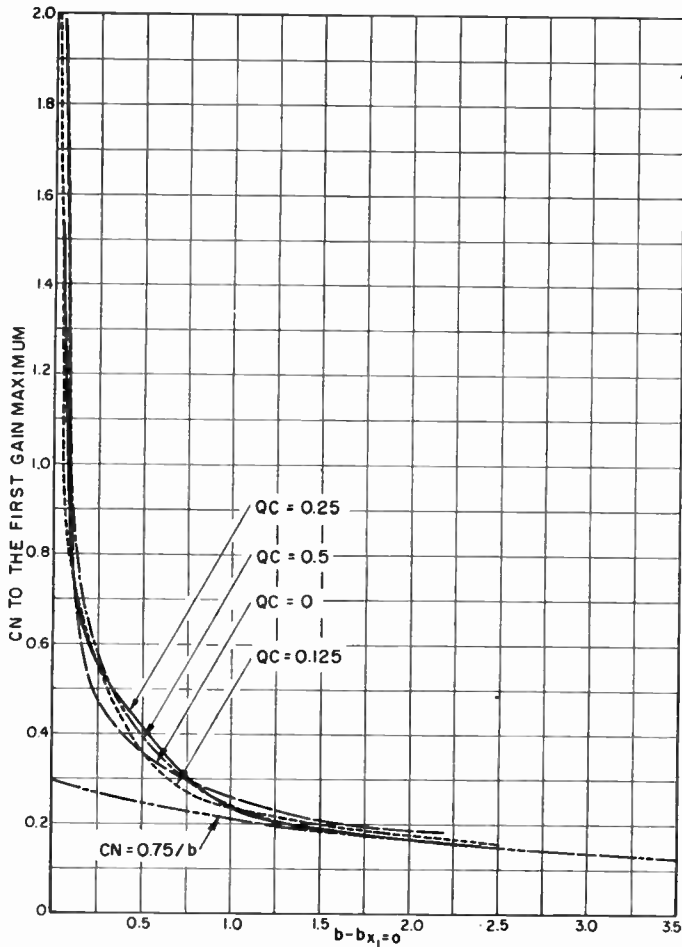


Fig. 8—CN to the first gain maximum vs injection velocity ($C=0.1, d=0$).

LARGE-SIGNAL PERFORMANCE

Saturation Gain

The large-signal performance of a beating-wave device has been evaluated using the large-signal theory of the traveling-wave amplifier.¹ Significant large-signal gain is found for large values of $b > b_{x_1=0}$ when the input-signal level, ψ , is appreciable compared to CI_0V_0 . A typical gain curve is shown in Fig. 9 with the input-signal level to the RF structure as the parameter. A periodicity in the large-signal gain vs distance curves is found similar to that previously shown with the linear theory. The gain is seen to decrease as the drive level is increased, but the power output and efficiency increase as the drive level is increased.

The composite results of the large-signal calculations may be plotted in summary form to show several interesting facets of the nonlinear performance of the Crestatron. As seen in Fig. 10 the "saturation" gain as a function of the drive level to the RF structure goes through a maximum at a value of ψ dependent upon the value of b . It should be noted that the optimum length, *i.e.*, for maximum output, changes as the drive level changes. When the tube is operated at a b value which gives maximum small-signal gain or maximum satura-

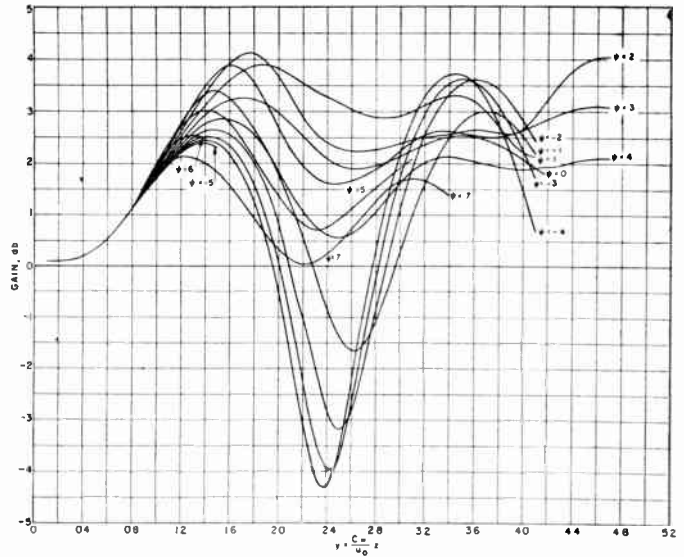


Fig. 9—Theoretical large-signal gain vs length ($C=0.1, QC=0.25, B=1.0, d=0, b=3.5$).

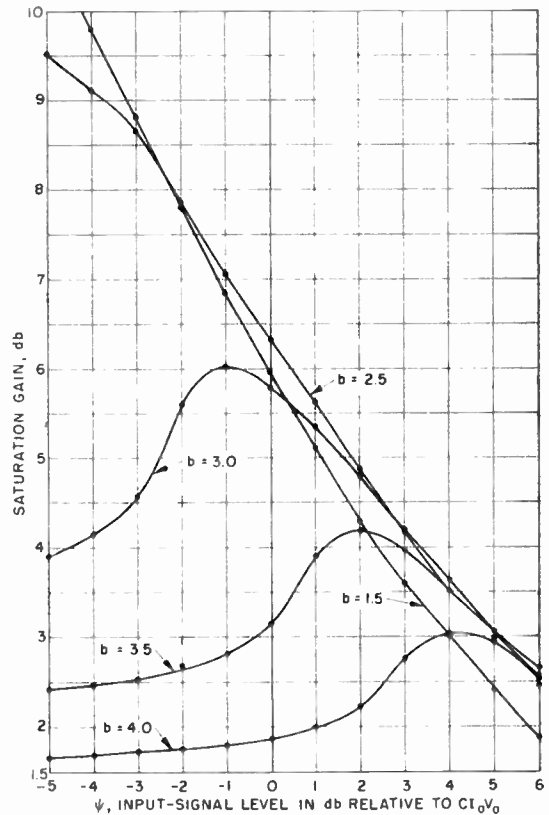


Fig. 10—Theoretical saturation gain vs input-signal level with injection velocity as the parameter ($C=0.1, QC=0.125, B=1, d=0, b_{x_1=0}=2.33$).

tion efficiency, an increase in the drive level results in a smooth transition to the beating-wave type of operation and the gain decreases smoothly. For very high drive levels the gain is low and relatively independent of the injection velocity. This relationship is also in line with that predicted from the linear theory. The value of CN

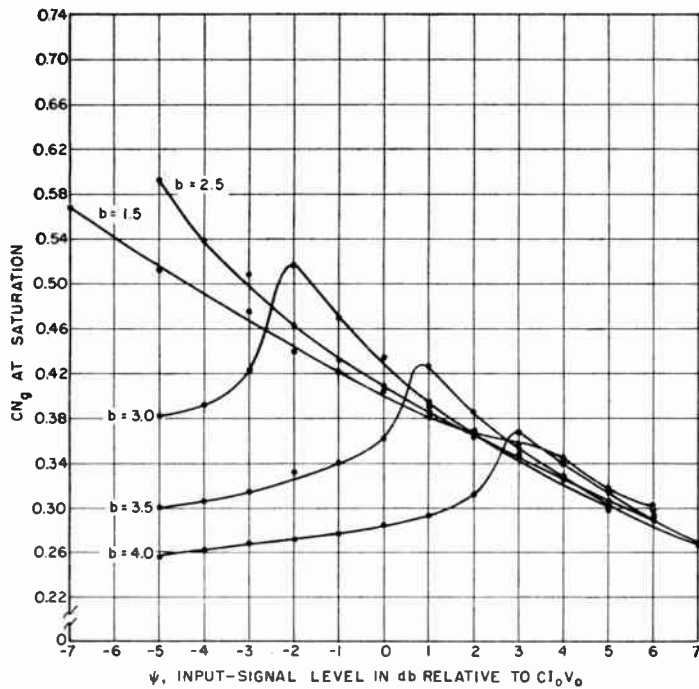


Fig. 11—Theoretical saturation length vs input-signal level with injection velocity as the parameter ($C=0.1, QC=0.125, B=1.0, d=0, b_{x_1=0}=2.33$).

to the first maximum of the gain curve can also be plotted as a function of both the drive level and the value of b as shown in Fig. 11.

A considerable amount of previously unexplained experimental information has been obtained by Caldwell and Hoch² and other workers which verifies the existence of gain in a forward-wave amplifier due to the beating between the waves propagating on the RF structure. A comparison of the calculated gains using the linear and nonlinear theories along with some data extracted from Caldwell and Hoch's paper is presented in Fig. 12. It is seen that the agreement is very good between the theoretical results and the experimental data. Similar experimental data have been obtained in this laboratory which substantiate the theory even more clearly. (It is planned to publish complete experimental data on a series of Crestatrons in a later paper.) Since the value of d was approximately 0.025 for the experimental data, it is difficult to choose a reference b where x_1 is nearly zero. A value of $b=2.9$ was used, but had a larger value been used the agreement would have been even better.

Caldwell and Hoch found in addition that the saturation power output increased as the drive level was increased, keeping the voltage constant. This phenomenon is also predictable from the nonlinear theory; a comparison is shown in Fig. 13. The amount of increase in the saturation power level for input-signal levels comparable to or greater than $CI_0 V_0$ is some 4 db over that for very small input-signal levels. This increase in power output is probably due to the fact that this type of operation extracts the energy associated with all three cir-

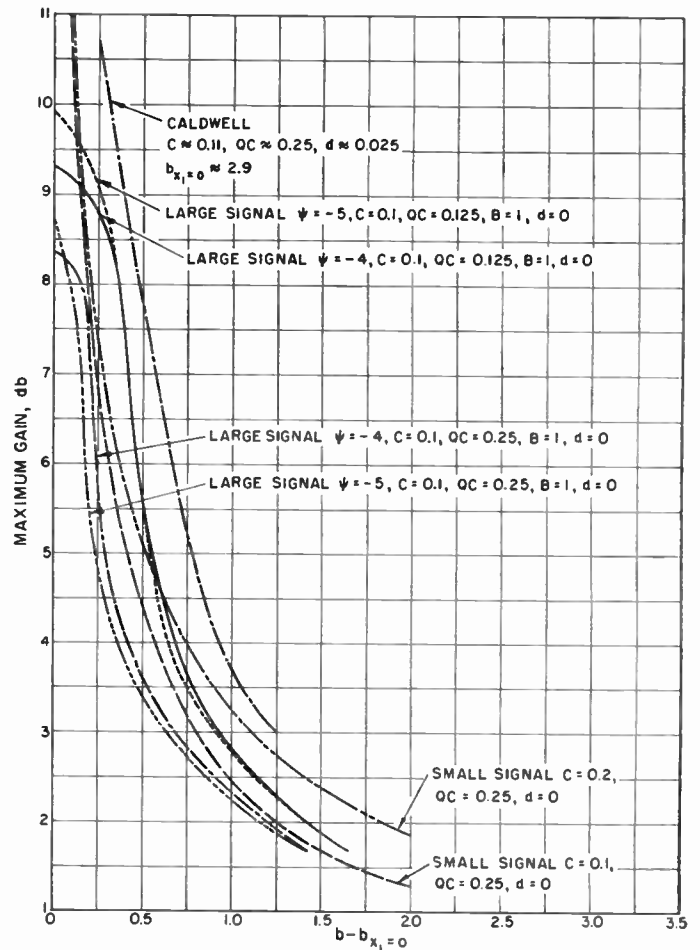


Fig. 12—Comparison of theoretical and experimental gain.

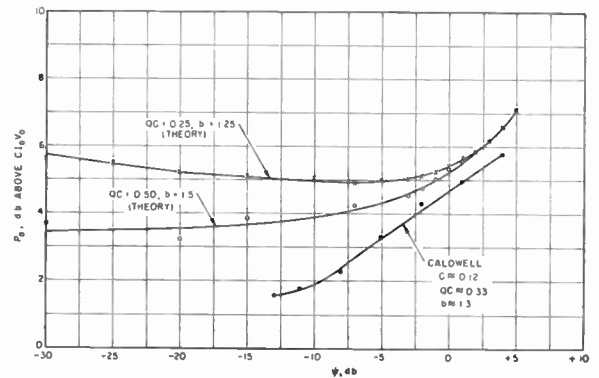


Fig. 13—Variation of saturation level with input-signal level ($C=0.1, B=1.0, d=0$).

cuit waves rather than only that of the growing wave as in the case of the conventional traveling-wave amplifier.

Efficiency

The saturation efficiency also increases as the drive level is increased, resulting in a relatively high efficiency for the Crestatron. Efficiency curves as a function of the drive level and the injection velocity are shown in Fig. 14. It is seen that the saturation efficiency for high drive approaches a value relatively independ-

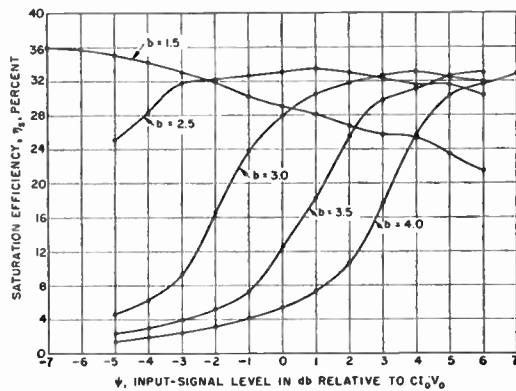


Fig. 14—Theoretical saturation efficiency vs input-signal level with injection velocity as the parameter ($C=0.1$, $QC=0.125$, $B=1.0$, $d=0$, $b_{z_1=0}=2.33$).

ent of the value of b in this type of device. In calculating the saturation efficiency of the Crestatron the input power is significant and, hence, one must consider only the energy conversion efficiency and subtract out the input-power level from the calculations. For values of b just slightly greater than that for which the wave growth constants become zero the efficiency is fairly constant as the drive level is varied. Continual increase in the drive power when b is adjusted for maximum saturation efficiency with small input-signal level results in a gradual decrease in the saturation efficiency.

The saturation efficiency is apparently higher at high values of drive when the voltage is adjusted for beating-wave operation than when the voltage is adjusted for maximum saturation output for a small input-signal level. This increase in efficiency is probably due in part to the fact that $1+Cb$ is approximately 1.3 or 1.4 in the Crestatron, as opposed to around 1.2 in the growing wave mode of operation and hence has considerably more energy to give up to the wave while slowing down.

MAGNETIC FIELD REQUIREMENT

The limiting stream perveance which can be transmitted through a cylindrical drift tube or helix due to space-charge spreading is given by⁸

$$\text{Perveance} = 38.6 \times 10^{-6} \left(\frac{d}{l} \right)^2, \quad (23)$$

where

d = helix diameter, and
 l = helix length.

The following familiar relations for traveling-wave tubes are recalled:

$$CN_s = \left(\frac{FK_s I_0}{4V_0} \right)^{1/3} \frac{l f}{u_0}, \quad (24a)$$

$$u_0 = (2\eta V_0)^{1/2} = \lambda_s f, \quad (24b)$$

$$\frac{u_0}{v_0} = 1 + Cb, \quad (24c)$$

and

$$\gamma a = 2\pi a / \lambda_g. \quad (24d)$$

The helix impedance FK_s used in (24a) may be written as

$$FK_s = \frac{506FK_s'(1 + Cb)}{V_0^{1/2}}, \quad (25)$$

where

F = the impedance reduction factor due to dielectric loading and space harmonics, and

K_s' = sheath-helix impedance as given by Pierce⁹ in Fig. A6.5.

Combining (23)–(25) yields

$$CN_s = 0.054 \frac{(FK_s')^{1/3}}{(1 + Cb)^{2/3}} (\gamma a) \left(\frac{l}{d} \right)^{1/3}. \quad (26)$$

From (26) can be calculated the maximum length of structure which can be used when no magnetic focusing field is present and the stream is allowed to spread under the influence of space-charge forces. Of course, the stream must be injected in a convergent manner, aimed toward the center of the structure, and then allowed to expand, resulting in a divergent stream at the output end. Allowance will also have to be made for stream spreading due to the presence of RF fields on the structure. The following typical values of the parameters in (26) are used to evaluate CN_s :

$$\begin{aligned} \gamma a &= 1.5 \\ (FK_s')^{1/3} &= 2.2 \\ (1 + Cb)^{2/3} &= 1.3 \\ \left(\frac{l}{d} \right)^{1/3} &= 2.5. \end{aligned}$$

Using the above values gives

$$CN_s = 0.34.$$

This value of CN_s is compatible with the lengths required for Crestatron operation. Hence under some conditions it may be possible to operate the Crestatron with little or no magnetic focusing field. Electrostatic focusing systems are sometimes possible depending upon the structure type.

CONCLUSION

A theoretical investigation of traveling-wave tube operation when $b > b_{z_1=0}$ has revealed that gain can be

⁸ J. R. Pierce, "Theory and Design of Electron Beams," D. Van Nostrand Co., Inc., New York, N. Y., p. 151; 1954.

⁹ J. R. Pierce, "Traveling-Wave Tubes," D. Van Nostrand Co., Inc., New York, N. Y.; 1950.

achieved due to a beating between the three small-signal waves which are set up at the input of the amplifier. These waves propagate along the RF structure with constant amplitudes and different velocities and hence beat with one another. Gain is achieved by terminating the circuit at a point where these waves add in phase to give an increased output. The gains achievable are moderate and increase with increasing C but decrease with increasing QC . The gain also decreases as the injection velocity as measured by b is increased.

Nonlinear calculations indicate the same type of behavior as both the voltage and drive level are increased; and it has been shown that the saturation power output increases with the drive level. The saturation efficiency is high for this type of operation and the CN bandwidth can be as large as ± 50 per cent.

In order to check the theory experimentally a beating-wave device called the Crestatron has been designed and tested. Measurements of gain indicate excellent agreement with the theory as do comparisons with data taken by other workers. Since the RF structure length of the Crestatron is extremely short it has been shown that it is theoretically possible to operate the device with little or no magnetic focusing field.

ACKNOWLEDGMENT

The author acknowledges the benefit of discussions during the course of this work with his associates in the Electron Physics Laboratory, University of Michigan, Ann Arbor, and in particular the assistance of Y. C. Lim and L. E. Stafford in solving the equations on a digital computer.

CORRECTION

The IRE Standards Committee has requested that the list of Committee Personnel which appeared with the "IRE Standards on Audio Techniques: Definitions of Terms, 1958," on page 1928 of the December, 1958 issue of PROCEEDINGS, be corrected as follows.

Subcommittee on Audio Definitions

D. S. DEWIRE, *Chairman* 1956-1958

L. D. RUNKLE, *Chairman*, 1955-1956

H. W. Bibber 1957-1958

D. S. Dewire 1955-1956

W. E. Darnell 1955-1958

W. F. Dunklee 1955-1958

C. W. Frank 1955-1958

A. A. McGee 1956-1958

G. H. Grenier 1955-1956

L. D. Runkle 1956-1958

R. E. Yaeger 1955-1958

Committee on Audio Techniques

D. S. DEWIRE, *Chairman* 1958

IDEN KERNEY, *Chairman* 1956-1958

D. E. MAXWELL, *Chairman* 1954-1956

A. P. EVANS, *Vice-Chairman* 1958

D. S. DEWIRE, *Vice-Chairman* 1956-1958

IDEN KERNEY, *Vice-Chairman* 1954-1956

Theory and Experiments on Shot Noise in Silicon P - N Junction Diodes and Transistors*

B. SCHNEIDER† AND M. J. O. STRUTT†, FELLOW, IRE

Summary—Experiments with silicon junction diodes and transistors have shown that previous theoretical expressions for the noise of such elements do not hold for silicon. New theoretical expressions are derived on the basis of recombination-generation in the depletion layer. These new expressions are satisfactorily checked by experiments in the case of low-level current injection. At high-level injection, however, deviations occur, for which no exact theory is known.

INTRODUCTION

EXPERIMENTS have shown that the theoretical expressions of noise in p - n junction diodes and transistors coincide reasonably well with experimental values in the case of germanium at low current densities.^{1,2} With silicon, however, significant deviations occur.³ It is well known that the characteristic curves of silicon p - n diodes and transistors show deviations from those of the corresponding germanium types.^{4,5} In the low current density region, theoretical expressions for these characteristic curves of silicon devices have been put forward,^{4,6,7} which show satisfactory coincidence with experimental values. In this paper, new expressions for the shot noise of silicon-junction diodes and transistors are derived on the basis of the theory of Sah, Noyce, and Shockley.⁴ It is then shown that these new expressions are in satisfactory agreement with experimental values.

DIFFERENTIAL ADMITTANCE OF P - N JUNCTION DIODES

In germanium p - n junction diodes current flow is mainly caused by diffusion and is, to a good approximation, given by Shockley's equation

$$I_D = I_o \left[\exp \left(\frac{qV}{kT} \right) - 1 \right]. \quad (1)$$

Here, I_o is the saturation current, q the magnitude of electron charge, V the applied voltage, k Boltzmann's constant, and T the absolute temperature (degrees Kelvin). The positive direction of currents and voltage is counted from the p -side to the n -side of the junction.

From (1) the real part of the differential admittance Y_D is found to be

$$\text{Re}(Y_D) = \frac{dI_D}{dV} = I_o \frac{q}{kT} \exp \left(\frac{qV}{kT} \right) = \frac{q}{kT} (I_D + I_o). \quad (2)$$

If the diode is biased in the forward direction and $qV > 3kT$, say, we obtain approximately

$$\text{Re}(Y_D) \approx \frac{q}{kT} I_D. \quad (3)$$

These equations are approximately valid in the case of low diode current densities. They break down, also, for germanium p - n junction diodes, if high-level current injection occurs, *i.e.*, for high current densities.⁸

In the case of silicon p - n junction diodes, considerable recombination and generation of carriers occurs in the depletion layer. As a result of this, a recombination-generation current flows through the junction diode, called I_R in this paper. According to Sah, Noyce and Shockley,⁴ this current is given by the expression

$$I_R = A \frac{\pi}{2} \frac{n_i k T w}{\tau_o (V_D - V)} \exp \left(\frac{qV}{2kT} \right). \quad (4)$$

Here, A is the cross-section area of the junction, n_i is the density of holes or electrons in an intrinsic specimen of the material under consideration, w is the width of the depletion layer, V_D is the diffusion voltage (or contact voltage) of the p - n junction, and τ_o is the mean lifetime of electrons and holes (if the lifetimes of either are equal). The current I_R , which is for short called "recombination current," gives rise to an admittance Y_R , the real part of which is, by (4),

$$\text{Re}(Y_R) = \frac{qI_R}{2kT} \left[1 + \frac{kT}{q(V_D - V)} \right]. \quad (5)$$

If we apply a forward bias voltage V , the second term within square brackets is mostly small with respect to unity, and hence, by (5),

* W. Guggenbuehl, "Theoretische Ueberlegungen zur physikalischen Begründung des Ersatzschaltbildes von Halbleiterdioden bei hohen Stromdichten," *Arch. elekt. Übertragung*, vol. 10, pp. 483-485; September, 1956.

* Original manuscript received by the IRE, September 15, 1958; revised manuscript received, December 8, 1958. This work was made possible by grants from the Swiss Federal Fund for Scientific Research, and from the Swiss Federal Institute of Technology.

† Swiss Federal Institute of Technology, Zürich, Switzerland.

¹ W. Guggenbuehl and M. J. O. Strutt, "Theory and experiments on shot noise in semiconductor junction diodes and transistors," *Proc. IRE*, vol. 45, pp. 839-854; May, 1957.

² A. van der Ziel, "Noise in junction transistors," *Proc. IRE*, vol. 46, pp. 1019-1038; June, 1958.

³ B. Schneider, "Untersuchungen des Hochfrequenzrauschens von neueren Transistoren," (High frequency noise of modern transistors), Communication Nachrichtentechnische Gesellschaft Session, Karlsruhe, Ger., September 24, 1957.

⁴ C. T. Sah, R. N. Noyce, and W. Shockley, "Carrier generation and recombination in p - n junctions and p - n junction characteristics," *Proc. IRE*, vol. 45, pp. 1228-1243; September, 1957.

⁵ J. L. Moll, "The evolution of the theory for the voltage-current characteristic of p - n junctions," *Proc. IRE*, vol. 46, pp. 1076-1082; June, 1958.

⁶ W. Shockley and W. T. Read, Jr., "Statistics of recombination of holes and electrons," *Phys. Rev.* vol. 87, pp. 835-842; September, 1952.

⁷ R. N. Hall, "Electron-hole recombination in germanium," *Phys. Rev.*, vol. 87, p. 387; July, 1952.

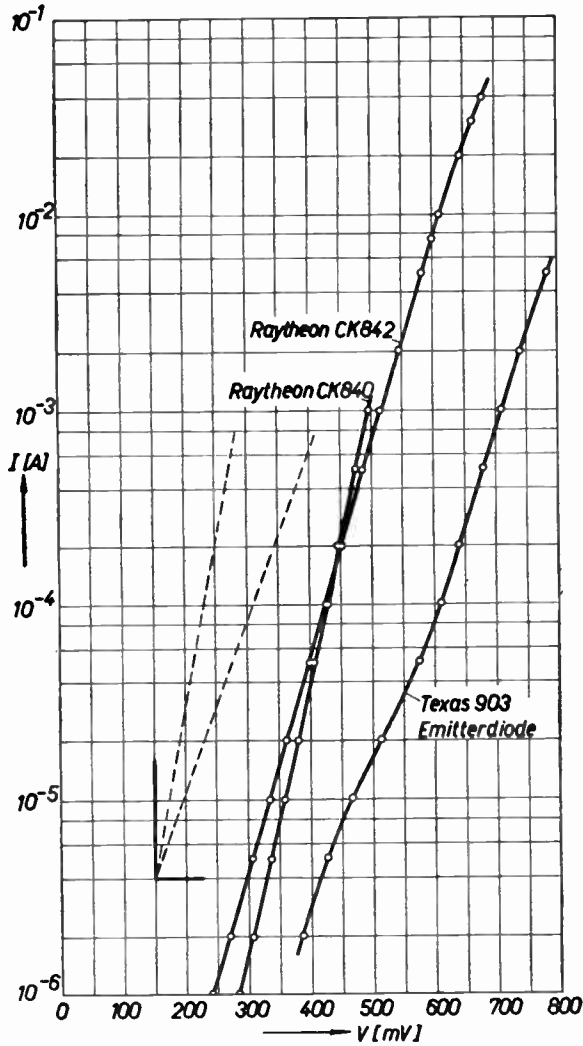


Fig. 1—Characteristic curves of diode current (vertical) vs diode voltage (horizontal) for three different silicon diodes (full curves), one of these being the emitter diode of a silicon transistor (Texas 903). The two broken curves show the slopes pertaining to pure diffusion (on the left) and to pure recombination (on the right).

$$\text{Re}(Y_R) \approx \frac{qI_R}{2kT} \tag{6}$$

From (4) we cannot directly see why I_R is much more relevant in silicon $p-n$ junction diodes than in germanium diodes. In order to see this, the recombination current I_R must be compared with the saturation currents I_o (which is the reverse current of a far negatively biased diode) in both cases. A simple argument⁶ then shows that I_R is much more important, relatively to I_o with silicon than with germanium $p-n$ junction diodes.

In general, a diffusion current, as well as a recombination current, will flow in a $p-n$ junction diode, thus yielding a total current I ,

$$I = I_D + I_R \tag{7}$$

The total differential admittance $Y = Y_D + Y_R$ has a real part, given by (3) and (6) for a forward bias voltage of sufficient magnitude

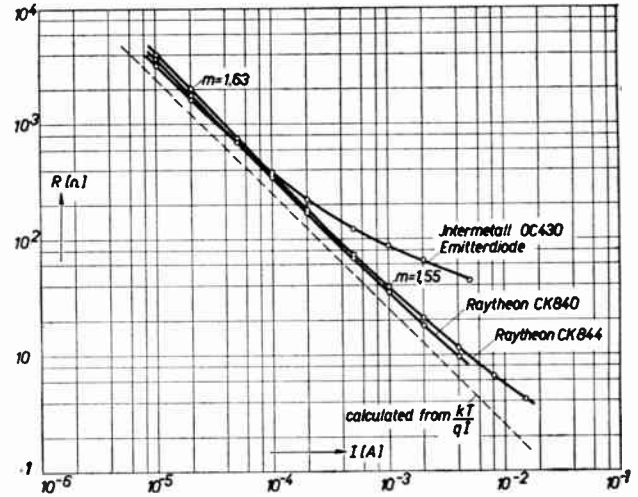


Fig. 2—Reciprocal value R of the real part of the diode admittance Y (vertical in ohms) vs diode current in amperes (horizontal) for three different silicon diodes. Some calculated values of m have been inserted [see (8)]. The broken curve pertains to pure diffusion.

$$\text{Re}(Y) \approx \frac{qI_D}{kT} + \frac{qI_R}{2kT} = \frac{qI}{mkT} \tag{8}$$

By (8), a multiplier m has been defined, which is obviously dependent on the ratio I_D/I_R . But, as will be shown experimentally, m is approximately constant within a limited range of the current I in some practical cases.

In Fig. 1, some experimental curves are shown, from which it is seen that m is between 1 and 2. In Fig. 2 some experimental values of $R=1/\text{Re}(Y)$ are shown. Except in one case (OC 430), the values of m are fairly constant within considerable ranges of the current I . The one case referred to obviously contains a series resistance, which affects the R -curve already from 0.1 ma upwards. Furthermore, high-level current injection starts at about 0.2 ma with this particular diode. With the diodes CK 840 and CK 844 of Fig. 2, series resistances are small and high-level current injection starts above 1 ma.

NEW THEORETICAL EXPRESSIONS FOR SHOT NOISE IN SILICON $P-N$ JUNCTION DIODES

We shall deal here with shot noise only, as distinct from flicker noise. The latter starts at zero frequency and is manifest up to some upper frequency, dependent on the purity of the material in question. With pure material, the upper frequency may be less than 1 kc, whereas it may be more than 1 mc with impure material. The intensity of flicker noise for a fixed frequency interval, Δf , is approximately proportional to the inverse mean frequency f of this interval, Δf .

A formula for the mean-square shot-noise current of a $p-n$ junction diode, in which carrier motion is exclusively due to diffusion, has been derived

$$\overline{i_{nd}^2} = [4kT \text{Re}(Y_D) - 2qI_D] \Delta f \tag{9}$$

This derivation was first published, using special assumptions, by van der Ziel,⁹ and then was shown to be of general validity by Guggenbuehl and Strutt.^{1,10}

Inserting the value of (3) for $\text{Re}(Y_D)$ yields, in the case of a forward bias voltage (positive from p to n) of sufficient magnitude ($qV > 3kT$)

$$\overline{i_{nd}^2} = 4qI_D\Delta f - 2qI_D\Delta f = 2qI_D\Delta f. \quad (10)$$

These expressions (9) and (10) yield the mean-square value of a noise current i_{nd} due to a current generator, whereby the current generator is connected in parallel to the diode terminals.

It is, of course, also possible to describe the diode's shot noise by means of a noise voltage generator, connected in series to the diode. If Z_D is the impedance of the diode, then

$$\overline{v_{nd}^2} = 4kT \text{Re}(Z_D)\Delta f - 2qI_D |Z_D|^2 \Delta f. \quad (11)$$

The derivation of the expression (11) may be given, along similar lines, as the derivation¹ of (9).

Tentatively, one might assume the deviation of expressions (10) and (11) from experimental results with silicon diodes to be due to a series resistance incorporated in the diode outside the space-charge layer. Assuming the series impedance to be Z_s , and the diode current I , with a diode impedance (of the space-charge layer) $1/Y$, we obtain, instead of (11)

$$\overline{v_{nd}^2} = 4kT \text{Re}\left(\frac{1}{Y} + Z_s\right)\Delta f - 2qI \left|\frac{1}{Y}\right|^2 \Delta f. \quad (12)$$

Instead of a noise current generator, or of a noise voltage generator, the noise is also often described by the "equivalent noise resistance" R_{eq} . This is a resistance, connected by definition with the noise generator voltage v_{nd} by

$$\overline{v_{nd}^2} = 4kTR_{eq}\Delta f. \quad (13)$$

We shall now relate this equivalent noise resistance to the differential admittance of the diode.

In the case of diffusion without series impedance, *i.e.*, according to (9) and (2) we obtain

$$\frac{R_{eq}}{R_D} = \frac{1}{2} \left(1 + \frac{I_o}{I_D + I_o}\right) \quad (14)$$

if $V=0$ [see (1)], we have $I_D=0$, and, hence, $R_{eq}=R_D$. On the other hand, if $qV > 3kT$, we have (forward bias) $I_D \gg I_o$, and, hence, $R_{eq} = \frac{1}{2}R_D$. This important relationship (14) was sufficiently confirmed experimentally with germanium junction diodes.¹¹

⁹ A. van der Ziel, "Shot noise in junction diodes and transistors," *Proc. IRE*, vol. 43, pp. 1639-1646; November, 1955, and vol. 45, p. 1011; July, 1957.

¹⁰ W. Guggenbuehl and M. J. O. Strutt, "Theorie des Hochfrequenzrauschens von Transistoren bei kleinen Stromdichten," *Nachricht. Fachberichte, Beiheft der NTZ*, vol. 5, pp. 30-33; September, 1956.

¹¹ Guggenbuehl and Strutt, *op. cit.*, Fig. 18, footnote 1.

If we have diffusion with series resistance $\text{Re}(Z_s) = R_s$, we obtain in the case of a forward bias of sufficient magnitude ($qV > 3kT$)

$$R_{eq} = \frac{1}{2}R_D + R_s. \quad (15)$$

Now we consider the case of diffusion plus recombination-generation. It has been shown that recombination-generation is predominantly located at the center plane of the depletion space-charge layer, if the mean lifetimes of carriers in the semiconductors adjacent to this layer are not too different.⁴ The maximum of the recombination-generation rate U is exactly located at the center plane of the depletion layer, if the lifetimes, the mobilities, and the carrier densities are equal on opposite sides of the junction (symmetrical diode). In the case of an unsymmetrical diode the maximum of U is not appreciably displaced out of the center plane (see Appendix formula for distance d). We shall, for simplicity, assume generation-recombination to take place at the exact center plane of the depletion layer. The motion of carriers in this layer is assumed to be random without intercorrelation. A carrier is either captured (recombination) or generated at the center plane. In the first case a carrier moves from one of the boundary planes of the depletion layer to the center plane; in the second case it drifts from the center plane to either of the boundary planes. Thereby, each carrier which is generated or recombines in the depletion layer only goes through exactly one-half of the total thickness of this layer. In the diode circuit the effect is the same as if a carrier of charge $q/2$ were to go through the total depletion layer. According to W. Schottky's diode noise equation we obtain for the mean-square noise current $\overline{i_{np}^2}$ due to recombination-generation of holes, and for the mean-square noise current $\overline{i_{nn}^2}$ due to recombination-generation of electrons

$$\overline{i_{np}^2} = \overline{i_{nn}^2} = 2 \frac{q}{2} \frac{I_R}{2} \Delta f.$$

Here, it is assumed that one-half of the total recombination current I_R is due to holes, and one-half to electrons. The total mean-square noise current $\overline{i_{nr}^2}$ due to recombination-generation is, hence

$$\overline{i_{nr}^2} = \overline{i_{np}^2} + \overline{i_{nn}^2} = qI_R\Delta f. \quad (16)$$

We may apply (16) in order to obtain the equivalent of (9) in the case of recombination-generation shot noise. The result is¹²

$$\overline{i_{nr}^2} = 4kT \text{Re}(Y_R)\Delta f - qI_R\Delta f. \quad (17)$$

If we add the mean-square shot-noise current due to diffusion to the above expressions (16) and (17), bearing in mind that the two shot noise currents are uncorrelated, we obtain

¹² *Ibid.*, pp. 839-841.

$$\overline{i_n^2} = \overline{i_{nd}^2} + \overline{i_{nr}^2} = 4kT [\text{Re}(Y_R) + \text{Re}(Y_D)]\Delta f - 2q \left(I_D + \frac{I_R}{2} \right) \Delta f. \tag{18}$$

Here again, we apply (8) for the multiplication factor m and obtain

$$\overline{i_n^2} = 4kT \text{Re}(Y) - 2qI \frac{\Delta f}{m}, \tag{19}$$

where I is the total diode current and Y the total diode admittance. In the low-frequency region, we have, in the case of forward bias of sufficient magnitude ($qV > 3kT$)

$$\text{Re}(Y) \approx \frac{qI}{mkT}.$$

Hence, (19) in this case reduces to

$$\overline{i_n^2} = 2q \frac{I}{m} \Delta f. \tag{20}$$

This (20) may again be reverted to an equivalent noise resistance R_{eq} . We then obtain, if $\text{Re}(Y) = 1/R$

$$\frac{R_{eq}}{R} \approx \frac{1}{2}, \tag{21}$$

in the case of a forward bias of sufficient magnitude ($qV > 3kT$). It is noteworthy that the relation (21) in the case of diffusion plus recombination noise is quite similar to (14) for a forward bias of sufficient magnitude ($qV > 3kT$).

If an appreciable series resistance R_s is present in the diode, (21) must be altered slightly, correspondingly to (15). In this case, $R + R_s$ denotes the total diode resistance, and we have

$$R_{eq} = \frac{1}{2}R + R_s. \tag{22}$$

This equation may be extended so as to obtain the equivalent of (12) in the case that recombination-generation noise is included. We obtain

$$\overline{v_n^2} = 4kT \text{Re} \left(\frac{1}{Y} + Z_s \right) \Delta f - 2q \frac{I}{m} |Z|^2 \Delta f. \tag{12a}$$

If we take into account that recombination-generation of carriers is not concentrated at the center plane of the depletion layer, but has a certain distribution over the depletion layer, (16) is somewhat altered (see Appendix). However, the theoretical deviations from (16) are small. Likewise, if the recombination-generation is assumed to be concentrated at a plane, which, however, is somewhat displaced with regard to the center of the depletion layer, (16) is somewhat altered (see Appendix). In this case, also, the theoretical deviation from (16) is small.

NEW THEORETICAL EXPRESSIONS FOR SHOT NOISE IN SILICON JUNCTION TRANSISTORS

We consider junction transistors in the three possible connections: grounded base, grounded emitter, and grounded collector. First, the intrinsic transistor, consisting of emitter and of collector diode, biased properly, is treated. The admittance of the emitter diode is denoted by Y_{11} . Then, (19), applied to this diode, yields

$$|\overline{i_{ne}^2}| = 4kT \text{Re}(Y_{11})\Delta f - 2q \frac{I_E}{m_E} \Delta f, \tag{23}$$

where I_E is the emitter dc current, and m_E is the multiplication factor [see (8)] of the emitter diode.

The collector current is composed of two parts: first, the saturation current I_{∞} caused by generation of carriers at the edges of the depletion layer and in the depletion layer, second, the injected current from the emitter into the base layer minus recombination current in this layer. The first part is relatively so small in silicon transistors that it may be neglected as to its noise contribution. Hence, the collector diode gives rise to a noise-current generator

$$|\overline{i_{nc}^2}| = 2qI_c \Delta f. \tag{24}$$

The correlation between the two noise currents i_{ne} and i_{nc} is given by the equation

$$\overline{i_{ne}^* i_{nc}} = 2kTY_{21}\Delta f. \tag{24a}$$

The deviation may be carried out in exactly the same manner as has been done.¹³ In (24a) the term $-2kTY_{12}^* \Delta f$ has been neglected at the right side. Applying (23), (24) and (24a), according to calculations along exactly the same line as published previously,^{1,10} we obtain

$$4kTR_o F = 2qI_c \left| \frac{\frac{1}{Y_{11}} + R_b + R_o}{\alpha_{fb}} \right|^2 - 2q \frac{I_E}{m_E} |R_b + R_o|^2. \tag{25}$$

Here, F is the noise figure for the grounded base and for the grounded emitter connection, R_o is the source resistance (assumed to be at the same absolute temperature T , as the transistor), R_b the extrinsic base resistance, and α_{fb} the ac current amplification factor in the grounded base connection. The conditions, involved in (24), (24a) and (25) are similar to those stated for pure diffusion transistors^{1,10}

$$|Y_{11}| \gg |Y_{12}|, \quad |Y_{21}| \gg |Y_{22}|, \quad |Y_{22}R_b| \ll 1. \tag{26}$$

Here, Y_{11} , Y_{12} , Y_{21} , and Y_{22} are the admittances of the intrinsic transistor, as usual.

For the grounded collector connection, we may again

¹³ *Ibid.*, p. 843.

apply the procedure, published previously^{1,10} bearing in mind (23), (24), and (24a). We then obtain

$$\begin{aligned}
 4kTR_oF &= 4kT(R_o + R_b) + 2qI_c(R_o + R_b)^2 - |\alpha_{fb}|^2 2q \\
 &\times \frac{I_E}{m_E} \left| R_o + R_b - \frac{1}{Y_{21}} \right|^2 - 4kT |\alpha_{fb}|^2 \operatorname{Re} \left(\frac{R_o}{\alpha_{fb}} \right) \\
 &- 4kT |\alpha_{fb}|^2 R_b \operatorname{Re} \left(\frac{1}{\alpha_{fb}} \right) \\
 &+ \frac{4kT}{|Y_{11}|^2} \operatorname{Re} (Y_{11}). \quad (27)
 \end{aligned}$$

The conditions for (27) are again (26).

EXPERIMENTAL CONFIRMATIONS OF THEORETICAL NOISE EXPRESSIONS FOR SILICON JUNCTION DIODES AND TRANSISTORS

In order to obtain the above experimental confirmation, a measuring set was constructed, with which the noise of junction diodes, biased in the forward direction, may be determined. The equivalent noise resistance of such objects is often below the input noise resistance of low-noise tube circuits. Hence, a suitable transformer must be applied between the diode to be measured and the input tube circuit of the measuring set.¹⁴

The measuring set is shown schematically in Fig. 3.

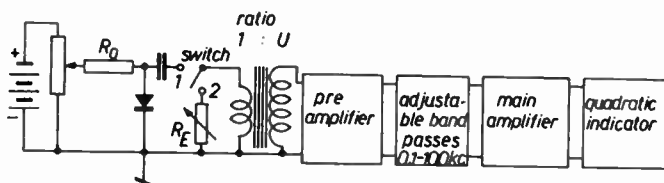


Fig. 3—Measuring setup for the determination of diode noise. For a description, see text.

If the switch at the input is connected to contact 1, an indication is obtained at the output indicator, due to diode noise, amplifier noise, and noise of the resistive parts of the transformer impedances. Then the switch is connected to contact 2, and the purely ohmic resistance R_E is adjusted until the same output indication is obtained. The value of R_E is determined and is then equal to the equivalent noise resistance of the diode under consideration. This determination of the diode's equivalent noise resistance R_{eq} may be carried out with sufficient accuracy if

$$R_{eq}u^2 \geq R_{eq \text{ ampl}} + R_{o2} + R_{o1}u^2$$

Here, u is the transformer ratio, $R_{eq \text{ ampl}}$ is the equivalent input noise resistance of the preamplifier, R_{o2} is the secondary, and R_{o1} the primary effective resistance of the transformer windings. The upper frequency of the

set is connected with the leakage inductance of the transformer. It has been possible, by this method, to determine equivalent noise resistances of less than one ohm with reasonable accuracy.

Some measured values of R_{eq} for silicon junction diodes are shown in Figs. 4, 5 and 6. As is seen from Fig. 4, the value of R_{eq} coincides satisfactorily with the value $\frac{1}{2}R$, *i.e.* with one-half of the diode's resistance, according to (21). On the other hand, the measured values of R_{eq} are distinctly above those, calculated from (10). In Fig. 5, measured values of R_{eq} as dependent on frequency at different dc values of the diode current I are shown. The values of R_{eq} tend to drop above about 20 kc. This is due to the frequency dependence of the diode's impedance $1/Y$. It is seen from Fig. 5, that R is still independent of frequency at the frequency, at which the values of Figs. 4 and 6 have been measured. At higher currents, a deviation of measured values of R_{eq} from $\frac{1}{2}R$ is shown in Fig. 4 and Fig. 6. This is due to high-level current injection, which invalidates the basis of our calculation.

The silicon diode Raytheon type 1 N 301 is manufactured according to the "bonded" procedure. It has a series resistance of about 26 ohms. The real part of its impedance $1/Y$ is independent of frequency up to above 70 kc. The curve *a* of Fig. 7 was calculated from (22), taking into account the said series resistance. This curve *a* coincides approximately with the measured values of R_{eq} , except at higher current values. This is due to high-level current injection, which starts below 1 ma with this diode. As a proof hereof, Fig. 8 shows measured values of the susceptance of this diode as dependent on dc diode current I . The susceptance goes negative at values of I above 1 ma, which is a sure sign for high-level current injection.⁸ Of course, high-level injection starts before the susceptance becomes negative. If we use (12) for the calculation of R_{eq} , curve *b* of Fig. 7 is obtained, which shows definitely worse agreement with measured values of R_{eq} than curve *a*.

In order to apply (25) to calculate the noise figure of transistors, the value of m_E must be known. The experimental determination of m_E is not straightforward. One method makes use of measurements of the differential emitter diode admittance. According to (8), the value of m_E may then be deduced. However, this method yields accurate values of m_E only for small current values. As soon as high-level current injection starts, (8) is no longer satisfied. Besides, an ohmic series resistance, which cannot be exactly determined, will be of increasing importance with increasing forward current. As an example, reference is made to Fig. 2, in which one curve pertains to the emitter diode of a silicon transistor type OC 430. Here, deviations from (8) already occur above a dc emitter current of 0.1 ma.

Another method for the determination of m_E could be based approximately on measurements of the dc current amplification factor α_{FB} . The emitter current of silicon transistors consists of two parts, one due to dif-

¹⁴ W. Nomenmacher, "Rauschspannungsmessungen an niederohmigen Bauelementen mit Hilfe eines Röhrenverstärkers mit vorge-schaltetem Uebertrager," *Nachricht. Z.* vol. 11, pp. 559-563; November, 1957.

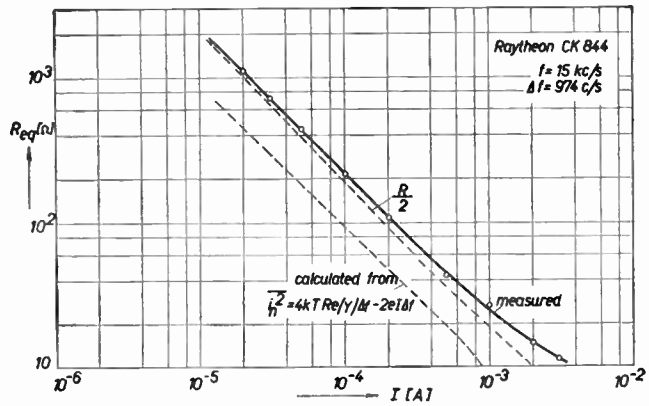


Fig. 4—Equivalent noise resistance R_{eq} in ohms (vertical) as measured (full curve) as dependent on diode current in amperes (horizontal). The broken curve marked $\frac{1}{2}R$ is calculated by taking one-half of the reciprocal value R of the real part of the measured diode differential admittance. The other broken curve is calculated from (10).

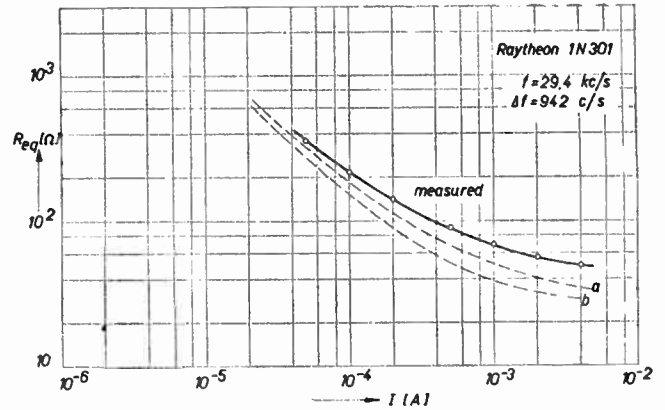


Fig. 7—Similar to Fig. 4, but for again another type of diode. Full curve is measured values of R_{eq} . Broken curve marked a is calculated from (22). Broken curve marked b is calculated from (12).

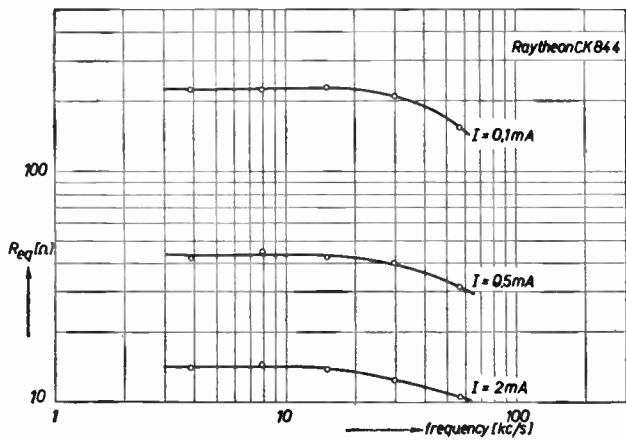


Fig. 5—Measured equivalent noise resistance R_{eq} as dependent on frequency at three values of diode current.

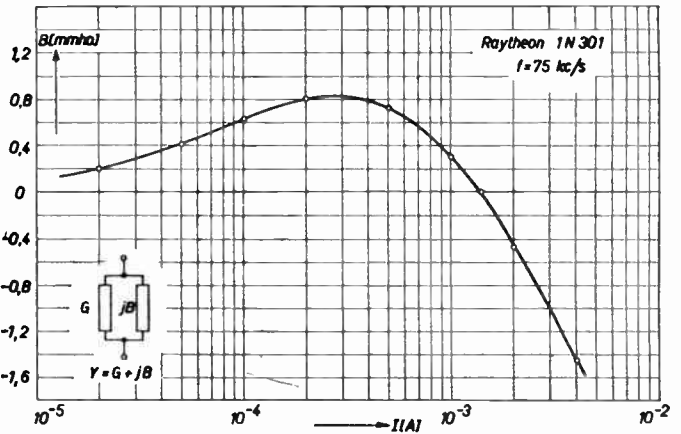


Fig. 8—Differential susceptance in mmhos (vertical) as dependent on diode current (horizontal), of a silicon diode.

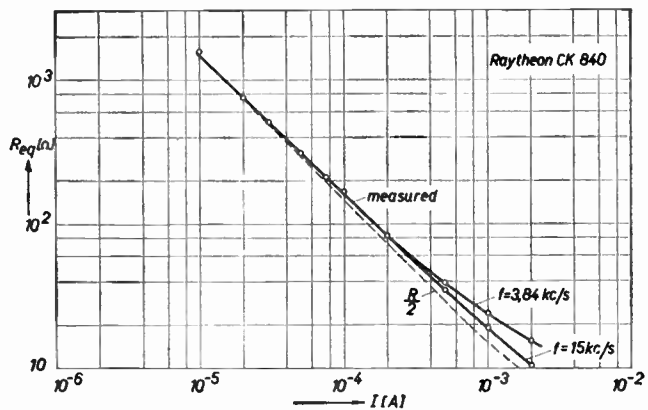


Fig. 6—Similar to Fig. 4, but for another type of diode. Measured values of R_{eq} at two different frequencies are full curves. The deviation between the curves $f = 3.84$ kc and $f = 15$ kc is caused by flicker noise. Broken curve is calculated from $\frac{1}{2}R$.

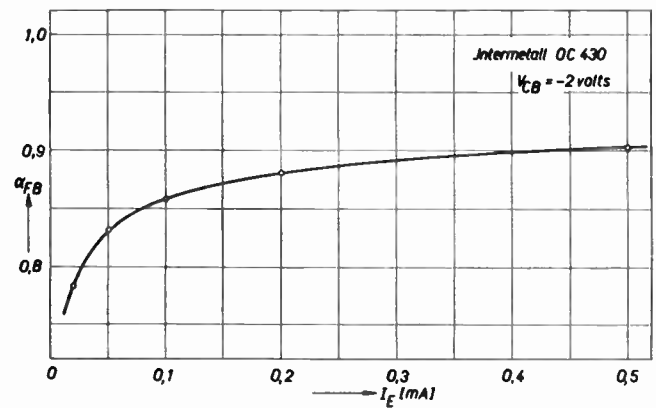


Fig. 9—DC current amplification factor α_{FB} of a silicon transistor, as dependent on emitter current.

fusion and the other due to recombination-generation. As the latter part consists of majority carriers on the n -side as well as on the p -side of the depletion layer, it offers no contribution to the minority current injected into the base layer. If the emitter current diminishes,

the recombination-generation current becomes more important in comparison to the diffusion current. Hence, the value of α_{FB} is correspondingly lower. This is confirmed by measurements, shown in Fig. 9. In order to evaluate the recombination current part of the emitter current, and hence, m_E from α_{FB} , the emitter efficiency, the surface recombination and the volume recombination of the base layer should be known, which is hardly

ever true. Thus, this method is not applicable.

If α_{FB} is near unity, recombination in the emitter depletion layer must be slight. Measured values of the noise figure F in grounded base connection of an alloyed silicon transistor type OC 470 are shown in Fig. 10 as being dependent on frequency. In the calculated curve, recombination was neglected, i.e., $m_E=1$ in (25). The discrepancy between the curves of Fig. 10 is not very marked. It is partly due to flicker noise inherent in the measured curve at lower frequencies. At higher frequencies the measured curve rises less steeply than the calculated curve. This is due to parallel capacity to the base resistance, which occurs in this transistor.

In Fig. 11, which is similar to Fig. 10 but for a different type of transistor, having a lower value of α_{FB} , recombination must be taken into account in order to obtain calculated curves, which are reasonably near to measured values. At high frequencies the rise of the measured curve is less steep than that of calculated curves, due to the capacity parallel to R_b , as mentioned above.

In both Figs. 10 and 11, measured values are above calculated values, taking recombination into account. This may be ascribed to high-level emitter current injection. As is shown in Fig. 12, the curve, calculated with recombination, fits the experimental values well at very low currents and deviates at higher currents. The curve, calculated without recombination, fits experimental values badly.

In cases of high-level current injection, the theory set forth here, which pertains to low current densities (no space charge caused by carriers), is only in part agreement with measured values. A better agreement could be expected from an extension of the theory to high level current injection.

A conjecture has been made previously¹ on the influence of high-level injection on noise. This conjecture may be extended here to include the case of recombination-generation noise. Referring to the above expression (19), the space charge in the semiconductor portions adjacent to the depletion layer, created by high-level injection, will probably tend to weaken the contribution embodied in the second term of (19). Hence, the total mean-square noise current will rise. This seems to be confirmed by the Figs. 4, 6, 7, 10, and 11.

APPENDIX

CALCULATION OF NOISE DUE TO RECOMBINATION-GENERATION

Assuming a linear potential variation across the junction, the rate U of recombination-generation in the depletion layer is approximately given by:

$$U(\xi) \approx \frac{n_i \exp\left(\frac{qV}{2kT}\right)}{\tau_{po} \exp Q + \tau_{no} \exp(-Q)}$$

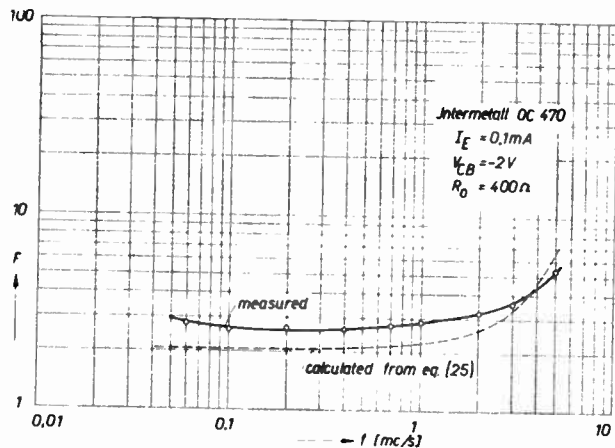


Fig. 10—Noise figure F (vertical) of a silicon transistor at fixed values, as indicated, of emitter current I_E , voltage V_{CB} and source resistance R_0 , measured in grounded base connection, as dependent on frequency (horizontal). The value of α_{fbo} of α_{fb} at low frequency is 0.970. The broken curve is calculated from (25).

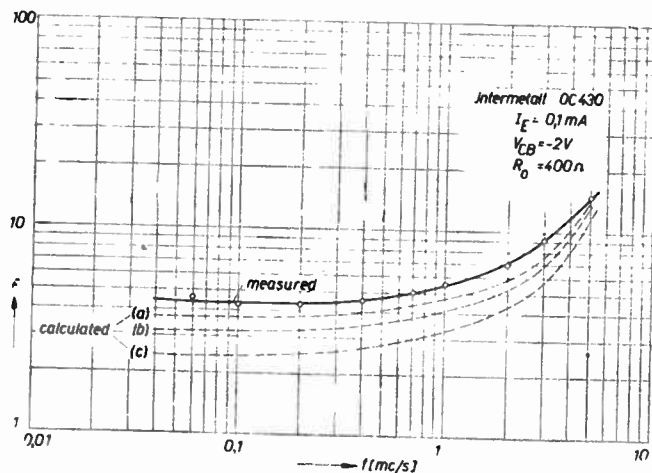


Fig. 11—Similar to Fig. 10, but for another type of silicon transistor. Here the value of α_{fbo} is 0.885. The calculated broken curves are a) from (25) inserting the most probable value of m_E , b) from (25) at $m_E=1$, but inserting the most probable value of Y_{11} and c) at $m_E=1$ and with a value of Y_{11} ignoring recombination.

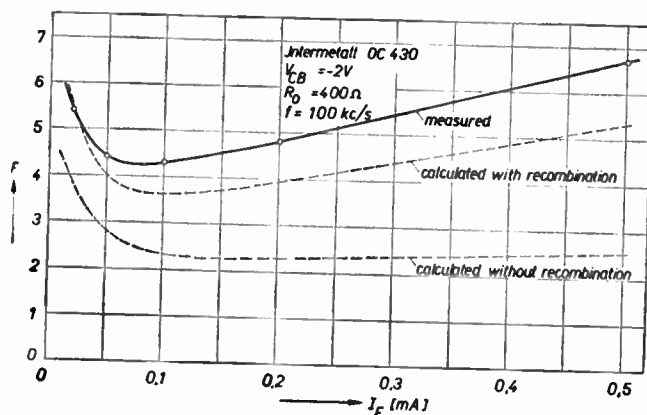


Fig. 12—Noise figure F (vertical) of the same silicon transistor of Fig. 11, as dependent on emitter current at fixed values, as indicated, of V_{CB} , R_0 and frequency. Broken curves calculated as indicated.

where

$$Q = \frac{q}{kT} \cdot \frac{V_D - V}{w} \xi.$$

V_D is the diffusion voltage, w is the width of the depletion layer, ξ a coordinate along the axis of the depletion layer, which is zero at the maximum of U , τ_{po} is the lifetime of holes injected into n -type material of high dotation, τ_{no} is the lifetime of electrons injected into p -type material of high dotation, n_i is the density of electrons or holes in intrinsic material.

A picture of the depletion layer with densities of acceptors, donors, holes, and electrons is shown in Fig. 13. The maximum of U , if the lifetimes τ_{po} and τ_{no} are not too different, is at the place where $p(x) = n(x)$.¹⁶ Taking account of the following relations for w_p and w_n , we obtain for the distance d ,

$$w_n \approx \frac{w p_p}{n_n + p_p} \quad w_p \approx \frac{w n_n}{n_n + p_p}$$

$$d = w_p + x_1 = \frac{w}{2} \left[1 + \frac{kT}{q(V_D - V)} \ln \frac{p_p}{n_n} \right]. \quad (28)$$

The second term within square brackets is usually small with respect to unity and, therefore, the maximum of U in unsymmetrical diodes is not considerably displaced out of the center of the depletion layer.

First we consider the influence on noise of the distribution over the depletion layer of the carrier-recombination-generation. To carry this out, we suppose the maximum of U to be at the center of the depletion layer (symmetrical diode). In a part of the depletion layer between x and $x+dx$ the recombination current contribution is

$$dI_R = qU(x)A dx,$$

where A is the cross-section area of the junction. This contribution dI_R may be separated into a part, due to electrons

$$dI_{Rn} = q \frac{\frac{w}{2} - x}{w} U(x)A dx,$$

and a part, due to holes

$$dI_{Rp} = q \frac{\frac{w}{2} + x}{w} U(x)A dx.$$

These parts each involve a noise current, the mean-square values of which are

¹⁶ Sah, Noyce, and Shockley, *loc. cit.*, pp. 1230-1231.

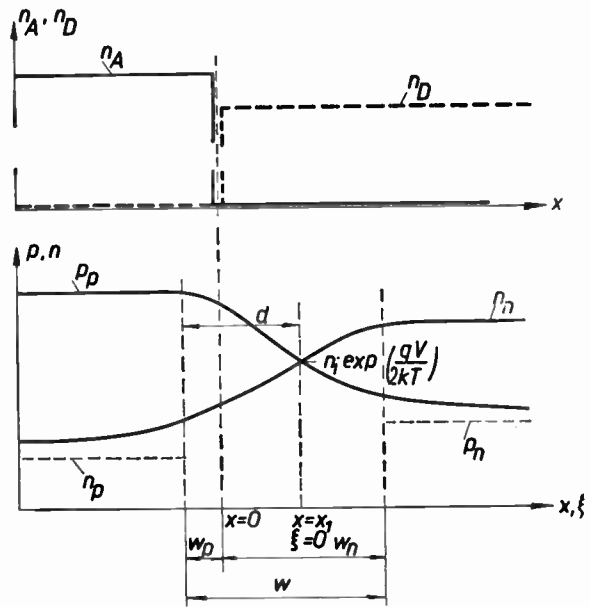


Fig. 13—The upper part shows the density n_A of acceptors, and the density n_D of donors in a cross-section of a p - n junction diode. The lower part shows the density n of electrons and the density p of holes in a p - n junction diode, where n_n is the density of electrons in n -material at thermal equilibrium, n_p the density of electrons in p -material at thermal equilibrium, p_n the density of holes in n -material at thermal equilibrium and p_p the density of holes in p -material at thermal equilibrium. The depletion layer is between $\xi = -x_1 - w_p$ and $\xi = w_n - x_1$.

$$d(\overline{i_{nn}^2}) = 2q \frac{\frac{w}{2} - x}{w} q \frac{\frac{w}{2} - x}{w} U(x)A dx \Delta f,$$

and

$$d(\overline{i_{np}^2}) = 2q \frac{\frac{w}{2} + x}{w} q \frac{\frac{w}{2} + x}{w} U(x)A dx \Delta f.$$

The total differential mean-square noise current due to recombination-generation is

$$d(\overline{i_{nr}^2}) = q^2 A U(x) \left[1 + \left(2 \frac{x}{w} \right)^2 \right] dx \Delta f.$$

This should be integrated along the depletion layer (see Fig. 13) from $x = -(w/2)$ to $x = +(w/2)$, assuming that $w_p = w_n$ in Fig. 13, *i.e.*, that $n_A = n_D$. By symmetry, and owing to the rapid decrease of $U(x)$ on both sides of $x=0$, we obtain approximately

$$\overline{i_{nr}^2} = 2q^2 A \Delta f \int_0^\infty U(x) \left[1 + \left(2 \frac{x}{w} \right)^2 \right] dx$$

or

$$\overline{i_{nr}^2} = q I_R \Delta f \left[1 + 8 \left(\frac{kT}{q(V_D - V)} \right)^2 \right]. \quad (29)$$

The second term within square brackets is usually small, compared with the first one, and hence, (29) yields approximately (16).

We now assume that recombination-generation is concentrated at $\xi=0$, but that this place is not the center of the depletion layer (unsymmetrical diode) (see Fig. 13). The electron contribution to the total recombination current is (see Fig. 13):

$$I_{Rn} = I_R \frac{w-d}{w}$$

and the hole contribution is

$$I_{Rp} = I_R \frac{d}{w}.$$

The path of the electrons being $w-d$ and that of the holes d , the corresponding mean square noise currents are

$$\overline{i_{nn}^2} = 2q \frac{w-d}{w} I_R \frac{w-d}{w} \Delta f,$$

$$\overline{i_{np}^2} = 2q \frac{d}{w} I_R \frac{d}{w} \Delta f.$$

Inserting (28) for the distance d , we obtain

$$\overline{i_{nr}^2} = qI_R(1+c^2)\Delta f,$$

where

$$c = \frac{kT}{q(V_D - V)} \ln \frac{p_p}{n_n}.$$

Again, the second term within brackets is small with respect to the first one and, hence, we obtain approximately (16).

LIST OF SYMBOLS

- τ_{po} —lifetime for holes injected into n -type material of high dotation.
 τ_{no} —lifetime for electrons injected into p -type material of high dotation.
 τ_o —lifetime for electrons and holes when $\tau_{po} = \tau_{no}$.

U —recombination rate.

V_D —diffusion voltage in a p - n junction.

m —multiplication factor to describe the empirical characteristics.

m_E —multiplication factor of the emitter junction in transistors.

w —width of the space-charge layer.

w_n — n -material portion of the space-charge layer.

w_p — p -material portion of the space-charge layer.

I_D —diffusion current in a p - n junction.

I_R —recombination current in a p - n junction.

I —total current in a p - n junction.

Y_D —diffusion differential admittance.

Y_R —recombination differential admittance.

Y — $Y_D + Y_R$ = total differential admittance of a p - n junction.

Z_D — $1/Y_D$ = diffusion differential impedance.

Z_S —series impedance of the p - n junction.

R_D — $\text{Re}(Z_D)$ = diffusion differential resistance.

R — $1/\text{Re}(Y)$ at low frequencies = total differential resistance.

R_s —series resistance.

i_{np} —noise current caused by holes.

i_{nn} —noise current caused by electrons.

i_{nr} —recombination noise current.

i_{nd} —diffusion noise current.

i_{ne} —noise current of the emitter diode.

i_{nc} —noise current of the collector diode.

v_n —noise voltage.

v_{nd} —diffusion noise voltage.

α_{fb} —ac current amplification factor in grounded base connection.

α_{fb} —dc current amplification factor in grounded base connection.

ACKNOWLEDGMENT

The authors wish to express their sincere thanks to G. Spescha who has contributed to the experimental setup of Fig. 3.

A Constant-Temperature-Operation Hot-Wire Anemometer*

J. M. L. JANSSEN†, SENIOR MEMBER, IRE, L. ENSING†, MEMBER, IRE AND J. B. VAN ERP†

Summary—The behavior of a hot-wire anemometer is analyzed using signal flow diagrams, especially for the case of a constant-temperature-operation anemometer, comprising a dc bridge and a dc differential amplifier.

The influence of static bridge unbalance and of the amplifier's gain for in-phase input signals on the over-all dynamic characteristics is analyzed, and requirements for the amplifier are derived. A chopper-stabilized amplifier is employed, which automatically maintains static bridge balance under all operating conditions.

The signal-to-noise ratio for comparable instruments having constant-current operation and constant-temperature operation is shown to be equal.

Results of measurements are reported; they are in fair agreement with the developed theory.

A nonlinear circuit is described, which delivers a voltage directly proportional to the instantaneous air velocity.

LIST OF SYMBOLS

- M = time constant of hot wire.
 M', M'' = main time constant of over-all control system.
 ω = angular frequency.
 C = heat capacitance of hot wire.
 λ = quantity as defined by (18).
 a, b = constants occurring in King's equation.
 Φ, Ψ = quantities as defined by (64) and (65).
 R = hot-wire resistance at operating temperature.
 R_a = hot-wire resistance at air temperature.
 R_1, R_2, R_3 = resistances of the branches of the bridge (see Fig. 2).
 T = hot-wire temperature.
 T_a = temperature of the air.
 I = total bridge current.
 I_a = bridge current supplied by amplifier.
 I_e = bridge current supplied by external source.
 E = voltage across hot wire.
 E_1 = voltage across bridge resistance R_1 .
 E_b = bridge unbalance voltage.
 E_d = equivalent drift at input of amplifier.
 E_i = in-phase component of the amplifier's input voltage.
 P = heat flow to wire due to electrical heating ($=I^2R$).
 II = heat flow from wire due to cooling.
 W = resulting heat flow to wire ($=P-II$).
 S, S', S_0 = loop gain.
 S_d, S_d' = dynamic loop gain.
 q = quantity as defined by (40).

f = rejection factor of difference amplifier [see (38)].

Λ = relative static bridge unbalance [see (35)].

g_0 = static transconductance of controlling amplifier.

K_1 = quantity as defined by (4).

τ = per-stage time constant of amplifier.

cco = abbreviation for "constant-current operation."

cto = abbreviation for "constant-temperature operation."

$r, t, i, i_a, i_e, e, e_1, e_b, p, h, w$, etc., are variations of $R, T, I, I_a, I_e, E, E_1, E_b, P, H, W$, etc., respectively.

I. INTRODUCTION

IN the investigation of turbulent air flow use is often made of hot-wire anemometers. These instruments are based on the cooling effect of the air stream on a heated wire. The wire is heated by an electrical current and placed in the air flow; variations in the velocity of the air flow, due to turbulence, cause the resistance of the wire to vary. The variations in the wire's resistance give rise, in turn, to variations in the voltage across the wire, which after being amplified give an image of the air velocity variations. Thus the characteristic properties of the flow can be determined.

In order that the variations in the wire's resistance may follow the variations in air velocity as closely as possible, it is necessary to keep the heat capacitance of the hot wire per unit length as small as possible. For this reason very thin wires (diameter 3μ) are used. These wires are part of a probe, which is introduced into the turbulent flow. To fix the wire to the probe a special spot-welding technique has been developed [1].

In view of the small dimensions of the eddies in a turbulent flow the length of the hot wire has to be limited. Otherwise the effects of several eddies on the wire resistance are bound to neutralize each other to a certain extent. A length of about 1 mm would be appropriate. If a tungsten wire with a diameter of 3μ is used, the resistance at room temperature will then be about 10 ohms.

Two different methods [2]–[6] can be distinguished in hot-wire anemometry: 1) constant-current operation (referred to in this paper as cco), and 2) constant-temperature operation (here referred to as cto).

With cco (see Fig. 1) the ratio of voltage variations across the hot wire to air velocity variations drops off with frequency according to $1/\sqrt{1+(\omega M)^2}$, M being the time constant of the wire and ω being the angular fre-

* Original manuscript received by the IRE, September 19, 1958.

† Royal Dutch/Shell Lab., Delft, of N. V. de Bataafsche Petroleum Maatschappij, The Hague, Holland.

ncy. In order to compensate for this linear distortion, the signal has to be passed through a filter with an inverse frequency characteristic. M , however, is not a constant for a particular wire but varies with wire temperature and air velocity. For this reason the filter characteristics must be readjusted if the operating conditions are changed. This is very time-consuming and tedious work. Compensation becomes increasingly inaccurate for large air velocity variations because M can then no longer be considered a constant during a single cycle.

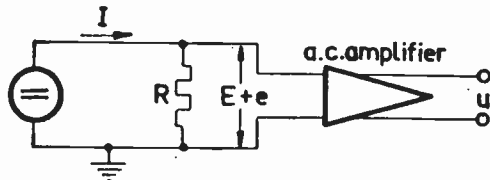


Fig. 1—Hot-wire anemometer with constant-current operation.

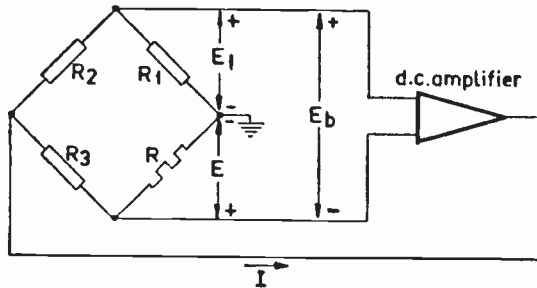


Fig. 2—Hot-wire anemometer with constant-temperature operation.

The necessity to study large velocity fluctuations containing frequencies of several tens of kilocycles per second has led to the development of cto anemometers. The wire is incorporated into a feedback system, e.g., by means of a bridge circuit and dc amplifier (see Fig. 2). In this way the main time constant of the instrument becomes $M/1+S$, where M is the time constant of the hot wire and S is the loop gain. The fact that the controlling amplifier introduces an additional phase lag at high frequencies gives rise to stability problems.

Eli Ossosky [6] derived the conditions that have to be complied with by the dc amplifier of Fig. 2 in order to avoid parasitic high-frequency oscillations. He starts from the assumption that the bridge is balanced for the adjusted mean values of air velocity and heating current. In our experience, it was found to be impossible to maintain the bridge in balance during measurement. Moreover, it was found that a slight bridge unbalance often gave rise to self-oscillation of the feedback system. This led to an investigation of the influence of the static bridge unbalance on the dynamic characteristics. From this study, the requirements regarding the static gain and the zero stability of the control amplifier were derived.

Based on this study, a cto hot-wire anemometer was constructed, which has the novel features of drift-stabilization and linearizing.

A chopper stabilizing circuit is provided in the controlling amplifier in order to maintain bridge balance under all operating conditions.

The relation between the air velocity and the hot-wire current with cto is nonlinear. At small amplitudes, therefore, the ratio between bridge current variations and air velocity variations changes with the static value of the air velocity, and at large amplitudes nonlinear distortion occurs. In the constructed instrument, this nonlinearity is compensated by a nonlinear circuit with an inverse characteristic which derives a voltage directly proportional to the air velocity from the bridge current.

II. FREQUENCY RESPONSE OF THE HOT WIRE

In this section the response of the hot-wire temperature to variations in air velocity is discussed. Since the temperature of the wire determines its resistance, this section covers at the same time the response of the hot-wire resistance to variations in air velocity. Knowledge of this resistance response enables one to find the response of the total electric measuring circuit in which the hot wire is incorporated.

Fig. 3 shows a signal flow graph [7] of the hot wire. The difference between the heat flows to and from the wire "charges" or "discharges" its heat capacitance C , giving rise to a temperature variation t . The associated transfer function is $1/j\omega C$.

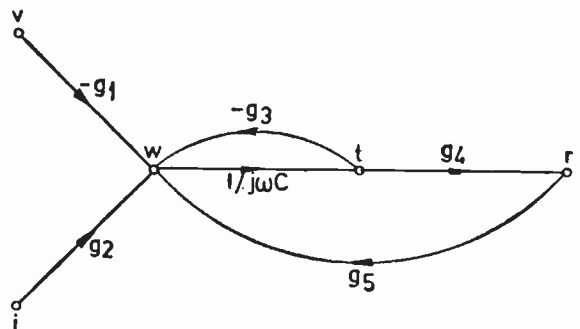


Fig. 3—Signal flow graph of hot wire.

There are four heat flows which in the analysis can be considered separately, although physically they are interdependent as shown in Fig. 3. They are: 1) the cooling due to an increase v in air velocity, 2) the heating due to an increase i in the current through the wire, 3) the cooling due to an increase t in temperature, and 4) the heating due to an increase r in wire resistance.

There are no time effects in any of the above-mentioned heat flows. Thus the associated transfer functions indicated in Fig. 3 are all constants. The same is true for the transfer function g_4 relating resistance to temperature variations.

The signal flow graph shows a negative feedback $-g_3$ and a positive feedback $g_4 \cdot g_5$. The stability condition for a constant current anemometer ($i \equiv 0$) is $g_4 \cdot g_5 < g_3$.

which condition is always satisfied in practice [see discussion of (22)].

The transfer function from v to r is

$$\frac{r}{v} = -g_1 \cdot \frac{r}{w} = -g_1 \cdot \frac{g_4 \cdot M/C}{1 + j\omega M} \quad (1)$$

with

$$M = \frac{C}{g_3 - g_4 \cdot g_5} \quad (2)$$

The above result is in agreement with results found by Betchov [8].

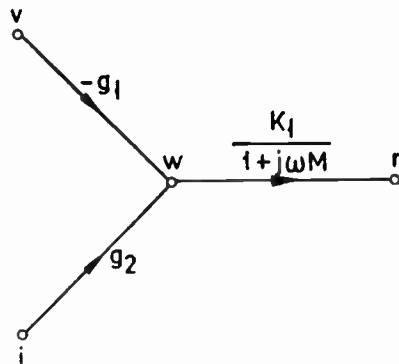
In constant-temperature operation another transfer function is equally of interest, namely

$$\frac{r}{i} = g_2 \cdot \frac{r}{w} \quad (3)$$

It has the factor

$$\frac{r}{w} = \frac{g_4 \cdot M/C}{1 + j\omega M} = \frac{K_1}{1 + j\omega M} \quad (4)$$

in common with the transfer function r/v , as is shown in the simplified signal flow graph of Fig. 4.



$$\frac{r}{w} = \frac{g_4 \cdot M/c}{1 + j\omega M} = \frac{k_1}{1 + j\omega M}$$

Fig. 4—Simplified signal flow graph of hot wire.

The constants g_1 and g_3 can be found from King's equation which describes the cooling of a small cylinder in an air flow [9]. The constants g_2 and g_5 follow directly from Joule's law, while the constant g_4 is determined by the temperature coefficient of the wire resistance.

King's equation reads:

$$H = (a + b\sqrt{V})(T - T_a) \quad (5)$$

in which

H = the heat flow from the wire.

V = the air velocity.

T = the wire temperature.

T_a = the air temperature.

a and b are constants, dependent on wire dimensions.

If P is the heat flow to the wire due to electrical heat-

ing, then the following equation holds under static conditions

$$H = P = I^2 R \quad (6)$$

where

I = the current through the wire.

R = the resistance of the wire.

It follows from (5)

$$h = \frac{b \cdot (T - T_a)}{2\sqrt{V}} \cdot v + (a + b\sqrt{V})t. \quad (7)$$

This equation also holds when the temperature is a function of the place along the wire because all quantities in the right-hand part of (7) except t and T are constant along the wire. In that case T stands for the average temperature and t for the average temperature variation. Hence, in Fig. 3:

$$g_1 = \frac{b(T - T_a)}{2\sqrt{V}} \quad (8)$$

$$g_3 = a + b\sqrt{V}. \quad (9)$$

As

$$p = d(I^2 R) = 2IRi + I^2 r \quad (10)$$

it follows that

$$g_2 = 2IR = \frac{2P}{I} \quad (11)$$

$$g_5 = I^2. \quad (12)$$

Further

$$g_4 = \frac{dR}{dT} = \frac{r}{t} \quad (13)$$

at the values of R , T and V at which the operation takes place.

Substitution of the equations for g_1 , g_2 , g_3 and g_5 in those for the time constant M [see (2)] and in the transfer functions r/w [see (4)], r/v [see (1)] and r/i [see (3)], yields, if use is made of (6):

$$M = \frac{C(T - T_a)}{P(1 - \lambda)} \quad (14)$$

$$\frac{r}{w} = \frac{R}{P} \cdot \frac{\lambda}{1 - \lambda} \cdot \frac{1}{1 + j\omega M} \quad (15)$$

$$\frac{r}{v} = \frac{R}{2V} \cdot \frac{b\sqrt{V}}{a + b\sqrt{V}} \cdot \frac{\lambda}{1 - \lambda} \cdot \frac{1}{1 + j\omega M} \quad (16)$$

$$\frac{r}{i} = 2 \cdot \frac{R}{I} \cdot \frac{\lambda}{1 - \lambda} \cdot \frac{1}{1 + j\omega M} \quad (17)$$

with

$$\lambda = \frac{g_4 \cdot (T - T_a)}{R}. \quad (18)$$

Eqs. (15), (16) and (17) could be rewritten as transfer functions for the relative variations in r , w , v and i by transferring R , P , V and I to the left hand side of the equations. Then the basic difference between these equations would lie only in the fact that the factor $b\sqrt{V}/a+b\sqrt{V}$ is present in (16) and absent in the others. This factor accounts for the fact that only the fraction $b\sqrt{V}/a+b\sqrt{V}$ of the cooling is caused by the air velocity V , while all of the heating is caused by the current I . For the $3\text{-}\mu$ tungsten wire the ratio between $b\sqrt{V}$ and a runs from 0 to about 2 at an air velocity of about 16 m/sec.

The factor 2 in the denominator of (16) stems from the square root in King's equation, while the same factor in the numerator of (17) stems from the second power of the current in Joule's law.

In the practical case of a tungsten wire, the temperature coefficient of the resistivity is approximately constant in the temperature range used. Thus

$$g_4 = \frac{r}{t} \approx \frac{R - R_a}{T - T_a} \tag{19}$$

Substituting (19) into (18) gives

$$\lambda = 1 - \frac{R_a}{R} \tag{20}$$

Substituting this equation into (14) for the time constant M results in

$$M = \frac{C(T - T_a)}{R_a I^2} \tag{21}$$

or

$$M = \frac{C(T - T_a)}{P} \cdot \frac{R}{R_a} \tag{22}$$

From (2) it is seen that the previously mentioned stability condition for c_{co} , $g_4 g_5 < g_3$, is satisfied if M is positive. From (21) it follows that this condition is indeed satisfied.

Eq. (22) gives the time constant M as the ratio of the heat $C(T - T_a)$ accumulated in the wire and the static heat flow P with the correction factor R/R_a .

In constant-temperature operation, an increase in air velocity causes the factor P in (22) or the factor I^2 in (21) to increase because the parameters T and R are kept constant. Thus the time constant M of the hot wire alone is in this case inversely proportional to the electric power supplied to the wire or inversely proportional to I^2 .

Using (5) and (6), (22) can be written

$$M = \frac{C}{a + b\sqrt{V}} \cdot \frac{R}{R_a} \tag{23}$$

This equation shows that at constant air velocity V the time constant is proportional to the hot-wire resistance R which depends on the operating temperature chosen.

III. FREQUENCY RESPONSE OF A CONSTANT-TEMPERATURE-OPERATION HOT-WIRE ANEMOMETER

In a constant-temperature hot-wire anemometer the wire temperature is controlled by automatic adjustment of the current through the wire. To this end variations in the wire resistance which indicate the variations of the wire temperature are measured in a Wheatstone bridge circuit. The bridge output voltage is amplified, and the amplifier output current is supplied to the Wheatstone bridge, as shown in Fig. 2. The heating due to the current variations should balance the cooling due to the velocity variations.

In this section the response of the amplifier's output current to variations in air velocity will be discussed.

In the practical bridge arrangement, maximum efficiency has been obtained by making $R_2 \gg R_3 \gg R$, so that the full output current passes through the hot wire, and the voltage variations e across the hot wire are not carried over to R_1 . Under these conditions, the branch voltages can be written

$$E_1 = \frac{R_1}{R_2} R_3 I, \text{ hence } e_1 = \frac{R_1}{R_2} R_3 i \tag{24}$$

and

$$E = RI, \text{ hence } e = rI + Ri. \tag{25}$$

If the bridge is balanced for static conditions,

$$R = \frac{R_1}{R_2} R_3 \tag{26}$$

and (24) can be written

$$e_1 = Ri. \tag{27}$$

In that case the bridge output voltage is found from (25) and (27) to be

$$e_b = e_1 - e = rI. \tag{28}$$

From this expression it is obvious that the bridge output is related only to variations in the hot-wire resistance.

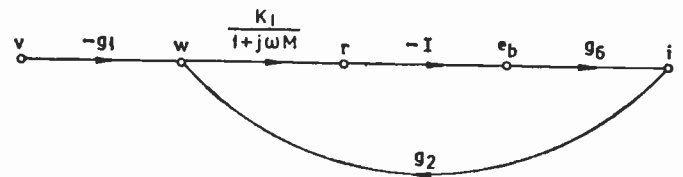


Fig. 5—Signal flow graph of cto anemometer in the idealized case of static bridge balance and zero transconductance of the amplifier for in-phase input signals.

Fig. 5 gives a signal flow graph of the cto anemometer for the above-mentioned idealized conditions. This figure differs from Fig. 4 in that the transfers $-I$ and g_6 are added, $-I$ being the transfer function of the bridge and g_6 being the transconductance of the amplifier. The latter is a function of the frequency. The amplifier's bandwidth is necessarily much larger than the frequency of the turbulence to be studied. The trans-

conductance g_6 can therefore, for a first approximation, be considered constant. The static loop gain of the feedback loop is

$$S = K_1 I g_6 g_2 = 2R \frac{\lambda}{1 - \lambda} g_6 = 2R \left(\frac{R}{R_a} - 1 \right) g_6. \quad (29)$$

In the constructed instrument $S \gg 1$ so that the transfer function from v to i as derived from Fig. 5 can be written

$$\frac{i}{v} = \frac{g_1}{g_2} \frac{S}{1 + S} \frac{1}{1 + j\omega M'} \approx \frac{g_1}{g_2} \frac{1}{1 + j\omega M'} \quad (30)$$

with

$$M' = \frac{M}{1 + S} \approx \frac{M}{S}. \quad (31)$$

From (31) it is obvious that the time constant M' of the hot wire incorporated into the feedback loop can be made very small by providing a large loop gain S . Thus the cutoff frequency can be shifted from a few hundred cycles per second for the hot wire in an open circuit to several tens of kilocycles per second in the closed circuit.

From (30) it is seen that the static transfer from v to i is approximated by g_1/g_2 and thus is independent of the amplifier's transconductance g_6 . It follows from Fig. 4 that the quotient g_1/g_2 is also equal to the quotient of r/v and r/i as given in (16) and (17), respectively, so that (30) can be written

$$\frac{i}{v} = \frac{I}{4V} \frac{b\sqrt{V}}{a + b\sqrt{V}} \frac{1}{1 + j\omega M'}. \quad (32)$$

A few practical figures can now be derived. For a hot wire of 3μ , with a length of 1 mm, the "cold" resistance R_a is about 10 ohms, and the cutoff frequency $1/(2\pi M)$ is about 200 cps at zero mean air velocity to 2000 cps at an air velocity of 40 meters per second (see Section VII).

To raise the cutoff frequency to 20 kilocycles per second, a static loop gain S of about 100 is necessary. A practical value of R_a/R is $\frac{2}{3}$, which makes $R = 15$ ohms.

Now the amplifier's necessary transconductance follows from (29):

$$g_6 = \frac{S}{2R \left(\frac{R}{R_a} - 1 \right)} \approx 7 \text{ mho.} \quad (33)$$

In the constructed instrument, values between 5 and 15 mhos are obtained, depending on the range of the output current chosen.

In the foregoing it has been presumed that the bridge is balanced in the static condition. In practice, however, there will always be a certain unbalance, e.g., due to drift of the controlling amplifier or to a change in the mean air velocity.

Another complication of practical importance is caused by the nonzero transconductance of the amplifier for an in-phase input voltage, i.e., a voltage between both input terminals and earth.

The influence of these undesired properties on the over-all transfer function will now be analyzed.

The output signal of the bridge follows from (24) and (25):

$$e_b' = e_1 - e \left(\frac{R_1}{R_2} R_3 - R \right) i - rI = \Lambda Ri - rI \quad (34)$$

with

$$\Lambda = \frac{R_1}{R_2} \frac{R_3}{R} - 1. \quad (35)$$

Λ is a measure of the static bridge unbalance. Comparing (28) and (34) shows that in the latter a term proportional to the bridge unbalance Λ is added.

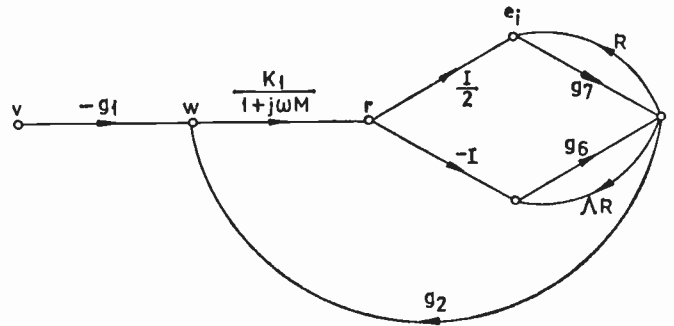


Fig. 6—Signal flow graph of cto anemometer in the general case of an amplifier with a finite rejection factor $f = g_6/g_7$ and a static bridge unbalance Λ .

In the signal flow graph (Fig. 6) this term is represented by a feedback path across the amplifier's transconductance g_6 .

To find the influence of a transconductance for in-phase input signals of the controlling amplifier, make the in-phase signal component

$$\frac{e_1 + e}{2} = e_i \quad (36)$$

or, using (24), (25) and (35),

$$e_i = iR \left(1 + \frac{\Lambda}{2} \right) + \frac{rI}{2}$$

which at small values of Λ can be approximated by

$$e_i \approx iR + \frac{rI}{2}. \quad (37)$$

This equation is represented in the flow graph, Fig. 6, by the transfers R and $I/2$ from i and r to e_i . The transconductance of the amplifier for in-phase input signals is in Fig. 6 represented by g_7 . Make

$$g_7 = \frac{g_6}{f} \quad (38)$$

where f is the rejection factor of the amplifier and the ratio of the gains for the anti-phase input signal e_b and the in-phase input signal e_i [10].

The static loop gain of the main feedback loop $i-w-r-i$ in Fig. 6 is now

$$S' = \frac{S \left(1 - \frac{1}{2f}\right)}{1 - g_6 R \left(\Lambda + \frac{1}{f}\right)} \approx \frac{S}{1 - q} \quad (39)$$

if

$$q = g_6 R \left(\Lambda + \frac{1}{f}\right). \quad (40)$$

From (39) it is seen that the loop gain S is increased or decreased by the additional loops in Fig. 6, depending on the sign of q .

The over-all transfer function from v to i is now

$$\frac{i}{v} = \frac{g_1}{g_2} \frac{S'}{1 + S'} \frac{1}{1 + j\omega M''} \approx \frac{g_1}{g_2} \frac{1}{1 + j\omega M''} \quad (41)$$

where

$$M'' = \frac{M}{1 + S'} \approx \frac{M}{S'} \quad (42)$$

or

$$M'' = M'(1 - q). \quad (43)$$

From (43) and (40) it is seen that a static bridge unbalance Λ and/or a finite rejection factor f of the amplifier for in-phase input signals have a considerable influence on the reduction of the hot wire's time constant. As g_6 and g_7 depend in a different way on the frequency, the rejection factor f in (40) is also frequency dependent.

IV. STABILITY REQUIREMENTS

The idealized case of Fig. 5, where the amplifier is drift-free and not sensitive for in-phase input signals, has already been analyzed extensively by Eli Osssofsky [6].

The dynamic loop gain as derived from Fig. 5 is

$$S_d = -g_2 g_6 I \frac{K_1}{1 + j\omega M} \quad (44)$$

in which g_2 and K_1 are scalar factors, given by (11) and (4). In the case of a 3-stage amplifier with equal time constants τ per stage, the transconductance g_6 can be written

$$g_6 = \frac{g_0}{(1 + j\omega\tau)^3} \quad (45)$$

where g_0 represents the amplifier's transconductance at low frequencies. The influence of the drift correction amplifier (see Fig. 7) at zero and very low frequencies is discussed later on. Making

$$S_0 = g_2 g_0 I K_1 \quad (46)$$

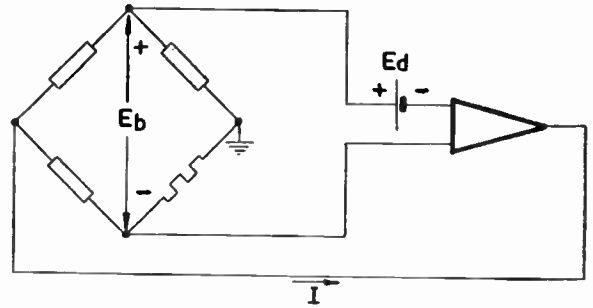


Fig. 7—If the amplifier's drift is equivalent to an input voltage variation E_d , a bridge unbalance voltage $E_b \sim E_d$ is generated by the feedback loop.

leads to

$$S_d = \frac{-S_0}{(1 + j\omega\tau)^3 (1 + j\omega M)} \quad (47)$$

Eq. (47) is equivalent to (11b) of Eli Osssofsky [6]. To allow a static loop gain S_0 of 100, the ratio M/τ should be 500 or greater to prevent self-oscillation.

Turning to the case of Fig. 6, the loop gain can be derived to be

$$S_d' = \frac{1}{1 - q} \frac{-S_0 \left(1 - \frac{1}{2f}\right)}{(1 + j\omega\tau)^3 (1 + j\omega M)} \approx \frac{-S_0}{(1 - q)(1 + j\omega\tau)^3 (1 + j\omega M)} \quad (48)$$

where q is given by (40).

Comparing (47) and (48) shows that the loop gain is increased or decreased by the additional feedback loops of Fig. 5, depending on the signs and magnitudes of f and q .

An increase in loop gain increases the bandwidth requirements for maintaining dynamic stability. To find the full dynamic requirements, it is necessary to study the frequency response (48), taking into consideration that q and f are functions of frequency.

Apart from dynamic instability, there is the possibility of "static" instability if the static loop gain $S_0/1 - q$ becomes positive. Thus the condition for "static" stability is

$$q < 1 \quad (49)$$

which is safely met if both parts of q are small enough, e.g.,

$$g_6 R \Lambda < 0.3 \quad (50)$$

and

$$\frac{g_6 R}{f} < 0.3. \quad (51)$$

Sources of bridge unbalance Λ are drift of the controlling amplifier and changes in the mean air velocity.

Drift of the amplifier is equivalent to a drift voltage source put in series with the input leads of the amplifier,

for instance, E_d in Fig. 7. Because of the feedback, this voltage is balanced by a bridge output voltage

$$E_b = E_d \frac{S}{1 + S} \approx E_d \tag{52}$$

Because

$$E_b = \Delta E = \Delta IR \tag{53}$$

(50) can be written

$$\frac{g_s E_d}{I} < 0.3. \tag{54}$$

Practical values $g_s = 10$ mho at $I = 30$ ma and substituted in (54) give the amplifier's drift requirements

$$E_b = E_d < 1 \text{ mv.} \tag{55}$$

In the long run this requirement can only be met if use is made of a chopper stabilized amplifier [12], as shown in Fig. 8. The chopper dc amplifier in this arrangement lifts the static gain of the amplifier by about a factor 500, thus reducing the drift of the amplifier by about the same factor.

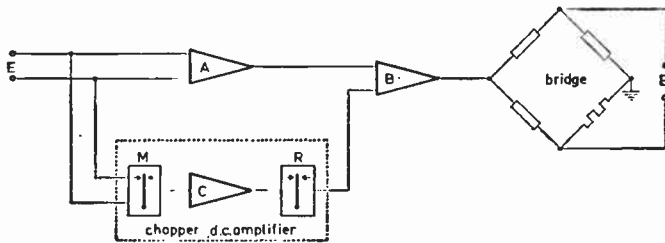


Fig. 8—A chopper dc amplifier is added to the circuit to meet the drift requirements. The blocks A and B represent wide-band dc amplifiers. The chopper dc amplifier consists of the modulator M, the ac amplifier C and the synchronous rectifier R.

Changes in the mean air velocity cause changes in the mean bridge current I , which maintain the hot wire at its correct resistance. Values found in practice are about 20 ma at zero air velocity to 100 ma at an air velocity of 40 m/sec. With an average transconductance in this range of $g_s = 10$ mhos, the variation in the amplifier's input (or bridge output) voltage needed to bring about this output current variation is 6 mv, which is higher than the figure quoted in (55). In the arrangement shown in Fig. 8, however, the static gain is increased by about a factor 500, so that the actual input voltage variation needed is not 6 mv, but only $12 \mu\text{v}$. Thus the chopper stabilizer offers the additional advantage of correcting automatically for changes in the mean air velocity.

The amplifier's rejection requirements are found from (52):

$$f > \frac{g_s R}{0.3} \tag{56}$$

Putting $R = 15$ ohms and $g_s = 10$ mhos into (56) gives

$$f > 500. \tag{57}$$

The rejection requirements for the chopper dc amplifier are much more exacting because at zero and very low frequencies it lifts the gain of the amplifier by about a factor 500. Thus the rejection factor of the chopper amplifier should exceed $500 \times 500 = 250,000$.

V. SIGNAL-TO-NOISE RATIO

It seems to be commonly held [6] that the SNR of comparable hot-wire anemometers is less favorable in the case of those having constant temperature operation since these require, for reasons of stability, a considerably larger bandwidth in the controlling amplifier than do those employing constant current operation.

It is the authors' opinion that this statement in its above-given general form is not valid; it is certainly not only the bandwidths of the different controlling amplifiers which determine the SNR at the instrument output terminals.

All the noise (thermal, shot, partition, secondary emission) in a certain frequency band can effectively be replaced by a single noise source at the input of the amplifier. The only basic difference between the setup of a cto and a cco hot-wire anemometer is, then, that the former has a feedback loop and the latter has not. However, it is well known that feedback does not influence the SNR for noise sources at the input of a system. If, therefore, the quality of the first stage of the controlling amplifiers and the over-all bandwidth of the measuring setup are equal for the cto and the cco systems, their SNR will also be equal.

If in the case of comparable instruments (*i.e.*, instruments designed for measuring turbulence up to the same maximum frequency) the bandwidth of the controlling amplifier is larger for the cto hot-wire anemometer than for the cco instrument, it goes without saying that the amount of high-frequency noise in the case of cto is larger at the output of the controlling amplifier. However, at the output of the hot-wire anemometer as a whole the additional noise is cut off in the low-pass output filters that determine the over-all bandwidth.

VI. METHOD OF MEASURING THE OVER-ALL TRANSFER FUNCTION

It is extremely difficult, if not impossible, to measure the transfer function i/v directly by varying the air velocity. It is possible, however, to measure this transfer function in an indirect way by introducing an electrical disturbance into the control circuit [6].

The measuring setup is shown in Fig. 9. An external current i_e from a high-impedance source is introduced into the circuit, and the response of the amplifier output current i_a is measured. For the idealized case that $q = 0$ (no static bridge unbalance, infinite rejection of in-phase inputs), the transfer function is found from the signal flow graph of Fig. 10,

$$\frac{i_a}{i_e} = - \frac{S}{1 + S} \cdot \frac{1}{1 + j\omega M'} \approx - \frac{1}{1 + j\omega M'} \tag{58}$$

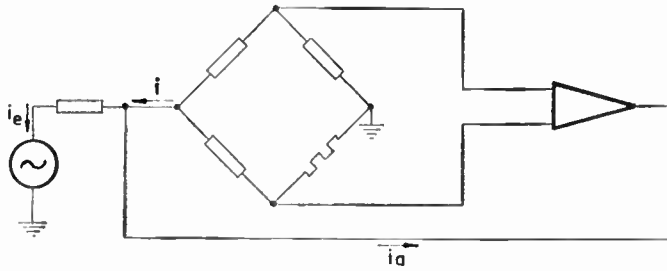


Fig. 9—A sinusoidal current i_e is injected into the circuit to find the frequency response of the cto anemometer.

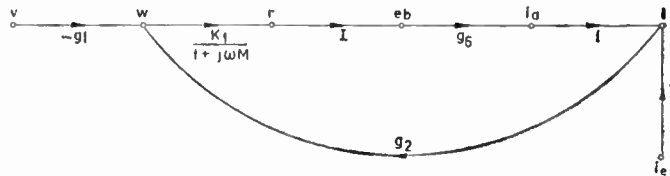


Fig. 10—Signal flow graph of the circuit given in Fig. 9 for $q=0$; that is at zero bridge unbalance and infinite rejection of in-phase input signals.

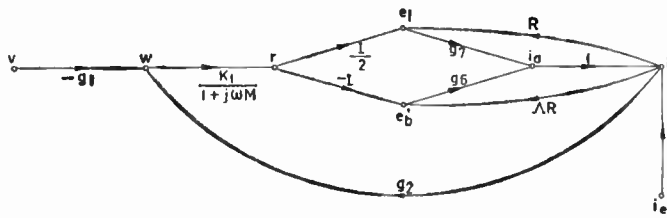


Fig. 11—Signal flow graph of the circuit of Fig. 9 in the practical case of a static bridge unbalance Λ and an amplifier with a finite rejection factor $f=g_6/g_7$.

where S and M' are given by (29) and (31), respectively.

Comparing (30) and (58) one notices that the transfer functions i/v and i_a/i_e differ only by a scalar factor. Thus to find the transfer characteristics of i/v one could instead measure i_a/i_e which is more attractive since i_e can easily be varied sinusoidally or stepwise.

In the case of a finite rejection factor f and a static bridge unbalance, the signal flow graph of Fig. 11 is valid with the transfer function

$$\frac{i_a}{i_e} \approx \frac{1}{1-q} \left(q - \frac{1}{1+j\omega M''} \right). \quad (59)$$

The response consists then of two parts: one part is a proportional response, the other part is governed by the transfer function $1/(1+j\omega M'')$. The proportional part can be either positive or negative depending on the sign of q .

Both the sign and the magnitude of the proportional part q can be found simply by varying i_e stepwise. The step response of the proportional part is another step; the step response of the other part is a first-order exponential function with a time constant M'' . The ratio of the static values of the proportional and the exponential parts of the total step response is then equal to $-q$.

Thus, in the case where $q \neq 0$, this method can likewise be used to find the transfer characteristic of i/v .

VII. RESULTS OF MEASUREMENTS AND CALCULATIONS

Eq. (21) can be rewritten as follows:

$$M = \left(\frac{\pi}{4} \right)^2 \cdot d^4 \cdot \beta \cdot \gamma \frac{T - T_a}{\rho_a \cdot I^2}. \quad (60)$$

Here

d = the diameter of the hot wire.

β = the density of the hot-wire material.

γ = the specific heat of the hot-wire material.

T = the hot wire temperature.

T_a = the air temperature.

ρ_a = the specific resistance of the hot-wire material at the temperature of the air.

I = the heating current.

From (60) it is possible to calculate the time constant. For a tungsten wire with diameter 3μ , operated under the following conditions: $I = 20$ ma, $T - T_a \approx 100^\circ\text{C}$, $V = 0$ m/sec, M is found to be about 0.6 msec.

Another way of determining M is by direct measurement. This can be done in the same bridge circuit as given in Fig. 2. In this case, however, the loop is not closed. In the setup of Fig. 12 the amplifier A_1 is only used as a means to amplify the voltage e_b , which in (28) was found to be proportional to the variations r in the hot-wire resistance. Another amplifier A_2 is used to amplify the voltage e_1 , which is a measure of the current i [see (24)].

At static bridge balance and complete rejection of in-phase signals, the signal flow graph of Fig. 13 is valid, from which is found

$$\frac{e_4}{i} = - \frac{SR_4}{1 + j\omega M}. \quad (61)$$

At static bridge unbalance and incomplete rejection of in-phase signals, the signal flow graph of Fig. 14 is valid, which results in an over-all transfer:

$$\frac{e_4}{i} = - R_4 \left(\frac{S}{1 + j\omega M} - q \right).$$

In the case of an open circuit, however, it is easy to compensate the incomplete rejection of in-phase signals by introducing a static bridge unbalance to make $q = 0$.

The output voltages e_1 and e_5 in the setup of Fig. 12 were compared on an oscilloscope. Thus the ratio r/i was measured as a function of the frequency. This resulted in the locus of Fig. 15, which indeed shows the behavior of a first-order system as was found in Section II.

The time constant M as derived from Fig. 15 is about 0.8×10^{-3} seconds. This is in fair agreement with the value calculated above from (60), especially if one takes into consideration that a small amount of dust on the wire has a considerable influence on the time constant. Moreover, owing to the fourth power of the wire diameter d occurring in (60), an error of 10 per cent in d brings about a change of about a factor 1.5 in the time constant M .

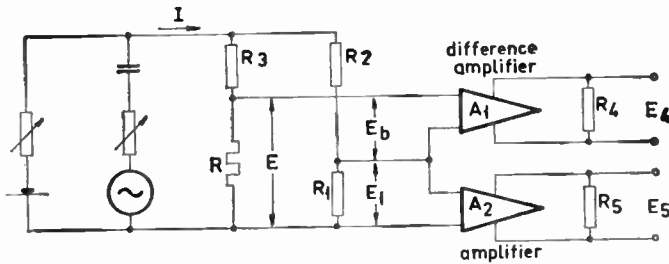


Fig. 12—Arrangement for measuring the hot wire's frequency response.



Fig. 13—Signal flow graph of the circuit of Fig. 12 under idealized conditions.

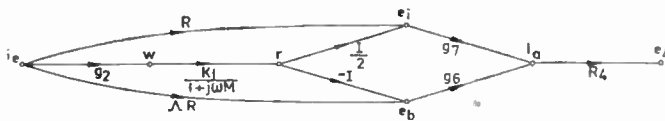


Fig. 14—Signal flow graph of the circuit of Fig. 12 under practical conditions.

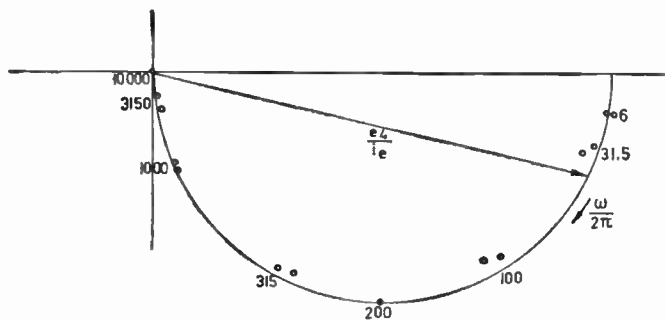


Fig. 15—Measured locus of the hot wire's frequency response.

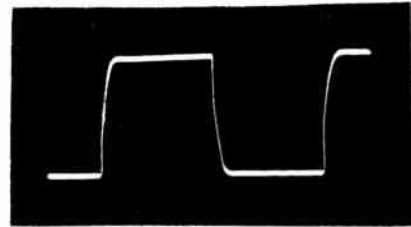
The scatter in the results of the measurements could in part be due to the fact that several burnouts of the hot wire prevented the various measurements from being carried out with one wire.

An effective way of testing the over-all performance of a cto hot-wire anemometer is by introducing a step signal i_e into the setup of Fig. 9.

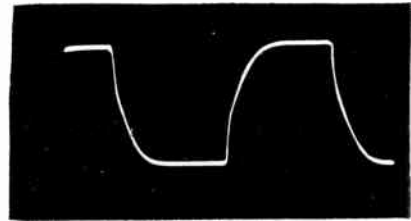
Fig. 16(a) and 16(b) give the response of i_a to a square wave disturbance in i_e with frequencies of 3000 and 10,000 cps, respectively; both figures are for zero air velocity. It is seen that the response of i_a consists of two parts, the amplitude ratio of these two parts being equal to q [see (59)]. From Fig. 16(b) one finds $q = -0.8$.

The drift correction amplifier maintains the static unbalance of the bridge well within $\pm 100 \mu v$, so that the contribution of Λ to q [see (40)] is negligible. The value of f is now found from (40) by putting $g_6 = 10$ mhos and $R = 15$ ohms at $q = -0.8$ and $\Lambda = 0$:

$$g = \frac{g_6 R}{q} = -190.$$



(a)



(b)

Fig. 16—(a) Response of i_a to a square-wave disturbance in i_e with a basic frequency of 3000 cps. Zero air velocity. (b) Same as (a) but with a basic frequency of 10,000 cps.

Thus the absolute value of f does not meet requirement (57), but since the sign is negative, f causes negative feedback. In a future design an attempt should be made to improve this figure.

Making $R = 15$ ohms, $R/R_a = 1.5$, $g_6 = 10$ mhos and $q = -0.8$ in (29) and (39) one finds

$$S = 150 \text{ and } S' = 80.$$

By means of (42) it is now possible to calculate M'' . From the measured value of $M = 0.8$ msec one finds $M'' = 10 \mu\text{sec}$, which is in good agreement with the time constant of the exponential part of Fig. 16(b) [see (59)].

From $M'' = 10 \mu\text{sec}$ we can calculate the 3-db point to be 16×10^3 cps. Direct measurement of the 3-db point by means of sinusoidal variations in i_e yielded a value which was about 20×10^3 cps.

In the tests in which Fig. 16(a) and 16(b) give the response of the amplifier current i_a , the air velocity chosen was zero since there is then only one kind of signal entering the control circuit.

To find the over-all performance of a hot-wire anemometer measurements under various operating conditions are necessary because the time constant of the wire depends on the air velocity. At air velocities not equal to zero, i_e should be made sufficiently high to be well above the signal level of the turbulence.

It was found that the constructed cto hot-wire anemometer showed a drop of 1 per cent in the modulus of the transfer function i/v at a frequency of about 20×10^3 cps under the following conditions:

$$V \approx 3 \text{ m/sec}$$

$$\frac{R}{R_a} = 1.57$$

$$I = 65 \text{ ma.}$$

Fig. 17(a) and 17(b) gives a picture of the response of i_a to a square-wave disturbance in i for $V \neq 0$. These figures are partly blurred due to the turbulence signal. It should be noted that Fig. 17(a) and 17(b) shows a certain overshoot, which is not present in Fig. 16(a) and 16(b). This phenomenon is to be ascribed to a lower value of M [see (21)], and the influence of M on the dynamic loop gain according to (48).

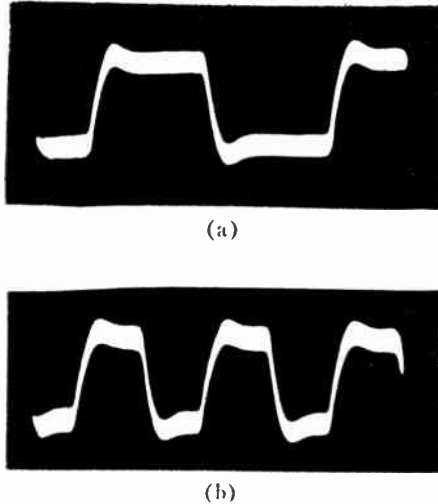


Fig. 17—(a) Response i_a to a square-wave input i_a with a basic frequency of 10,000 cps. Air velocity not zero. (b) Same as (a) but with a basic frequency of 20,000 cps.

VIII. LINEARIZING

From King's equation (5) and the power equation (6) it follows that the relation between the bridge current I and the air velocity V will be

$$V = \left[\frac{\frac{R}{T - T_a} I^2 - a}{b} \right]^2 \tag{62}$$

or

$$V = \{(\Phi I)^2 - \Psi\}^2 \tag{63}$$

with

$$\Phi = \sqrt{\frac{R}{b(T - T_a)}} \tag{64}$$

and

$$\Psi = \frac{a}{b} \tag{65}$$

The parameters Φ and Ψ depend on the hot-wire dimensions and the hot-wire temperature T .

The block diagram of the linearizer is given in Fig. 18. A variable resistor R_s in series with the bridge is used to adjust the parameter Φ . Two squarers perform the squaring operations of (63). The parameter Ψ is introduced in a subtracting unit between the two squarers.

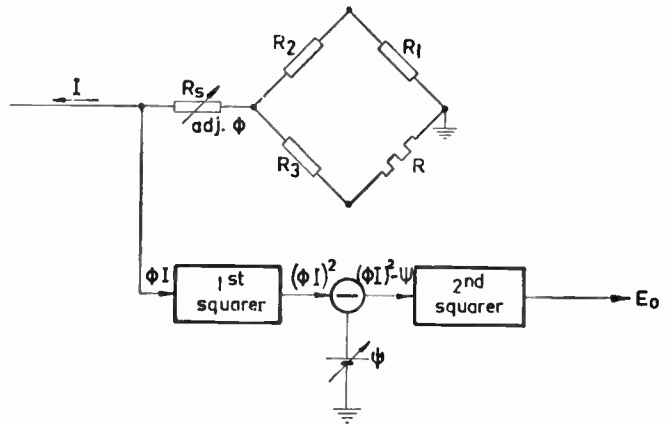


Fig. 18—Block diagram of linearizer. The output E_0 is proportional to the measured air velocity.

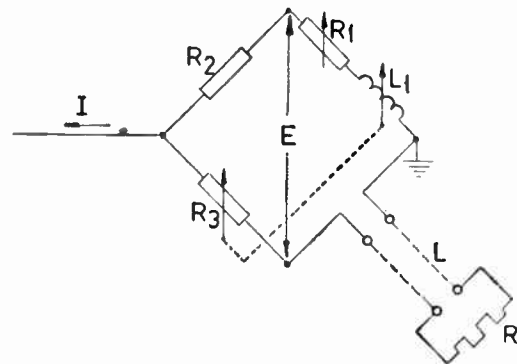


Fig. 19—Bridge arrangement.

During a test the parameters Φ and Ψ were adjusted so as to obtain maximum output at an air velocity of 40 m/sec and quarter-scale output at 10 m/sec. Succeeding measurements showed the output voltage E_0 to be proportional to the air velocity within 2 per cent.

IX. CONSTRUCTION

The starting point for the design and construction was to make an instrument for the kilocycle range, provided with linearizing and suitable for use by people without experience in electronics.

The restricted frequency range allowed the hot wire to be connected to the bridge by means of a connecting cable. The other elements of the bridge (see Fig. 19) are located in the instrument. The equilibrium value of the hot wire's operating resistance is read directly from the positions of two switches in the branches R_1 and R_3 respectively. R_3 is for coarse adjustment in 3 steps and R_1 for fine adjustment in 11 steps. The total range of R is from 4.5 to 44 ohms.

The series self-inductance L of the hot-wire probe leads and connecting cable is corrected by means of a self-inductance L_1 in series with R_1 . As

$$\frac{L_1}{L} = \frac{R_1}{R} = \frac{R_2}{R_3} \tag{66}$$

and L and R_2 are constant; the value of L_1 is related only to that of R_3 .

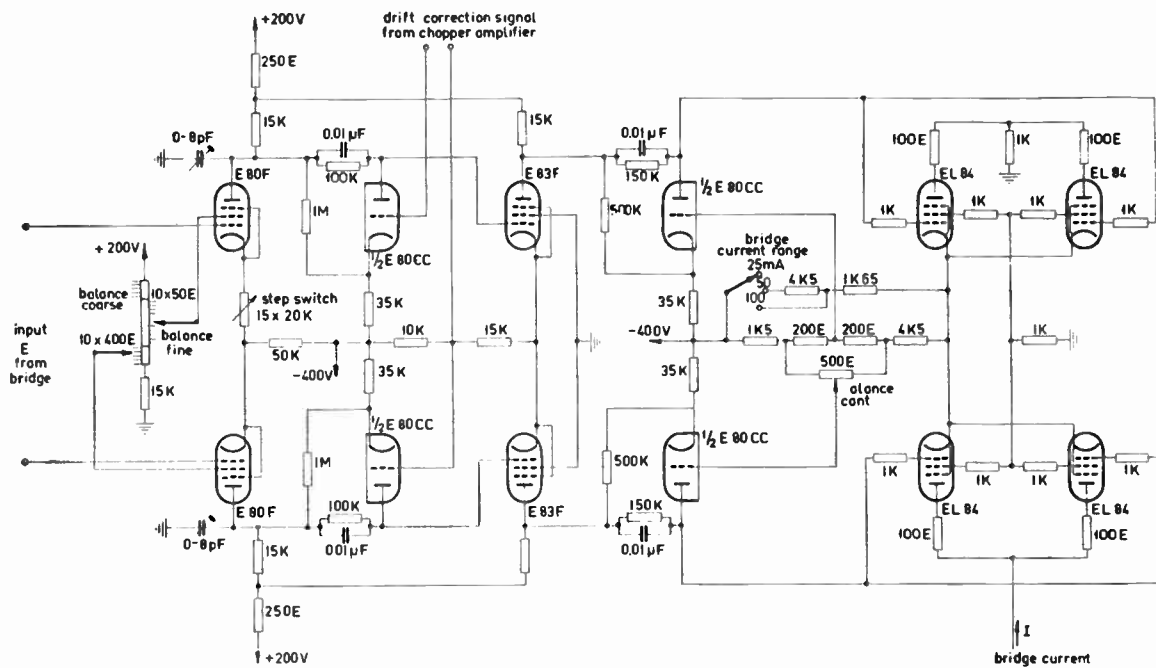


Fig. 20—Control amplifier.

The dc amplifier (Fig. 20) is a further development of Ossfosky's amplifier [6]. To obtain a large rejection factor for in-phase signals, the input tubes are equalized by means of an adjustable resistance in series with one of the cathodes. In a more advanced design, the rejection factor could be considerably improved without any equalizing means at all by applying the technique described by Klein [10]. Initial balance is adjusted by means of two tap switches in the screen grids supply of the first stage and by a potentiometer in the voltage divider between the second and the output stages. The bridge current range is chosen by means of an adjustable resistor in the common cathode circuit of the output stage. The drift correction signal from the chopper amplifier is injected in one of the Mezger type voltage dividers [11] between the first and the second amplifier stages.

The chopper amplifier is shown in Fig. 21. The input filter has two sections. The first section is symmetrical and serves to attenuate in-phase ac components, the second to attenuate anti-phase ac components. To obtain a good rejection factor both statically and dynamically for in-phase signals, the amplifier has a differential input stage. To prevent insulation currents setting up a static difference input signal across R_1 and R_2 , a system of guarding (not shown in Fig. 21) was needed in the chopper circuit.

The output chopper rectifier is followed by a filter for reducing the ripple voltage.

The entire chopper amplifier circuit now contains three low-pass filter sections, *i.e.*, two at the input and one at the output. To prevent instability in the closed loop due to the phase lag of these filters, the time constant of the output filter was increased to 800 seconds.

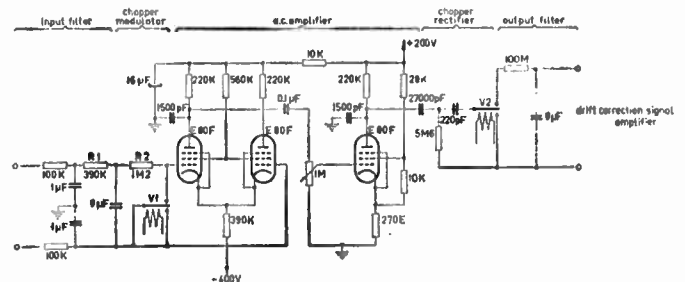


Fig. 21—Drift correction amplifier.

An electronic galvanometer is permanently connected to the bridge output. Its circuit is a simplified version of that of the drift correction amplifier. It serves as a continuous indicator of the bridge unbalance voltage but does not load the bridge, and the indicator is not damaged by overload, *e.g.*, in the case of hot-wire burnout.

The block diagram of the linearizer is shown in Fig. 18. The electronic circuit is given in Fig. 22. The squarers are of the diode function generator type [12].

Fig. 23 shows the complete anemometer without hot-wire probe. The upper panel contains the control amplifier, the chopper amplifiers for the galvanometer and the drift correction, the linearizer, an attenuator and a pre-amplifier for the ac output signal. The center panel contains low-pass filters, an integrator circuit for studying macro-scale eddies, a differentiator circuit for studying micro-scale eddies [13], [14], and a rms voltmeter.

The lower panel contains supply units for the stabilized dc supply, not only of anode and screen voltages, but also of the filament currents of several critical tubes in the circuits.

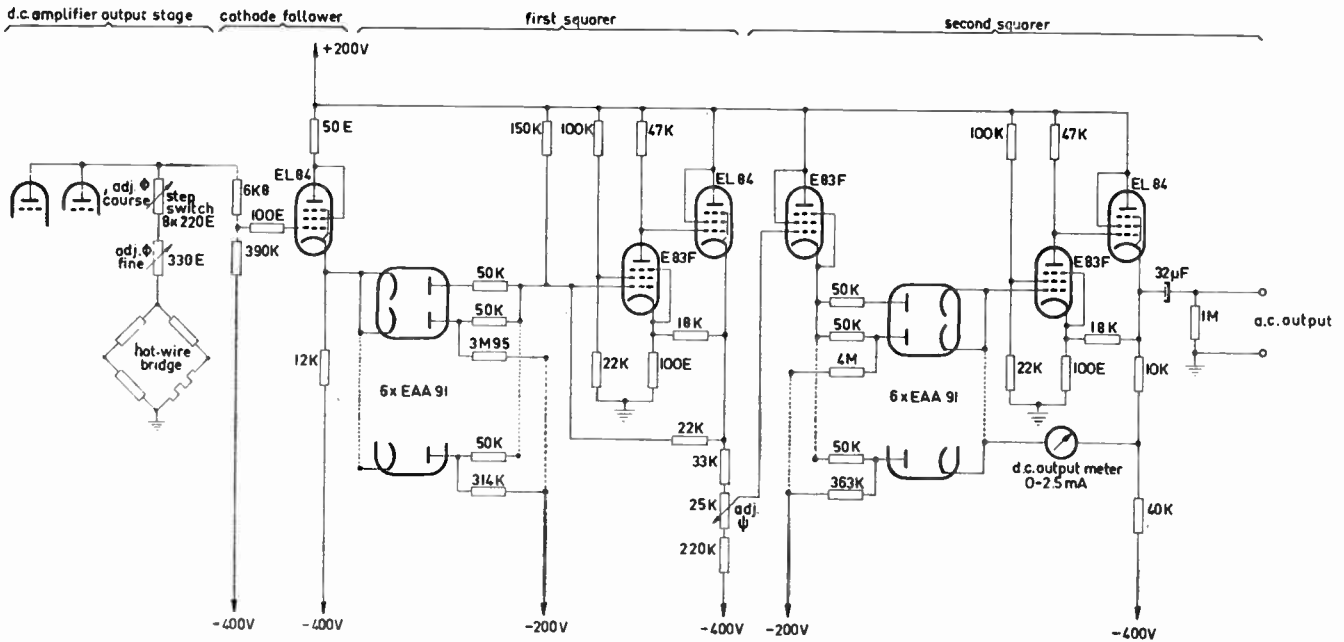


Fig. 22—Linearizer.

X. OTHER TYPES OF CTO HOT-WIRE ANEMOMETERS

Various ways of controlling the resistance of the hot wire other than that described above are possible. The main features by which these systems can be distinguished are: 1) the way in which the hot-wire resistance is measured, and 2) the method by which the hot wire is heated.

In the system which is the subject of this paper, the measuring of the resistance and the heating of the hot wire are both accomplished by means of a dc current. This has a drawback in that the heating current interferes with the measuring signal when the bridge is not well balanced.

However, in a system which measures the hot-wire resistance by means of a RF current and which heats the hot wire with a dc current (or reversed: measuring with dc and heating with RF current) as has been suggested by Ziegler [4] one can obtain a system in which the heating does not influence the measurement. Figs. 24 and 25 give two possible systems; Figs. 26 and 27 give their respective signal flow graphs.

It is seen that the nonessential loops can in this way be eliminated. However, the number of elements in the control loop is increased, each element adding to the total phase lag in the loop.

It remains to be seen whether the advantages of a system where measurement and heating of the hot-wire resistance do not influence each other are a sufficient compensation for the stability problems that will occur as a result of the additional phase lags in the control loop.

Other possible systems would be those using radio frequency currents both for measuring and for heating.

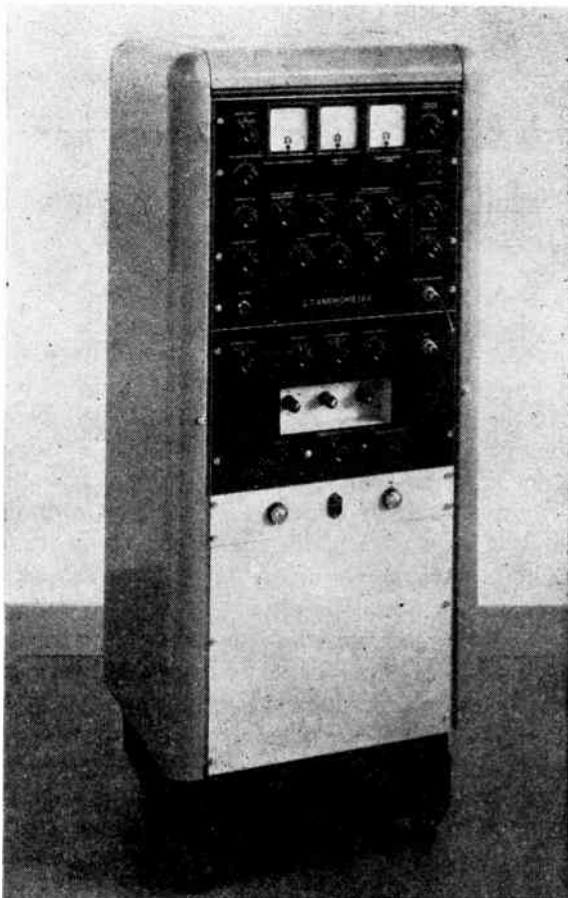


Fig. 23—The constructed constant-temperature operation hot-wire anemometer.

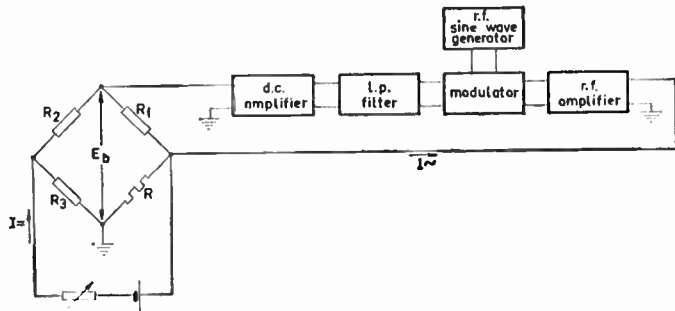


Fig. 24—CTO anemometer with dc bridge supply and ac heating current supply.

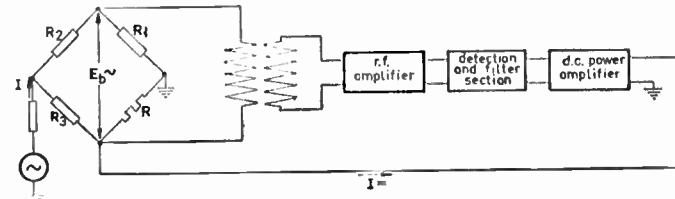


Fig. 25—CTO anemometer with ac bridge supply and dc heating current supply.

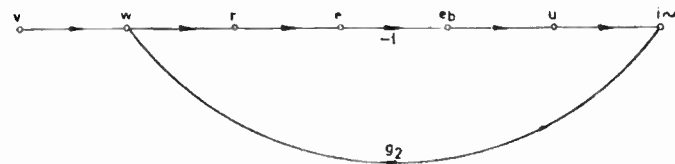


Fig. 26—Signal flow graph of the circuit of Fig. 24.

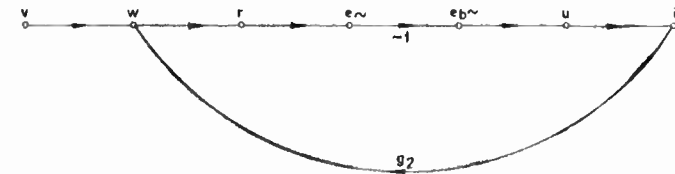


Fig. 27—Signal flow graph of the circuit of Fig. 25.

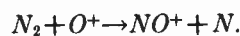
BIBLIOGRAPHY

- [1] Hegge Zijnen, van der B. G. "On the construction of hot-wire anemometers for the investigation of turbulence," *Applied Scientific Research*, vol. A2, pp. 351-363; 1949-1951.
- [2] Dryden, H. L., and Kuethe, A. M. "The Measurement of Fluctuations of Air Speed by the Hot-Wire Anemometer," National Advisory Committee for Aeronautics, Washington, D. C., Rep. No. 320; 1929.
- [3] Runyon, R. A., and Jeffries, R. J. "Empirical Method for Frequency Compensation of the Hot-Wire Anemometer," National Advisory Committee for Aeronautics, Washington, D. C., Tech. Note 1331; June, 1947.
- [4] Ziegler, M. "The Construction of a Hot-Wire Anemometer with Linear Scale and Negligible Lag," *Laboratorium voor Aerodynamica et Hydrodynamica der Technische Hogeschool te Delft, in Verhandelingen der Kon. Ned. Akademie van Wetenschappen te Amsterdam, Afdeling Natuurkunde, Mededeling 29*; 1934.
- [5] Weske, J. R. "A Hot-Wire Circuit with Very Small Time Lag," National Advisory Committee for Aeronautics, Washington, D. C., Tech. Note 881; February, 1943.
- [6] Ossofsky, E. "Constant-temperature operation of the hot-wire anemometer at high frequency," *Review of Scientific Instruments*, vol. 19, pp. 881-889; December, 1948.
- [7] Mason, S. J. "Feedback theory—further properties of signal flow graphs," *PROCEEDINGS OF THE IRE*, vol. 44, pp. 920-926; July, 1956.
- [8] Betchov, R. "Théorie non-linéaire de l'anémomètre à fil chaud," *Proceedings Royal Netherlands Academy of Sciences*, vol. 52, pp. 195-207; March, 1949.
- [9] King, L. V. "On the convection of heat from small cylinders in a stream of fluid: determination of the convection constants of small platinum wires with application to hot-wire anemometry," *Philosophical Transactions of the Royal Society of London*, vol. A 214, pp. 373-432; May, 1914.
- [10] Klein, G. "Rejection factor of difference amplifier," *Philips Research Reports*, vol. 10, pp. 241-259.
- [11] Mezger, G. R. "A stable direct-coupled amplifier," *Electronics*, Vol. 17, pp. 106-110, 352-353; July, 1944.
- [12] Korn, G. A., and Korn, T. M. "Electronic Analog Computers," McGraw-Hill Book Co., Inc., New York, N.Y. 2nd ed.; 1956.
- [13] Townsend, A. A. "The measurement of double and triple correlation derivatives in isotropic turbulence," *Proceedings of the Cambridge Philosophical Society*, vol. 43, pp. 560-570; 1947.
- [14] ———, "On the fine-scale structure of turbulence," *Proceedings of the Royal Society of London*, vol. A 208, pp. 534-542; September, 1951.
- [15] Kovásznay, L. S. G. "Development of Turbulence-Measuring Equipment," National Advisory Committee for Aeronautics, Washington, D. C., Tech. Note 2839; January, 1953.
- [16] Laurence, J. C., and Landes, L. G. "Applications of the constant-temperature hot-wire anemometer to the study of transient air-flow phenomena," *ISA Journal*, vol. 26, pp. 128-132; December, 1953.

CORRECTION

Herbert Friedman, author of "Rocket Observations of the Ionosphere," which appeared on pages 272-280 of the February, 1959 issue of PROCEEDINGS has requested that the following correction be made to his paper.

Eq. (2) on page 275, should read:



IRE Standards on Antennas and Waveguides: Waveguide and Waveguide Component Measurements, 1959*

59 IRE 2. S1

COMMITTEE PERSONNEL

Subcommittee on Waveguide and Waveguide Component Measurements

A. A. OLINER, *Chairman* 1955–1958

H. JASIK, *Chairman* 1954–1955

E. G. Fubini 1954–1955

A. A. Oliner 1954–1955

P. A. Loth 1955–1958

K. Packard 1955–1958

W. E. Waller 1955–1958

Committee on Antennas and Waveguides

G. A. DESCHAMPS, *Chairman* 1957–1958

A. A. OLINER, *Vice-Chairman* 1957–1958

H. JASIK, *Chairman* 1955–1957

G. A. DESCHAMPS, *Vice-Chairman* 1955–1956

P. H. SMITH, *Chairman* 1954–1955

H. JASIK, *Vice-Chairman* 1954–1955

K. S. PACKARD, *Secretary* 1957–1958

R. L. MATTINGLY, *Secretary* 1954–1956

J. Blass 1957–1958

H. Jasik 1957–1958

D. C. Ports 1954–1958

P. S. Carter 1954–1958

E. T. Jaynes 1954–1955

S. W. Rubin 1957–1958

M. J. DiToro 1957–1958

R. W. Klopfenstein 1957–1958

W. Sichak 1954–1958

G. A. Deschamps 1954–1955

O. E. Kienow 1954–1955

G. Sinclair 1954–1958

J. E. Eaton 1954–1955

D. J. LeVine 1957–1958

P. H. Smith 1955–1958

H. A. Finke 1954–1957

P. A. Loth 1954–1958

K. Tomiyasu 1955–1958

P. W. Hannan 1957–1958

R. L. Mattingly 1957–1958

W. E. Waller 1954–1958

W. C. Jakes, Jr. 1955–1957

A. A. Oliner 1954–1956

M. S. Wheeler 1955–1958

K. S. Packard, Jr. 1954–1956

Committee on Standards 1958–1959

R. F. SHEA, *Chairman*

J. G. KREER, JR., *Vice-Chairman*

C. H. PAGE, *Vice-Chairman*

L. G. CUMMING, *Vice-Chairman*

J. Avins

P. S. Carter

A. B. Glenn

D. E. Maxwell

R. L. Pritchard

W. F. Bailey

A. G. Clavier

V. M. Graham

H. R. Minno

P. A. Redhead

M. W. Baldwin, Jr.

G. A. De champs

R. A. Hackbusch

E. Mittelmann

R. Serrell

J. T. Bangert

S. Doba, Jr.

R. T. Haviland

L. H. Montgomery, Jr.

W. A. Shipman

W. R. Bennett

P. Elias

A. G. Jensen

G. A. Morton

H. R. Terhune

J. G. Brainerd

G. A. Espersen

I. Kerney

R. C. Moyer

E. Weber

D. R. Brown

D. Frezzolini

A. E. Kerwien

J. H. Mulligan, Jr.

R. B. Wilcox

T. J. Carroll

E. A. Gerber

G. S. Ley

W. Palmer

W. T. Wintringham

Wayne Mason

Measurements Coordinator

J. G. KREER, JR.

* Approved by the IRE Standards Committee, December 18, 1958. Reprints of this Standard, 59 IRE 2. S1, may be purchased while available from the Institute of Radio Engineers, 1 East 79th Street, New York, N. Y., at \$0.75 per copy. A 20 per cent discount will be allowed for 100 or more copies mailed to one address.

SECTION 1—GENERAL

1.1 Introduction

THIS STANDARD is concerned with measurements of the quantities which characterize a waveguide or waveguide component and the associated electromagnetic fields. The term "waveguide," as used here, is a generic term which includes transmission lines and uniconductor waveguides as special cases.

The measurements are described in general terms. For the specific details of procedure and equipment, the reader is directed to numerous references (Sec. 6), which form an indispensable part of this Standard.

Definitions of terms employed in this Standard are given in Sec. 5. These definitions are presented both to insure precision of meaning with regard to the measured quantities and to clarify possible conceptual differences in the usage of terms common to both microwave and low-frequency circuit practice. As an example of the latter, the term "match" has different significance in the two usages.

Section 2 is concerned with measurements in a waveguide having uniform characteristics. Sections 3 and 4 are concerned with components which are connected to or located in waveguides.

This Standard is limited to measurements in linear, reciprocal systems, and unless otherwise stated to single frequency sources. For example, it does not apply to special devices such as nonreciprocal ferrite components and crystal detectors.

1.2 Measurement Techniques

In general, the equipment required for waveguide measurements includes a signal source of the appropriate frequency and a suitable detector. In addition depending on the nature of the measurement being made, equipment such as attenuators, slotted lines, impedance bridges, sampling devices, and terminations may also be required. The exact form of this equipment will vary depending upon the nature of the waveguide, the frequency range, and the particular method used for the measurement.

Regardless of the equipment used, there are certain basic precautions which must be taken if the measurements are to be meaningful. The signal supplied by the source should be stable and free of harmonics and other spurious components and should be free of undesired modulation. In many cases, this requirement may be relaxed if the detector is selective enough so as not to respond to the undesired signals. Leakage into a detector either directly from the signal source, through undesired paths in the component, or from external sources should be guarded against. If the detector is used at other than a constant level, it is often necessary to know accurately the response law of the detector. In connecting the measuring equipment to the device being measured, care should be taken to minimize

unwanted discontinuities or reflections. If high precision is required, such discontinuities as do exist must be separately determined and accounted for in the data reduction. In certain kinds of measurements, it is desirable that the impedance of the source be matched to the characteristic impedance of the waveguide being used. For the case of balanced transmission line systems, care must be taken that the probe and detector respond only to the balanced component of the existing fields. This is a special case of the more general problem involving measurements in waveguides which can support multimode transmission, and it is obvious for such cases that the detector should respond only to the mode of interest.

SECTION 2—MEASUREMENTS IN WAVEGUIDES [1], [2]

2.1 Measurement of Voltage

(a) In transmission lines carrying a TEM mode, it is possible to measure the total voltage across the line (*i.e.*, the line integral, in the transverse plane, of the electric field strength) at frequencies below a few hundred mc with a reasonable degree of accuracy by using vacuum tube voltmeters or crystal diode voltmeters which are available commercially. In making this type of measurement, care should be taken to insure that the voltmeter does not unduly load the line. In addition, the voltmeter leads should not couple to any field other than that being measured.

(b) In a balanced transmission line system it is necessary that a balanced type of voltmeter be used. This may consist of an unbalanced voltmeter with a balance-to-unbalance transformer of known ratio. A second method of measuring a balanced voltage is to use a quarter-wave shunt stub of balanced transmission line with an ammeter shorting the line at the far end. The voltage across the line is equal to the current times the characteristic impedance of the stub line.

(c) In uniconductor waveguides, total voltage is not usually of interest. However, measurement of electric field strength is frequently of interest (see Sec. 2.3).

2.2 Measurement of Current [1], [3]

(a) In a transmission line carrying a TEM mode, the total current flowing in either conductor can be measured with a reasonable degree of accuracy at frequencies below several hundred mc with a thermo-couple type ammeter. At frequencies much lower than this, a thermo-ammeter is sometimes used.

(b) In a balanced transmission line system, the total current may be measured by inserting ammeters in series with each conductor or by using a single ammeter and a suitable coupling loop such that the loop couples only to the balanced component of the current [4]. If unbalanced currents are present, as may be evidenced by a difference in the meter readings on the two sides of the line or by other methods (see Sec. 2.12), it will be necessary to locate and remove the sources of the unbalance before proceeding with the measurement.

(c) In a uniconductor waveguide, the definition of total current has no practical importance. However, the local current density at a point on the surface can be determined by measuring the magnetic field strength at that point (see Sec. 2.4).

2.3 Measurement of Electric Field Strength [5]

The component of the electric field in a specified direction at a point in space is usually obtained by measuring the voltage induced in a small linear probe oriented in the specified direction. Care must be taken that the transmission line leading to the probe does not itself affect the field nor the probe pickup. It is important that the amount of power absorbed or scattered by the probe be small compared to the total power in the guide.

Although it is possible to make absolute electric field strength measurements by calibrating the probe, relative measurements are usually of most interest.

2.4 Measurement of Magnetic Field Strength [5]

The component of the magnetic field in a specified direction at a point in space is usually obtained by measuring the voltage induced in a small loop type probe oriented in the specified direction. Care must be taken that the transmission line leading to the probe does not itself affect the field nor the probe pickup. It is important that the amount of power absorbed or scattered by the probe be small compared to the total power in the guide.

It should be noted that a loop type probe will always have a certain amount of response to the electric field as well as to the magnetic field. This response can be minimized by keeping the loop and the associated meter balanced and by keeping sizes as small as possible. Balance can be checked by physically reversing the loop.

When measuring the magnetic field strength on a metallic surface, a small rectangular slot in the surface is sometimes used as the probing device. For this case, the voltage across the slot is measured.

Although it is possible to make absolute magnetic field strength measurements by calibrating the probe, relative measurements are usually of most interest.

2.5 Power Measurements [6]–[9]

(a) In a matched lossless transmission line carrying a TEM mode, the power absorbed by the load (which is equal to the incident power) can be determined from the characteristic impedance (Z_0) of the line and either the total voltage (V) or the total current (I). If the line is mismatched, the power (P) absorbed by the load can be computed from the value of either of these quantities at both a maximum and minimum.

$$P = \frac{V_{\max} V_{\min}}{Z_0} = I_{\max} I_{\min} Z_0.$$

The absorbed power is sometimes measured by the three meter method in which either voltage or current

readings are taken along a line at three appropriately spaced points [10].

(b) In a matched lossless waveguide, the incident power can be determined by measuring the power dissipated in the matched load or by extracting and measuring a known fraction of that power. If the waveguide is mismatched, the incident power can be determined by extracting, and measuring a known small fraction of the forward traveling wave by means of a directional coupler.

(c) There are several common methods of measuring the power in a matched load.

1. Measurement of resistance change. This method includes the use of devices such as bolometers and thermistors [7].
2. Calorimetric methods [7].
3. Thermo-electric (*e.g.*, thermo-couple) methods [7].

2.6 Measurement of Waveguide Wavelength [11]–[13]

A common means of measuring waveguide wavelength employs a movable probe for observing the standing wave along a length of the waveguide which is terminated by a mismatched load. The use of a short-circuit termination as the mismatched load will improve the accuracy of the measurement. A half wavelength in the waveguide is equal to the distance between adjacent minima of the standing wave. In the case of completely enclosed waveguides it is necessary to provide a non-radiating longitudinal slot for the movable probe. Commercial slotted sections are available for most standard waveguides.

An equivalent procedure uses a fixed probe and a movable short circuit to position successive minima of the standing wave at the probe.

An alternate method employs a cavity arrangement wherein the waveguide under measurement is terminated at both ends by short circuits, one of which is adjusted for two successive resonances of the cavity.

For waveguides of simple cross section it is possible to compute the waveguide wavelength from a measurement of the frequency and a knowledge of the dimensions of the waveguide cross-section.

2.7 Measurement of Attenuation Constant [14]

The attenuation constant is the real part of the propagation constant and is the attenuation per unit length, expressed in nepers/unit length.

(a) The methods of measuring attenuation constant fall into two main groups, one based on transmission and one on reflection procedures.

(b) Transmission type procedures involve the measurement of the insertion loss of a known length of the waveguide under test by the methods of Sec. 3.1.

(c) Reflection type measurements require a knowledge of the magnitude of the input reflection coefficient of a known length of waveguide terminated in a load of known reflection coefficient [15].

(d) A variation on the reflection type measurement, particularly useful for waveguides of unusual cross-

section, employs the measurement of the Q of a cavity consisting of the length of waveguide under test, short-circuited at both ends (see Sec. 3.8) [16]. The end losses must be small or separable.

2.8 Measurement of Input Impedance [17], [18]

It is necessary to distinguish between input impedance and normalized input impedance. Input impedance is generally significant in transmission lines carrying a TEM mode; in uniconductor waveguides it is practicable to measure normalized input impedance. Input admittance is the reciprocal of input impedance.

At frequencies below several hundred mc, lumped constant bridges are useful in determining impedance [17]. At higher frequencies, impedance may be found by measuring the normalized impedance in a transmission line of known characteristic impedance carrying a TEM mode.

2.9 Measurement of Normalized Input Impedance [18]-[21]

The quantities Z' , the normalized input impedance, Y' , the normalized input admittance, and ρ , the complex voltage reflection coefficient, are simply related in the following manner

$$Z' = \frac{1}{Y'} = \frac{1 + \rho}{1 - \rho}.$$

Another associated quantity, the standing wave ratio (S) is related to the magnitude of ρ as

$$S = \frac{1 + |\rho|}{1 - |\rho|}.$$

Methods of measuring normalized input impedance may be classified under distributed constant bridge methods, standing wave ratio techniques, and procedures involving the separation of incident and reflected traveling waves.

(a) One class of distributed constant bridges consists of comparison devices which either directly compare the unknown with a known normalized impedance, or which effect the comparison through variable ratios [18], [21]-[24]. Another type of distributed constant bridge determines the complex ratio of the electric and magnetic field strengths [25], [26]. A number of commercially available bridges fall into these categories.

(b) Standing wave ratio techniques include a number of methods based upon the sampling of the field variation in a waveguide terminated by the unknown impedance. The most common of these procedures employs a sliding probe [20]. Other methods include the use of multiple fixed probes [27], or sweep methods such as frequency sweeping or the Chipman line procedure [28], [29].

(c) Procedures involving the separation of incident and reflected traveling waves, such as those employing directional couplers, yield directly the reflection coefficient magnitude only [30]. Phase information is some-

times obtained by the introduction of a known (usually capacitive) susceptance in a known location [31], [32].

2.10 Measurement of Dielectric Voltage Breakdown [33], [34]

(a) In a waveguide, it is possible to measure the dielectric breakdown of a particular region if its power-handling ability is less than that of the remainder of the line under test. Conditions affecting the lowest power level at which corona or arcing (breakdown) first appears include pressure, temperature, frequency, ionization, extraneous material, and magnitude of standing wave at the location of the breakdown.

(b) To measure power capacity, breakdown is induced by raising the applied power or lowering the ambient pressure, whichever is more convenient, and noting the pressure, temperature, and load conditions at breakdown. Breakdown may be observed by various methods including sight, sound, increased reflection, change in generator output, changes in transmission properties, or heating effects. Power capacity under most other conditions of pressure, temperature, and load reflection may then be computed. If an accurate measurement of the applied peak power is not available, due to irregular waveform, etc., a comparison may be made between a component of known breakdown, and the part under test [35]. Repeatability of results may be improved by irradiation.

(c) The variation of high-frequency breakdown with pressure and distance may be computed by a simple rule [33], [36] except under conditions of relatively low pressure and small distances, where the observed power capacity will be significantly greater than the computed value [33].

(d) Under short-pulse high-power conditions, it is possible to obtain stable states of "breakdown probability" less than unity, in which only a certain percentage of applied pulses break down. The peak power for zero probability of breakdown is known as the "threshold" and is generally computed by extrapolation from observed percentages of pulses breaking down at higher powers. The entire range between the threshold and unity breakdown probability is known as the "over-voltage" region. For convenience in testing, a point within the over-voltage region corresponding to a fairly low probability (one or two arcs per minute) is commonly chosen as indicating failure, or alternatively a point approaching 100 per cent arcing may be so designated.

There are various methods for increasing the gradient available from a particular generator, such as decreasing electrode spacing, decreasing radius of curvature of an electrode, establishing a standing wave with a voltage maximum at the region of interest, or setting up a resonance condition with an electric field maximum at the region of interest [36a], [36b].

(e) Corona

Corona is a particular type of high-voltage discharge differing from arcing principally in the magnitude and

continuity of current involved. At low frequencies and high pressures, the difference is clearly evident: corona is a relatively low-current, often stable, discharge originating at a point of high gradient and diffusing into space; as the gradient is increased, there is a rapid transition to breakdown by arcing, which is a high-current cumulative discharge between two points, generally resulting in complete failure of the system during the arc. At high frequencies, however, electron oscillation within the region of high gradient can reduce the cumulative action of an arc to such a degree that the transition region between corona and arcing becomes entirely obscured, particularly at reduced pressures. For this reason, high-frequency breakdown is often considered to comprise all detectable discharges, including corona.

2.11 Measurement of Mode Purity

In recent years, especially for the higher frequencies, increasing use is being made of waveguides which may propagate several modes simultaneously. Generally, however, only one of these modes is of interest; the remainder are referred to as undesired or spurious modes. Two quantities are of interest in this connection: mode purity and spurious mode level. Mode purity generally refers to the desired mode and is defined as the ratio of power present in the forward-traveling wave of the desired mode to the total power present in the forward-traveling waves of all modes. Spurious mode level involves a ratio of the power present in the forward-traveling wave of a particular undesired mode to that in the desired mode; this ratio is commonly expressed in decibels.

(a) The amount of power present in the forward-traveling wave of any given mode is best measured by the use of a mode-selective device such as a coupled line transducer [37], [38]. In general, a separate device of this type is required for each mode of interest. Such a procedure enables one to completely determine the spurious mode level or to find the numerator of the mode-purity expression. The denominator of the mode-purity expression, the total power present in the forward-traveling wave of all modes, can be measured by any of the means indicated in Sec. 2.5 which are not mode-dependent; e.g., a calorimetric method.

(b) The proportion of power in the forward-traveling waves of each of the propagating modes present may be measured directly by terminating the line in a mode-independent match and by appropriately probing the field distribution in the cross section. Such a probing procedure is rather difficult, however, and is feasible only for simple, stable field configurations and for a few modes present. Since at any given cross-section plane an arbitrary but constant time phase between the modes may exist, it is generally necessary to take measurements at more than one cross-section plane. In view of these difficulties, the probing is considered useful only for qualitative analyses.

(c) In the specific but valuable case of the TE_{01} mode

in circular waveguide in which the TE_{02} mode is beyond cutoff, the radial resistive card mode filter [37] is sufficiently selective to permit the transmitted power to be regarded as being in the TE_{01} mode only and, therefore, to permit a direct measurement of the power in that mode.

(d) If the TE_{11} mode in a particular orientation in circular waveguide is designated as the desired mode, the orthogonal TE_{11} mode may be considered as a spurious mode. This latter mode may be excited by ellipticities or irregularities in the waveguide. The resulting polarization will, in general, be elliptical and may vary with location along the waveguide. Elliptical polarization may be completely described by the axial ratio and the orientation of the major axis of the ellipse of polarization. Mode purity may be determined at any particular cross section by noting the ratio of minimum to maximum field strength (axial ratio) and the angular position of the minimum with respect to the desired reference direction [39]. This measurement may be made by circumferential rotation of a radial detecting probe.

If the axial ratio is designated as $\tan \alpha$, and the angle between the direction of the maximum and the reference direction of the desired TE_{11} component is β , the level of the undesired TE_{11} component, $\tan^2 \gamma$, and the mode purity, $\cos^2 \gamma$, can be obtained from

$$\cos 2\gamma = \cos 2\alpha \cos 2\beta.$$

2.12 Measurement of Transmission Line Unbalance

(a) In the case of uniconductor waveguides or coaxial transmission lines, the question of unbalance does not usually arise. For a coaxial line, the total current on the inner conductor must always be equal and opposite to the total current on the inner surface of the outer conductor. The only balance problem which commonly occurs with a coaxial line is for the case when the generator or load is connected to the line in such a way that currents are caused to flow on the outer surface of the outer conductor. For this case, the presence of current on the outer conductor can be detected by a measurement of the magnetic field strength on the outer surface as outlined in Sec. 2.4.

(b) For a balanced transmission line system operating properly, the voltages (relative to ground) on the conductors are push-pull voltages, and the currents in the conductors are push-pull currents. When the system becomes unbalanced, this is evidenced by the presence of push-push voltages and currents in addition to the push-pull voltages and currents. The amount of the system unbalance is measured by the ratio of the push-push voltage component to the push-pull voltage component or by the ratio of the push-push current to the push-pull current (Sec. 2.1).

(c) One excellent method for measuring the ratio of unbalanced to balanced currents involves the use of a transmission line arrangement and shielded loop pickup

with a configuration such that in one position, the loop reads a value proportional to the unbalanced component of the current, while in a second position perpendicular to the first position, the loop reads a value proportional to the balanced component of the current [40]. This technique is one of the most accurate although it requires a careful set-up.

(d) A simple method for measuring the relative amount of unbalance involves the measurement of the voltage or the current on each conductor as a function of position [41] by one of the methods described in Secs. 2.1 or 2.2. If unbalance is present, then the standing wave on one conductor will be displaced from the standing wave on the second conductor. The amount of unbalance is related to the relative amount of displacement between the two standing waves. Unfortunately, this method will not give the absolute unbalance ratio since the voltage or current measurements give only the magnitude of either of these quantities. In order to determine the absolute ratio between the unbalanced and balanced quantities, it is necessary to know the complex values of either the voltage or the current in each of the two conductors at a given cross section.

SECTION 3—MEASUREMENT OF ONE-PORT AND TWO-PORT WAVEGUIDE COMPONENTS

It should be recalled that the performance of any waveguide component is affected by and must be specified with respect to the input and output waveguides between which it is inserted. The input and output ports need not be in the same kind of waveguide nor utilize the same mode of transmission, recalling, of course, that each port is identified with a single mode. As mentioned in Sec. 1, these measurement methods apply to linear, passive, reciprocal waveguide components.

3.1 Measurement of Insertion Loss [42]–[44]

According to the definition of insertion loss used in this Standard (see Sec. 5), both the load and the generator must be respectively matched to the waveguides which connect them to the waveguide component under test. It should be noted that this is not always the condition for maximum power transfer through the component. The insertion loss measured under these conditions is the sum of the dissipative and reflection losses.

Measurement of insertion loss can be made by noting the change in power level at a matched detector upon insertion of the component. An alternative method is a substitution method in which a matched calibrated variable attenuator is inserted in place of the component and adjusted to obtain the original power level at the detector. This attenuator may be part of the original measurement system, in which case the insertion loss is equal to the change in attenuation of the calibrated attenuator. When the input and output waveguide connections do not permit direct insertion of the component under test, it may be possible to make

this measurement for high-loss components by including a low-loss adapter where convenient. The loss of the adapter should be small compared to the tolerable error of the measurement.

For very low-loss components, the method described in Sec. 3.9 is preferable.

3.2 Measurement of Input SWR

This measurement is made by measuring the standing-wave ratio (SWR) in the waveguide connected to the input port of the component, with the output port (if any) match-terminated. Any of the methods described in Sec. 2.9 (b) and (c) can be used. For lossless or symmetrical components, the result would be the same regardless of which port is used as the input.

3.3 Measurement of Input Impedance

This measurement is made by measuring the input impedance looking into one of the ports, with the other port (if any) match-terminated. Any of the methods described in Sec. 2.8 can be used. For components which are unsymmetrical, this impedance is not necessarily the same at both ports.

3.4 Measurement of Normalized Input Impedance

This measurement is made by measuring the normalized input impedance looking into one of the ports, with the other port (if any) match-terminated. Any of the methods described in Sec. 2.9 can be used. For unsymmetrical components, this impedance is not necessarily the same at both ports.

3.5 Measurement of Phase Shift

The phase shift through a waveguide component at a single frequency is the phase difference under matched conditions between corresponding incident and transmitted field quantities at the input and output ports, respectively, of the component, ignoring multiples of 2π radians. Since the phase difference will vary with load conditions, phase shift has been defined under matched conditions.

Phase shift measurements are based on the comparison of the phases of two signals by interference methods. The two signals may be obtained by sampling with directional devices at the input and output ports of the component under test [45], or they may be the signals transmitted through the waveguide containing the component under test and a reference waveguide of known phase shift [46], when equiphase signals are applied to the two waveguides. The comparisons may be made by employing hybrid junctions or by applying the two signals to opposite ends of a slotted section of waveguide [45] with suitable isolation to eliminate reflections. When a slotted section is employed in this manner, the position of a voltage minimum is observed with the component in the test apparatus. The phase shift of the component is then equal to twice the displacement of the minimum expressed in electrical degrees. Comparison procedures using a hybrid junction

employ null indications which require the use of a calibrated phase shifter in one of the arms [46]. A difference in the levels of the two signals being compared results in a finite minimum rather than a null indication. This effect does not affect the accuracy, but may influence the precision of the measurement.

The phase shift can also be determined by use of a sliding-short-circuit method to determine the appropriate component of the scattering matrix, as described in Sec. 3.9.

3.6 Measurement of Envelope Delay [47]

The quantity "envelope delay" (τ) in seconds is related to the rate of change of phase shift (ϕ) in radians with frequency (f) in cycles per second by the definition

$$\tau = \frac{1}{2\pi} \frac{d\phi}{df}$$

For a nondispersive waveguide component, such as an air-filled TEM waveguide, the envelope delay is identical with the delay of the envelope of the wave.

The envelope of a wave passing through a dispersive waveguide component is distorted, so that the concept of the delay of the envelope loses meaning when the dispersion is high. While the delay of the distorted envelope cannot be strictly defined in a dispersive medium, to the degree to which the quantity is definable it is given by (τ).

The quantity $d\phi/df$ is obtained by measurements of the phase shift at several frequencies in the vicinity of the frequency at which the delay is to be evaluated. In measuring phase shift, the methods and restrictions of Sec. 3.5 are applicable.

The envelope delay may also be measured directly by the use of short pulses and oscillographic presentation of the time between input and output pulses.

3.7 Measurement of Power-Handling Capacity [33], [34], [48], [49]

The power-handling capacity of a waveguide component is limited by the occurrence of dielectric voltage breakdown, or by the effects of heating, or a combination of both. The energy in a single pulse may have to be limited to avoid overheating.

The limitation of power capacity by heating must be judged for each individual component. In some cases, radio frequency power cables for example, this limitation is measured by applying equivalent low-frequency power to the component.

The methods and restrictions applicable to the measurement of the dielectric voltage breakdown of a waveguide component are described under Sec. 2.10.

3.8 Measurement of Q [50], [51]

As here used, the Q of a resonant waveguide circuit is 2π times the ratio of the energy stored to the energy dissipated per cycle in that circuit. The following discussion applies to the Q at resonance of components ex-

hibiting a simple resonance response and having a Q high enough (ordinarily about 10 or greater) to produce the desired accuracy of measurement.

If the circuit consists of a component under test, coupled to its associated loads, the resultant Q is termed the loaded $Q(Q_l)$ of the circuit, and is commonly referred to as the Q_l of the component under these conditions. For the component alone, without its coupling mechanisms, the pertinent quantity is the unloaded $Q(Q_u)$. These quantities are related by

$$\frac{1}{Q_l} = \frac{1}{Q_u} + \frac{1}{Q_e}$$

where Q_u results from dissipation in the component itself, and Q_e from dissipation in the external circuit through the coupling mechanism.

The Q of a component such as an inductor or a capacitor at any frequency is understood to mean the Q which would be obtained by resonating that component with a lossless element at that frequency.

Q_l may be measured directly, while Q_u is a derived quantity. The Q_l of a component depends on the particular coupling mechanisms; matched external loads are commonly used. In the case of a very loose coupling, the external losses become negligible, and Q_l approaches Q_u .

There are three basic methods of measuring the loaded $Q(Q_l)$. These are, first, the measurement of the transmission through the component as a function of frequency; second, the measurement of the time rate of decay of energy stored in the component at a given frequency, and third, the measurement of the input impedance of the component as a function of frequency.

(a) For the first method, it is necessary to determine the difference (Δf) between frequencies at which the power transmission differs by 3 decibels from the transmission at the resonance frequency, f_0 . Then Q_l is obtained from the relation

$$Q_l = \frac{f_0}{\Delta f}$$

If the component is symmetrically coupled to match-terminated lines of equal characteristic impedance, a measurement of its insertion loss (Sec. 3.1) at resonance will permit the unloaded $Q(Q_u)$ to be computed from the relation

$$\frac{1}{Q_u} = \frac{1-a}{Q_l}$$

where a = voltage transmission coefficient. The quantity a is related to the insertion loss (L) by

$$L = 20 \log_{10} (1/a) \text{ in decibels.}$$

It should be noted that when the insertion loss is low, this method may be inaccurate because of the difficulty in measuring the insertion loss to a sufficient degree of accuracy.

For example, if the resonator is a two-port component

which is designed for maximum transmission at resonance, the measurement may be made as follows. With a constant available power from the generator, the transmitted power is observed as a function of frequency in the vicinity of resonance, and the frequencies above and below resonance at which the transmitted power has been reduced by 3 decibels from the peak value at resonance are recorded. The transmitted power level may be determined by one of the methods described in Sec. 2.5. When the available power varies with frequency, the insertion loss of the component should be measured by one of the methods of Sec. 3.1 and 3-decibel change in insertion loss used to determine the appropriate frequency difference, Δf .

If the resonator is a two-port component designed for maximum absorption at resonance, the measurement procedure is similar to the above, except that the attenuation by the component is considered instead of transmission.

At low frequencies, a special case of this method is the measurement of bandwidth between frequencies where the voltage or current has fallen to 0.707 of its maximum value with a constant current or voltage source, respectively, and gives the unloaded $Q(Q_u)$.

(b) The second method of measurement, often referred to as a "decrement" measurement, is useful when the circuit has a sufficiently high Q so that it is simpler to make time interval measurements rather than frequency difference measurements.

It involves measuring the time interval (τ) required for the field strength at any point in the circuit to decay to $1/e$ (approximately 0.368) of its initial value after the generator output power has been suddenly interrupted. It is also necessary to measure the frequency (f) of the circuit resonance. The Q then follows from the relation

$$Q_t = \pi \tau f.$$

(c) The third of these methods, applicable to one-port components, is based on the relation

$$Q_u = \frac{\omega}{2G} \frac{dB}{d\omega} = \frac{\omega}{2G'} \frac{dB'}{d\omega} \quad \text{at } \omega = \omega_0,$$

where G and B are the components of the input admittance seen at a plane at which $B=0$ at resonance, G' and B' are the components of the normalized input admittance at the same plane, and ω is the angular frequency. There exists a variety of specific methods for evaluating the necessary quantities, and the methods for measuring input admittance and normalized input admittance are those described in Secs. 2.8 and 2.9 herein.

3.9 Measurement of Scattering Matrix Elements by Sliding-Short-Circuit Methods [52]

3.9.1 General Discussion

The measurement of the scattering matrix elements or the equivalent circuit of a waveguide component by

the sliding-short-circuit method is often the most accurate and convenient way of determining any or all of its properties. Sliding-short methods have the advantage of greater accuracy in that no relative power measurements are required, and no calibrated attenuators or carefully matched loads are needed. In the case of lossless components, only distance and frequency measurements are involved. These methods are also useful in measuring components through mismatched junctions.

The choice of scattering matrix or equivalent circuit representation depends on the application and the nature of the component to be measured. For example, if the component is to be employed with a matched load following it, particularly if only the transmission and reflection coefficients are of interest, the scattering matrix is clearly preferable. If the component is representable by a simple shunt or series element, use of the equivalent circuit is indicated. Even if the component does not permit a simple representation the pictorial features of an equivalent circuit may still be found useful, or a graphical procedure may be employed from which some pertinent partial information may be readily obtained. For all choices of representation the data is taken in basically the same fashion; the treatment of the data, however, depends on the representation desired. In this section the scattering matrix elements are considered. The equivalent circuit determinations are treated in Sec. 3.10.

3.9.2 Basic Measurement Procedure

The measurement set-up for the sliding-short method requires placing the component under test between a slotted section and sliding-short-circuit [53], [54]. The basic procedure consists of moving the sliding-short-circuit through a succession of known positions and determining the position of the voltage minimum (and VSWR if the component is dissipative) in the slotted section for each of the sliding-short-circuit positions.

3.9.3 Parameters Derived from the Measurement

The measured data, obtained in the manner indicated above, may be appropriately treated to yield the elements S_{11} , S_{12} , and S_{22} of the scattering matrix. These elements are complex, with magnitude and phase given by

$$S_{11} = |S_{11}| e^{j\phi_{11}}, \quad S_{12} = |S_{12}| e^{j\phi_{12}}, \quad S_{22} = |S_{22}| e^{j\phi_{22}}.$$

The magnitudes, but not the phases, of the elements are independent of input and output reference plane locations. The choice of reference plane locations is arbitrary; it may be based on physical convenience or computational simplicity. An example of the latter would be a choice such that ϕ_{11} and ϕ_{22} are both zero.

The scattering matrix elements have the following physical meaning: S_{11} is the input voltage reflection coefficient obtained when a matched load is placed at the output port; S_{22} is defined similarly to S_{11} except that

the component is reversed; S_{12} is the voltage transmission coefficient which is the ratio of the complex voltages of the wave transmitted past the component to that incident on it. Usually the $|S_{12}|^2$ is of particular interest, rather than the complex quantity S_{12} , since it is directly the power transmission coefficient of the component.

When the component is placed between a load and generator, each of which is matched to its waveguide, the magnitudes of the scattering matrix elements are simply related to the insertion loss (L_I), the reflection loss (L_R), and the dissipative loss (transmission loss, L_D) of the component. These relations are:

$$L_I = 10 \log_{10} \frac{1}{|S_{12}|^2}$$

$$L_R = 10 \log_{10} \frac{1}{1 - |S_{11}|^2}$$

$$L_D = 10 \log_{10} \frac{1 - |S_{11}|^2}{|S_{12}|^2}.$$

Another quantity of interest which can be derived from the above measurements is the minimum or intrinsic loss. This is the insertion loss (L_I) obtained when reactive elements producing maximum power transfer are placed at both ports of the two-port component. The resulting network, including these reactive elements, will be bilaterally matched ($S_{11} = S_{22} = 0$).

3.9.4 Dissipative Loss

The dissipative loss of a component may be obtained accurately by the sliding-short-circuit method without analyzing the data completely and obtaining the complete scattering matrix. The measurement procedure described under 3.9.2 above is followed; however, the procedure requires the power flow through the component to be opposite that for which the transmission characteristics are desired [55]. If the component possesses similar input and output connections, reversal of the component is all that is required. The data obtained are then plotted on the reflection coefficient chart. The radius (R) normalized to the chart radius of the resulting circular locus is then related to the dissipative loss, *i.e.*,

$$L_D = 10 \log_{10} \frac{1}{R}.$$

3.9.5 Complete Scattering Matrix

The complete scattering matrix for a component, which includes the phases of the above elements, may be determined by means of a method due to Deschamps [53], [56]–[58]. This method imposes an additional requirement on the measurement procedure outlined under 3.9.2 in that the short-circuit locations are most conveniently taken in pairs spaced a quarter guide wavelength apart. The resulting data are then plotted on the reflection coefficient chart, and the magnitudes

and phases of the scattering matrix elements are separately obtained by means of graphical constructions.

3.9.6 Relation to Other Parameters

Some of the elements of the scattering matrix as determined by the method of 3.9.5 above are related simply to other parameters of the component as follows:

- Input SWR = $\frac{1 + |S_{11}|}{1 - |S_{11}|}$
- Normalized input impedance = $\frac{1 + S_{11}}{1 - S_{11}}$
- Phase shift = angle of $S_{12} = \phi_{12}$.

3.9.7 Lossless Components

The scattering matrix of a lossless component is characterized by only three independent numbers, in contrast to six for a lossy component. The elements of the scattering matrix of a lossless component are related in the following fashion:

$$|S_{11}| = |S_{22}|,$$

$$|S_{12}|^2 = 1 - |S_{11}|^2,$$

$$2\phi_{12} = \phi_{11} + \phi_{22} \pm \pi.$$

In the measurement method referred to in 3.9.5 above, the data circle on the reflection coefficient chart becomes coincident with the unit circle, and the graphical constructions become somewhat simplified [53], [56]–[58].

An alternative measurement procedure for lossless components is the tangent relation method [53], [54], [58]. The measured data are taken in the manner described under 3.9.2 above. If the positions of the voltage nulls in the input and output waveguides relative to the chosen reference planes, T_1 and T_2 , (measured away from the junction as shown in Fig. 1) are denoted by D and S , respectively, a simple plot of D vs S as indicated in Fig. 2 yields three real parameters D_0 , S_0 and γ which characterize the lossless component. D_0 and S_0 are the values of D and S at the point of maximum slope, (γ). These parameters are related to the scattering matrix elements by:

$$|S_{11}| = |S_{22}| = \frac{\gamma + 1}{\gamma - 1}.$$

$$|S_{12}| = \frac{2\sqrt{-\gamma}}{1 - \gamma}$$

$$\phi_{11} = \frac{4\pi}{\lambda_0} D_0$$

$$\phi_{22} = \frac{4\pi}{\lambda_0} S_0 + \pi$$

$$\phi_{12} = \frac{2\pi}{\lambda_0} D_0 + S_0 + n\pi, \quad (n = 0, 1).$$

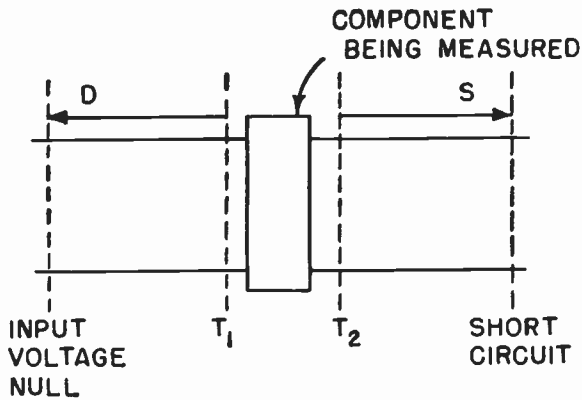


Fig. 1

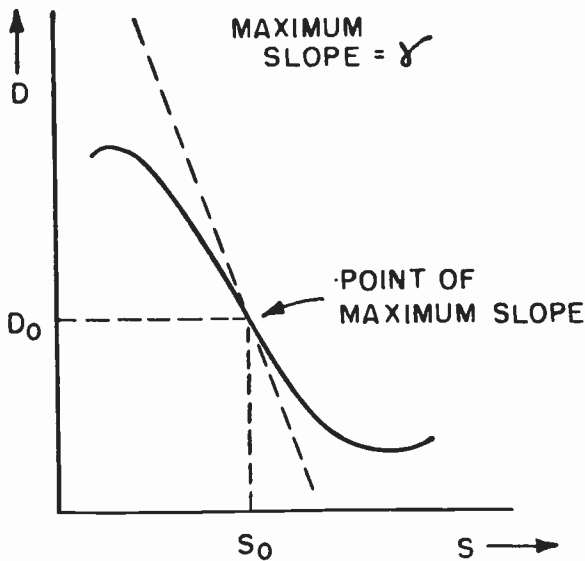


Fig. 2

Note: $(-\gamma)$ is a positive number and the sign of S_{12} is not determined.

3.9.8 Measurements Through a Junction

In certain cases it is necessary to perform measurements through a reflecting and possibly lossy junction or component such as an adapter. A modification of the graphical constructions described in 3.9.5 above may be employed to separate out the parameters of the component under test [57], [59], [60]. If the junction is lossless, an alternative and simpler procedure is available which employs the tangent relation method [61], [62]. Preliminary measurements of the junction alone are necessary in both methods.

3.9.9 Components with Small Loss

The measurement of the scattering parameters of a component with small dissipative loss is sometimes inaccurate or difficult because of the high values of SWR that need to be measured. These values of SWR can be lowered so that they fall into a more accurately measurable range by the deliberate addition of dissipative loss into the overall system. A simple additional meas-

urement suffices to determine the effect of this added loss, which can then be subtracted out in order to obtain the properties of the component alone. A common and useful means for obtaining this added loss is a lossy shorting plunger [63].

3.10 Measurement of Equivalent Circuit Parameters by Sliding-Short-Circuit Methods [52], [53]

3.10.1 General Discussion

An equivalent circuit representation for an arbitrary dissipative component contains six real parameters (which appear as three complex parameters if the tee or pi network form is used). Symmetry in the component and in the location of the reference planes reduces this number to four; for the case of an unsymmetrical lossless component the number becomes three, while for a symmetrical lossless component only two independent real parameters are required. These parameters may be combined into any one of a variety of pictorial forms, in which the numerical values of the parameters vary with the reference plane location (since a different length of waveguide is absorbed into the equivalent circuit representation). It is sometimes convenient, by appropriate adjustment of the reference plane locations, to simplify the form of the equivalent circuit. The equivalent circuit for a lossless component can always be reduced to a shunt or series form or to a single ideal transformer by appropriate shifting of the reference plane locations; except in special cases, however, these final reference plane locations are not known in advance. Such reductions in form are also possible for lossy components; however, since only two reference plane shifts are available, the number of parameters for an arbitrary lossy component can be reduced only to four (or to three for a symmetric lossy component). The parameter values of an equivalent circuit are valid only at the frequency at which the measurement was made, and, in general, no inference may be drawn as to the frequency dependence of the parameters. This situation is similar to that occurring with the scattering matrix representation; however, for special cases, such as a very thin transverse iris in a uniconductor waveguide which is not operated near the cutoff frequency of the next mode, the frequency dependence may be inferred and this property of the equivalent circuit representation may be found useful.

3.10.2 Equivalent Circuits

A large variety of equivalent circuits may be found to correspond, at the same set of reference planes, to a given impedance matrix, of elements Z_{11} , Z_{22} , and Z_{12} . One of these equivalent circuits is the tee circuit of Fig. 3. In a similar manner, the pi circuit corresponds directly to the admittance matrix in Fig. 4. Another circuit representing the impedance matrix Z which is useful for lossless components is shown in Fig. 5 which contains an ideal transformer.

$$n = Z_{11}/Z_{12}$$

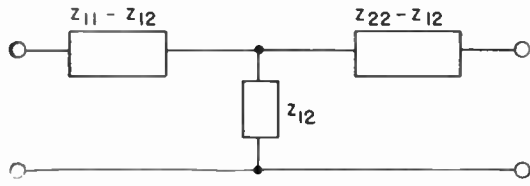


Fig. 3

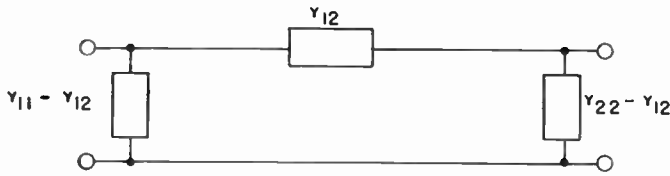


Fig. 4

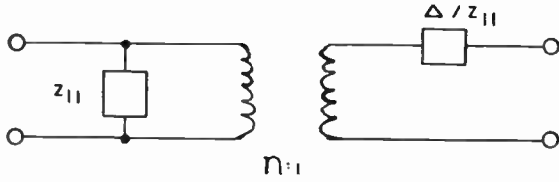


Fig. 5

where

$$\Delta = Z_{11}Z_{22} - (Z_{12})^2.$$

If the component is lossless, appropriate shifts of both the input and output reference planes reduce this network to one consisting of the shunt element only, or the transformer only [54]. The relations between the network parameters and the impedance matrix elements indicate readily that to eliminate the series element, Δ must be zero, or that to eliminate the transformer, Z_{11} must equal Z_{12} . A dual circuit corresponds to the admittance matrix.

3.10.3 Shunt or Series Networks

When the component under test can be represented by a purely shunt or series equivalent circuit at particular reference planes, the parameters may be determined from a single input impedance measurement. For a series network, the normalized resistance and reactance are given directly by the normalized input impedance to the component when a short circuit is placed at the output reference plane. For a shunt network, the normalized conductance and susceptance follow directly from the measurement of the normalized input admittance to the component when an open circuit is placed at the output reference plane.

3.10.4 Simplified Method for Symmetrical Components

When the component is symmetrical but not representable by a purely shunt or series equivalent circuit, the parameters may be determined by measuring the input impedances at the input reference plane corresponding to both a short and an open circuit termination at the output reference plane. The normalized impedance matrix elements Z_{11}' , Z_{22}' , and Z_{12}' are related to the measured quantities by [53]:

$$\begin{aligned} Z_{11}' &= Z_{22}' = Z_{oc}' \\ (Z_{12}')^2 &= Z_{oc}'(Z_{oc}' - Z_{sc}') \\ Z_{11}'Z_{22}' - (Z_{12}')^2 &= Z_{sc}'Z_{oc}' \end{aligned}$$

where Z_{oc}' and Z_{sc}' are the measured normalized input impedances at the input reference plane corresponding to an open circuit and a short circuit, respectively, at the output reference plane. Note that the sign of Z_{12}' is not determined by these relations. The above relations are also valid for the admittance matrix elements if all the normalized impedances are replaced by normalized admittances, and if the role of open and short circuits is reversed.

Note: If the component is unsymmetrical, the above procedure can be generalized by requiring an additional terminating impedance and its corresponding input impedance measurement. However, the relations then become more involved, and the usefulness of the procedure becomes questionable.

3.10.5 Lossless Components

For lossless components, the tangent relation method furnishes an alternative procedure to the preceding ones in Sec. 3.10. This method is more accurate because additional points are taken and the data are averaged in a systematic fashion. The measurement procedure, which employs a sliding short circuit, is the same as that described under 3.9.2. If, then, the positions of the voltage nulls in the input and output waveguides relative to the chosen reference planes are denoted by D and S , respectively, a simple plot of D vs S (see figures associated with 3.9.7) yields three real parameters D_0 , S_0 , and γ which characterize the lossless component [53], [54], [58]. These parameters (defined in Sec. 3.9) are related to the normalized reactance matrix elements by:

$$\begin{aligned} \frac{X_{11}}{X_{01}} &= -\frac{\alpha\beta + \gamma}{\beta - \alpha\gamma}, \\ \frac{X_{22}}{Z_{02}} &= \frac{1 + \alpha\beta\gamma}{\beta - \alpha\gamma}, \\ \frac{X_{11}X_{22} - (X_{12})^2}{Z_{01}Z_{02}} &= -\frac{\alpha - \beta\gamma}{\beta - \alpha\gamma}, \end{aligned}$$

where

$$\begin{aligned} \alpha &\equiv \tan \frac{2\pi}{\lambda_{g1}} D_0, \\ \beta &\equiv \tan \frac{2\pi}{\lambda_{g2}} S_0, \end{aligned}$$

and where the subscripts 1 and 2 refer to the input and output waveguides, respectively. The above relations are also valid for the elements of the susceptance matrix if X is replaced everywhere by B , and Z by Y , and if

$$\alpha = -\cot \frac{2\pi}{\lambda_{g1}} D_0$$

$$\beta = -\cot \frac{2\pi}{\lambda_{g2}} S_0.$$

These relations are also useful for determining the appropriate reference plane shifts required for obtaining simplified equivalent circuit forms.

3.10.6 Lossy Components

Methods also exist for lossy components in which the equivalent circuit parameters are obtained by sliding-short methods. One of these methods is applicable to unsymmetrical lossy components, and yields an equivalent circuit which is almost shunt or almost series, and in which the lossy and lossless portions are separated from each other [53], [58], [64]. A second method, suited to symmetrical lossy components, is based on the representation of the lossy portion by an ideal attenuator [65], [66]. For the same degree of accuracy, the effort involved in the analysis of the measured data to yield the final equivalent circuit in these methods is about the same as that required in the procedure discussed in 3.9.5 for determining the complete scattering matrix.

SECTION 4—MEASUREMENTS OF MULTI-PORT WAVEGUIDE COMPONENTS [67], [68]

Multi-port components are herein considered as those having more than two ports. The ports need not be in the same kind of waveguide nor utilize the same mode of transmission, recalling that each port shall be identified with only a single mode. Again, only linear, passive, reciprocal networks are treated.

In general, the measurements of multi-port components reduce to the measurements described in Secs. 3.1 through 3.8 with a specified pair of ports comprising the input and output with the remainder of the ports match-terminated. In addition, certain properties of multi-port junctions consist of a comparison of the transmission properties of specific pairs of ports. It should be noted that the reflection of a specified port and transmission of a port pair may be substantially affected by the load conditions at the other ports.

Terms commonly used to describe the coefficient of transmission from one port to another in a multi-port waveguide component are "coupling" and "isolation." Isolation (sometimes called "decoupling") is identical with insertion loss, whereas coupling is the negative of insertion loss, expressed in decibels. The use of these terms depends on the intent of the application; coupling usually refers to a definite desired transmission coefficient between a particular pair of ports, whereas isolation refers to a transmission coefficient which should be as small as possible. The term "unbalance" may be used to refer to the difference between the insertion losses between an input port and each of two output

ports where these are desired to be as nearly equal as possible.

4.1 Measurement of Coupling [69], [70]

The coupling between any two ports of a multi-port component is specified by the insertion loss between these ports and is measured by the methods of Sec. 3.1. The numerical value attached to the term "coupling" is the negative of the insertion loss when expressed in decibels or, equivalently, the reciprocal when expressed as a power ratio.

A common example of a four-port component is the symmetrical directional coupler represented by Fig. 6. For this component, the negative (or reciprocal) insertion loss from port 1 to port 4, or from port 2 to port 3, would be termed the forward coupling, or simply the "coupling" of the directional coupler. These couplings are related to the elements S_{41} and S_{32} , respectively, of the scattering matrix of the component. For an unsymmetrical directional coupler, the elements S_{41} and S_{32} may be different, and the term coupling should be associated with the direction of use.

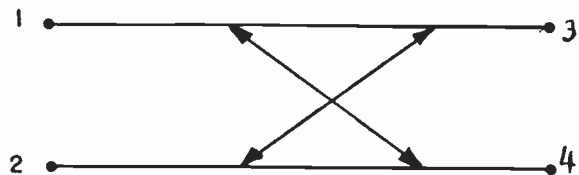


Fig. 6—Symmetrical directional coupler.

4.2 Measurement of Isolation

The isolation between any two ports of a multi-port component is given directly by the insertion loss between these ports when the other ports are match-terminated. The accuracy of the isolation measurement may be critical to departures from matched load conditions on the other ports of the component.

Special techniques are available to correct for the inaccuracies introduced by the loads [71]. The measurement is generally made with a sensitive detector circuit.

A typical four-port component for which the measurement of isolation is significant is the hybrid tee shown in Fig. 7 [71]. The isolation between the E and H arms of this component is the insertion loss between ports 1 and 2; the isolation between collinear arms is the insertion loss between ports 3 and 4. These isolations, which are not necessarily equal, are related to the scattering matrix elements S_{21} and S_{43} , respectively.

The insertion loss between ports 1 and 2 or ports 3 and 4 of the symmetrical directional coupler of Fig. 6 is the isolation of the component; its negative (in decibels) is also frequently called the "backward coupling" of the coupler.

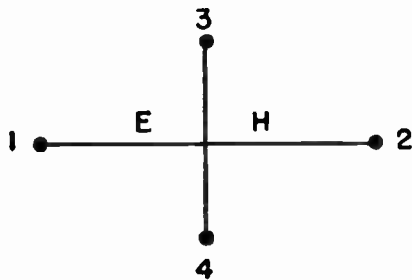


Fig. 7—Hybrid tee.

4.3 Measurement of Unbalance [72]

Small inequalities between the supposedly equal transmissions (magnitude and phase) from a common port to other ports, in turn, of a multi-port component are of interest in components such as simple tees, hybrid tees, and n -port power dividers. The power unbalance is the difference, in decibels, between the insertion losses between an input port and each of two output ports.

The outputs may be measured simultaneously or in sequence by matched detectors, or the difference in outputs may be observed with an appropriate amplitude or phase comparison circuit. In the case of simultaneous measurement, the accuracy may be improved by interchanging detectors, and averaging.

An alternative method for measuring unbalance consists of observing the small output from the input port when the output pair of ports are simultaneously fed equal magnitude signals of opposite phase.

4.4 Measurement of Directivity [73]

In the case of a directional coupler, the difference in insertion loss from one port of one waveguide to each of the two ports of the other waveguide is known as the directivity. In Fig. 6, for power fed into port 1, directivity is the insertion loss between ports 1 and 2 less the insertion loss between ports 1 and 4, with the insertion loss expressed in decibels.

SECTION 5—DEFINITIONS

Attenuation Constant. Of a traveling plane wave at a given frequency, relative rate of decrease of amplitude of a field component (or of voltage or current) in direction of propagation in nepers per unit length.

Characteristic Impedance (of a Two-Conductor Transmission Line). For a traveling transverse electromagnetic wave, the ratio of the complex voltage between the conductors to the complex current on the conductors in the same transverse plane with the sign so chosen that the real part is positive.

Electric (Magnetic) Field Strength. The magnitude of of the electric (magnetic) field vector.

Input Impedance of a Transmission Line. The impedance between the input terminals with the generator disconnected.

Insertion Loss (of a Waveguide Component). The change in load power, due to the insertion of a waveguide component at some point in a transmission system, where the specified input and output waveguides connected to the component are reflectionless looking in both directions from the component (match-terminated). This change in load power is expressed as a ratio, usually in decibels, of the power received at the load before insertion of the waveguide component to the power received at the load after insertion.

Note 1: A more general definition of insertion loss does not specify match-terminated connecting waveguides, in which case the insertion loss would vary with the load and generator impedances. In this Standard, match-terminated connecting waveguides will be assumed unless otherwise specified.

Note 2: When the input and output waveguides connected to the component are not alike or do not operate in the same mode, the change in load power is determined relative to an ideal reflectionless and lossless transition between the input and output waveguides.

Matched Termination (for a Waveguide). A termination producing no reflected wave at any transverse section of the waveguide.

Matched Transmission Line. See Matched Waveguide.

Matched Waveguide. A waveguide having no reflected wave at any transverse section.

Mode of Propagation (Transmission). A form of propagation of guided waves that is characterized by a particular field pattern in a plane transverse to the direction of propagation, which field pattern is independent of position along the axis of the waveguide.

Note: In the case of uniconductor waveguides the field pattern of a particular mode of propagation is also independent of frequency.

Mode Purity. The ratio of power present in the forward-traveling wave of a desired mode to the total power present in the forward-traveling waves of all modes.

Normalized Impedance (Relative to a Given Waveguide). An impedance divided by the characteristic impedance of the waveguide.

Note: The relation between voltage, current and power chosen for the characteristic impedance must also be taken for the impedance to be normalized, in which case the normalized impedance will be independent of the convention used to define the characteristic impedance.

Port (for a Waveguide Component). A means of access characterized by a specified reference plane and a specified propagating mode in a waveguide which permits power to be coupled into or out of a waveguide component.

Note 1: At low frequencies the port is synonymous with a terminal pair.

Note 2: To each propagating mode at a specified reference plane there corresponds a distinct port.

Reflection Coefficient (in a Transmission Medium). At a given frequency, at a given point, and for a given mode of transmission, the ratio of some quantity associated with the reflected wave to the corresponding quantity in the incident wave.

Note: The reflection coefficient may be different for different associated quantities, and the chosen quantity must be specified. The "voltage reflection coefficient" is most commonly used and is defined as the ratio of the complex electric field strength (or voltage) of the reflected wave to that of the incident wave.

Reflection Coefficient (of a Transition or Discontinuity). For a transition or discontinuity between two transmission media, the reflection coefficient at a specified point in one medium which would be observed if the other medium were match-terminated.

Scattering Matrix. A square array of complex numbers consisting of the transmission and reflection coefficients of a waveguide component.

As most commonly used, each of these coefficients relates the complex electric field strength (or voltage) of a reflected or transmitted wave to that of an incident wave. The subscripts of a typical coefficient S_{ij} refer to the output and input ports related by the coefficient. These coefficients, which may vary with frequency, apply at a specified set of input and output reference planes.

Standing Wave Ratio. At a given frequency in a uniform waveguide, the ratio of the maximum to the minimum amplitudes of corresponding components of the field (or the voltage or current) along the waveguide in the direction of propagation.

Note: Alternatively, the standing wave ratio may be expressed as the reciprocal of the ratio defined above.

Transmission Coefficient (of a Transition or Discontinuity). For a transition or discontinuity between two transmission media, at a given frequency, the ratio of some quantity associated with the transmitted wave at a specified point in the second medium to the same quantity associated with the incident wave at a specified point in the first medium, the second medium being match-terminated.

Transmission Line. A waveguide consisting of two or more conductors.

Transmission Loss. In the transmission of power past two points, the ratio, usually expressed in decibels, of the net power passing the first point to the net power passing the second.

Uniconductor Waveguide. A waveguide consisting of a

cylindrical metallic surface surrounding a homogeneous dielectric medium.

Note: Common cross-sectional shapes are rectangular and circular.

Uniform Waveguide. A waveguide in which the physical and electrical characteristics do not change with distance along the axis of the guide.

Waveguide. A system of material boundaries capable of guiding waves.

Waveguide Component. A device designed to be connected at specified ports in a waveguide system.

Waveguide Wavelength. For a traveling wave in a uniform waveguide at a given frequency and for a given mode, the distance along the guide between similar points at which a field component (or the voltage or current) differs in phase by 2π radians.

SECTION 6—REFERENCES

- [1] F. E. Terman and J. M. Pettit, "Electronic Measurements," McGraw-Hill Book Co., Inc., New York, N. Y., ch. 1; 1952.
- [2] M. C. Selby, "High Frequency Voltage Measurement," Nat. Bur. of Standards Circular 481; 1949.
- [3] "Radio Instruments and Measurements," Nat. Bur. of Standards Circular C74, pp. 139-175.
- [4] E. J. Sterba and C. B. Feldman, "Transmission lines for short-wave radio systems," *PROC. IRE*, vol. 20, p. 1163; July, 1932.
- [5] D. D. King, "Measurements of Centimeter Wavelength," D. Van Nostrand Co., Inc., New York, N. Y., pp. 272-278; 1952.
- [6] R. A. Schrack, "Radio Frequency Power Measurements," Nat. Bur. of Standards Circular 536; 1953.
- [7] C. G. Montgomery, "Technique of Microwave Measurements," M.I.T. Rad. Lab. Ser., McGraw-Hill Book Co., Inc., New York, N. Y., vol. 11, ch. 3; 1947.
- [8] Ref. 5, ch. 3.
- [9] "The Handbook of Microwave Measurements," Microwave Res. Inst., Polytechnic Inst. of Brooklyn, Brooklyn, N. Y., sec. IV; 1954.
- [10] Ref. 6, p. 11; see also F. E. Terman, "Radio Engineers' Handbook," McGraw-Hill Book Co., Inc., New York, N. Y., p. 938; 1953.
- [11] Ref. 5, ch. 4.
- [12] Ref. 7, ch. 5.
- [13] Ref. 9, sec. 1.
- [14] Ref. 9, sec. 8.
- [15] H. M. Barlow and A. L. Cullen, "Microwave Measurements," Constable and Co., Ltd., London, Eng., pp. 238-239; 1950.
- [16] Ref. 7, pp. 821-822.
- [17] Ref. 1, ch. 3.
- [18] Ref. 1, ch. 4.
- [19] Ref. 5, ch. 6.
- [20] Ref. 7, ch. 8.
- [21] Ref. 7, ch. 9.
- [22] Ref. 15, ch. 5.
- [23] Ref. 1, pp. 159-160.
- [24] Ref. 5, pp. 235-238.
- [25] Ref. 1, pp. 157-158.
- [26] Ref. 5, pp. 241-242.
- [27] Ref. 5, pp. 197-199.
- [28] Ref. 1, pp. 168-169.
- [29] Ref. 5, pp. 205-211.
- [30] Ref. 7, p. 896.
- [31] Ref. 1, p. 160.
- [32] Ref. 5, pp. 239-241.
- [33] L. Gould, "Handbook on Breakdown of Air in Waveguide Systems," Microwave Associates; 1956.
- [34] Ref. 9, sec. 7.
- [35] D. Dettinger and R. D. Wengenroth, "A standard waveguide spark gap," *IRE TRANS. ON MICROWAVE THEORY AND TECHNIQUES*, vol. MTT-1, pp. 39-47; March, 1953.
- [36] H. A. Wheeler, "Air breakdown chart for radar pulses," *Electronics*, vol. 25, p. 148; August, 1952.
- [36a] L. Young, "A hybrid-ring method of simulating higher powers than are available in waveguides," *Proc. IEE*, vol. 101, pt. 3, pp. 189-190; May, 1954.

- [36b] P. J. Sferazza, "Traveling wave resonator," *TeleTech.*, vol. 14, pp. 84-85, 142-143; November, 1955.
- [37] S. E. Miller and A. C. Beck, "Low loss waveguide transmission," *Proc. IRE*, vol. 41, pp. 354, 357, 358; March, 1953.
- [38] S. E. Miller, "Coupled wave theory and waveguide applications," *Bell Sys. Tech. J.*, vol. 31, pp. 661-719; May, 1954.
- [39] A. P. King, "Dominant wave transmission characteristics of a multimode round waveguide," *Proc. IRE*, vol. 40, p. 968; August, 1952.
- [40] O. M. Woodward, "Balance measurements," *Electronics*, vol. 26, pp. 188-191; September, 1953.
- [41] K. Tomiyasu, "Unbalanced terminations on a shielded-pair line," *J. Appl. Phys.*, vol. 21, pp. 552-556; June, 1950.
- [42] Ref. 7, pp. 804, 853.
- [43] Ref. 9, sec. 3.
- [44] R. W. Beatty, "Mismatch errors in the measurement of ultrahigh frequency and microwave variable attenuators," *J. Res. NBS*, vol. 52, pp. 7-9; January, 1954.
- [45] Ref. 1, pp. 270-271.
- [46] Ref. 7, pp. 570-571.
- [47] Ref. 1, pp. 275-277.
- [48] W. W. Mac Alpine, "Heating of radio-frequency cables," *Elec. Commun.*, vol. 25, pp. 84-99, March, 1948; *AIEE Trans.*, vol. 68, pt. 1, pp. 283-288; 1949.
- [49] R. C. Mildner, "The power rating of radio-frequency cables," *AIEE Tech. Paper*, No. 49-78; 1948.
- [50] Ref. 7, pp. 330-342.
- [51] Ref. 9, sec. 5.
- [52] H. M. Altschuler and L. B. Felsen, "Network methods in microwave measurements," *Proc. Symp. on Modern Advances in Microwave Techniques*, Polytechnic Inst. of Brooklyn, Brooklyn, N. Y.; November, 1954.
- [53] Ref. 9, sec. 6.
- [54] N. Marcuvitz, "Waveguide Handbook," M.I.T. Rad. Lab. Ser., McGraw-Hill Book Co., Inc., New York, N. Y., vol. 10, ch. 3; 1951.
- [55] R. W. Beatty, "Determination of attenuation from impedance measurements," *Proc. IRE*, vol. 38, pp. 895-897; August, 1950.
- [56] G. A. Deschamps, "Determination of reflection coefficients and insertion loss of a waveguide junction," *J. Appl. Phys.*, vol. 24, pp. 1046-1050; August, 1953.
- [57] J. E. Storer, L. S. Sheingold and S. Stein, "A simple graphical analysis of a two-port waveguide junction," *Proc. IRE*, vol. 41, pp. 1004-1013; August, 1953.
- [58] "Instruction Manual on Equivalent Circuit Measurement of Waveguide Structure," Rep. R-284-52, Microwave Res. Inst. Polytechnic Inst. of Brooklyn, Brooklyn, N. Y.; March, 1953.
- [59] G. A. Deschamps, "A Hyperbolic Protractor for Microwave Impedance Measurements and Other Purposes," Federal Telecommunication Labs., Nutley, N. J.; 1953.
- [59a] G. A. Deschamps, "A new chart for the solution of transmission time and polarization problems," *Elec. Commun.*, vol. 30, pp. 247-256; September, 1953.
- [60] F. L. Wentworth and D. R. Barthel, "A simplified calibration of two-port transmission line devices," *IRE TRANS. ON MICROWAVE THEORY AND TECHNIQUES*, vol. 4, pp. 173-175; July, 1956.
- [61] Ref. 58, p. 24.
- [62] A. A. Oliner, "The calibration of the slotted section for precision microwave measurements," *Rev. Sci. Instr.*, vol. 25, pp. 13-20; January, 1954.
- [63] H. M. Altschuler and A. A. Oliner, "Microwave measurements with as lossy variable termination," *Proc. IEE (London)*, Monograph No. 179R; May, 1956.
- [64] L. B. Felsen and A. A. Oliner, "Determination of equivalent circuit parameters for dissipative microwave structures," *Proc. IRE*, vol. 42, pp. 477-482; February, 1954.
- [65] H. M. Altschuler, "A method of measuring dissipative four-poles based on a modified Wheeler network," *IRE TRANS. ON MICROWAVE THEORY AND TECHNIQUES*, vol. 3, pp. 30-36; January, 1955.
- [66] K. Tomiyasu, "Intrinsic insertion loss of a mismatched microwave network," *IRE TRANS. ON MICROWAVE THEORY AND TECHNIQUES*, vol. 3, pp. 40-44; January, 1955.
- [67] Ref. 9, secs. 12, 13.
- [68] L. B. Felsen and A. A. Oliner, "Comment on 'A single graphical analysis of a two-port waveguide junction' by J. E. Storer, L. S. Sheingold, and S. Stein," *Proc. IRE*, vol. 42, pp. 1447-1448; September, 1954.
- [69] Ref. 9, sec. 13.06.
- [70] Ref. 9, sec. 12.05.
- [71] Ref. 9, sec. 12.04.
- [72] E. W. Matthews, Jr., "Characteristics of microwave comparators," *IRE TRANS. ON INSTRUMENTATION*, no. PG1-4, pp. 109-112; October, 1955.
- [73] Ref. 9, sec. 13.08.
- [74] E. L. Ginzton, "Microwave Measurements," McGraw-Hill Book Co., Inc., New York, N. Y.; 1958.

Correspondence

Stereo Frequency Response*

These comments are stimulated by those submitted by Sobel¹ who suggested that the frequency response necessary for stereo reproduction might be considerably curtailed from the maximum frequency response to which the ear responds. Sobel proposed that work might be done which could result in such a determination.

Extensive work has been done in this respect by the two foremost acoustical experts in the world. It has definitely been proven that the full frequency range the ear accommodates is not only preferred by compara-

tive listener tests, but is necessary from the standpoint of an analysis of the separate effects of the binaural and stereophonic phenomena. This work has been described by Dr. Harry F. Olson, Director, Acoustical and Electromechanical Research Laboratory, RCA Laboratories, Princeton, N. J., and Dr. Harvey Fletcher, Director of Scientific Research, Brigham Young University, Provo, Utah, formerly Director of Physical Research, Bell Telephone Laboratories.

An account of Dr. Olson's work, concerning the listener preference tests, appears in his book.² In section 12.29, he describes extensive listening tests (after Chin and Eisenberg) which indicated that the listeners preferred a curtailed range of frequencies for reproduced monaural music. In section 12.30,

he points out that the reason for this choice by the listeners was undoubtedly due to distortions in the reproduction equipment, and goes on to describe listener tests which employed live music and acoustical filters which resulted in a preference of the listeners for the full range for the case of both music and speech. The obvious result of these extensive tests is that when the reproduction is natural enough, the listener prefers the full range.

Similar frequency preference tests were conducted by Dr. Olson using stereophonic sound reproduction and are described in section 12.31. The subjective tests of frequency range preference were conducted for speech and music reproduced in auditory perspective employing a two-channel stereophonic sound system. The full frequency range was a flat response to 15,000 cycles. "The comparison range was a flat response to 5000 cycles. The results of these tests indicate a preference for a full frequency range" (for music). "The frequency preference for speech

* Received by the IRE, January 23, 1959. The author submitted this letter for comments to both Dr. Olson and Dr. Fletcher, and they agreed that the material is factual and correct.

¹ A. Sobel, "A possible simplification of stereophonic audio systems," *Proc. IRE*, vol. 46, p. 1426; July, 1958.

² H. F. Olson, "Acoustical Engineering," D. Van Nostrand Co., Inc., Princeton, N. J.; 1957. The pertinent material is given in ch. 12, sec. 12.29-12.32, pp. 600-610.

also indicates a preference for the full frequency range."

The work of Dr. Fletcher concerns the analysis of the separate stereo and binaural effects. In chapters 12 and 13 of his book² he points out that the binaural and stereo effects are dependent upon three factors: the *phase* effect, the *amplitude* effect, and the *sound quality*. A consideration of any one of these alone does not give the full effect. Many measurements have been taken considering the phase effect alone with blind-folded listeners who indicated the location of the image as the phase was varied while the amplitude was held constant. These measurements indicated that the phase effect becomes uncertain above approximately 1000 cycles. This reference, which considers only one of the three pertinent factors, may be responsible for Sobel's assumption that only a limited frequency response might be required to supply the full stereo effect.

In Chapter 13, "Auditory Perspective," Dr. Fletcher considers stereophonic transmission where two or more loudspeakers are employed. Much data are given which show the intricate nature of the amplitude perception of the stereophonic effect by the ear. A graph reproduced on page 225 shows that the amplitude perception of the stereophonic effect is greatest in the range of frequencies between 5000 and 15,000 cycles. He concludes that: "Of the factors influencing angular localization, loudness differences of direct sound seem to play the most important part; for certain observing positions the effect can be predicted reasonably well from computations."

On page 228 this statement is made: "If the quality from the various loudspeakers differs, the quality of sound is important to localization. In general, localization tends towards the channel giving the most natural or 'close-up' reproduction, and this effect can be used to aid the loudness differences in producing angular localization." This is an interesting point. It shows that AM-FM stereo, or the FM multiplex stereo of the type which employs full fidelity on the main channel of the FM transmitter and a curtailed fidelity on the multiplex sub-carrier channel, result in an improper localization. An interesting additional fact in this respect is the experiment described on page 216 in which different frequency ranges of speech and music were applied to the two channels. In the case of speech, "... the brain was able to combine the sounds obtained from the two ears to complete the proper picture. However, when music was transmitted a different situation resulted. This was particularly true when listening to music from the piano. In this case the tones appeared first in one ear and then in the other ear depending upon the pitch. This causes confusion and gives a very weird sort of sensation." The obvious conclusion of these extensive measurements is that while curtailed frequency response on one of the loudspeaker systems may give an apparent stereo effect, the full and most desirable effect cannot be obtained. A further conclusion is that with the compatible¹ system of FM multiplex

stereo, which balances the frequency response of the two loudspeakers, the degradation produced by unequal frequency response is removed.

It is my feeling that we are in a formative stage with respect to stereo. Much is known about it, as is evidenced by the published material mentioned above. However, as this system is brought more and more into practice by the stereo tapes, disks, and broadcasting systems, still more will be learned to enhance it further. Hence, nothing should be done at this time which would place any limitation on such further developments. In addition, it appears that stereo is providing a new tool for the maestro. Interesting effects of separation are being employed by the stereo disk manufacturers such as very realistic soft-shoe dancing which dances from one loudspeaker to the other and gives a further imaginative effect of the listener being "there." Such devices as the two-studio technique which uses one microphone, in one studio with one group of musicians, another microphone in another studio with another group of musicians, and glass panels that permit both to be seen by the maestro, may appear as stunts with a certain amount of deceit. However, out of such stunts there will inevitably emerge new techniques which will further enhance musical reproduction for the greater enjoyment of the listening public. A free hand should be allowed in every respect. The listeners will judge which is good and which is bad, but they must have the opportunity for the best frequency response, distortion characteristics, and other factors, to make such judgment.

Sobel is to be commended for bringing the subject up as he did. I hope that these comments provide a clarification.

MURRAY G. CROSBY
Crosby Laboratories, Inc.
Syosset, N. Y.

¹ M. G. Crosby, "A compatible system of stereo transmission by FM multiplex," *J. Audio Eng. Soc.*, vol. 6, pp. 70-73; April, 1958.

Directional Bridge Parametric Amplifier*

Mr. S. H. Autler in his letter¹ describes a proposed maser amplifier that does not require non-reciprocal elements. A similar system utilizing varactor diodes has been used at the Bell Laboratories.

The operation of this system can be seen from Fig. 1. A signal in arm 1 of the hybrid divides equally between arms 2 and 3. This signal is amplified by the varactors and reflected back to the hybrid. When the phase adjustment of the varactors and phase

shifters shown on the figure in arms 2 and 3 are such that the returned signals at the hybrid are 180° out of phase, we have addition of the signals in arm 4 and cancellation in arm 1.

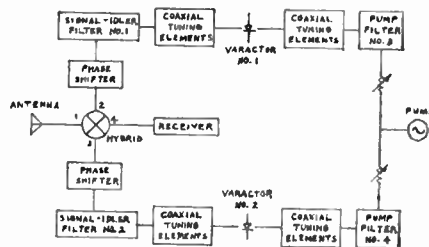


Fig. 1—Directional bridge parametric amplifier.

The noise figure of this directional bridge amplifier for a matched antenna and ideal balanced hybrid is the same as the single varactor. Heffner and Wade² have shown that the noise figure of a varactor is given by

$$F = 1 + \frac{G_1}{G_g} + \frac{G}{G_g} \frac{\omega_1}{\omega_2} + \text{higher terms.}$$

Normally,

$$\frac{G_1}{G_g} \approx 0 \quad \text{and} \quad \frac{G}{G_g} \approx 1.$$

hence the noise figure of the varactor in the degenerate mode (signal frequency approximately equal to idler frequency) is

$$F \approx 1 + \left[\frac{\omega_1}{\omega_2} \right] \approx 3 \text{ db.}$$

Of course, a mismatched antenna or unbalanced hybrid will cause an increase in noise figure above the 3-db figure.

The experimental circuit follows Fig. 1 closely. A broad-band coaxial hybrid was used. A varactor diode with its associated tuning elements was placed in each side arm (2 and 3). Means of controlling phase shift were placed between the filters and hybrid. Filters 1 and 2 pass the signal and idler frequencies but reject the pump. Filters 3 and 4 pass the pump but reject the signal and idler. The pump is fed from a common source through separate attenuators to the diodes. DC bias was supplied separately to the diodes.

The experimental results of the directional bridge amplifier operating at 530 mc (pump at 1060 mc) are promising. Gains up to 25 db have been obtained although the margin of stability was small. For a 10-db gain, the following results were obtained. A pump power of about 4 milliwatts was required. A bandwidth of approximately .6 mc was obtained. The hybrid balance at 530 mc was such that the VSWR in the input arm 1 was $1.02 \pm .01$. The average of the measured noise figures was 3.8 db which compares favorably with the theoretical noise figure of 3 db for this mode of operation.

* Received by the IRE, January 8, 1959.

¹ S. H. Autler, "Proposal for a maser-amplifier system without nonreciprocal elements," *Proc. IRE* vol. 46, pp. 1880-1881; November, 1958.

² H. Heffner and G. Wade, "Gain Bandwidth and Noise Characteristics of the Variable Parameter Amplifier," Stanford Electronics Lab., Stanford University, Stanford, Calif., Tech. Rep. No. 28.

Further experiments indicate that the directional bridge parametric amplifier can be used as a tunable amplifier by varying pump frequency, tuning, and phase shift. The range of operation would be limited by the broad-band nature of the hybrid. This directional bridge amplifier can be used at any frequency where a hybrid and a maser or reactance device are available.

L. U. KIBLER
Bell Telephone Labs.
Holmdel, N. J.

Minimum Insertion Loss Filters*

The recent letter by La Rosa¹ can be used, together with the papers referenced in the letter, to formulate a general problem whose solution has not been obtained yet: "Given the requirements for a band-pass filter in terms of bandwidths, selectivity, and such other requirements as particular problems suggest, choose the shape of the response and the design criteria that minimize the insertion loss in the center of the pass bands."

La Rosa shows that in a particular case a symmetrical filter meets the minimum loss conditions. On the other hand, Dishal has shown that, for the case of Butterworth or Chebyshev shapes, asymmetrical filters are required to minimize the mid-band loss. Despite the apparent contradiction, both answers, of course, are correct and show that the general solution depends upon the initial requirements.

The importance of the problem is great enough to warrant effort by other researchers, and the purpose of this note is to formulate the general problem and invite attention to it.

EUGENE G. FUBINI
Airborne Instruments Lab.
Mineola, N. Y.

* Received by the IRE, November 13, 1958.

¹ La Rosa, "Optimum coupled-resonator band-pass filter," *Proc. IRE*, vol. 47, pp. 329-330; February, 1959.

AGU Committee for the Study of the Metric System in the United States*

Pursuant to the resolution adopted unanimously at the business session of the American Geophysical Union on May 7, 1958,¹ President Ewing appointed a Committee on the study of the Metric System in the United States.

* Received by the IRE, January 30, 1959.
¹ *AGU Trans.*, p. 558; June, 1958.

METRIC SYSTEM QUESTIONNAIRE

1. Indicate professional field of interest in the AGU. _____
2. What approximate percentages of units used in your work are
Metric _____ British _____
Other _____
3. Would it be to your advantage if a complete conversion to the metric system could eventually be made?
Yes _____ No _____
4. How long a period of time should be allowed for the conversion, in years?
10 _____ 20 _____ 30 _____ 40 _____ 50 _____
Longer _____
5. Should the centigrade system of temperature measurement be adopted?
Yes _____ No _____
6. Do you believe that U. S. export trade is suffering due to the use of British units?
Yes _____ No _____ No Opinion _____
7. Do you believe that the eventual adoption of the metric system is inevitable?
Yes _____ No _____
8. In the event of a one-time conversion to the metric system, do you believe that the cost would be prohibitive?
Yes _____ No _____
9. In the event a Joint Committee were established to study the problem, circulate questionnaires, accumulate statistics, and report, it should be sponsored by (check one):
Professional societies _____
Educational institutions _____
Industry _____
Government _____
How should the study be financed?
Would you be willing to assist such a study group?
Financially _____
As an advisor _____
10. Additional remarks at any length are welcomed.

Bills for the exclusive adoption of the metric system in the United States have been presented to Congress more than once, but they failed, the principal reason being that the effective date proposed was entirely too soon after passage of the bill. An early effective date would undoubtedly work a severe hardship on the adult population not familiar with the metric system, and it would make obsolete a prohibitive amount of everyday items of weights and measures. A solution would appear to be a bill to make the metric system the only official system of weights and measures in the United States, effective in not less than one generation, 33 years, after passage of the bill. Following this action by the Congress, the grade schools and high schools would begin immediately to teach children the metric along with the English system and, during the transition period, would place more and more emphasis on the metric system. By the end of the transition period, the English system would still be taught, but the emphasis would be completely reversed from what it is today. In a generation, most items of equipment involving weights and measures normally become obsolete or worn out and are replaced. Also, persons engaged in professions and trades now using the English system exclusively would normally pass on to retirement during

this period and would be replaced by a new generation thoroughly educated and trained in the metric system. A long transition period should result in a smooth change to this simplified decimal system under which 90 per cent of the world's people now live.

QUESTIONNAIRE

The accompanying questionnaire is directed to readers for the purpose of gathering statistical information to indicate the degree of interest in this matter. The metric committee of the American Geophysical Union will welcome any comments. Those submitting replies are urged to suggest solutions to difficulties which may be foreseen in the adoption of the metric system. Signature of these replies is optional.

Additional copies of the questionnaire are available upon request. A small effort on your part to complete and mail this questionnaire will be of invaluable help to the Committee. Address all correspondence to:

The Executive Secretary
American Geophysical Union
1515 Massachusetts Avenue N. W.
Washington 5, D. C.

FLOYD W. HOUGH
Committee Chairman

Low Noise Parametric Amplifier*

In this note the authors report preliminary analytical and experimental results obtained with a cavity-type parametric amplifier at S-band in which through variable coupling the effect of diode losses on noise figure can be minimized at the expense of pump power. In this way, excess noise temperatures of 100°K have been obtained at room temperature. By cooling the diode with liquid nitrogen temperature, the excess noise temperature was reduced to 50°K.

In what follows it is assumed that the reader is acquainted with the referenced literature.^{1,2,3} The noisiness of the amplifier is described by its "excess noise temperature T_c "⁴ which is related to the "noise figure F "⁵ as follows:

$$\frac{T_c}{T_0} = F - 1 \quad (1)$$

where

$$T_c = \frac{N_c}{kBG}$$

* Received by the IRE, January 19, 1959.
¹ J. M. Manley and H. E. Rowe, "Some general properties of nonlinear elements," Part II, *Proc. IRE*, vol. 46, pp. 850-860; May, 1958.
² S. Bloom and K. K. N. Chang, "Theory of parametric amplification using nonlinear reactances," *RCA Rev.*, vol. 18, pp. 578-596; December, 1957.
³ H. Heffner and G. Wade, "Gain, band width and noise characteristics of the variable parameter amplifier," *J. Appl. Phys.*, vol. 29, pp. 1321-1331; September, 1958.
⁴ J. C. Helmer and M. W. Müller, "Calculation and measurement of the noise figure of a maser amplifier," *IRE TRANS. ON MICROWAVE THEORY AND TECHNIQUES*, vol. MTT-6, pp. 210-215; April, 1958.
⁵ H. A. Haus and R. B. Adler, "Optimum noise performance of linear amplifiers," *Proc. IRE*, vol. 46, pp. 1517-1533; August, 1958.

N_e = excess output noise power generated between input and output terminals of the device
 G = power gain
 B = effective bandwidth = $1/G \int_0^\infty G(f) df$
 T_0 = reference temperature (290°K)

Our analysis is based on the equivalent circuit of Fig. 1. A single cavity supports both signal and idler frequencies and an ideal circulator is symbolically indicated by arrows showing direction of unattenuated power-flow. The subscripts g, d, p refer to generator, signal, diode, and pump respectively. The coupling coefficients k are defined as follows:

$$k_{sd} = Q_s/Q_{sd}, \text{ etc. } k_{sp} = Q_s/Q_{sp}, \text{ etc.}$$

where

Q_s is the unloaded signal circuit Q
 Q_{sd} is the external signal circuit Q loaded by the diode
 Q_{sp} is the external signal circuit Q loaded by the generator.

In addition, we define the following quantity:

$$\mu_g = Q_{sd}/Q_{sp}$$

This coefficient measures directly the degree of coupling between the generator and diode. Extension of the above model to include a separate idler cavity is obvious. The gain and bandwidth expressions for this model are, of course, identical with the published ones provided the admittances and Q 's are properly interpreted. The excess noise temperature and the critical pump power (power necessary for onset of oscillations) can be given for the general case in terms of the above quantities by (2) and (3).

$$T_e = T_s \frac{1}{k_{sg}} + T_d \frac{1}{\mu_g} + \alpha \frac{\omega_s}{\omega_i} \frac{k_{id}}{k_{id} + 1} \cdot \left(1 + \frac{1}{k_{ru}} + \frac{1}{\mu_g}\right) \left(T_d + T_i \frac{1}{k_{id}}\right) \quad (2)$$

$$P_{CR} = \frac{\omega_s C}{Q_{sd}^2} \left(\frac{C}{\mathcal{E}}\right)^2 \left(1 + \mu_g + \frac{1}{k_{sd}}\right) \left(1 + \frac{1}{k_{id}}\right) \left(1 + \frac{1}{k_{rd}}\right) \left(\frac{\omega_i}{\omega_p}\right) \left(\frac{\omega_p}{\omega_s}\right)^2 \quad (3)$$

where

$C_d = C + \mathcal{E}'$ defines diode nonlinearity
 Q_d = diode Q at signal frequency
 T_s = temperature of signal circuit
 T_i = temperature of idler circuit
 T_d = diode temperature
 T_v = temperature of generator resistance.

For the single cavity experiment in which the noise performance is measured with a broadband noise source, the above expressions reduce to (4) and (5).

$$\frac{T_e}{T_0} = \frac{T_s}{T_0} \frac{1}{k_{sg}} + \frac{T_d}{T_0} \frac{1}{\mu_g} \quad (4)$$

$$P_{CR} = 4 \frac{\omega_s C}{Q_{sd}^2} \left(\frac{C}{\mathcal{E}}\right)^2 \left(1 + \mu_g + \frac{1}{k_{sd}}\right) \cdot \left(1 + \mu_g + \frac{1}{k_{id}}\right) \left(1 + \frac{1}{k_{pd}}\right) \quad (5)$$

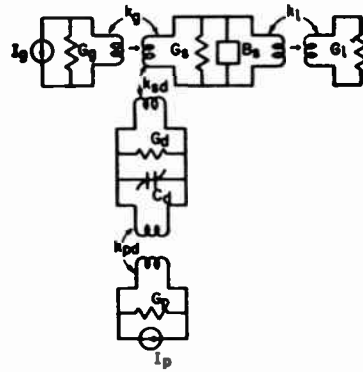


Fig. 1—Equivalent circuit of single-cavity parametric amplifier using ideal circulator.

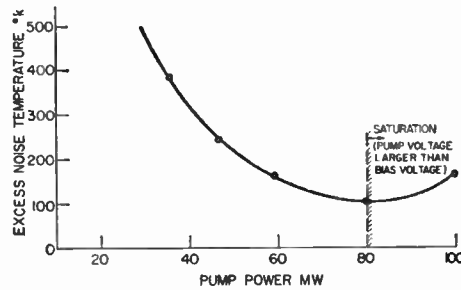


Fig. 2.

Eqs. (4) and (5) show the important characteristic that the amplifier's noise temperature can be reduced at the expense of increased pump power. This is obtained by increasing μ_g , i.e., reducing the diode-to-signal-circuit coupling relative to the generator-to-signal circuit coupling.

From (4) and (5) both noise figure and pump power for a specific amplifier can be rather accurately predicted because the diode parameters as well as the relative coupling coefficients (ratios of Q 's) can be measured or evaluated. A verification of these relations was performed with an S-band (3100 mc) waveguide cavity amplifier with pump power equal to about twice the signal frequency. This amplifier was so designed that the diode coupling to the signal cavity could be varied. Provision was also made for cooling the diode with liquid nitrogen temperature without cooling the circuits. Noise figure was measured both with an argon discharge lamp and, in an absolute measurement, by reference to the noise from a matched load cooled to liquid nitrogen temperature. In these measurements, because idler and signal frequencies were about the same, noise from the reference noise source was fed to both signal and idler channels. This means that there was no contribution from the idler channel to the excess noise temperature and that (4) did apply.

The diodes used in these experiments were gold bonded diodes produced expressly for this purpose by the Semiconductor Division of Hughes Products. At this stage of development, the diode Q at 3000 mc and 2 volt reverse bias was about 15.

A typical variation of amplifier noise temperature with pump power measured with this amplifier is shown in Fig. 2. These

experimental results were found in agreement with the theoretical relations (4) and (5).

By cooling the diode to liquid nitrogen temperature (78°K), the minimum amplifier noise temperature was reduced to 50°K, while the pump power necessary to maintain constant gain was decreased by 25 per cent. This was also found consistent with (4) and (5).

The authors are indebted to K. M. Johnson for the data presented in Fig. 2. and to M. R. Currie for helpful discussions.

R. C. KNECHTLI
 R. D. WEGLEIN
 Physics Laboratory
 Hughes Aircraft Co.
 Culver City, Calif.

Rotating Loop Reflectometer for Waveguide*

The rotating inductive loop described by Tischer¹ has been successfully used by us as a reflectometer in S-band waveguide; limited access precluded the use of a slotted line or a directional coupler. However, considerable skill in adjusting the loop and compensating probe is called for when it is required to measure VSWR of the order of 1.01, and this setting is very easily disturbed. I therefore feel that a variant of the method requiring much less critical adjustment might be of some interest.

In principle, if a pure inductive loop is inserted through the wall of a waveguide and rotated, at a position where the magnetic field of the mode is circularly polarized, the signal induced in it will remain constant independent of its orientation. However, there is also an electric field at this position, and, in practice, a simple wire loop connected to a crystal detector behaves as a capacitive probe as well as an inductive loop; previous techniques have used a separate probe, critically coupled to the loop to cancel out the capacitive component of the signal.

Here the effect of pure inductance is achieved by closing the loop, through another loop which is then only inductively coupled to the mode in a second waveguide. One position satisfying this condition is at the center of a plane short circuit placed across a rectangular guide propagating the H_{01} or H_{01} modes. A capacitive probe inserted here perpendicular to the surface is completely decoupled from the electric field, but a loop can be orientated for maximum magnetic coupling. The device is illustrated in Fig. 1. Symmetry and careful positioning of the loops in both waveguides are necessary, and any higher modes excited in the secondary guide should be isolated from the detector.

* Received by the IRE, November 27, 1958.
¹ F. J. Tischer, "Rotatable inductive probe in waveguides," Proc. IRE, vol. 43, pp. 974-980; August, 1955.

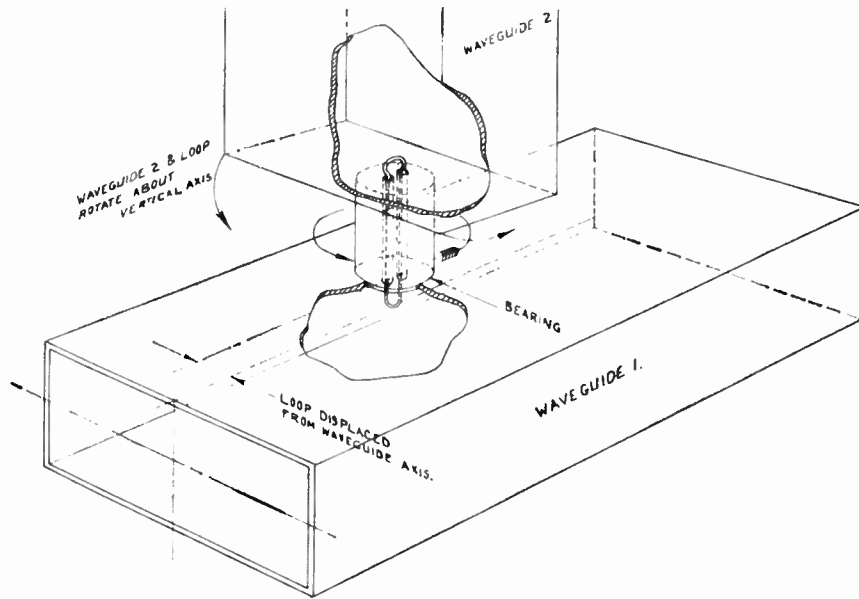


Fig. 1—Rotating loop reflectometer.

Nevertheless the adjustments are much less critical than for the earlier device. Thus, pure inductive coupling is obtained without need for a compensating probe, and, in addition, the loop may readily take various sizes and shapes according to the application.

The principle was confirmed with a makeshift model used as a reflectometer in rectangular guide. This gave, for example, an apparent VSWR of about 1.01 when a high precision slotted line instrument indicated a VSWR of 1.003. Unfortunately, very little development has been carried out, but with suitable refinements a greater accuracy should be obtained. A particularly valuable application is as a reflectometer for use in rectangular and circular waveguides of nonstandard sizes because only a small hole through the guide wall is required and the rotating mechanism may then be clamped in position.

P. J. HOUSELEY
Admiralty Signal and
Radar Est.
Portsmouth, England

Gain Measurements on a Pulsed Ferromagnetic Microwave Amplifier*

The dependence of gain on pump power has been measured for a ferromagnetic microwave amplifier¹ using polycrystalline yttrium iron garnet. The amplifier operates in the "quasi-degenerate" mode in which one cavity serves as the resonant circuit for both the signal and the idle frequency fields. A

second resonant cavity is used for the pump signal. Coupling between the signal-idle cavity and the external transmission line is obtained with a single capacitive probe, so that the device is a reflection-type negative-resistance amplifier. To reduce heating effects a pulsed source is used for the pump power; the device amplifies only when the pump is on.

With the CW signal f_s tuned to approximately one half the pump frequency, the power reflected from the signal-idle cavity was measured as a function of the peak pump power incident on the pump cavity. The reflected power was measured relative to the incident signal power by adjusting a precision attenuator to give the same amplitude of power at the input of a microwave receiver as that measured with a short inserted immediately in front of the cavity. The reflected power was allowed to build up for 1.5 μ sec after the beginning of the pump pulse before it was measured. The power gain was defined as the ratio of the power reflected from the signal-idle cavity to the power incident on the cavity at the signal frequency. The pump power was measured with a directional coupler and a bolometer. The incident signal frequency power was varied from 2×10^{-7} watts to 2×10^{-3} watts for these measurements to test for possible signal saturation. At signal levels greater than 10^{-2} watts severe arcing occurred in the signal-idle cavity at high gains. The results of this experiment are shown in Fig. 1.

Using the expression of Suhl¹ for the negative quality factor (Q_s) of the ferrite one can derive the following expression for the gain of a reflection-type ferrite amplifier under transient conditions:

$$g(t) = 1 - \frac{4Q_L^2}{Q_e Q_u} \frac{\left(1 - \frac{Q_u}{Q_L} \frac{P}{P_c}\right)}{\left(1 - \frac{P}{P_c}\right)^2} \left[1 - \frac{P}{P_c} e^{-Bt/2}\right]^2 \quad (1)$$

where Q_L , Q_e , and Q_u are, respectively, the loaded, external, and unloaded quality factors of the signal-idle cavity

$$\frac{1}{Q_L} = \frac{1}{Q_e} + \frac{1}{Q_u};$$

P is the pump power incident on the cavity; P_c is the value of pump power which gives infinite steady state gain (i.e., the value of P which drives the precession angle to the critical value given by Suhl for electromagnetic operation¹); t is the time elapsing after the beginning of the pump pulse; and B is the amplifier bandwidth, which for large gain is

$$B = \frac{2\pi f_s}{Q_L} \left(1 - \frac{P}{P_c}\right) \left(1 + \frac{P}{P_c}\right) \quad (2)$$

In deriving (1) and (2) it has been assumed that the ferromagnetic precession angle is directly proportional to the amplitude of the field at the pump frequency; i.e., high power saturation effects² have been neglected. If these effects were included, one would expect P/P_c to be replaced by some other more slowly varying function of P .

It was not possible to measure P_c by independent means in this experiment because of the pulsed operation of the device (see next paragraph) but a reasonable fit of (1) to the data can be obtained if one assumes $P_c = 5.0$ kw. The theoretical transient gain and steady-state gain are indicated in Fig. 1.

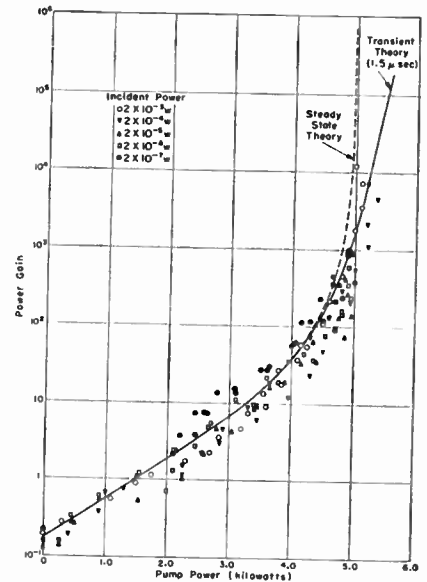


Fig. 1—Power gain as a function of pump power.

The rather wide scatter of the experimental points may have been caused by fluctuations in the pump frequency and power, and by phase instabilities resulting from the near equality of the signal and idle frequencies.

In an effort to determine the noise properties of the device the output power of the amplifier at one half the pump frequency was measured at various values of pump power with no signal input. On the assumption that the output power resulted from the amplification of noise present in the amplifier and in the external room temperature load, the

* Received by the IRE, December 11, 1958.

¹ H. Suhl, "Theory of the ferromagnetic microwave amplifier," *J. Appl. Phys.*, vol. 28, pp. 1225-1236; November, 1957.

DC Characteristics of a Junction Diode*

Moll¹ has pointed out the problems involved in comparing theory and experiment for *p-n* junction diodes. Thus, the well-known expression of Shockley, $I = I_0(e^{\alpha^*V} - 1)$ with $\alpha^* = q/kT$, holds only for heavy doping or very small applied voltages. For an intrinsic base, Spenke² shows that the largest value for α^* is $q/2kT$. For intermediate doping, α^* is certainly smaller than q/kT , and for large forward bias one again has $q/2kT$, as quoted by Moll. We wish, therefore, to describe a diode for which, by including the field, all these relationships can be connected analytically.

This is a planar, narrow-base, abrupt-junction diode with unequal doping (injection into base only). For later use two restrictions are re-stated: width of base, $W \ll (D_p\tau_p)^{1/2}$ (neglect of recombination) and number of ionized acceptors in emitter region, $N_a \gg$ number of ionized donors in base, N_d .

Fig. 1 is a schematic diagram of the diode. We use the boundary conditions

$$p = p_0 e^{\alpha V_1}, \quad x = 0; \quad \alpha = q/kT \quad (3)$$

$$p = p_0, \quad x = W. \quad (4)$$

Because of (1) and (2), the net electron current in the base can be set equal to zero, and the hole current, J_p , must be constant. Using the definitions of electron and hole current

$$J_n = q\mu_n n E + qD_n \nabla n = 0 \quad (5)$$

$$J_p = q\mu_p p E - qD_p \nabla p \quad (6)$$

together with the neutrality condition

$$p - n + N_d = 0 \quad (7)$$

we have for the field in the base,

$$E = \frac{J_p + qD_p \nabla p}{q\mu_p p} \quad (8)$$

and also

$$E = - \frac{D_p \nabla p}{\mu_p (p + N_d)}. \quad (9)$$

Solving for ∇p between these two equations:

$$\nabla p = - \frac{J_p}{qD_p} \left(\frac{p + N_d}{2p + N_d} \right). \quad (10)$$

Integrating (10) and using (3) and (4), the total current obtained is

$$J = J_p = qD_p N_d / W \left[2p_0 / N_d (e^{\alpha V_1} - 1) - \ln \left(\frac{N_d + p_0 e^{\alpha V_1}}{N_d + p_0} \right) \right]. \quad (11)$$

These relations have been derived by Rittner³ in connection with transistor theory.

* Received by the IRE, January 9, 1959.
 1 J. L. Moll, "The evolution of the theory for the voltage-current characteristic of *p-n* junctions," *Proc. IRE*, vol. 46, pp. 1076-1082; June, 1958.
 2 E. Spenke, "Forward and back characteristics of a *p-n*-metal rectifier," *Z. Naturf.*, vol. 11a, no. 6, pp. 443-456; 1956.
 3 L. S. Rittner, "Extension of the theory of the junction transistor," *Phys. Rev.*, vol. 94, pp. 1161-1171; June 1, 1954.

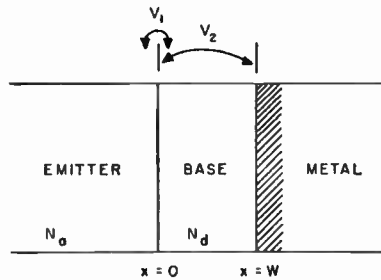


Fig. 1—The narrow-base diode.

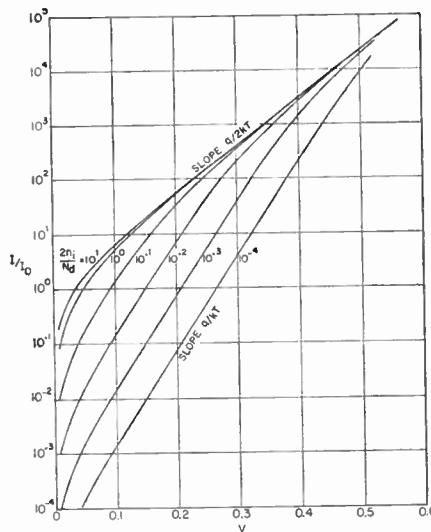


Fig. 2—Forward characteristics of the narrow-base diode.

Eliminating ∇p between (8) and (9), we have

$$E = \frac{J_p}{q\mu_p(2p + N_d)} \quad (12)$$

for the field in the base region. The voltage drop across the base, V_2 is then given by

$$V_2 = \int_0^W E(x) dx = \int_{p_0 e^{\alpha V_1}}^{p_0} \frac{J_p}{q\mu_p(2p + N_d)} \left(\frac{dx}{dp} \right) dp \quad (13)$$

which can be evaluated to give

$$V_2 = 1/\alpha \ln \left(\frac{N_d + p_0 e^{\alpha V_1}}{N_d + p_0} \right). \quad (14)$$

Since $V_{total} = V_1 + V_2$, V_2 can be eliminated in (14) and solve for V_1 to get

$$\alpha V_1 = -N_d/2p_0 \left\{ 1 - \left[1 + 4p_0/N_d (p_0/N_d + 1) e^{\alpha V} \right]^{1/2} \right\}. \quad (15)$$

The equilibrium concentration of holes in the base, p_0 , can be written as

$$p_0 = -N_d/2 \left\{ 1 - \left[1 - (2n_i/N_d)^2 \right]^{1/2} \right\} \quad (16)$$

where (7) and the equilibrium relation $n p = (n_i)^2$ are used. Substituting (15) and (16) into (11) finally leads to

$$I = I_0/a \left\{ (1 + a^2 e^{\alpha V})^{1/2} - (1 + a^2)^{1/2} - \ln \left[\frac{1 + (1 + a^2 e^{\alpha V})^{1/2}}{1 + (1 + a^2)^{1/2}} \right] \right\} \quad (17)$$

where $I_0 = 2qD_p n_i A/W$, $A = 2n_i/N_d$, A is the junction area, and n_i is the intrinsic concentration of electrons in the material.

It is readily seen that (17) reduces to $I = I_0 a / 4 (e^{\alpha V} - 1)$ for small values of the parameter a . This is also the result obtained by direct application of the Shockley theory to a similar diode with heavy base doping.

For large values of a , (17) reduces to $I = I_0 (e^{\alpha V/2} - 1)$, the result of Spenke for intrinsic base material.

The gradual change in α^* from q/kT to $q/2kT$ is illustrated in Fig. 2, which shows (17) for a series of values of the parameter a . For large V , α^* is seen to approach $q/2kT$ for any doping.

The range of validity of this equation can be estimated from the condition

$$e^{\alpha V/2} \ll N_d/n_i.$$

Valuable discussions with A. Brodzinsky are gratefully acknowledged.

I. LADANY
 U. S. Naval Research Lab.
 Washington, D. C.

Suppression of Undesired Radiation—Directional HF Antennas and Associated Feed Lines*

Concerning RF transmission lines of the open type,¹ the statement "Yet, the provisions presently made for detecting such deficiencies are totally inadequate in almost all installations, both commercial and military, to the knowledge of the author," deserves some comment. The "deficiencies" referred to are unbalanced components on the line.

In our point-to-point HF transmitting installations, it has been the practice to use a balance-indicating voltmeter, similar to the type shown in Fig. 8 by Brueckmann, for the past nine years. Our circuit has the additional feature of being tunable over the 4-26 mc range to minimize pick-up from lines and frequencies other than that being measured. It is known as a type BNY-1197. The original design was by G. T. Royden.

In its portable form, this balance indicator consists of a small metal box with a wooden handle and two hooks for attachment to any point on the line. The need for such a device was recognized long ago, and all of our major installations are equipped with one or more of these units.

In discussing the demerits of using RF ammeters, the author also states, "Yet, two ammeters are presently standard equipment for monitoring." Here again, we wish to differ.

In the latest Mackay 10-kw and 30-kw transmitters, the output monitor consists of a built-in balance indicator and a built-in relative output voltage indicator. There are

* Received by the IRE, August 26, 1958.
 1 H. Brueckmann, "Suppression of undesired radiation of directional HF antennas and associated feed lines," *Proc. IRE*, vol. 46, pp. 1510-1516; August, 1958.

no ammeters. Transmitters so equipped have been in operation for several years.

The transmitter balance indicator plus the portable unit are essential in keeping our lines reasonably well balanced. Yet I would be the first to admit that, even so, open lines leave a great deal to be desired. In a large installation there are so many lines and so many bends and irregularities before the antenna feed point is reached, that the maintenance of truly balanced conditions throughout the system becomes difficult.

CHRISTOPHER BUFF
Mackay Radio and Telegraph Co., Inc.
P. O. Box 6
Brentwood, L. I., N. Y.

A UHF Ruby Maser*

A ruby maser has been operated at signal frequencies tunable over the range 380–450 mc. In the experimental arrangement, the magnetic levels $M = +\frac{1}{2}$ and $M = -\frac{1}{2}$ of paramagnetic pink ruby were used for the signal, and X-band pumping was carried out between levels $M = +\frac{3}{2}$ and $M = +\frac{1}{2}$. At the required low magnetic field strength of approximately 70 oer, maser operation was observed to be only slightly dependent on the angle between the dc magnetic field and the crystal axis; amplification and oscillation were obtained for any angle of orientation, with optimum performance at 90°. The observed slight dependence of the maser action on the angle of orientation at the low fields used here is expected on theoretical grounds.

In the mode of operation used, the X-band pumping frequency (approximately 11.8 kmc) is not a critical parameter so that tuning of the signal frequency over the range 380–450 mc required neither adjustment of the pump source nor variation of the magnetic field with regard to magnitude or direction. This feature makes the UHF ruby maser especially suitable for applications in which tuning is desired.

The ruby crystal (4 cm³ in volume) was located at the center of a teflon loaded cavity which was excited in a TE₀₁₁ pump mode. The construction and tuning of the signal frequency lumped circuit was carried out in a manner similar to that used by Kingston¹ in the design of a potassium-chromicyanide maser. The dc magnetic field was supplied by a small permanent magnet in which the field strength was adjusted by varying the gap between the pole faces.

As an amplifier, typical operational data included a gain of 15 db and a bandwidth of 100 kc with the maser at a temperature of 1.7°K. As an oscillator, the power output was less than 1 μw.

G. K. WESSEL
Electronics Lab.
General Electric Co.
Syracuse, N. Y.

* Received by the IRE, December 15, 1958.

¹ R. H. Kingston, "A UHF solid-state maser," *Proc. IRE*, vol. 46, p. 916; May, 1958.

Incoherent Scattering of Radio Waves by Free Electrons with Applications to Space Exploration by Radar*

Gordon¹ has discussed the use of a powerful radar to measure electron temperatures of the ionosphere. An interesting adjunct to these experiments would be to investigate Bailey's suggestion² of controlling the electron temperature of the ionosphere by means of radio waves of frequency 1.2 mc, the gyro frequency of ionospheric electrons. A section of the ionosphere could be illuminated by 1.2 mc radiation and the increased width in the frequency spectrum of the back scattered radar signal measured.

L. H. GINSBERG
U.S.I. Technical Center
Div. of U. S. Industries, Inc.
Bound Brook, N. J.

* Received by the IRE, December 1, 1958.

¹ W. E. Gordon, "Incoherent scattering of radio waves by free electrons with applications to space exploration by radar," *Proc. IRE*, vol. 46, pp. 1824–1829; November, 1958.

² V. A. Bailey, "Control of the ionosphere by means of radio waves," *J. Atmos. Terres. Phys.*, vol. 12, No. 13, pp. 216–217; 1958.

WWV Standard Frequency Transmissions*

Since October 9, 1957, the National Bureau of Standards radio stations WWV and WWVH have been maintained as constant as possible with respect to atomic frequency standards maintained and operated by the Boulder Laboratories, National Bureau of

WWV FREQUENCY*

January, 1959 1600 UT	Thirty-Day Moving Average Seconds Pulses on 15 MC, Parts in 10 ¹⁰ †
1	-30
2	-30
3	-30
4	-30
5	-30
6	-30
7	-30
8	-29
9	-29
10	-29
11	-29
12	-29
13	-29
14	-28
15	-28
16	-28
17	-28
18	-28
19	-28
20	-28
21	-28
22	-28
23	-28
24	-28
25	-28
26	-28
27	-28
28	-28
29	-29
30	-29
31	-29

* Received by the IRE, February 24, 1959.

† WWVH frequency is synchronized with that of WWV.

‡ No adjustment was made in the control oscillator at WWV this month.

Standards. On October 9, 1957, the USA Frequency Standard was 1.4 parts in 10⁹ high with respect to the frequency derived from the UT 2 second (provisional value) as determined by the U. S. Naval Observatory. The atomic frequency standards remain constant and are known to be constant to 1 part in 10⁹ or better. The broadcast frequency can be further corrected with respect to the USA Frequency Standard, as indicated in the table below. This correction is *not* with respect to the current value of frequency based on UT 2. A minus sign indicates that the broadcast frequency was low.

The WWV and WWVH time signals are synchronized; however, they may gradually depart from UT 2 (mean solar time corrected for polar variation and annual fluctuation in the rotation of the earth). Corrections are determined and published by the U. S. Naval Observatory.

WWV and WWVH time signals are maintained in close agreement with UT 2 by making step adjustments in time of precisely plus or minus twenty milliseconds on Wednesdays at 1900 UT when necessary; one retarding time adjustment was made during this month at WWV and WWVH on January 28, 1959.

NATIONAL BUREAU OF STANDARDS
Boulder, Colo.

History of the Problem of Conversion of Heat to Electricity by Thermionic Emission*

Hatsopoulos and Kaye state in their paper¹ that the first electronic and thermodynamic study on the conversion of heat to electricity by thermionic emission was given by Hatsopoulos.²

The first properly documented scientific study of the fundamental problems of the conversion of heat to electricity by thermionic emission is that of Schlichter,³ which was finished sometime prior to August 2, 1914.

Schlichter states¹ (literal translation): "We arrive at the following result: The total practical efficiency of the simple thermionic element is very small, if one uses Platinum and similar materials as electrodes on account of their low electron emission with respect to the radiation loss. It is not possible to reduce this radiation loss at a given emissivity in proportion to this emissivity. The practical efficiency could be increased only by selection of an electrode material with a sufficiently high melting

* Received by the IRE, January 5, 1959.

¹ G. N. Hatsopoulos and J. Kaye, "Analysis and experimental results of a diode configuration of a novel thermoelectron engine," *Proc. IRE*, vol. 46, pp. 1574–1579; September, 1958.

² G. N. Hatsopoulos, "The thermoelectric engine," Sc.D. dissertation, M.I.T., Cambridge, Mass.; May, 1956.

³ W. Schlichter, "Spontaneous emission from glowing metals and the thermionic element," (in German), inaugural dissertation, University of Göttingen, Ger., August, 1915. Published by Barth, Leipzig, Ger., 1915. See also *Ann. Phys.*, vol. 47, pp. 573–640; 1915.

⁴ *Ibid.*, inaugural dissertation, pp. 97–98.

point and extraordinary higher electron emission than that of Platinum. There does not exist a material of this kind among those which have been so far investigated."

"It does not seem to be entirely impossible to prepare such a material artificially by treatment of its surface. If one should succeed in this manner to reduce the constant ϕ to about one third of its value for Platinum maintaining the same constant A , a material with the required high electron emission would be produced. Thus the technical problem would also be solved. Neglecting the radiation loss, economically working thermionic elements are definitely possible within the limits set by the remaining physical laws."

It is evident from the text of Schlichter's dissertation (1a and 1b) that he was not familiar with the work of Child (1911),⁵ Langmuir (1913),⁶ and Schottky (1914).⁷

HENRY J. MILLER
P.O. Box 35
South Orange, N. J.

Author's Comment⁸

Professor Hatsopoulos and I seriously doubt that we should reply to the statements raised by Dr. Miller. Let me indicate that we never claimed that we were the first ones to think of thermionic emission as a new means of conversion of heat directly into electricity. We clearly stated⁹ that the idea was quite old but that the first detailed electronic and thermodynamic analysis on this subject was given in a quantitative fashion by one of the authors in 1956. Miller's remarks indicate that his first reference, Wilhelm Schlichter, discussed the idea only in a qualitative fashion without giving any detailed electronic and thermodynamic analysis.

J. KAYE
Mass. Inst. Tech.
Dept. of Mech. Eng.
Cambridge, Mass.

⁵ C. D. Child, "Discharge from hot CaO," *Phys. Rev.*, vol. 32, pp. 492-511; May, 1911.

⁶ I. Langmuir, "The effect of space charge and residual gases on thermionic currents in high vacuum," *Phys. Rev.*, vol. 2, pp. 402-403; 450-486; December, 1913.

⁷ W. Schottky, "Action of space charge in thermionic currents in high vacuum," (in German), *Phys. Zeit.*, 1914, vol. 15, pp. 526-528; 1914.

⁸ Received by the IRE, January 21, 1959.

⁹ *Op. cit.*, p. 1575.

An Approximation of Transient Response from Frequency Response Data*

The determination of a system transient response, if the frequency response is known, has been studied in many publications.

A method that simplifies Dawson's¹ procedure is presented here.

If the system frequency response is known as

$$H(j\omega) = A(\omega) + jB(\omega), \quad (1)$$

then the impulse response is

$$h(t) = \frac{-2}{\pi} \int_0^{\infty} B(\omega) \sin \omega t d\omega. \quad (2)$$

Usually $B(\omega)$ is quite small for large values of ω such that the approximation.

$$B(\omega) \cong 0 \quad \omega > \omega_0,$$

will not change the integral for $h(t)$.

Therefore,

$$h(t) \cong \frac{-2}{\pi} \int_0^{\omega_0} B(\omega) \sin \omega t d\omega. \quad (3)$$

Also $B(\omega)$ can be described by a Fourier series for $0 < \omega < \omega_0$ as

$$B(\omega) = \sum_{n=1}^{\infty} \sin \frac{n\omega}{\omega_0} \quad (4)$$

where

$$b_n = \frac{2}{\omega_0} \int_0^{\omega_0} B(\omega) \sin \frac{n\pi\omega}{\omega_0} d\omega. \quad (5)$$

But, using the approximate equation for $h(t)$,

$$b_n = -\frac{\pi}{\omega_0} h\left(\frac{n\pi}{\omega_0}\right) \quad (6)$$

or

$$h\left(\frac{n\pi}{\omega_0}\right) = -\frac{\omega_0}{\pi} b_n$$

$$h\left(\frac{nT_0}{2}\right) = \frac{-2b_n}{T_0}. \quad (7)$$

Thus the determination of the transient response at discrete values of time, $t = nT_0/2$, reduces to the determination of Fourier series coefficients, which is relatively simple and well tabulated.

The example worked out by Dawson was a closed looped unity feedback system with a forward transfer function,

$$G(j\omega) = 5(1 + j\omega)^2 / ((j\omega)^3(1 + j0.05\omega)^2).$$

Dawson determined the coefficients b_n to be (assuming $\omega_0 = 17.6$),

$$b_1 = -0.781 \quad b_2 = -0.519$$

$$b_3 = -0.66 \quad \text{and} \quad b_4 = 0.134.$$

Setting these values in (7) yields,

t	$h(t)$	$h_a(t)$
.179	4.38	4.39
.358	2.91	2.87
.536	.37	.30
.715	-.75	-.77

The values $h_a(t)$ are determined by the inversion of the closed loop transfer function.

$$h_a(t) = 0.09e^{-.726t} - 6.36e^{-2.8t} + 3.58e^{-28.13t} + 22.76e^{-4.17t} \sin(4.18t + 6.8^\circ).$$

Comparison of the two columns shows the approximation to be quite close to actual values.

J. D. GRAHAM
Elec. Eng. Dept.
Marquette University
Milwaukee, Wis.

* Received by the IRE, January 16, 1959.

¹ C. H. Dawson, "Approximation of transient response from frequency response data," *Trans. AIEE*, vol. 72, pt. 11, pp. 289-291; 1953.

Space-Charge Capacitance of a P-N Junction*

When estimating the space-charge capacitance of a p-n junction, the space-charge density is often assumed to follow a definite function of position (that of excess donor density) for an appropriate distance. It always turns out that the incremental capacitance per unit cross section is ϵ/d , where ϵ is the dielectric constant and d the breadth of the space-charge layer, just like the capacitance of the corresponding parallel-plate condenser.

Though often implied, this is no coincidence. Given any fixed curve c for the space-charge density (see Fig. 1) the incremental charges $\pm dq$ will add at the boundaries of the space-charge region and thereby cause an additional field and hence an additional potential difference equal to that produced by these charges on condenser plates separated by the distance d .

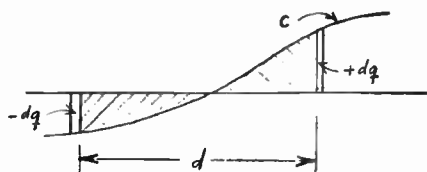


Fig. 1

HELGE JØRSBOE
The Technical University of Denmark
Copenhagen, Denmark

* Received by the IRE, December 18, 1958.

On Direct Coupled Transistor Amplifier Stages*

A transistor is used frequently to perform the function of current amplification. If a transistor current amplifier must have a relatively constant current amplification to zero frequency, reactive elements cannot be used in the coupling or bias circuits. In this case high current amplification and good stability of the quiescent operating point with respect to temperature variations become inconsistent requirements unless temperature-sensitive elements are used to enhance the thermal stability of the circuit.

Temperature instability of the operating point in a transistor amplifier stage has two basic sources. First, the conductance of the emitter junction increases with increasing temperature.¹ Second, the collector cut-off current increases exponentially with increasing temperature. These effects will result in a temperature-sensitive operating point unless the emitter current is made substantially independent of the parameters of the transistor. In practice this is usually accom-

* Received by the IRE, August 7, 1958; revised manuscript received, November 20, 1958.

¹ J. S. Schaffner and R. F. Shea, "The variation of the forward characteristics of junction diodes with temperature," *Proc. IRE*, vol. 43, p. 101; January, 1955.

J. M. L. Janssen (SM'56) was born in Arnhem, The Netherlands, on September 14, 1918. He attended the Technological University of Delft,



J. M. L. JANSSEN

where he received the physical engineering degree in 1941. From 1942 to 1949 he worked with Philips Research Laboratories, Eindhoven, on the development of electronic measuring equipment.

In 1949 Mr. Janssen joined the Royal Dutch Shell Laboratory, Delft, where he was placed in charge of the Measurement and Control Department the following year.

In 1957 he was transferred to the Bataafse Petroleum My., The Hague, as head of their Data Processing and Computer Center.



J. E. Rowe (A'51-M'55) was born in Highland Park, Mich., in 1927. He received the B.S. degree in electrical engineering and in mathematics in 1951, the M.S. degree in electrical engineering in 1952, and the Ph.D. degree in electrical engineering in 1955, all from the University of Michigan, Ann Arbor.



J. E. ROWE

Since 1951 he has been associated with the University of Michigan Research Institute, engaging in fundamental research on microwave systems, microwave devices, and electromagnetic field theory. Formerly a lecturer and assistant professor of electrical engineering, he is now an associate professor of electrical engineering and head of the Electron Physics Laboratory at the University of Michigan.

Dr. Rowe is a member of the American Institute of Electrical Engineers, the American Mathematical Society, and the Society for Industrial and Applied Mathematics. He is also a member of Sigma Xi, Phi Kappa Phi, Tau Beta Pi, and Eta Kappa Nu.

Bruno Schneider was born on August 6, 1929, in Zürich, Switzerland. He studied electrical engineering at the Swiss Federal Institute of Technology from 1950 to 1954, and received the M.S. degree in 1954. Since that time he has been an assistant, and later Research Fellow, in the Department of Advanced Electrical Engineering, Swiss Federal Institute of Technology, Zürich, Switzerland.



B. SCHNEIDER

Mr. Schneider worked on a variety of transistor circuit problems, and has done research on junction diode and transistor noise. He has published several papers on temperature and other stabilization of transistor circuits, and on semiconductor noise.



Max J. O. Strutt, for a photograph and biography please see page 925 of the May, 1958 issue of PROCEEDINGS.



Jan B. van Erp was born in Laras, Simoeloengoen, Sumatra, on September 15, 1929. After graduating as an electrical engineer in January, 1955, from the Technological University of Delft, Netherlands, he worked several years as a research engineer in the measurement and control department of the Royal Dutch/Shell Laboratory at Delft.



J. B. VAN ERP

In January, 1958, he came to the United States to gain experience in the field of nuclear engineering. At present he is at the Argonne National Laboratory, Lemont, Ill., doing work on the kinetics, control, and instrumentation of nuclear reactors. Since January, 1959, Mr. Van Erp has been with "Euratom," Brussels, Belgium.

Lawrence J. Varnerin (SM'58) was born in Boston, Mass., on July 10, 1923. He received the B.S. degree in 1947 and the Ph.D. degree in 1949, in physics from the Massachusetts Institute of Technology.



L. J. VARNERIN

From 1949 to 1952, he worked on deionization phenomena in gases at Sylvania's Electronics Division. From 1952 to 1957, he worked on surface physics, high vacuum studies and ionic pumping at the Westinghouse Research Laboratories. He then joined Bell Telephone Laboratories in 1957 where he has worked on gas discharges and high-frequency germanium transistors. He is presently concerned with components development.

Dr. Varnerin is a member of the American Physical Society.



Ronald L. Wigington (M'57) was born in Topeka, Kan., on May 11, 1932. He received the B.S. degree in engineering physics from the University of Kansas, Lawrence, Kan., in 1953 and is currently attending graduate school at the University of Maryland, College Park, Md.



R. L. WIGINGTON

From 1953 to 1954, he worked on millimeter wave problems in klystron exploratory development at the Bell Telephone Laboratories. While service on the Army from 1954 to 1956, he was assigned as an electronics engineer to the Department of Defense. Since that time he has been a civilian employee of the Department of Defense, working in the fields of millimicrosecond instrumentation and high-speed computation.

Mr. Wigington is a member of Tau Beta Pi, Sigma Pi Sigma, Pi Mu Epsilon, and is an associate member of Sigma Xi.

IRE Awards, 1959

Medal of Honor Award



E. LEON CHAFFEE

For his outstanding research contributions and his dedication to training for leadership in radio engineering.

Joint Winners of the Morris Liebmann Memorial Prize



CHARLES H. TOWNES



NICOLAAS BLOEMBERGEN

For important fundamental contributions to the maser.

**Browder J. Thompson
Memorial Prize**



FRANKLIN H. BLECHER

For his paper entitled "Design Principles for Single Loop Transistor Feedback Amplifiers" which appeared in the September, 1957 issue of the IRE TRANSACTIONS ON CIRCUIT THEORY.

**W. R. G. Baker
Award**



RICHARD D. THORNTON

For his paper entitled "Active RC Networks" which appeared in the September, 1957 issue of the IRE TRANSACTIONS ON CIRCUIT THEORY.

**Vladimir K. Zworkin
Television Prize**



PAUL WEIMER

For contributions to photoconductive-type pickup tubes.

**Harry Diamond
Memorial Award**



JACK W. HERBSTREIT

For original research and leadership in radio-wave propagation.

New Fellows



A. E. ANDERSON

For contributions to transistor switching circuits.



S. J. ANGELLO

For contributions in the field of solid-state rectifiers.



MAURICE APSTEIN

For contributions to the improvement of electronic ordnance devices.



V. A. BABITS

For contributions to engineering education and pioneering in television.



J. M. BARSTOW

For contributions to the transmission of monochrome and color television.



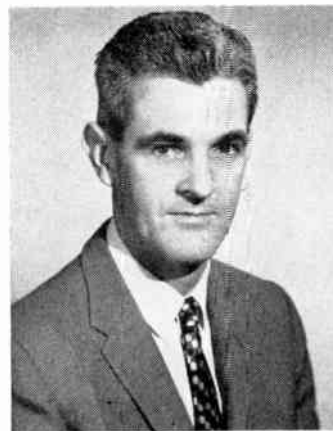
ROSS BATEMAN

For contributions in the field of ionospheric scatter propagation.



A. H. W. BECK

For contributions to the development of the thermionic valve.



J. T. BOLLJAHN

For contributions to the fundamental theory and design of antennas.



J. M. BRIDGES

For contributions to precision tracking radar and component reliability.

New Fellows



J. T. BROTHERS

For contributions and leadership in the field of electronic components.



W. C. BROWN

For contributions in the field of microwave tubes.



J. A. BRUSTMAN

For contributions in the development of digital computing systems.



C. C. CHAMBERS

For leadership in electrical engineering education.



S. B. COHN

For contributions to the theory and design of microwave components.



H. F. DART

For contributions to the electronic profession.



B. J. DASHER

For pioneering contributions in the field of network synthesis and engineering education.



J. T. DEBETTENCOURT

For contributions to radio wave propagation theory and systems.



S. M. DEL CAMP

For contributions in the development and standardization of electronic components.

New Fellows



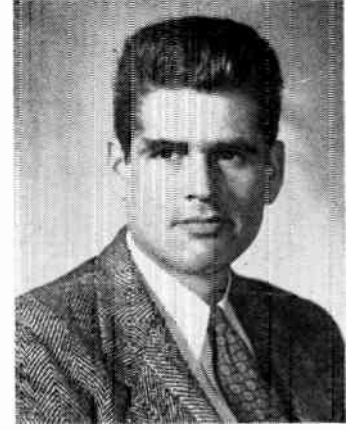
J. L. DENNIS

For contributions and leadership in the field of aeronautical navigation.



J. M. EARLY

For contributions in the development of high frequency transistors.



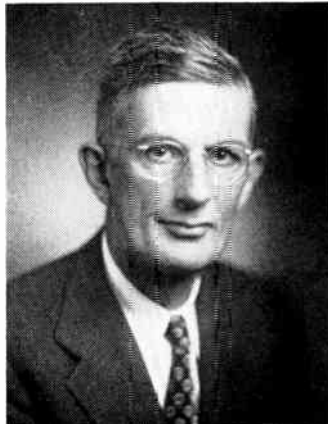
PETER ELIAS

For contributions to information theory and to engineering education.



H. T. ENGSTROM

For contributions in the development and utilization of high-speed computers.



D. K. GANNETT

For contributions to the transmission of television and sound broadcasting signals.



W. E. GOOD

For pioneering development in microwave spectroscopy and contributions to color television receivers.



R. E. GRAHAM

For contributions in the field of radar tracking systems and television research.



GEORGE GRAMMER

For contributions in single sideband radio telephony and for publication of technical information.



J. W. E. GRIEMSMANN

For contributions to microwave research.

New Fellows



J. H. HAMMOND, JR.

For pioneering work in radio control and communication.



E. H. HANSEN

For contributions to the development of motion picture sound recording and reproduction.



E. F. HERZOG

For contributions to military electronics.



W. A. HIGINBOTHAM

For contributions to pulse circuits and nuclear instrumentation.



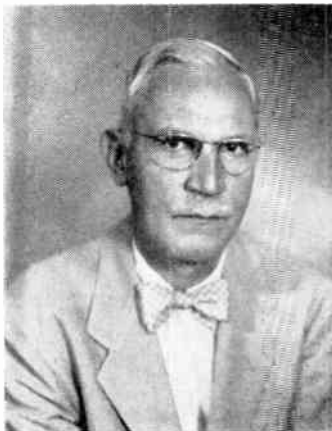
L. N. HOLLAND

For contributions to engineering education.



HEINZ HORN

For contributions in the development of ultra-high frequency and submarine cables.



A. W. HORTON

For contributions to long distance telephony, electronic switching and military electronics.



H. E. KALLMANN

For contributions to transient response analysis of networks and to instrumentation.



M. V. KIEBERT, JR.

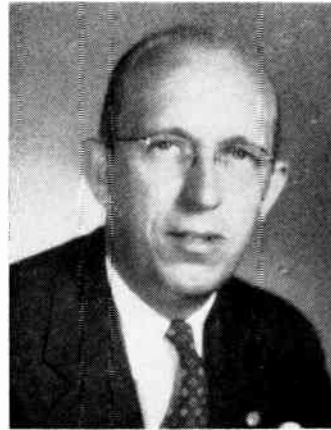
For contributions to telemetry and automatic data reduction.

New Fellows



D. D. KING

For contributions to microwave technology and electronic countermeasures.



T. P. KINN

For contributions in the field of industrial heating.



L. K. LEE

For contributions in the development of subminiature components and production techniques.



W. R. LE PAGE

For contributions to electronic engineering education and literature.

D. K. LIPPSCOTT
(deceased)

For outstanding service in the field of patent law.



L. B. LUSTED

For technical achievements and leadership in relating medicine and electronics.



J. R. MACDONALD

For contributions to the theory of electronic circuits and electrical properties of solids.



S. J. MASON

For contributions in the fields of active networks and engineering education.



FRANK MASSA

For pioneering in electroacoustical engineering.

New Fellows



D. O. McCoy

For research in the field of radio astronomy.



R. D. McCoy

For contributions in the fields of servo-control systems and analog computers.



DAVID MIDDLETON

For contributions to the theory of noise in electronic systems.



SIDNEY MILLMAN

For contributions in the fields of magnetrons, travelling-wave amplifiers, and backward-wave oscillators.



B. B. MINNICK

For the development of electronic components and for service to the radio engineering profession.



C. W. MUELLER

For contributions to the development of electronic tubes and solid-state devices.



J. H. MULLIGAN, JR.

For contributions in the fields of network theory, feedback systems, and engineering education.



T. M. ODARENKO

For contributions to the development of radio transmission systems, techniques, and components.



R. W. OLSON

For leadership in geophysical research.

New Fellows



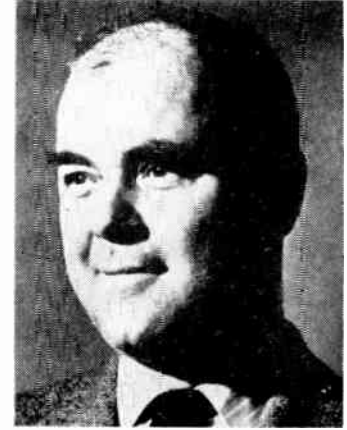
P. F. ORDUNG

For contributions to network theory and to electrical engineering education.



R. D. PARKER

For pioneer developments of teleprinter and data transmission systems.



G. W. PATTERSON

For leadership in the development of machine logic and switching theory.



EUGENE PETERSON

For analysis and application of nonlinear devices in communication.



A. J. POTE

For contributions to high-power accelerators, radio-frequency heating, and communication systems.



W. R. RAMBO

For contributions to military electronics.



A. C. ROCKWOOD

For contributions to standardization of electron devices.



HORST ROTHE

For contributions in the fields of electron tubes and the theory of noise.



H. P. SCHWAN

For outstanding leadership in the medical electronic field.

New Fellows



L. C. SIMPSON

For contributions to broadcasting and telecommunication systems.



D. H. SLOAN

For contributions to high-power electron tubes.



O. J. M. SMITH

For contributions in the fields of electrical measurement and feedback control systems.



H. M. STEARNS

For contributions in the fields of microwave tubes and Doppler radar.



M. W. P. STRANDBERG

For research in the field of microwave spectroscopy.



J. C. TELLIER

For contributions to receiver design and transistorization.

P. M. G. TOULON
(deceased)

For contributions to the control of gaseous conducting devices and in the field of color television.



J. G. TRUXAL

For fundamental contributions to the theory of feedback control systems.



J. H. VOGELMAN

For contributions to military electronics.

New Fellows



H. J. VON BAEYER

For contributions to development of radio communication techniques and systems.



J. D. WALLACE

For contributions in the fields of radio transmitters, antennas, and propagation.



YASUSHI WATANABE

For contributions in the development of feedback amplifiers, transistor electronics, and to engineering education.



S. E. WEBBER

For contributions to high-power klystron amplifiers.

Scanning the Transactions

Synthesis by Computer. Designers of circuits and components are finding the digital computer an increasingly important tool for solving design formulas and for analyzing the performance of the resulting designs, especially when lengthy repetitive calculations are involved. In many cases, however, design formulas are only approximate and yield results which do not exactly match the desired performance specifications. The designer must then go the rest of the way toward the final design by trial and error methods, varying his parameters and analyzing the results over and over until the performance converges on the specification. Now it appears that this synthesis procedure, too, is being taken over by the computer. A computer was recently programmed not only to analyze each successive design, but also to decide which parameters to adjust next and by how much for the next trial run, so that entire cut-and-try process was carried out automatically in one rapid operation. Incidentally, the problem chosen for the experiment was the synthesis of a stagger-tuned three-cavity filter, which probably represented the first time a computer was used to solve a microwave circuit problem. (L. Young, "Microwave filter design using an electronic digital computer," IRE TRANS. ON MICROWAVE THEORY AND TECHNIQUES, January, 1959.)

Broadcasters, too, are turning to computers. With new radio stations being added to the crowded broadcast band and existing stations trying to increase their power and improve their coverage, the problem of designing an antenna that will give good coverage without interfering with other stations is becoming increasingly intricate. Low-power stations are starting to use directional arrays with up to six towers—something considered uneconomical only a few years ago—to obtain the odd-shaped radiation patterns now required. And, if a station proposes to operate at night, sky-wave as well as ground-wave propagation must be taken into account. According to FCC rules this means that in addition to the horizontal radiation patterns, a complete azimuthal pattern must be computed for every five degrees of elevation up to sixty degrees. Thus not one, but 13 complex patterns have to be determined—a job ideally suited to the digital computer. (S. Bergen, "Calculation of directional antenna patterns using digital computer techniques," IRE TRANS. ON BROADCAST TRANSMISSION SYSTEMS, January, 1959.)

Vitamin pills and railroad car wheels would have been the last things you would expect to find discussed in an IRE publication a half dozen years ago. But so rapidly have electronic techniques been adopted throughout science and industry that today almost any subject is fair game. Convincing evidence, if any is needed, may be found in the January issue of the IRE TRANSACTIONS ON INDUSTRIAL ELECTRONICS. Vitamin pills? A photo-electric detection system is described which can accurately count and control the packaging of 15,000,000 capsules a day. Railroad car wheels? Positioning servos make possible a fully automated repair shop where old wheels are reconditioned and new ones are machined, bored, transferred and pressed on the axles—all automatically. What other jobs are being done electronically? Here is only a small sample: control of nuclear reactors, inspection of metal castings for structural flaws, reading 500 strain gauges at the rate of 50 per second, safety devices for preventing overspeed or overtorque of high-speed rotating machinery, and automatic machining of finished parts by numerical control systems.

Noise in stereo disk recordings, which is sometimes considered to be greater than in monaural recordings, has been

found partly to originate from the geometry of the record playback system rather than from the recording channel itself. It arises from the fact that the pivot point about which the recording stylus moves is apt to be slightly different from the pivot for the playback stylus. This difference introduces a slight loss in playback level of the vertical component and some harmonic distortion. Moreover, because the pivot point is not in the plane of the record, a vertical motion of the stylus is accompanied by a horizontal component in the direction of the motion of the disk. This component alternately adds to or subtracts from the average groove velocity, resulting in frequency-modulation noise. These findings suggest that manufacturers can effect an improvement in the quality of stereo recordings by a careful and uniform selection of the vertical pivot point of tone arms. (D. Cronin, "Modulation noise in two-channel disk recordings," IRE TRANS. ON AUDIO, November-December, 1958.)

Hypodermic needles have never been a popular item with those on the receiving end. It now appears that those on the other end have had their problems, too. It seems that the victim's blood has a tendency to coagulate inside the needle, making it very difficult to clean. Ultrasonics, which has been used recently to clean everything from laundry to teeth to metal parts, has been found to provide a neat solution to the problem. Using ordinary tap water as the medium, an ultrasonic technique has been developed which not only removes dried blood quickly and effectively, but also makes it possible to sterilize the needle at the same time. While this development may be of small comfort to you in your hour of pain, it should be of substantial interest to hospital and laboratory technicians everywhere. (F. Nesh and J. R. Andreotti, "An ultrasonic cleaner for hypodermic needles and similar small bore apparatus," IRE TRANS. ON ULTRASONICS ENGINEERING, February, 1959.)

Megawatt traveling-wave tubes, predicted in a PROCEEDINGS paper three years ago, have now become a reality. At that time an experimental model had been operated at 300 kw pulsed power output, indicating that a megawatt tube was entirely feasible. Now this goal has actually been achieved, opening up a whole new range of power capabilities for the traveling-wave tube which will be of major interest to system designers as well as to microwave tube specialists. (M. Chodorow, *et al*, "The design and characteristics of a megawatt space-harmonic traveling-wave tube," IRE TRANS. ON ELECTRON DEVICES, January, 1959.)

Two bibliographies of special interest were published in January. The first was contained in a report of an URSI Subcommittee on antennas and waveguides. The report gives an authoritative summary of recent developments, primarily in the U. S., in some of the more active areas of antenna and diffraction theory, accompanied by 169 literature references. The second bibliography gives what is probably the most complete list yet to be compiled of papers dealing with masers and parametric amplifiers. The list of 121 references is appended to an excellent review of the methods of operation and the performance that has been achieved by these important new types of microwave amplifiers. (R. S. Elliott, *et al*, URSI Report on antennas and waveguides, and annotated bibliography," IRE TRANS. ON ANTENNAS AND PROPAGATION, January, 1959; H. Heffner, "Solid-state microwave amplifiers," IRE TRANS. ON MICROWAVE THEORY AND TECHNIQUES, January, 1959.)

Books

Gmelins Handbuch der Anorganischen Chemie: Germanium, 8th Ed. Rev., edited by E. H. Erich Pietsch.

Published (1958) by Verlag Chemie, GMBH, Weinheim/Bergstrasse, Germany. 576 pages+XI,IV pages. 290 figs. 6 1/2 X 10. DM337.—(In German)

The new volume of "Gmelins Handbuch" on germanium is a very exhaustive and detailed summary of all that is known about the physical and chemical properties of germanium and germanium compounds. Over 300 pages are devoted to electrical and optical properties of germanium, including a thorough coverage of *p-n* junctions, diodes, transistors, photocells, and other devices. The volume is indexed according to subject matter; the index is in German and English and is very complete, although there is no author index.

The treatments of the various subject headings are in the nature of review articles, with copious references to technical literature. The caliber of these reviews is generally high, and the coverage of the literature very inclusive. The book should prove very useful to investigators who wish an over-all view of a given topic and will also provide a guide to further study of the technical articles themselves.

Unfortunately, the survey of the literature is complete only up to 1955. This point limits the usefulness of the volume as a general literature survey, although the fact that the major effort of research and development work has shifted from germanium to other materials in the past few years makes this a less serious shortcoming than it might otherwise have been. The editors have been liberal in including a large number of illustrations and diagrams to accompany the text.

In summary, this edition of "Gmelins Handbuch" on germanium should provide the research worker or development engineer with a conveniently indexed, comprehensive, and reasonably complete review of what knowledge is currently available about germanium, germanium electron devices, and germanium compounds.

J. P. MCKELVEY
Westinghouse Res. Labs.
Pittsburgh 35, Pa.

Dynamical Analogies, 2nd edition, by Harry F. Olson

Published (1958) by D. Van Nostrand Co., Inc., 120 Alexander St., Princeton, N. J. 269 pages+8 index pages+xi pages. Illus. 6 1/2 X 9 1/4. \$6.75.

H. F. Olson's "Dynamical Analogies" is a modification of the book of the same title first published in 1943. Except for minor changes, the first eleven chapters are essentially the same as the earlier edition. New chapters entitled, "Noise and Distortion," "Feedback," "Mobility Analogies," and "Mechanical Analogies" have been introduced. They constitute about 70 pages in addition to the 200 pages of the previous chapters.

The book as a whole presents in clear, readable form, with interesting diagrams, the extensive experience of the author in the application of analogies to the solution of dynamical problems in electroacoustics. The short chapter on noise and distortion gives formulas for calculating the noise due to thermal agitation of the air particles, the atoms in the vibrating system as well as the electrons in a conductor. The description of distortion in dynamical systems is short and nonanalytical.

The chapter on feedback should be quite useful. It assembles in one place, in systematic form, the dynamical formulas relating to the stabilization of a system that contains in it internal disturbance. Examples involving hydraulic regulator, an engine governor, power steering in automobiles, and an electronic feedback amplifier are discussed.

It is pleasant to see the addition of the chapter on mobility analogy. Many of us have made extensive use of this type of analogy in our work and writings and believe that it should be given emphasis in any book on this subject. The principal reference to this subject used by Olson is Floyd A. Firestone who has been the important leader in presenting the mobility concept to electroacoustic readers in this country.

The final chapter on the magnetic analogy rounds out the text. The material in this chapter, although not new to workers in the field, is an important part of the text as a whole.

The reviewer recommends this book to all who wish to apply the tool of electrical circuit theory to the solution of mechano-acoustic problems.

LEO. L. BERANEK
Bolt, Beranek and Newman
Cambridge, Mass.

Sampled-Data Control Systems, by Eliahu I. Jury

Published (1958) by John Wiley and Sons, Inc., 440 Fourth Ave., N. Y. 16, N. Y. 403 pages+5 index pages+6 bibliography pages+9 appendix pages+25 problems pages+xv pages. Illus. 6 X 9 1/4. \$16.00.

The theory and practice of sampled-data control systems have been developing rapidly during recent years, and Dr. Jury, who has contributed heavily to this development, has written an excellent book.

This reviewer has been particularly impressed by the wealth of subjects that have been more than adequately covered. Written for the graduate student and practicing engineer who have mastered the fundamentals of feedback system theory and the theory of complex variables, the purpose of the book as outlined by the author is "—to develop a basic theory that can be applied to sampled-data systems, to other allied fields such as circuits, networks and computers, and to the general field of systems engineering." As is to be expected in any book dealing with control systems, careful attention

is given to the problems of analysis and synthesis, with five chapters concerned with the former and three with the latter.

In the first chapter the concept of a sampled-data system is introduced and the mathematical description of the sampling process is given. The *z*-transform method is defined, and its relationship to the Laplace transform is shown clearly. With these fundamentals established, other useful concepts are developed. These include the sampled-data system transfer function, inverse *z*-transform, transformation theorems and stability. As in the remainder of the book, the presentations include the supporting mathematics. The chapter concludes by examining the characteristics of hold circuits. A fairly complete table of *z*-transform pairs is given also.

As the *z*-transform method is limited to yielding results at the sampling instants only, the second chapter introduces the modified *z*-transform which removes this restriction. The same subjects investigated for the *z*-transform are presented from the point of view of the modified *z*-transform approach. Tables of modified *z*-transforms are given together with a table showing the transfer functions for various feedback loop configurations.

Chapter three is devoted to the root-locus method of analysis of sampled-data systems. An illustration of the use of the root-locus in system compensation is given in some detail. The remaining material in this chapter covers constant overshoot loci, equations for overshoot and peak time and the correlation between frequency-locus and root-locus.

In chapter four, standard frequency response methods of analysis are extended to sampled-data systems. The relationship of the sampled-data frequency spectrum to the continuous frequency spectrum is presented. Once this is done, the techniques of the Nyquist diagram and Bode plots follow in a logical manner.

Chapters five through seven take up the problems of synthesis. Chapter five deals with discrete compensation methods, *i.e.*, the use of digital computers, or a number of delay elements. Three interesting examples are worked in detail. Chapter six discusses system compensation through the use of continuous networks. The synthesis portion of the book concludes in chapter seven which goes into the physical realization of the discrete compensators. There is enough material presented in the synthesis chapters to gain an appreciation for the practical difficulties that occur. Facing a real problem, the designer should have obtained enough insight to choose between the digital and continuous compensation methods; the one having extreme flexibility, the other usually much simpler in equipment requirements.

Chapter eight presents some of the methods for analyzing continuous systems by sampled-data techniques. Included are the fictitious hold method and the *z*-form and

modified z -form methods. The chapter concludes by applying the method of z -transforms to the solution of difference equations with constant and periodic coefficients.

The final chapter takes a closer look at the methods of sampling analysis by presenting a clear picture of what is involved in the assumption that the sampled signal can be treated as a train of impulses. The P -transform method is then derived to be used in systems in which the sampling pulse width is not negligible in comparison to the system time constant.

All in all, the book presents the sampled-data picture remarkably well and should be welcomed by those desiring to learn about this subject, and by those who desire a comprehensive reference.

In addition, the excellence of the choice of problems and of the many drawings should be mentioned.

RUBIN BOXER
Servomechanisms, Inc.
Santa Barbara, Calif.

Handbook of Automation, Computation, and Control, Vol. 1: Control Fundamentals, edited by E. M. Grabbe, S. Ramo, and D. E. Wooldridge

Published (1958) by John Wiley and Sons, Inc., 440 Fourth Ave., N. Y. 16, N. Y. 974 pages+20 index pages+xxx pages. Illus. 64×94. \$17.00.

"Control Fundamentals" is the first of a set of three volumes whose objective is to give "problem solvers" in the fields of automation, computation, and control a condensed presentation of "the available theory and information on general mathematics, feedback control, computers, data processing, and system design." Volumes 2 and 3, which have not appeared yet, will cover "Computers and Data Processing" and "Systems and Components."

To a gratifying extent the editors and the twenty-nine contributors of Volume 1 succeed in covering a great deal of the basic knowledge required by control systems engineers. The following are some of the chapter headings (there are twenty-four chapters in all): "Sets and Relations," "Matrix Theory," "Finite Difference Equations," "Operational Mathematics," "Conformal Mapping," "Boolean Algebra," "Statistics," "Numerical Analysis," "Operations Research" (which includes discussions of game theory, allocation models, waiting time models, etc.), "Information Theory," "Relation Between Transient and Frequency Response," "Feedback System Compensation," "Noise, Random Inputs and Extraneous Signals," "Nonlinear Systems," and "Sampled-Data Systems and Periodic Controllers."

Each chapter is essentially a condensation of most of the fundamental results of a special body of theory, and for the most part good lists of references are provided. As a result the user of the "handbook" will find that it can be a good point of departure for many of his present needs in the realm of basic theory, if it doesn't already provide him with all he wants to know. The minimum previous training he will need is included in the technical portion of most undergraduate engineering curricula.

In a work of this kind, where the subject matter is so broad, it is unavoidable that many users will not find sufficient variety or depth of material. The editors have to stop somewhere, of course. We suggest, however, that certain additional subjects could be usefully included, perhaps in a supplementary volume. The following areas, in this reviewer's opinion, deserve such treatment: calculus of variations, dynamic programming, analysis of automata and neural networks, classical mechanics (with emphasis on the ballistics of space missiles), theories of self-optimizing and adaptive systems, multidimensional control systems, final-value control systems, and aspects of human psychology involved in matching control systems to their users and operators.

These lacks, however, do not detract from the value of the huge amount of basic information that has already been packed into this volume. We believe it will serve as an excellent reference work.

JACK SKLANSKY
RCA Laboratories
Princeton, N. J.

Nonlinear Problems in Random Theory, by Norbert Wiener

Published (1958) by The Technology Press, M.I.T., Cambridge, Mass., and John Wiley and Sons, Inc., 440 Fourth Ave., N. Y. 16, N. Y. 128 pages+3 index pages+ix pages. Illus. 6×94. \$4.50.

This interesting monograph represents some of Professor Wiener's most recent work in random theory. Here, he is particularly concerned with nonlinear problems in a variety of fields. A brief review of the topics discussed will give the reader an idea of the scope of his interests. The book itself consists of 15 lectures which were recorded and subsequently reproduced in mimeographed notes. These lectures contain a description of a class of Gaussian random processes, in particular, the Brownian Motion processes and their representations. Considerable attention is given to a treatment of both linear and nonlinear functionals of such processes. After four preliminary lectures, Professor Wiener applies his methods first to a discussion of frequency modulation. Two types of frequency-modulation problems are considered. Type 1 is a linear frequency modulation where the random variations in frequency appear as a linear functional of the driving stochastic mechanism. Type 2 imparts a quadratic stochastic driving mechanism. The result of suitable operations then yields the desired spectral density of the frequency-modulation process. This in turn is applied to a study of brain waves, and "random time," in lecture 8. In lecture 9, some questions of using Brownian processes to describe probabilities in quantum theory are considered. In lectures 10 and 11 Professor Wiener next applies these ideas to still another area of interest, specifically the problem of analyzing and synthesizing nonlinear electrical systems. Here a typical problem is to determine the operational characteristics of an unknown linear or nonlinear "black box." In lectures 12 and 13 his methods are applied to coding and decoding problems. Finally, in lectures 14 and 15, some new approaches to the description of statistical mechanical systems, such as a

three-dimensional gas subject to various types of force fields, are outlined.

While this book is not directed towards the average engineer there is probably no technical reader who will not enjoy and profit from some of the discussions. Those who will find it most useful, perhaps, are the communication engineers, although physicists and engineers with an interest in hydrodynamics, statistical mechanics, and quantum mechanics will find interesting ideas in the various lectures. Nonlinear problems occur, of course, in all the areas mentioned. Moreover, they have received considerable attention in recent years. Although the present book does give a powerful approach to such problems, with much new material, it should be pointed out that considerable progress has also been made along similar lines by a number of other investigators in the last decade. For example, similar questions involving nonlinear functionals, the distributions of noise processes after nonlinear devices, and studies of frequency modulation, have been considered by Kac, Siegert, Darling and others, and in the case of frequency modulation by Middleton, to mention but a few.¹ This excellent introduction to the subject which Professor Wiener has given us would be enhanced still further if a more comprehensive bibliography and reference to those and related studies had been made available to the reader.

In summary, we are indebted to Professor Wiener for a glimpse into new problems and techniques involving random processes. His monograph is timely, with a delightfully informal style, depending much on the way it was originally recorded and a vigorous approach, which suggests new discoveries to come. [A number of typographical errors are easily corrected by the reader, (cf. Eqs. (4.13), (5.12), (5.34), (6.9), (6.15), (6.16), (6.26), (6.30).)]

DAVID MIDDLETON
Concord, Mass.

¹ See, for example, M. Kac and A. J. F. Siegert, "On the theory of noise in radio receivers with square law detectors," *J. App. Phys.* vol. 18, p. 383; (1957).
A. J. F. Siegert, "Passage of stationary processes through linear and nonlinear devices," *IRE TRANS. ON INFORMATION THEORY*, vol. 3, p. 4; March, 1954.
D. A. Darling and A. J. F. Siegert, "A systematic approach to a class of problems in the theory of noise and other random phenomena—part I," *IRE TRANS. ON INFORMATION THEORY*, vol. 3, p. 32; March, 1957.

A. J. F. Siegert, "Part 11, Examples," *ibid.*
D. Middleton, "The distribution of energy in randomly modulated waves," *Phil. Mag. ser. 7*, vol. 42, p. 689; 1951.

Fundamentals of Advanced Missiles by Richard B. Dow

Published (1958) by John Wiley and Sons, Inc., 440 Fourth Ave., N. Y. 16, N. Y. 555 pages+11 index pages+xvi pages. Illus. 6×94. \$11.75.

This book represents an excellent introduction to the field of guided missilery. It is indeed a summary, but it makes a success of an attempt to relate fundamental principles and their applications to the major technical areas in which missile designers must be proficient. The term "advanced" in the title is misleading unless one considers that all missiles are "advanced." The text is really at an introductory level but makes a welcome addition to the library of specialists who want a broad look at missile problems

or to the beginner who needs to know some of the problems ahead.

The author has contrived to gather an excellent summary of a broad field and to bridge the gap between fundamentals and applications by a careful arrangement of topics. For example, principles of propulsion and properties of fuels are discussed in the chapter on fluid mechanics; forces on the airframe, dynamic stability, and automatic control systems follow the introductory material on dynamics; reliability, signal to noise problems, and kill probability are included in the chapter on probability and statistics; and properties of microwaves, wave propagation, circuit elements such as magnetrons and klystrons, beam characteristics, and infrared radiation are discussed as a prelude to radar and guidance chapters.

The result is a logical presentation of most of the subsystem elements required to make up the airborne portion of a guided missile weapon system.

The chapter on systems is lacking in attention to a discussion of exchange or trade-off ratios, growth factors, subsystem integration, and the broader implications and scope of systems engineering but does present several typical system analyses.

The extensive use of footnotes adds much useful information without detracting from the readability of the book. The Table of Contents is sufficiently detailed to be of major assistance in locating material in general and the index is moderately well done. The author is to be commended for this addition to the literature on guided missile design.

C. W. BESSERER
Space Technology Lab.
Los Angeles, Calif.

Microwave Propagation in Snowy Districts, edited by Y. Asami

Published (1958) by the Research Institute of Applied Electricity, Hokkaido University, Sapporo, Japan. 198 pages. Illus. 74 X 104.

This book can be of great value to any engineer engaged in establishing or maintaining a communication system in a region where snow and ice are listed among the facts of life. The only fault I have to find with the book is its title. The book does deal with propagation through snow and over snow-covered terrain, but it is also concerned with the accretion of snow and ice on antennas. Y. Asami, editor, and co-author of two of the eight papers in the book, is Chairman of a committee of the Institute of Electrical Communication Engineers of Japan, which has been studying the problems involved in microwave communication in snowy districts. As a result, a book has been produced which examines these problems and their solutions with great thoroughness, both experimentally and theoretically.

The book contains eight papers by a total of nine authors and co-authors. The substance of the book is to be found in the first five papers. The first two cover the mechanism of ice-formation on antennas, the physical properties of this ice, and dielectric properties of many different forms of snow and ice, and the variation of these properties with frequency, temperature,

and time. In the third paper the effect of ice and snow accretion on antenna performance, both as regards attenuation and antenna matching, is considered experimentally and theoretically. Then, in logical order, the problem of anti-icing and de-icing by electric heating is discussed. The fifth paper deals with the reflection coefficient of snow-covered terrain and the formation of atmospheric ducts over such a surface.

The subjects of the last three papers are the statistical examination of propagation data and a theory of space diversity. Although these papers are interesting in themselves, they do not fall within the main theme, and occupy only 36 of the 198 pages.

The papers are of the nature of comprehensive summaries of the present state of knowledge in the field, and yet contain much information which is original to the Japanese authors. The book is to be highly recommended to anyone faced with the task of communication in snowy districts.

LORNE H. DOHERTY
Natl. Res. Council of Can.
Ottawa, Ontario, Canada

Junction Transistor Electronics, by Richard B. Hurley

Published (1958) by John Wiley and Sons, Inc., 440 Fourth Ave., N. Y. 16, N. Y. 461 pages + 11 index pages + xvii pages. Illus. 6 X 94. \$12.50.

The term "transistor electronics" has been used to cover a wide range of subject matter, from the physics of junction-transistor operation to a description of transistor applications. Mr. Hurley's book is concerned with fundamentals of transistor circuits and is intended for the circuit man. According to the author, the text is aimed primarily at the electronics engineer who has had first courses in vacuum-tube electronics and electric circuits.

The first two chapters, on physics of semiconductors and of transistor operation, are intended to be more descriptive than rigorous. Accordingly, these chapters—along with similar material in later portions of the book—should be approached with some caution. For example, in Chapter 2, the author speaks of "forward carriers diffuse through a depletion layer." In Chapter 8, in discussing high-level operation of a *p-n-p* transistor, when a large number of holes is injected into the base from the emitter, the author states that charge neutrality is preserved by causing an "equal number of electrons to be drawn in from the emitter" (rather than from the base contact).

At the end of the second chapter, the author derives an equivalent circuit for the transistor based on its physical operation. Except for the criticism noted above, this reviewer is glad to see this approach. Thus, at the outset, the student is aware of the physical phenomena taking place in the junction transistor, rather than just being given an equivalent circuit with numbers to be obtained from a manufacturer's data sheet.

Subsequently, the physically derived equivalent circuit is converted to the usual equivalent-Tee circuit, and Chapter 3 contains a tabulation of gain and impedance equations in terms of the Tee parameters. The remainder of the first half of the book

comprises chapters on audio-frequency, amplifiers, power amplifiers, and dc amplifiers, biasing, noise, feedback, and ends with an interesting chapter on regulated power supplies.

In some respects, a different arrangement of material might have been desirable. For example, as noted above, junction-transistor operation is described in Chapter 2, alone with derivation of an equivalent circuit, but characteristic curves are not discussed until six chapters later. Similarly, biasing schemes are discussed in Chapter 5, following a discussion of the operation of audio-amplifiers in Chapter 4. Actually, the author had anticipated these criticisms because in the Preface he indicates that his arrangement of material and treatment is based on his own experience in the field and by the reactions of his students.

Explanations of transistor circuits are facilitated by liberal use of numerical examples. Polarities and magnitudes of voltages across the terminals of transistors and other components are indicated in many circuit diagrams; this is quite helpful to the student. Each chapter has a dozen or more references. Some of these, however, refer to material of limited availability (e.g., company reports), which occasionally is somewhat frustrating to a reader.

The second half of the book begins with a chapter on high-frequency equivalent circuits. Most of these, in this reviewer's opinion, are too complicated for practical circuit use. Moreover, some of the more widely used equivalent circuits, e.g., Giacometto's hybrid- Π , are not discussed. Subsequent chapters are devoted to internal feedback, video and tuned amplifiers, oscillators, and modulators. In general, the material here is not presented in as much detail as in the first half of the book. However, the style of the first half of the book returns in Chapters 19-21, which are devoted to switching circuits. Also included here is a discussion of binary arithmetic and logic circuits. The final chapter is devoted to the subject of saturable reactor circuits.

In summary, then, this book is a text rather than a reference work. Its principal applications probably will be in teaching a circuit man the fundamentals of transistor circuits—but not transistor physics.

R. L. PRITCHARD
Texas Instruments Inc.
Dallas, Texas

Handbook of Physics, edited by E. U. Condon and Hugh Odishaw

Published (1958) by McGraw-Hill Book Co., Inc., 330 W. 42 St., N. Y. 36, N. Y. 1402 pages + 10 index pages + 13 appendix pages + xxvi pages. Illus. 74 X 104. \$25.00.

The "Handbook of Physics" gathers in one volume much of the detailed information essential to a comprehensive knowledge of physics. Prepared by a staff of about ninety specialists, this handbook is intended as a judicious selection from the vast literature of physics of "what every physicist should know."

In contrast to the "Handbook of Chemistry and Physics" and the "American Institute of Physics Handbook," for example, the present volume is not concerned

with exhaustive compilations of widely ranging experimental data and practical technological information. Unlike the recently published "Fundamental Formulas of Physics" (an excellent reference work in its own right), the "Handbook of Physics" places emphasis less on the listing of formulas, and more on a consideration of formulas in their proper perspective.

In effect, it is a carefully organized collection of abridged textbooks covering every major branch of physics. Its scope is perhaps best indicated by a brief survey of its principal parts: mathematics; mechanics of particles and rigid bodies; mechanics of deformable bodies; electricity and magnetism; heat and thermodynamics; optics; atomic physics; the solid state; and nuclear physics. For the most part, each chapter is the counterpart of a full-length textbook or treatise. The chapters on electricity and magnetism, for example, are as follows: basic electromagnetic phenomena; static electric and magnetic fields; electric circuits; electronic circuits; electrical measurements; conduction; metals and semiconductors; dielectrics; magnetic materials; electrolytic conductivity and electrode processes; and conduction of electricity in gases.

Since most of the chapters are written on a level which should be found comprehensible to a nonspecialist, the student is

likely to find the Handbook useful not only as a reference work, but also as a means of gaining entry into a new field. In most chapters, the lay of the land is sketched out in bold strokes, and usually there is ample bibliographical material to guide further pursuit. The working scientist is likely to find the Handbook more convenient to have on his desk than an odd assortment of undergraduate and possibly graduate textbooks, particularly because it is well indexed, and because it contains a very useful appendix on units and conversion factors. For advanced work, of course, the Handbook is no replacement for the more than fifty volume "Encyclopedia of Physics" (Handbuch der Physik).

The large size and weight (5.8 pounds) of the Handbook pose a practical handling problem, but this minor disadvantage is offset by its overall convenience. This has been verified in practice by three months use on this reviewer's desk.

The editors, E. U. Condon and H. Odishaw, have exercised a great deal of wisdom in their choice of subject matter, though each reader is likely to wish that certain subjects had been treated in greater detail. For instance, this reader would have preferred a more thorough coverage of mathematical physics, possibly at the expense of other topics. A fair question is: Why is group

theory, a branch of mathematics widely used in physics, treated in little more than one page, when thirty-one pages are devoted to an article entitled "Fundamental Constants of Atomic Physics," which can be found in substantially the same form elsewhere? From the standpoint of gaining a liberal education in physics, the general reader is more likely to profit from reading this article than a comparable article on group theory. However, the balance would appear to be in favor of the group theory article in a reference work.

This volume is naturally at its best on the more elementary subjects, and on those least sensitive to recent developments. A few of the advanced chapters, which attempt to summarize the status of a rapidly changing field (such as microwave spectroscopy), appear slightly out of date.

In summary, the "Handbook of Physics" is well written, well organized, and well indexed, and as such is a welcome addition to the reference literature. It is also beautifully printed in a pleasing typography. It is highly recommended to students and working scientists in all branches of science and technology. It makes a nice gift for an aspiring scientist.

FRANK HERMAN
RCA Labs.
Princeton, N. J.

Abstracts of IRE Transactions

The following issues of TRANSACTIONS have recently been published, and are now available from the Institute of Radio Engineers, Inc., 1 East 79th Street, New York 21, N. Y. at the following prices. The contents of each issue and, where available, abstracts of technical papers are given below.

Sponsoring Group	Publication	Group Members	IRE Members	Non-Members*
Antennas & Propagation	Vol. AP-7, No. 1	\$2.50	\$3.75	\$7.50
Audio	Vol. AU-6, No. 6	0.55	0.85	1.65
Electron Devices	Vol. ED-6, No. 1	2.55	3.85	7.65
Engineering Writing & Speech	Vol. EWS-2, No. 1	1.30	1.95	3.90
Industrial Electronics	Vol. IE-8	1.65	2.50	4.95
Military Electronics	Vol. MIL-3, No. 1	0.50	0.75	1.50
Ultrasonics Engineering	Vol. UE-7	0.95	1.40	2.85

* Libraries and colleges may purchase copies at IRE Member rates.

Antennas and Propagation

VOL. AP-7, No. 1, JANUARY, 1959

Propagation of a Ground Wave Pulse Around a Finitely Conducting Spherical Earth from a Damped Sinusoidal Source Current—J. R. Jöhler and L. C. Walters (p. 1)

The form of the transient electromagnetic ground wave which has been propagated over a finitely conducting spherical earth from a source current dipole can be calculated by a direct quadrature evaluation of the Fourier integral. The method is illustrated in this paper by a calculation of the transient field radiated by the particular case of the damped sinusoidal source current dipole. At short distances from the source, the earth was assumed to be a plane and the displacement currents in the earth were neglected. The pulse was then calculated by a direct evaluation of the Fourier integral and the integration was verified by special operational methods (inverse Laplace transformation). The form of this pulse was then predicted at great distance from the source by a direct evaluation of the Fourier integral in which the displacement currents in the earth and the earth's curvature were introduced into the Fourier transform. The form of the tran-

sient signal was found to be dispersed by the propagation medium. The most noteworthy attribute of this dispersion is a stretching of the period of the wave so that the form of the source is somewhat obscured by the filtering action of the medium.

On the Measurement of Virtual Height—I. Kay (p. 11)

A time dependent definition of the virtual height of a reflected wave train is suggested. This definition is such that its accuracy increases as the width of the incident pulse increases. Moreover, it is theoretically possible to obtain an estimate of the virtual height with as small an error as desired, no matter what the nature of the reflecting medium.

Suppose an incident pulse having width W and a carrier frequency ω_0 produces a reflected wave which, when measured at a fixed point $x=0$ in space, is $R(\omega_0, w, t)$. The suggested definition of the virtual height $h'(\omega_0)$ is

$$h'(\omega_0) = \lim_{w \rightarrow \infty} c \left\{ \int_{-\infty}^{\infty} |R(\omega_0, w, t)|^2 dt / \int_{-\infty}^{\infty} |R(\omega_0, w, t)|^2 dt - \int_{-\infty}^{\infty} |I(\omega_0, w, t)|^2 dt / \int_{-\infty}^{\infty} |I(\omega_0, w, t)|^2 dt \right\},$$

where c is the free space velocity of light. This relation for $h'(\omega_0)$ holds for any physically reasonable incident wave train and is independent of its envelope shape.

An example is given of a reflected wave whose virtual height cannot be determined by inspection in the usual manner. The expression given here for the virtual height provides the correct result.

Back-Scattering Measurements with a Space-Separation Method—H. J. Schmitt (p. 15)

A method for the experimental determination of the back-scattering cross section of arbitrarily shaped obstacles is suggested, which, in a manner analogous to the Michelson interferometer in optics, makes use of a semitransparent mirror in order to separate the incident wave and the reflected wave. A measurement setup is described, and possible sources of error are discussed. The accuracy of measurements is investigated by comparing the measured values of the back-scattering cross section of circular metallic disks with the results obtained from the exact theory.

Scattering of a Surface Wave by a Discontinuity in Reactance—Alan F. Kay (p. 22)

The following two-dimensional scattering problem is solved exactly by a Wiener-Hopf procedure. The incident field is a TM surface wave traveling in the positive x direction and guided by a reactive surface in the plane $z=0$. The surface has normal reactance X_0 if $x<0$, and X_1 if $x>0$. X_0 and X_1 are assumed positive and real. The discontinuity produces reflected and transmitted surface waves and a radiated field. Closed form expressions are found for the magnitudes of these fields. The reflected, radiated, and transmitted power flows, relative to that of the incident field, are plotted in universal curves. Conservation of energy is verified exactly.

Spherically Symmetric Lenses—Alan F. Kay (p. 32)

A design procedure is given for finding the index variation of a spherically (or cylindrically) symmetric lens which will produce, with some restrictions, any desired shaped beam pattern. Applications are made to a broad beam Luneberg lens, a bistatic Luneberg reflector, and a bistatic Eaton-Lippmann lens, and other examples are worked out. The practical impor-

tance of the index singularity at the center of lenses of the Eaton-Lippmann type is treated.

On the Design of Some Rhombic Antenna Arrays—A. A. de Carvalho Fernandes (p. 39)

The expression of the field radiated by a rhombic antenna, taking into consideration both the vertical and the horizontal polarization components, is used to establish the theory of the array of two stacked rhombics and of the array of four rhombics in a stacked and interlaced arrangement. The main conclusions obtained are that for convenient values of the vertical and horizontal spacings between the antennas of the array, there is a greater concentration of power radiated along the directions of the main lobe of the pattern and, as a result, these arrays show an appreciable gain over a conventional rhombic. Practical rules for the design of these arrays for point-to-point and broadcasting are given in some detail.

Radiation Field of an Elliptical Helical Antenna—J. Y. Wong and S. C. Loh (p. 46)

Rigorous expressions for the radiation field of a helical antenna of elliptical shape are derived on the assumption of a traveling-wave type of current distribution along the helix conductor. The analysis is valid for integral and nonintegral numbers of turns. These expressions for the general helix are employed to determine the fields for the limiting case of a circular helical antenna, and the results are essentially the same as those derived by both Knudsen and Kornhauser. Allowing the ellipse to degenerate to the other limiting case, a solution for the radiation field is obtained for the planar or commonly known zig-zag antenna. Therefore, it is possible to achieve a truly circularly polarized field with an elliptical helix of slight ellipticity.

The Rectangular Loop Antenna as a Dipole—R. W. P. King (p. 53)

An integral equation for the current in a rectangular loop of wire is derived for a loop that is driven by two generators located at the centers of one pair of opposite sides. The EMF's are equal in magnitude and in phase in the sense that they maintain currents in the generators that are in the same direction relative to the coordinate system and, therefore, in opposite directions from the point of view of circulation around the loop. An approximate solution is obtained for the distribution of current around the loop and for the driving-point impedance. It is shown that the solution for the rectangle of wire reduces to that of the symmetrically driven folded dipole when one dimension is made electrically small and to a section of transmission line driven simultaneously at both ends when the other dimension is made small. The loop that is electrically small in both directions is also examined.

Properties of Slotted Dielectric Interfaces—R. E. Collin (p. 62)

A theoretical analysis of slotted dielectric interfaces based on an application of the Rayleigh-Ritz method is presented. Formulas for calculating the equivalent circuit parameters are derived for arbitrary polarization and angles of incidence. Numerical results are given which show that the slotted dielectric interface behaves essentially as a homogeneous anisotropic dielectric interface. Formulas and numerical values of the equivalent dielectric constants are also given.

Traveling-Wave Cylindrical Antenna Design—A Graphical Synthesis Method—Peter Folds (p. 74)

A simple graphical method is given for the synthesis of a special line source system. The elements of the line source system are excited with equal amplitudes and continuously increasing phases. The sources lie on a cylindrical surface. The shape of this surface depends on the given pattern functions.

Theoretical Research on Tropospheric

Scatter Propagation in the United States 1954-1957—H. Staras and A. D. Wheelon (p. 80)

This paper outlines recent progress in the theory of tropospheric scatter propagation in the United States. In the past three years, the emphasis of theoretical research has shifted from the analysis of the average signal level to the analysis of the signal statistics and to the underlying hydrodynamics of atmospheric turbulence. As might be expected in such a new and complex field, there is far from unanimity of opinion as to the "best" model to explain the myriad experimental results.

URSI Report on Antennas and Waveguides, and Annotated Bibliography—H. V. Cottony, et al. (p. 87)

Recent developments in some of the more active areas of antenna and diffraction theory are summarized. Although concerned primarily with U.S.A. activity, some reference is made to the literature of other countries where closely allied work is in progress. Fields included in this survey are broad-band antennas, wide-angle microwave optics, antennas for ionospheric scatter propagation, traveling-wave antennas, slot radiators, diffraction, and scattering theory.

Recent work in broad-band antennas has been concerned mainly with trying to hold both radiation pattern and impedance independent of frequency. The problem has been approached successfully through development of that class of antenna shapes which depends on angles only. The equiangular spiral is a simple example.

In microwave optics the requirements for wide-angle scanning of antenna beams have been met largely by using new light-weight, low-loss dielectrics to construct suitable lenses such as a spherical Luneberg lens. Using the geodesic analog of the Luneberg lens in one plane a scan of 40 beamwidths without aberrations has been obtained.

The very high gain required for antennas suitable for VHF ionospheric scatter propagation has been obtained through use of long horizontal rhombics and, more recently, by corner reflector antennas driven by collinear arrays of dipoles. The latter antennas have the important advantage for this application of much lower sidelobe level.

Traveling-wave antennas have received much attention in recent years because of their inherent adaptability to flush-mounted applications. Among the forms considered are corrugated surfaces and single or double dielectric-clad surfaces. The launching problem has been studied rather intensively and recent interest has been shown in the synthesis and scanning aspects for slow-wave structures. Progress has continued in the exploitation of fast-wave systems, with major advances centering on the launching problem and the polarization problem. Strip lines are taking an important place as feeding systems for traveling-wave antennas.

Recent years have been marked by considerable research activity on flush-mounted microwave antennas. Such antennas often take the form of slots or apertures in the metallic surfaces of aircraft. The radiation pattern of the slot radiator depends upon the shape of the metallic surface in which it is cut, and for complicated shapes resort is made to experiment. However, certain simple geometric shapes have been treated mathematically. These shapes include the circular cylinder, half plane, wedge, sphere, elliptic cylinder, oblate and prolate spheroid, and cones. Various combinations of these shapes on which work also has been done are the semicircular boss on a flat ground plane, the cylindrically tipped wedge, and the spherically tipped cone.

The problem of radiation from apertures in a metallic surface is closely related to the re-

reciprocal problem of calculating the currents excited on the surface by an incoming wave. As a direct consequence of the reciprocity theorem there is an intimate connection between slot radiators, diffraction, and scattering. The result is that the extensive body of knowledge classed as diffraction and scattering must be considered as an integral part of antenna theory. During the past three years there has been a very considerable effort in obtaining new exact solutions, several new approximate solutions, and a better physical understanding of the mechanisms involved in scattering. All of the geometric shapes mentioned above have received attention, and much experimental work has also been done. For the future it can be expected that this intensive effort will continue with emphasis on the asymptotic approaches of Kline and Keller, the method proposed by Logan, and Fock's method of obtaining asymptotic results based on local analysis.

Communications

Preliminary Results of Measurements on Doppler Shift of Satellite Emissions—P. R. Arndt (p. 99)

Suppressed Sidelobe Antenna of 32 Elements—Grote Reber (p. 101)

Measuring the Capacitance Per Unit Length of Two Infinite Cones of Arbitrary Cross Section—J. D. Dyson (p. 102)

The capacitance per unit length, and hence the characteristic impedance of two infinite cones, may be accurately measured by employing an extension of conventional guard techniques.

An appropriate gap is cut in one of the cones, converting the structure into a three-terminal capacitor. If the arm beyond the gap is long enough, the desired field distribution will be maintained past the gap and the capacitance per unit length of the isolated or guarded section may be measured by a conventional low-frequency capacitance bridge.

The Exact Solution of the Field Intensities from a Linear Radiating Source—Sheldon S. Sandler (p. 104)

Correction to "Determination of a Current Distribution over a Cone Surface Which Will Produce a Prescribed Radiation Pattern"—H. Unz (p. 104)

Fall Meeting of International Scientific Radio Union October 20-22, 1958, Pennsylvania State University (p. 105)

Abstracts of Papers from the Region Three Technical Meeting (p. 113)
Contributors (p. 115)

Audio

VOL. AU-6, NO. 6,

NOVEMBER-DECEMBER, 1959

PGA News (p. 117)

An Improved Method for the Measurement of Nonlinear Audio Design—James A. Aagaard (p. 121)

The three most common methods of measuring nonlinear distortion in audio equipment are the harmonic method in which harmonics of a single sinusoidal input signal are measured; the SMPTE, or modulation, method in which the modulation of a high audio frequency by a low frequency is measured; and the CCIF, or difference frequency, method in which the beat note between two closely spaced frequencies is measured. These methods are discussed with particular reference to the behavior which may be expected in applications where the equipment under test includes pre-emphasis or de-emphasis networks, or where the distortion is symmetrical. It is shown that in a number of cases a more satisfactory method for use at the higher audio frequencies would be the measurement of the third-order component, rather than

the second, produced in the CCIF method. A modification of the CCIF method using a sharp-cutoff low-pass filter is described which is capable of measuring both second- and third-order components. It is then shown that an instrument for this new method and the standard SMPTE method have many elements in common and that one instrument could be devised to make both forms of tests. The discussion is illustrated with the results of measurements made on a simulated distortion generator and on actual samples of audio equipment.

Modulation Noise in Two-Channel Disk Recordings—Daniel Cronin (p. 130)

Part of a modulation-noise problem encountered in two-channel stereo disk recording is shown to have its source not in the recording channel but in the geometry of the record-playback system. A relation is given to show the order of magnitude of this effect and some of the possible means of improvement are indicated.

Electromagnetic Efficiency of Heads in Magnetic Recording—Marvin Camras (p. 131)

A simple method is described for obtaining a figure of merit for response of magnetic recorder due to core losses and electrical characteristics.

Correspondence (p. 133)

Contributors (p. 133)

Annual Index 1958 (p. 136)

Electron Devices

VOL. ED-6, NO. 1, JANUARY, 1959

On Calculating the Current Gain of Junction Transistors with Arbitrary Doping—H. L. Armstrong (p. 1)

In transistors made by such techniques as solid-state diffusion, the doping density is not constant in the emitter and base regions. Tanenbaum and Thoinas have given an expression for the emitter efficiency of such a transistor. The present work extends that treatment, and gives an expression for the base transport factor. Thus the current gain can be calculated for any arbitrary distribution of doping density. It is found that, for constant doping densities, the results from this treatment reduce to those usually given (at least to the usual approximation), as they should.

Two cases of some practical interest are that in which the doping density varies monotonically from one side of the base to the other, as in the "drift transistor," and that in which the conductivity in the base region has a maximum somewhere within that region. Results for simplified forms of these two cases are presented in the form of graphs for convenience. Also, the result given by the present approximation for an exponential variation of doping density is compared with the exact calculation which can be made for this case.

Traveling-Wave Tube Efficiency Degradation Due to Power Absorbed in an Attenuator—C. K. Birdsall and C. C. Johnson (p. 6)

Traveling-wave tubes will oscillate if sufficient power is reflected at the input and the output of the tube; that is, if the loop gain is more than unity. As most tubes have large forward gain and matches (or loads) have some reflection, protection against oscillation is usually provided by return or backward loss. In most tubes the loss will be bilateral with the loss in the forward direction both absorbing power and reducing the rate of gain. The power absorbed subtracts from the power output and reduces the efficiency. This report presents the efficiency reduction due to power absorbed in the attenuator.

A Class of Waveguide-Coupled Slow-Wave Structures—J. Feinstein and R. J. Collier (p. 9)

The properties of an array of resonators coupled to a waveguide at their normally

short-circuited ends are investigated. Methods of obtaining both normal and abnormal dispersion are indicated. Experimental measurements of dispersion and electronic impedance are compared with theoretical calculations. The effect of system parameters upon these characteristics is illustrated.

A Gun and Focusing System for Crossed-Field Traveling-Wave Tubes—O. L. Hoch and D. A. Watkins (p. 18)

A problem encountered in the design of crossed-field traveling-wave tubes (particularly M-type amplifiers or backward-wave oscillators) is a limitation on current due to the restricted cathode size in the usual gun systems. The scheme considered here incorporates into a crossed-field device the techniques commonly used in O-type devices for designing converging Pierce-type strip-beam guns, which can increase the effective cathode area by perhaps ten times. A design procedure is presented for getting a well-formed beam from such a gun, which is magnetically shielded, through a fringing crossed-field region into the uniform-field region of interaction.

An analysis of electron flow through the fringing-field region, including the effect of space charge, is presented. A trajectory equation, solved on a digital computer, yields trajectories for the beam and design curves for various values of the important parameters. The results show the scheme to be feasible.

Results are also presented from tests on an experimental, demountable tube used to test the focusing scheme. About 90 to 95 per cent of the current entering the crossed-field region could be focused to the collector, and the system behaved generally as the design predicted. An evaluation of the experimental data showed the scheme to be useful.

Germanium P-N-P-N Switches—I. A. Lesk (p. 28)

Transistors having bases from 90 to 220 mils wide, with the base contact placed near the collector, have shown marked current gain increases with current, peaking at values from 0.1 to 0.3. This effect is due to drift of the injected carriers in the base electric field set up by the emitter current. If the base contact is placed near the emitter, only very small values of α are obtained.

Germanium *p-n-p-n* diode and triode switches were made to operate primarily on the base field mechanism. They had one very wide (*p*-type) and one very narrow (*n*-type) base. The base contact for the switching triode may be placed either on the wide base but near the narrow base, or on the narrow base. In the latter case, much less current is required to switch the device from the high resistance to the high conductance region. When used as a transistor, the dc grounded base current gain of the *p-n-p-n* diode passes through unity at the turn-off current.

A *p-n-p-p+* structure, as a component part of the *p-n-p-n* triode with base contact on the wide base region, is shown to act as a switching diode in much the same way as the germanium *p-n-p-m* unit.

When the base contact is made to a narrow base bar-type transistor structure, overlap onto emitter and collector regions often results in a current gain that increases with current. This effect may also be utilized in making *p-n-p-n* switches.

Large-Signal Theory of UHF Power Triodes—A. D. Sutherland (p. 35)

Using a parallel plane model, an analysis is made of the UHF electronics of triodes operating under Class B conditions. The theory, in its most general form, includes the effects of space charge in both the grid-cathode region and the plate-grid region. However, most of the solutions contained in this paper were obtained by neglecting space-charge effects in the plate-grid region.

Over the wide range of UHF operating conditions investigated, it is found that the reduction of a triode's power output due to transit times is accounted for almost entirely by transit-time effects in the plate-grid region only. The principal effect of transit times in the grid-cathode region is to introduce a phase shift. This phase shift is quite important, however, for it contributes to a mechanism of regenerative feedback from output to input.

The reduction of transit-time effects for a fixed operating frequency is limited by four factors: temperature-limited saturation of the cathode emission current, reliable mechanical spacing considerations, electrode dissipation capabilities, and amplifier bandwidth requirements. It is shown that there exists an optimum plate-grid spacing which leads to the highest possible RF output power consistent with the required bandwidth of the amplifier.

The Design and Characteristics of a Megawatt Space-Harmonic Traveling-Wave Tube—M. Chodorow, E. J. Nalos, S. P. Otsuka, and R. H. Pantell (p. 48)

The tube described in this paper has a pulsed output power of one megawatt with 9.6 per cent bandwidth, where bandwidth is defined as the 3 db points for saturation power. Saturation gain is about 20 db, which is 6 db below the low-level gain. This is a space-harmonic S-band structure, designed to operate at a beam voltage of 10^6 volts and perveance of 2×10^{-6} . Field configurations for the lowest and next higher pass bands are drawn, based upon a field analysis and cold measurements. The impedance determined by perturbation measurements is compared to the impedance for the forced sinusoid inside a closed region, and it is found that the tube has about four times the minimum storage energy necessary to obtain the same bandwidth.

The Effect of a Space Charge on Bunching in a Two-Cavity Klystron—T. G. Mihran (p. 54)

The effect of space charge on bunching in a two-cavity klystron has been analyzed by many investigators, but no rigorous theory exists for large-signal bunching in a finite beam klystron.

The various available theories are reviewed and compared with new experimental data on the subject. It is found that there is 25 per cent loss of bunching efficiency at the drift length which is currently accepted as optimum, namely, 90 degrees of an effective plasma wavelength. It is shown that to reduce this loss to 5 per cent, drift length should vary from 65 degrees of an effective plasma wavelength at $\gamma h = 0.5$ to 45 degrees at $\gamma h = 2$.

Reasoning qualitatively from these measurements, the optimum drift lengths for a multicavity klystron are suggested to be:

$$90^\circ : 90^\circ : \dots : 65^\circ : 45^\circ : 30^\circ$$

A Microwave Electron Velocity Spectrograph—P. B. Wilson and E. L. Ginzton (p. 64)

An electron-velocity spectrograph is described which can be used to measure the velocity distribution of electrons in a high-density electron beam modulated at microwave frequencies. The spectrograph employs a crossed electric and magnetic deflection system, has a resolution of less than one per cent in velocity, and a deflection region of very short length in order to minimize space-charge effects in the instrument.

Results of measurements made with the instrument on a Brillouin-focused, gap-modulated electron beam of microperveance one are given. Measurements made on the dc beam indicate that non-laminar flow effects are important for focusing fields of the order of and greater than the Brillouin focusing condition. Measurements of the RF velocity distribution at a point in the beam near the cavity gap have been found to agree with the predictions of kinematic bunching theory. A consequence of

small-signal, space-charge-wave theory is that RF velocities should go to zero at a point in the beam a quarter of a reduced plasma wavelength from the cavity gap. This is confirmed by measurements made with this spectrograph.

Independent Space Variables for Small-Signal Electron Beam Analysis—D. L. Bobroff (p. 68)

This paper gives a systematic account of three systems of independent space variables useful in small signal electron beam analyses—the familiar Eulerian, polarization, and hose systems. The continuity, dynamical, and power exchange equations are given for each of the three sets of variables, and the relative merits of each system are discussed. The inapplicability of the Lagrangian system to small signal beam problems is also indicated.

Effect of Transient Voltages on Transistors—H. C. Lin and W. F. Jordan, Jr. (p. 79)

During transient conditions, the maximum junction temperature is dependent on the energy delivered to the transistor. For resistive and capacitive loads, transient energy is delivered during the turn-on period because the internal space-charge capacity induces a forward current in the base, which is amplified. For an inductive load, energy is delivered during the turn-off period because of the high induced voltage. Analytical expressions are derived to show the different transistor parameters and circuit constants which influence the magnitude of transient energy. By far the most important parameter is the sustain voltage. If this voltage is exceeded in the resistive or capacitive load condition, the initial base current is amplified by a greatly increased current gain causing excessive dissipation. If the voltage induced in the inductive load exceeds the sustain voltage, the negative resistance collector characteristic may cause highly dissipative oscillations which usually destroy the transistor. The transistor may be protected from destruction by preventing the base from biasing in the reverse direction so as to avoid negative resistance.

The Germanium Microwave Crystal Rectifier—Alan C. MacPherson (p. 83)

The characteristics of the commercial germanium microwave mixer crystal are reviewed. The conventional theory for these devices is discussed and criticized on the grounds that minority carrier storage phenomena are completely ignored. A model which includes this effect is proposed, and conversion loss calculations which include the effect of spreading resistance are presented for a highly idealized version of this model. Some possible explanations for the dc characteristics and for the success of the conventional fabrication techniques are offered.

Transient Analysis of Junction Transistors—W. F. Gariano (p. 90)

The transient behavior of the surface barrier and diffused junction transistors may be represented by an equivalent network consisting of two diodes and a nonlinear base resistance. Expressions for the nonlinear resistance, the base-emitter voltage time response, and the collector current time response are derived and tested experimentally. The equivalent circuit allows us to predict hole storage time for direct-coupled transistor logic (DCTL) circuits.

Electron-Beam Flow in Superimposed Periodic and Uniform Magnetic Fields—J. R. Anderson (p. 101)

Theoretical and experimental results are presented on the focusing of an electron beam by means of a magnet structure which produces, along the axis of the beam, a periodic magnetic field superimposed on a uniform field. The relation between space-charge and magnetic-field parameters for minimum ripple is derived. The flow in superimposed uniform and periodic magnetic fields is shown to be degraded from the flow of electrons in a magnetic field

which has a sinusoidal variation along the axis. The results indicate the flow conditions to be expected, where such combined fields are unavoidable. The focusing of electron beams in this type of superimposed magnetic field and in Brillouin flow are compared.

Strapped Bifilar Helices for High-Power Traveling-Wave Tubes—D. A. Watkins and D. G. Dow (p. 106)

A method of increasing the peak-pulsed power output of broad-band traveling-wave tubes is described. The method involves the use of a modified bifilar helix for the slow-wave structure. The modification employs 1) special straps or 2) mode-selective attenuation to prevent backward-wave oscillation in the anti-symmetric mode. This results in the possibility of using helices in the symmetric mode at values of ka (circumference-to-free-space wavelength ratio) as large as 0.6 at the highest amplification frequency. This in turn makes possible an increase in peak-pulsed beam power of a factor of approximately sixteen times that possible with a single helix. Both analytical and experimental results regarding the behavior of the structures are presented showing the propagation characteristics. The experimental results include cold measurements to determine $\omega - \beta$ diagrams and measurements with an electron beam which yield experimental values of interaction impedance.

Dispenser Cathode Magnetrons—G. A. Espersen (p. 115)

The performance of a number of magnetrons using oxide nickel matrix L and impregnated types of cathodes is described. A discussion of the cathode structure, evacuation, seasoning, emission factor, arcing and life is included.

Experimental Notes and Techniques Method for Determining Specific Cooling Rates of Plate Materials in a Vacuum—C. W. Horsting, I. S. Solet, T. A. Sternberg, and P. Avakian (p. 119)

Contributors (p. 120)

Engineering Writing and Speech

VOL. EWS-2, NO. 1, JANUARY, 1959

Editorial (p. 1)

The Function and Design of the Scientific Message—Harry F. Arader (p. 2)

Use Your Readers Eyes—P. M. Beatts (p. 6)

Methods for the Study of Writing and Speech Techniques—Ralph E. Clark (p. 12)

Write Better Than You Talk—Frederick T. Van Veen (p. 15)

Selecting and Writing to the Proper Level—Joseph Racker (p. 16)

Engineering Writing "Up or Down"—M. L. Feistman (p. 22)

Can They See What You Say When You Speak—Edwin W. Still (p. 24)

Microphone Technique—Paul Taylor (p. 30)

Running Your Own Projector—James B. Angell (p. 33)

IRE Publications—The Section Bulletin—Alfred L. Cotcher (p. 34)

Contributors (p. 40)

Industrial Electronics

VOL. IE-8, JANUARY, 1959

Message From the Publications Chairman (p. 1)

A Numerically Controlled Manufacturing System—F. E. Booth (p. 2)

The process of machining a finished part from a numerical description involves a number of data processing steps, as well as the actual metal cutting operations. The approach to ac-

completing this purpose is generally organized in two major groups of equipment. One group consists of a general-purpose digital computer with associated input and output equipment. The second group of equipment consists of electronic machine control units, electrohydraulic servo drives, feedback units, and the machine tool itself. These equipment groups are described with reference to the Bendix system. Also, operating experience in existing installations is discussed.

A High-Speed Low-Level Scanner—K. Einstein (p. 17)

Pulse-Time Positioning Used for Safety Control of High-Speed Tester—M. E. Fitch (p. 25)

The operation and fail-safe features of the safety devices for a high speed bearing and shaft seal testing machine, operating between 10,000 rpm and 110,000 rpm, are discussed in this paper. The machine consists of an air turbine which drives a load through a flexible quill shaft. The safety devices interrupt the turbine air supply by a valve when either a predetermined torque or a preset speed is exceeded. Magnetic pickup signals generated by magnetic pins attached to the rotating shaft operate the safety devices. An electrical shutoff signal is developed during the first revolution of over-torque or overspeed. These safety devices, including the valve, must be fail-safe and operate in approximately 27 ms to prevent possible turbine disintegration due to centrifugal force in the event of load removal by quill breakage.

A Positioning Servo for Automatic Machine Tool Operation—F. H. London. (p. 31)

This paper describes a relay servo system used in the positioning of machine tools. Its primary application is in the manufacture of parts that have to fit accurately other parts on which all machining has been completed. A linear transducer uses the dimension of the machined part to obtain the reference signal, while a matched linear transducer provides the error signal for the servo system. A particular application of the servo system as used in a fully atomic railroad shop is described.

Automatic Packaging of Gelatin Capsules—S. H. McMillan (p. 34)

Shipping cartons are automatically filled from a 24 parallel channel feeder and photoelectric detection system. A doubly preset counter summarizes all 24 channels to first reduce speed and then stop the feed at a preset total count. One conveyor system serves four such feeder-counter combinations. The system has a counting capacity of approximately 200,000 capsules per minute.

A Nuclear Reactor Control System—D. J. Niehaus, R. R. Hoge, and A. B. Van Rennes (p. 38)

Electronic equipment used with nuclear reactors performs the functions of operational control of the reactor, surveillance of the reactor power and period, and protection against dangerous power excursions and periods. Transistorized circuits and duplicate channels of equipment provide the reliability which assures safe, continuous operation of the reactor.

Multichannel Swept Sonic Tester for Casting Quality Control—N. W. Schubring and J. E. Stevens (p. 46)

Automatic, production-type, sonic inspection based on the measurement of the fundamental vibrating frequency and/or decrement of a mechanically shocked casting has been in

operation in our foundries for several years. The method has been suitable for the detection of cracks, voids, porosity, mottle, shrink, etc., on many of the parts having simple geometries. However, the more complex castings can vibrate in many basic modes and these modes upon shock excitation may interact indistinguishably. Swept-frequency, continuous-wave, forced vibration obviates mode interaction and permits casting evaluation by comparison of the sonic energy absorption spectra. Center frequencies, bandwidths, and amplitudes of certain of the absorption peaks usually establish overall quality.

The multichannel Swept Sonic Tester evaluates a given casting by determining the presence of a response within each of several preselected bands. These channels have very sharp limits which are established by active, tunable, twin-T networks. Each channel is self-contained permitting the system to be extended to accommodate any degree of casting complexity by adding channels in building block fashion. The spectrum sweep, having an adjustable sweep width, sweep rate, and starting frequency, is accomplished by heterodyning a crystal oscillator with a reactance-controlled frequency-swept oscillator and approximately follows the derived ideal frequency vs time characteristic for conserving inspection time.

Management Views Automation—I. Travis (p. 59)

Military Electronics

VOL. MIL-3, NO. 1, JANUARY, 1959

Frontispiece—G. E. Valley (p. 1)

Guest Editorial—G. E. Valley (p. 2)

Systems Engineering and Weapon System Management—L. I. Davis (p. 4)

Systems Engineering for Usefulness and Reliability—W. C. Tinus and H. G. Och (p. 8)

With the increasing complexity and cost of weapon systems, it is becoming ever more important to provide a product that will be useful to the customer, that will provide reliable service, and that will have growth capabilities so that its useful life can be prolonged to meet the ever increasing enemy threat. The management of the research and development program for such large projects must provide detailed and careful planning and control in order to produce an integrated system on a minimum schedule.

System approach, now the byword of the electronic industry, means many things to many people. To the authors of this paper, it is the orderly arrangement of many details that are necessary to the sound planning of a large development effort.

Systems Engineering—R. H. Jewett and R. A. Montgomery (0. 12)

A description is given of practical systems engineering methods as applied to large military systems in an industrial environment. Particular emphasis is placed on a design approach which stresses minimum interconnections between subsystems and on system testing methods. Also discussed are system evaluation, management, and costs.

Weapons Systems Management—T. L. Phillips and I. A. Getting (p. 19)

Contributors (p. 23)

Ultrasonics Engineering

VOL. UE-7, FEBRUARY, 1959

PGUE Award (p. 1)

Biographical Notes on the Award Winners (p. 2)

An Ultrasonic Cleaner for Hypodermic Needles and Similar Small Bore Apparatus—F. Nesh and J. R. Andreotti (p. 3)

Most of the information dealing with ultrasonic cleaning devices is to be found in the advertising literature of the commercial houses manufacturing such equipment. G. G. Carr gives a rather comprehensive list of such concerns plus a discussion of the applications. Q. C. McKenna in his paper describes quite thoroughly the various techniques used in ultrasonic cleaning, with emphasis on its application to cleaning small parts. The ultrasonic equipment used at present for cleaning medical apparatus has not been effective in removing the coagulated blood from the inside of hypodermic needles. A design is described which has successfully removed the dried blood from hypodermic needles in a relatively short period of time. Preliminary experiments indicate that this system may also be sterilizing the needles at the same time as it is cleaning them.

Ultrasonic Atomization of Liquids—J. N. Antonevich (p. 6)

Observations of liquid films excited ultrasonically are described and discussed. These films atomized under ultrasonic excitation, and the rupture of capillary waves in the film is suggested as the prime cause of atomization. The atomization of a paint film by 20 kc vibrations was studied qualitatively. Highspeed motion pictures show sprays emanating from vibrating gas bubbles in the paint film. The particles produced were from 5μ to 500μ in diameter. Under the best atomizing conditions at 20 kc, the particle diameters were from 20μ to 70μ .

Theory of Magnetostrictive Delay Lines for Pulse and Continuous Wave Transmission—R. C. Williams (p. 16)

The theory presented is an analytic formulation of the characteristics of magnetostrictive delay lines. Assuming linear relationships between the elastic and magnetic variables involved, equations are derived that give analytic forms for the magnetostrictive and inverse magnetostrictive effect. The analytic expression for the magnetostrictive effect enables the strain pulse to be calculated in terms of the driving magnetic field. The expression for the inverse magnetostrictive effect gives the output magnetic flux density for an open-circuited receiver coil. The output voltage is then determined from this flux density.

Frequency response curves are obtained for two cases: 1) the ideal case, which refers to magnetic fields that terminate sharply at the extremes of the transmitting coil and receiving coils with perfect efficiencies; and 2) non-uniform and fringing magnetic fields at the transmitting coil and inefficient receiver coils. The response curves enable one to calculate the effective length of the coils needed to operate at the frequency which gives maximum gain. They also show that the nickel magnetostrictive delay line has an intrinsic conversion loss of 35 db. The voltage response is obtained by Fourier transform methods for input current step-functions for both of the above cases. These waveforms agree with experiment.

Biographical Notes on the Authors (p. 39)

Abstracts and References

Compiled by the Radio Research Organization of the Department of Scientific and Industrial Research, London, England, and Published by Arrangement with that Department and the *Electronic and Radio Engineer*, incorporating *Wireless Engineer*, London, England

NOTE: The Institute of Radio Engineers does not have available copies of the publications mentioned in these pages, nor does it have reprints of the articles abstracted. Correspondence regarding these articles and requests for their procurement should be addressed to the individual publications, not to the IRE.

Acoustics and Audio Frequencies.....	614
Antennas and Transmission Lines.....	615
Automatic Computers.....	616
Circuits and Circuit Element.....	616
General Physics.....	617
Geophysical and Extraterrestrial Phenomena.....	618
Location and Aids to Navigation.....	620
Materials and Subsidiary Techniques.....	620
Mathematics.....	623
Measurements and Test Gear.....	623
Other Applications of Radio and Electronics.....	624
Propagation of Waves.....	624
Reception.....	625
Stations and Communication Systems.....	625
Subsidiary Apparatus.....	626
Television and Phototelegraphy.....	626
Tubes and Thermionics.....	626
Miscellaneous.....	628

The number in heavy type at the upper left of each Abstract is its Universal Decimal Classification number. The number in heavy type at the top right is the serial number of the Abstract. DC numbers marked with a dagger (†) must be regarded as provisional.

ACOUSTICS AND AUDIO FREQUENCIES

- 534:061.3** 661
All-Union Acoustical Conference—V. A. Krasil'nikov. (*Akust. Z.*, vol. 4, pp. 105-106; January/March, 1958.) Report on a conference held in Moscow, June, 1957, at which 150 papers were read on propagation in inhomogeneous media, radiation and diffraction, waves of finite amplitude, ultrasonics, musical and physiological acoustics, and speech investigations.
- 534.2** 662
Amplitude and Phase Fluctuations in a Spherical Wave—V. N. Karavañnikov. (*Akust. Z.*, vol. 3, pp. 165-176; April/June, 1957.) Mathematical analysis of fluctuations produced by inhomogeneities of the medium.
- 534.2** 663
Correlation of Field Fluctuations—L. A. Chernov. (*Akust. Z.*, vol. 3, pp. 192-194; April/June, 1957.) Formulae are derived which establish a relation between the correlation function of the field fluctuation and the auto-correlation functions of the amplitude and phase fluctuations. See also 320 of 1957.
- 534.2-14** 664
Diffraction and Radiation of Acoustic Waves in Liquids and Gases: Part 2—M. D. Khaskind. (*Akust. Z.*, vol. 4, pp. 92-99; January/March, 1958.) General expressions are derived for the average value of hydrodynamic forces and moments acting on a body in the presence of diffraction and radiation. Part 1: 3665 of 1958.
- 534.21** 665
Waveguide Sound Propagation in One Type of Stratified Inhomogeneous Medium—Yu. L. Gazarian. (*Akust. Z.*, vol. 3, pp. 127-141; April/June, 1957.) An expression is derived for

The Index to the Abstracts and References published in the PROC. IRE from February, 1958 through January, 1959 is published by the PROC. IRE, May, 1959, Part II. It is also published by *Electronic and Radio Engineer*, incorporating *Wireless Engineer*, and included in the March, 1959 issue of that journal. Included with the Index is a selected list of journals scanned for abstracting with publishers' addresses.

the field of a spherical harmonic point source in a medium in which the sound velocity varies according to Epstein's law (see 319 of 1957). A solution is given to waveguide-type propagation in an inhomogeneous half space with a totally reflecting boundary.

- 534.21** 666
Acoustic Field in a Medium with a Homogeneous Surface Layer—A. N. Barkhatov. (*Akust. Z.*, vol. 4, pp. 13-18; January/March, 1958.) Experimental investigation of the propagation of sound through a space bounded by a homogeneous surface layer over a medium with a constant negative gradient of sound velocity.

- 534.21** 667
Sound Amplitude Fluctuations in a Turbulent Medium—B. A. Suchkov. (*Akust. Z.*, vol. 4, pp. 85-91; January/March, 1958.) Report of an experimental investigation of the fluctuation of sound waves propagated through atmospheric layers near the ground.

- 534.21** 668
On the Absorption of Sound Waves of Finite Amplitude—K. A. Naugol'nykh. (*Akust. Z.*, vol. 4, pp. 115-124; April/June, 1958.) Review of theory and comparison of results of calculations with experimental data, showing that waveform distortion, leads to a marked increase in absorption. In water, for example, at 100 kc, the absorption coefficient doubles for a pressure increase of the order of 0.01 atm.

- 534.21** 669
Attenuation of a Sound Beam Traversing a Layer of Discontinuity in Sound Velocity—A. N. Barkhatov and I. I. Shmelev. (*Akust. Z.*, vol. 4, pp. 125-127; April/June, 1958.) A note on the experimental determination of the attenuation of a sound wave traversing a transition layer between two homogeneous media. The application of geometrical theory to the phenomena is considered.

- 534.21** 670
Rayleigh-Type Waves on Cylindrical Surfaces—I. A. Victorov. (*Akust. Z.*, vol. 4, pp. 131-136; April/June, 1958.) Mathematical treatment of the propagation of Rayleigh-type elastic waves along a convex and a concave cylindrical surface.

- 534.21-8-14** 671
Ultrasonic Absorption in Viscous Liquids—I. G. Mikhailov. (*Akust. Z.*, vol. 3, pp. 177-182; April/June, 1957.) Ultrasonic absorption was measured in castor oil and other oils in the frequency range 0.26-30 mc. Results are tabulated.

- 534.232** 672
On the Theory of Piezoelectric Transducers—K. V. Goncharov. (*Akust. Z.*, vol. 4, pp. 37-46; January/March, 1958.) Investigation of the frequency characteristics of X-cut quartz plates, steel, Al, fused quartz and Mg. The effect of an adhering layer is considered in relation to its thickness and acoustic properties.

- 534.232-8** 673
Distributed Transducer—M. Greenspan and R. M. Wilmotte. (*J. Acoust. Soc. Am.*, vol. 30, pp. 528-532; June, 1958.) In an array of frequency characteristics by inactive material, the input voltages at successive inputs are delayed so that the speed of the electric wave travelling towards the load equals the speed of sound in the transducer material. High power and a wide frequency band can thus be obtained. See also 3012 of 1954 (Rabinow and Apstein).

- 534.232.001.4:534.522.1** 674
Visualization of Mode Conversion of an Ultrasonic Beam in Fused Quartz—V. J. Hammond and R. Carter. (*Nature, London*, vol. 182, p. 790; September 20, 1958.) The process is useful in investigating methods of bonding transducers to fused quartz for use in delay lines.

- 534.26** 675
Sound Scattering on Inhomogeneous Surfaces—Yu. P. Lysanov. (*Akust. Z.*, vol. 4, pp. 47-50; January/March, 1958.) Description of a mathematical method for the solution of a system of n equations determining the complex amplitude of waves scattered from a flat surface with periodically varying acoustic conductivity for the case of normal incidence.

- 534.26** 676
Scattering of Sound by a Thin Rod of Finite Length—L. M. Lyamshev. (*Akust. Z.*, vol. 4, pp. 51-58; January/March, 1958.) Mathematical analysis of the scattering of a plane monochromatic sound wave by a thin finite rod of circular cross-section shows that vibrations of the rod can produce an angular variation of the scattering characteristics.

- 534.374-8** 677
Ultrasonic Interference Filters with Variable Transmission Frequencies—B. D. Tartakovskii. (*Akust. Z.*, vol. 3, pp. 183-191; April/June, 1957.) The general theory of ultrasonic interference filters of single- and multi-layer type is developed. See 912 of 1953 (Curtis and Hadey).

- 534.522.1** 678
Diffraction of Light by Large-Amplitude Ultrasonic Waves—I. G. Mikhailov and V. A.

- Shutilov. (*Akust. Z.*, vol. 4, pp. 174-183; April/June, 1958.) The light intensity distribution is calculated according to the diffraction maxima for different waveforms. The results of calculations taking account of phase modulation are in good agreement with experimental data. See also *Ibid.*, vol. 3, pp. 203-204; April/June, 1957.
- 534.6:621.385.83:537.228.1** 679
An Electronic-Acoustical Converter—Yu. B. Semennikov. (*Akust. Z.*, vol. 4, pp. 73-84; January/March, 1958.) Methods of rendering an acoustical field visible are noted and a detailed treatment is given of the image-converter tube in which a piezoelectric plate is scanned by an electron beam. See 2184 of 1956 (Oshchepkov *et al.*).
- 534.781** 680
Masking of English Words by Prolonged Vowel Sounds—J. J. O'Neill and J. J. Dreher. (*J. Acoust. Soc. Am.*, vol. 30, pp. 539-543; June, 1958.) Results of tests are analysed.
- 534.79** 681
Temporary Threshold Shift and Masking for Noise of Uniform Spectrum Level—J. D. Miller. (*J. Acoust. Soc. Am.*, vol. 30, pp. 517-522; June, 1958.) An empirical relation between masking and temporary threshold shift is examined experimentally.
- 534.79** 682
Temporary Threshold Elevation Produced by Continuous and 'Impulsive' Noises—W. Spieth and W. J. Trittipoe. (*J. Acoust. Soc. Am.*, vol. 30, pp. 523-527; June, 1958.)
- 534.833** 683
Surface Absorption of Sound in Internally Lined Ducts—R. Piazza. (*Alta Frequenza*, vol. 27, pp. 44-53; February, 1958.)
- 534.843** 684
The Distribution of Normal Modes of Vibration in a Rectangular Room According to the Frequency Spectrum and Direction—Ma Da-Yu (D. Y. Maa). (*Akust. Z.*, vol. 4, pp. 168-173; April/June, 1958.) The angular distribution approaches a random one for an increase in the dimensions of the room, for a shift of the signal spectrum in the direction of higher frequencies, or for a widening of the frequency band.
- 534.844:534.6** 685
Testing the 'Echo Parameter' Criterion in Room Acoustics by Means of Measurements of Syllable Intelligibility—H. Niese. (*Hochfreq. und Elektroak.*, vol. 66, pp. 70-83; November, 1957.) Measurements of the "echo parameter" (see 2658 of 1957) at various points in four different halls are compared with subjective intelligibility tests at the same points. A close correlation between the results of objective and subjective tests is found.
- 534.845** 686
Acoustic Properties of Some Types of Sound-Absorbing Material—Z. N. Baranova and K. A. Velizhanina. (*Akust. Z.*, vol. 3, pp. 99-103; April/June, 1957.) The results of investigations are tabulated.
- 534.845:534.414** 687
Slit Resonators as Low-Frequency Sound Absorbers—D. G. Ragavan. (*J. Inst. Telecommun. Engrs. India*, vol. 4, pp. 213-219; September, 1958.) Theoretical values of resonance frequency, bandwidth, and maximum absorption agree fairly well with values obtained in test chambers and studios.
- 534.846** 688
Acoustical Design of the Alberta Jubilee Auditoria—T. D. Northwood and E. J. Stevens. (*J. Acoust. Soc. Am.*, vol. 30, pp. 507-516; June, 1958.) Impedance-tube and reverberation-chamber data were obtained for materials and components of the two auditoria. Measurements were made in the halls before their completion and concluded by a test concert.
- 534.851.089(083.74)** 689
IRE Standards on Recording and Reproducing: Methods of Calibration of Mechanically Recorded Lateral Frequency Records, 1958—(PROC. IRE, vol. 46, pp. 1940-1946; December, 1958.) Standard 58 IRE 19. S1.
- 621.395.61** 690
The Effect of Mechanical Vibrations on the Response of Various Types of Microphone—A. Chiesa. (*Alta Frequenza*, vol. 27, pp. 54-60; February, 1958.)
- 621.395.61** 691
The Effect on a Receiving System of a Set of Independent Noise Sources Located on the Surface of a Sphere of Finite Radius—V. I. Klyachkin. (*Akust. Z.*, vol. 4, pp. 153-160; April/June, 1958.) The concepts of concentration coefficient and directivity characteristic as applied to a receiving system in the field of a large number of independent noise sources distributed over a continuous surface are discussed, and concentration coefficients for several types of receiving system are determined.
- 621.395.623.7:534.831** 692
Methods of Generating High-Intensity Sound with Loud-speakers for Environmental Testing of Electronic Components Subjected to Jet and Missile Engine Noise—J. K. Hilliard and W. T. Fiala. (*J. Acoust. Soc. Am.*, vol. 30, pp. 533-538; June, 1958.)
- 621.395.623.8** 693
On a Method for Increasing the Stability of Sound Amplification Systems—L. N. Mishin. (*Akust. Z.*, vol. 4, pp. 64-72; January/March, 1958.) Description of a system of acoustic feedback in which the phase of the feedback is varied continuously. A mathematical justification is given for the choice of a particular value of phase deviation. Experimental results are given.
- 621.395.625.3** 694
Braking Action in Magnetic-Tape Recorders—G. Hartmann. (*Elektron. Rundschau*, vol. 12, pp. 45-49; February, 1958.) Consideration of the mechanics of the braking action shows that a constant braking moment is desirable. The shortcomings of practical methods are discussed, and a purely electrical braking system is suggested whose characteristics closely approach the ideal.
- ANTENNAS AND TRANSMISSION LINES**
- 621.372.2+621.396.11** 695
Transmission and Reflection of Electromagnetic Waves in the Presence of Stratified Media—Wait. (See 939.)
- 621.373.2.09** 696
Electric Waves on Delay Lines—F. Borgnis. (*Elektrotech. Z.*, vol. 79, pp. 383-385; June 1, 1958.) Propagation conditions for surface waves along plane slow-wave structures are examined.
- 621.372.221** 697
A Novel Construction Concept for Linear Delay Lines—D. Elders. (IRE TRANS. ON COMPONENT PARTS, vol. CP-4, pp. 24-28; March, 1957. Abstract, Proc. IRE, vol. 45, p. 1035; July, 1957.)
- 621.372.221** 698
The Significance of Phase and Group Delay—F. Kirschstein and H. Krieger. (*Nachrichtentech. Z.*, vol. 11, pp. 57-60; February, 1958.) The importance of the phase velocity in assessing distortion in coil-loaded transmission lines is shown experimentally.
- 621.372.8** 699
Critical Cross-Sections in Irregular Waveguides—B. Z. Katsenelenbaum. (*Dokl. Ak. Nauk SSSR*, vol. 123, pp. 53-56; November 1, 1958.) Mathematical analysis for the determination of the amplitude of any wave in a rectangular irregular slanting waveguide with ideal walls.
- 621.372.8.002.2** 700
Waveguide Manufacturing Techniques—T. Beardow. (*Brit. Commun. Electronics*, vol. 5, pp. 772-778; October, 1958.) Survey and comparison of techniques based on fabrication, casting, metal deposition, and printing methods.
- 621.372.821** 701
The Characteristic Impedance and Phase Velocity of High-Q Triplate Line—K. Foster. (*J. Brit. IRE*, vol. 18, pp. 715-723; December, 1958.) An exact solution is obtained for the impedance in the absence of the dielectric support sheet and an expression for the phase velocity derived. Comparison with experimental results shows that the line parameters can be calculated with an error of about 1 per cent.
- 621.372.823** 702
An Approximate Theory for Determining the Characteristic Impedances of Elliptic Waveguide—R. V. Harrowell. (*J. Electronics Control*, vol. 5, pp. 289-299; October, 1958.) Much similarity is found between the impedance behaviour of an elliptic waveguide sustaining an H_{c1} wave [see Chu, *J. Appl. Phys.*, vol. 9, pp. 583-591; September, 1938] and a rectangular guide sustaining an H_{10} wave. For a fixed broad dimension in each case the total axial wall current is not changed by reducing the length of the short dimension, and the impedance is modified only by the change in maximum voltage across the guide.
- 621.372.829** 703
Helix Waveguide Theory and Application—H. G. Unger. (*Bell Syst. Tech. J.*, vol. 37, pp. 1599-1647; November, 1958.) Generalized telegraphist's equations are derived for the curved helix waveguide, and coefficients obtained for conversion from normal modes of this waveguide to normal modes of the metallic waveguide. A radial wave impedance at the helix interface is used to calculate the effect of composite jacket structures in three applications of circular-electric-wave transmission. The analysis is confirmed by measurement.
- 621.372.829** 704
Attenuation of the TE_{01} Wave within the Curved Helix Waveguide—D. Marcuse. (*Bell Syst. Tech. J.*, vol. 37, pp. 1649-1662; November, 1958.) The helix waveguide has a coating of lossy dielectric and is shielded by a metallic pipe. A perturbation method is used to calculate the change in the field pattern of the TE_{01} mode caused by bending this waveguide; the additional field components produce an em field in the dielectric, which results in energy dissipation and attenuation. The attenuation can be reduced markedly by proper choice of dielectric thickness.
- 621.372.832.43** 705
Modified Two-Hole Directional Coupler—W. G. Voss. (*Electronic Radio Eng.*, vol. 36, p. 28; January, 1959.) The modification described enables a two-hole, interference-type coupler to be tuned to give perfect directivity at any wavelength within a wide frequency range.

- 621.372.85 706
On the Theory of Anisotropic Obstacles in Waveguides—W. Hauser. (*Quart. J. Mech. Appl. Math.*, vol. 11, Part 4, pp. 427-437; November, 1958.) "Variational principles for the approximate computation of the elements of the scattering matrix for anisotropic obstacles in waveguides are presented."
- 621.372.852 707
Variational Principles or Guided Electromagnetic Waves in Anisotropic Materials—W. Hauser. (*Quart. Appl. Math.*, vol. 16, pp. 259-272; October, 1958.) Approximate expressions are given for propagation in a waveguide partially filled with a material with tensor electromagnetic properties. Variational principles are used to obtain a solution for a rectangular guide containing an infinitely long ferrite slab.
- 621.396.67:621.372.54 708
A Three-Band Antenna Combining Network—Fife. (See 733.)
- 621.396.67.001.57 709
A Microwave Model Equipment for Use in the Study of the Directivity Characteristics of Short-Wave Antennas—D. W. Morris, E. W. Thurlow and W. N. Genna. (*P.O. Elec. Eng. J.*, vol. 51, pp. 126-131 and 173-179; July and October, 1958.) Report on investigations of the directivity characteristics of a rhombic antenna and a horizontal array of dipoles. The effect of nearby metallic structures on the performance of antennas was also studied.
- 621.396.677.4:621.396.11:551.510.535 710
A New Antenna to Eliminate Ground-Wave Interference in Inosopheric Sounding Experiments—R. S. Macmillan, W. V. T. Rusch, and R. M. Golden. (*J. Atmos. Terr. Phys.*, vol. 13, pp. 183-186; December, 1958.)
- 621.396.677.7:621.396.969.33 711
Slotted-Waveguide Array for Marine Radar—H. G. Byers and M. Katchky. (*Electronics*, vol. 31, pp. 94-96; December 5, 1958.) A rectangular waveguide with 126 inclined slots extends along the throat of a 30°-flare horn. A metal grating mounted across the horn aperture eliminates cross-polarisation radiation, and full-length chokes between waveguide and horn prevent back radiation. Advantages over a reflector-type antenna are noted.
- 621.396.677.8 712
Split Reflector for Microwave Antennas—R. L. Mattingley, B. McCabe, and M. J. Traube. (*Electronics*, vol. 31, pp. 86-88; December 19, 1958.) Impedance mismatch in pill-box (cheese) and other reflectors is reduced by dividing the reflector into two halves by a metal septum. Each half is fed by conjugate output ports of a short-slot hybrid coupler having suitable phase correction.
- 621.396.677.85 713
On the Axial Phase Anomaly for Microwave Lenses—G. W. Farnell. (*J. Opt. Soc. Amer.*, vol. 48, pp. 643-647; September, 1958.) Measurements of axial phase anomaly made on solid-dielectric lenses at 3 cm λ give results which generally agree with those calculated from scalar diffraction theory.
- 621.396.677.85 714
Experimental Investigation of a Homogeneous Dielectric Sphere as a Microwave Lens—R. N. Assaly. (*Can. J. Phys.*, vol. 36, pp. 1430-1435; October, 1958.) The emergent beam can be rotated through 360° by movement of the source alone. See also 996 of 1957 (Bekefi and Farnell).
- AUTOMATIC COMPUTERS
- 681.142:061.4 715
Electronic Computer Exhibition—(*Wireless World*, vol. 65, pp. 17-21; January, 1959.) Short notes on special features of computers shown in London from November 28 to December 4, 1958.
- 681.142:061.4 716
Learning Machines—(*Wireless World*, vol. 65, pp. 8-9; January, 1959.) A conditional-probability computer and character-recognition machines, exhibited at the symposium on "The Mechanization of Thought Processes" held at the National Physical Laboratory from November 24-27, 1958, are discussed.
- 681.142:537.227 717
Ferroelectric Storage Devices—S. Morleigh. (*Electronic-Eng.*, vol. 30, pp. 678-684; December, 1958.) The switching characteristics of ferroelectric materials, as required for use in digital storage systems, are examined. The properties of single-crystal BaTiO₃ capacitors are investigated experimentally.
- 681.142:621.318.57 718
A Track Switching System for a Magnetic Drum Memory—D. D. Majumder. (*Electronic Eng.*, vol. 30, pp. 702-705; December, 1958.)
- CIRCUITS AND CIRCUIT ELEMENTS
- 621.3.077.6:621-526 719
Phase-Selective Gate Rejects Quadrature—B. Fennick. (*Electronics*, vol. 31, pp. 92-93; December 19, 1958.) A phase-reference voltage controls two unmatched diodes which conduct only when the in-phase component is at maximum and the quadrature component at minimum. A circuit designed for a 400 cps servo amplifier is described.
- 621.314.22 720
Transformer Design for Zero Phase Shift—N. R. Grossner. (IRE TRANS. ON COMPONENT PARTS, vol. CP-4, pp. 82-85; September, 1957. Abstract, PROC. IRE, vol. 46, p. 384; January, 1958.)
- 621.316.825 721
Bounds for Thermistor Compensation of Resistance and Conductance—A. B. Soble. (IRE TRANS. ON COMPONENT PARTS, vol. CP-4, pp. 96-101; September, 1957. Abstract, PROC. IRE, vol. 46, p. 384; January, 1958.)
- 621.318.57:621.314.7 722
An Introduction to the Use of Transistors in Inductive Circuits—A. F. Newell. (*Mullard Tech. Commun.*, vol. 4, pp. 157-160; November, 1958.) The mechanism of a delayed switch-off effect, which is due to avalanche multiplication, is described, and a method of avoiding it in relay switching circuits is given.
- 621.318.57:621.314.7 723
Transistor Switch Design—A. Gill. (*Electronics*, vol. 31, p. 97; December 5, 1958.) Switching parameters are tabulated for eight types of transistor.
- 621.318.57:621.387 724
An Experimental Gas-Diode Switch—A. D. White. (*Bell Lab. Rec.*, vol. 36, pp. 446-449; December, 1958.) The ac impedance is a stable negative resistance of about 225 Ω for frequencies up to 30 kc.
- 621.319.4 725
Dielectric Films in Aluminium and Tantalum Electrolytic and Solid Tantalum Capacitors—J. Burnham. (IRE TRANS. ON COMPONENT PARTS, vol. CP-4, pp. 73-82; September, 1957. Abstract, PROC. IRE, vol. 46, p. 384; January, 1958.)
- 621.319.4:621.318.134 726
Ferrite-Cored Capacitors—R. Davidson. (*Research, London*, vol. 11, pp. 367-370; September, 1958.) Details are given of British capacitors with ferrite loading for improving their attenuation characteristics.
- 621.372.029.3(083.7) 727
IRE Standards on Audio Techniques: Definitions of Terms, 1958—(PROC. IRE, vol. 46, pp. 1928-1934; December, 1958.) Standard 58 IRE 3. S1.
- 621.372.2 728
A Review on the Analysis of Transients in Electrical Circuits Using the Laplacian Transformation—P. R. Rao. (*J. Inst. Telecommun. Engrs. India*, vol. 4, pp. 209-212; September, 1958.)
- 621.372.44:621.316.8 729
General Power Relationships for Positive and Negative Nonlinear Resistive Elements—R. H. Pantell. (PROC. IRE, vol. 46, pp. 1910-1913; December, 1958.) The method developed by Manley and Rowe (2988 of 1956) for the treatment of reactive elements is extended to resistors. Relations are derived which yield modulation efficiency, efficiency of harmonic generation and stability criteria.
- 621.372.5 730
How Quickly does a Twin-T respond?—M. Price. (*Can. Electronics Eng.*, vol. 2, pp. 40-41; September, 1958.) The response to three different input waveforms is examined using the Laplace transformation. In all cases the output transient is negligible after 1½ cycles of the resonance frequency of the network.
- 621.372.54 731
Filter Attenuation Characteristics—M. D. Johnson and D. A. G. Tait. (*Electronic Eng.*, vol. 30, pp. 710-711; December, 1958.) The use of hyperbolic functions is avoided, and formulae are derived which permit slide-rule computation.
- 621.372.54:621.376.3 732
The Magnitude of the Permissible Circuit Impedances of the Filters in I.F. Amplifiers for F.M. Systems—E. G. Woschni. (*Hochfreq. und Electroak.*, vol. 66, pp. 63-67; November, 1957.) Application of results obtained in 2672 of 1958.
- 621.372.54:621.396.67 733
A Three-Band Antenna Combining Network—S. L. Fife. (*Electronic Eng.*, vol. 30, pp. 720-722; December, 1958.) Three prototype filter sections of low-pass, band-pass and high-pass characteristics respectively for bands 1, 2, and 3 are combined in a masthead unit to provide a common output for the three antenna inputs.
- 621.372.543 734
Normalized Input-Admittance Curves of Two-Stage Band Filters and the Smallest Mismatch Circles for a Given Frequency Range—H. Hein. (*Nachrichtentech. Z.*, vol. 11, pp. 85-91; February, 1958.)
- 621.372.543 735
Band Filters with Electronic Bandwidth Control—C. Kurth. (*Elektron. Rundschau*, vol. 12, pp. 39-44; February, 1958.) The design of a two-stage filter with amplification in the feedback line is considered.
- 621.372.543 736
Null-Point Band Filters and Their Theoretical Treatment—E. Trzeba. (*Hochfreq. und Elektroak.*, vol. 66, pp. 90-94 and 95-107; November, 1957, and January, 1958.)
- 621.372.553:621.397.61 737
The Frequency and Time Characteristics of

- All-Pass Filters for Delay Equalization in Television Transmission**—H. Dobsch. (*Hochfreq., und Elektroak.*, vol. 66, pp. 67-70; November, 1957.) The basic circuits given by Bünemann (2240 of 1956) are considered.
- 621.372.632:621.3.072.6 738
Some Properties of a Frequency Stabilizing Circuit—L. L. Campbell. (IRE TRANS. ON COMMUNICATIONS SYSTEMS, vol. CS-5, pp. 10-12; September, 1957. Abstract, PROC. IRE, vol. 45, p. 1760; December, 1957.)
- 621.373 739
The Wave-Mechanical Damped Harmonic Oscillator—K. W. H. Stevens. (*Proc. Phys. Soc.*, vol. 72, pp. 1027-1036; December 1, 1958.) A wave-mechanics treatment is given of damped harmonic motion for the charge in a tuned circuit and the em field in a resonant cavity. The classical frequency appears in the time dependence of the eigenfunctions, and the classical damping as a decay in the eigenvalues.
- 621.373.14:621.396.96 740
High-Q Echo Boxes—A. Cunliffe and R. N. Gould. (*Electronic Radio Eng.*, vol. 36, pp. 29-33; January, 1959.) An investigation of the occurrence of unwanted modes in a tunable Ho cylindrical cavity. Suggestions for the suppression of these modes are given.
- 621.373.421.13 741
Generations of Oscillations with Equally Spaced Frequencies in a Given Band—D. Makow. (IRE TRANS. ON COMMUNICATIONS SYSTEMS, vol. CS-5, pp. 13-20; September, 1957. Abstract, PROC. IRE, vol. 45, p. 1760; December, 1957.)
- 621.373.43:621.396.96 742
The Application of Pulse-Forming Networks—A. Graydon. (IRE TRANS. ON COMPONENT PARTS, vol. CP-4, pp. 7-13; March, 1957. Abstract, PROC. IRE, vol. 45, p. 1035; July, 1957.)
- 621.373.431 743
Miller Sweep Circuit—C. S. Speight. (*Wireless World*, vol. 65, pp. 34-36; January, 1959.) Circuits are described in which both Miller integrator and Puckle flyback circuits are combined to produce a very linear time base.
- 621.373.431:621.314.7 744
Bistable Circuits using Unijunction Transistors—T. P. Sylvan. (*Electronics*, vol. 31, pp. 89-91; December 19, 1958.) The design and operation of various circuits are explained. Use of the negative-resistance region as one stable state decreases power requirements and increases switching speed. The application to ring-counter circuits is shown.
- 621.373.52 745
Transistor 20-kc/s Oscillator with 50mW Output—J. F. Berry and L. E. Jansson. (*Mullard Tech. Commun.*, vol. 4, pp. 122-127; November, 1958.) "A design procedure is described for transistor oscillators employing external feedback and an LC resonator. An example is given which delivers an output of 50m at 20kc, and which operates from a 9-volt battery. It is suitable for use as a bias oscillator for dictation machines."
- 621.373.52 746
Graphical Designing of Transistor Oscillators—W. R. McSpadden and E. Eberhard. (*Electronics*, vol. 31, pp. 90-93; December 5, 1958.) A method is described which is simple but yields results accurate enough for most engineering design calculations. A design example is given for a crystal-controlled oscillator to operate at 1 mc.
- 621.375.018.756 747
Summary of the Theory of Wide-Band Distributed Amplifiers Suitable for the Amplification of Very Short Pulses—D. Dosse. (*Nachrichtentech. Z.*, vol. 11, pp. 61-68; February, 1958.)
- 621.375.024:621-52 748
D.C. Amplifiers for Control Systems—L. S. Klivans. (*Electronics*, vol. 31, pp. 96, 98; November 21, 1958.)
- 621.375.121.2:621.396.621.22 749
An Electronic Multicoupler and Antenna Amplifier for the V.H.F. Range—K. Fischer. (IRE TRANS. ON COMMUNICATIONS SYSTEMS, vol. CS-5, pp. 43-48; December, 1957. Abstract, PROC. IRE, vol. 46, p. 515; February, 1958.)
- 621.375.2.024 750
A Triode-Connected Pentode with Stabilized Anode Current—B. C. Cox. (*J. Sci. Instr.*, vol. 35, pp. 471-472; December, 1958.) Drift in dc coupled circuits caused by heater supply voltage variation is minimized by the use of a triode-connected pentode stabilized by variation of grid current with emission.
- 621.375.2.132.3 751
The Influence of the Output Time-Constant of a Cathode Follower—C. Edwards. (*Electronic Eng.*, vol. 30, pp. 712-714; December, 1958.) A nomogram is derived for determining the maximum pulse amplitude, as a function of rise time and output time constant, that may be applied without causing positive grid current.
- 621.375.23:621.317.089.2 752
A Low-Capacitance Input Circuit—J. C. S. Richards. (*Electronic Eng.*, vol. 30, pp. 706-708; December, 1958.) Methods of reducing the effect of coaxial-cable capacitance are discussed. A probe containing only passive elements is used with a single triode-pentode valve feedback amplifier to give an input capacitance of 5 pf and a gain of unity over a bandwidth of 2 Mc.
- 621.375.4:621.318.57 753
Properties of Hook Transistors in Switching and Amplifying Circuits—L. M. Vallese. (*J. Brit. IRE*, vol. 18, pp. 725-732; December, 1958.) An analysis is given of the most significant properties of hook and *p-n-p-n* transistors in common-base, common-emitter and common-collector configurations.
- 621.375.4.029.3 754
Stagger-Tuned Transistor Video Amplifiers—V. H. Grinich. (IRE TRANS. ON BROADCAST AND TELEVISION RECEIVERS, vol. BTR-2, pp. 53-56; October, 1956. Abstract, PROC. IRE, vol. 45, p. 253; February, 1957.) See also 69 of January.
- 621.375.4.078 755
Transistor Circuits Based on the Half-Supply-Voltage Principle—B. G. Dammers, A. G. W. Uitjens, and W. Ebbinge. (*Electronic Applic.*, vol. 18, pp. 85-98; August, 1958.) Analysis shows that temperature stabilization of a transistor can be effected by a preceding dc coupled amplifying stage stabilized on the half-supply-voltage principle. Practical circuits are described for AF amplifiers and stabilized supply units. See also 71 of January (Dammers et al.).
- 621.375.9:538.569.4.029.64 756
Analysis of the Emissive Phase of a Pulsed Maser—H. H. Theissing, F. A. Dieter, and P. J. Caplan. (*J. Appl. Phys.*, vol. 29, pp. 1673-1678; December, 1958.) A discussion of the emission from a matched cavity at paramagnetic resonance. Results are given for transverse moment, output field, output power, and power gain as a function of time.
- 621.375.4+621.373.52 757
Transistor Circuit Engineering [Book Review]—R. F. Shea (ed.) Publishers: John Wiley, New York, and Chapman and Hall, London, 1957, 468 pp., 95 s. (*Nature, London*, vol. 182, pp. 756-757; September 20, 1958.)

GENERAL PHYSICS

- 537+538:061.3 758
Report of the Meeting of the Swiss Physical Society—(*Helv. Phys. Acta*, vol. 30, pp. 457-494; November 20, 1957.) The text is given of papers read at a meeting held at Neuchâtel, September 1957, including the following:
- a) **Electrical Properties of Silver Selenide** Ag₂Se—G. Busch and P. Junod (p. 470, in French).
- b) **Oscillatory Magnetic Resistance Variation of n-Type InSb at Low Temperatures and High Field Strengths**—G. Busch, R. Kern and B. Lüthi (pp. 471-472, in German).
- c) **The Field Parameters of Galvano- and Thermomagnetic Effects in Ferromagnets**—G. Busch, F. Hulliger, and R. Jaggi (pp. 472-474, in German).
- d) **Hall and Righi-Leduc Effects in Ferromagnetics**—D. Rivier (pp. 474-478, in French).
- e) **Effect of a Cubic Electric Field on the Fundamental Level of the Gd⁺⁺⁺ Ion**—R. Lacroix (pp. 478-480, in French).
- f) **Hyperfine Splitting in the Paramagnetic Resonance of Pr³⁺ in Ceramic LaAlO₃**—H. Gränicher, K. Hübner, and K. A. Müller (pp. 480-483, in German).
- g) **Improvements in an NH₃ Maser**—J. Bonanomi, J. De Prins, J. Herrmann, and P. Kartaschoff (pp. 492-494, in German).
- 537.122 759
Magnetic Susceptibility of an Electron Gas at High Density—K. A. Brueckner and K. Sawada. (*Phys. Rev.*, vol. 112, pp. 328-329; October 15, 1958.)
- 537.222 760
The Electrostatic Interaction of Two Arbitrary Charge Distributions—M. E. Rose. (*J. Math. Phys.*, vol. 37, pp. 215-222; October, 1958.)
- 537.226.1 761
Molecular Theory of the Dielectric Constant—L. Jansen. (*Phys. Rev.*, vol. 112, pp. 434-444; October 15, 1958.) A theory of the static dielectric constant is developed on a quantum-mechanical basis. By introducing the concept of "local field" a molecular version of the general theory is obtained. It is shown that such a molecular theory is fundamentally ineffective in accounting for the observed results within the experimental accuracy.
- 537.311.31:530.145 762
Quantum Theory of the High-Frequency Conductivity of Metals—M. Ya. Axbel'. (*Zh. Eksp. Teor. Fiz.*, vol. 34, pp. 969-983; April, 1958.) Development of the theory of conductivity of a metal in a high-frequency em field and a constant magnetic field. The amplitude of the quantum oscillations in the high-frequency case is usually larger than in the static case.
- 537.311.62 763
Quantum Oscillations of the High-Frequency Surface Impedance—M. Ya. Axbel'. (*Zh. Eksp. Teor. Fiz.*, vol. 34, pp. 1158-1168; May, 1958.) A quantum-mechanical formula is derived and cases involving constant magnetic fields both parallel and inclined to the surface are considered. From an experimental study of surface impedance in a strong magnetic field the shape of the Fermi surface and the velocity of the electrons in it can be determined.

- 537.533:621.385.029.6 764
Solution to the Equations of Space-Charge Flow by the Method of the Separation of Variables—P. T. Kirstein and G. S. Kino. (*J. Appl. Phys.*, vol. 29, pp. 1758–1767; December, 1958.) The steady-state behaviour of electron beams with high space-charge densities is analysed. The equations for irrotational, electrostatic laminar space-charge flow are set up in terms of the action function; these equations are reduced by separation of variables in cylindrical polar coordinates. The method may be extended to include the effect of magnetic fields.
- 537.56 765
Energy Spectrum of Plasma Electrons—G. Medicus. (*Elektrotech. Z.*, vol. 79, pp. 373–374; June 1, 1958.) Brief report on results obtained by the graphical method described earlier (731 of 1957).
- 537.56 766
Thermal Conductivity of an Electron Gas in a Gaseous Plasma—T. Sekiguchi and R. C. Herndon. (*Phys. Rev.*, vol. 112, pp. 1–10; October 1, 1958.) Experimental techniques used with Ne and He plasmas are described. Conductivity values obtained by two separate methods are in agreement and consistent with theory.
- 537.56:538.56 767
Kinetic Theory of Magneto-hydrodynamic Waves—K. N. Stepanov. (*Zh. Eksp. Teor. Fiz.*, vol. 34, pp. 1292–1301; May, 1958.) Analysis of the propagation of magneto-hydrodynamic waves in an ionized gas when the wave frequency is much greater than the frequency of "short-range" collisions. See also 2418 of 1957.
- 537.562 768
Microwave Method for Measuring the Probability of Elastic Collision of Electrons in a Gas—J. L. Hirshfield and S. C. Brown. (*J. Appl. Phys.*, vol. 29, pp. 1749–1752; December, 1958.) A plasma in a dc magnetic field has a transverse conductivity component whose reactive part depends on the magnetic field. By measuring the magnetic field necessary to make the reactive part zero the probability of the elastic collision of electrons in he is obtained.
- 537.562:538.56 769
Scattering of Microwave Radiation by a Plasma Column—F. I. Boley. (*Nature, London*, vol. 182, pp. 790–791; September 20, 1958.) Experiments conducted at 10 cm λ to determine the angular distribution of the e.m. radiation scattered by the positive column of a mercury discharge under resonant conditions are described. Results support the theory of Mackinson and Slade (3532 of 1954). See also 418 of 1958 (Dattner).
- 538.24:621.372.413 770
Microwave Faraday Rotation: Design and Analysis of a Bimodal Cavity—A. M. Portis and D. Teaney. (*J. Appl. Phys.*, vol. 29, pp. 1692–1698; December, 1958.) An equivalent circuit is developed for the cavity, and the coupling between degenerate modes is expressed in terms of the susceptibility tensor of the material producing the rotation. The results are compared with experimental data.
- 538.566 771
Propagation of Plane Electromagnetic Waves in Inhomogeneous Media—H. Osterberg. (*J. Opt. Soc. Amer.*, vol. 48, pp. 513–521; August, 1958.) The laws of propagation along the z direction are derived for infinite inhomogeneous media in which dielectric constant and electrical conductivity are functions of z and the magnetic permeability is constant. Homogeneous media are treated as special cases.
- 538.566 772
Electromagnetic Scattering by Thin Conducting Plates at Glancing Incidence—J. S. Hey and T. B. A. Senior. (*Proc. Phys. Soc.*, vol. 72, pp. 981–995; December 1, 1958.) A large signal is scattered back from a thin plate illuminated edge-on by a field whose magnetic vector is normal to the plate. Experimental measurements show that the currents in the plate are predominant near the edges; their relation to theoretical results is discussed.
- 538.566:516.6 773
A Helical Coordinate System and Its Applications in Electromagnetic Theory—R. A. Waldron. (*Quart. J. Mech. Appl. Math.*, vol. 11, Part 4, pp. 438–461; November, 1958.) The system described enables problems involving helical symmetry to be solved exactly.
- 538.566:535.42 774
The Edge Condition in Diffraction Problems—P. Poincelot. (*Compt. Rend. Acad. Sci., Paris*, vol. 246, pp. 3324–3325; June 16, 1958.) The diffraction of an em wave by a perfectly conducting solid is considered.
- 538.566:535.43]+534.26 775
Theory of Wave Scattering on Periodically Uneven Surfaces—Yu. P. Lysanov. (*Akust. Z.*, vol. 4, pp. 3–12; January/March, 1958.) Description of six approximate mathematical methods for calculating the scattering of sound or em waves over the sea or uneven ground. 79 references.
- 538.566.2:538.22 776
Magnetic Double Refraction of Microwaves in Paramagnetics—F. S. Imamutdinov, N. N. Neprimerov, and L. Ya. Shekun. (*Zh. Eksp. Teor. Fiz.*, vol. 34, pp. 1019–1021; April, 1958.) Investigation at 9375 mc of the rotation of the plane of polarization of an H_{11} wave in a circular waveguide containing a paramagnetic salt, and its dependence on the intensity of the static magnetic field perpendicular to the direction of wave propagation.
- 538.569.4:538.221 777
Spin-Wave Analysis of Ferromagnetic Resonance in Polycrystalline Ferrites—E. Schlömann. (*J. Phys. Chem. Solids*, vol. 6, pp. 242–256; August, 1958.) Dipolar interaction is taken into account by means of the spin-wave formalism. Crystalline anisotropy and the polycrystalline nature of the material cause the homogeneous mode of precession to interact with spin waves whose wavelength is of the order of, or larger than, the average linear grain size. The theory predicts a very strong frequency and shape dependence of the linewidth when the homogeneous mode is approximately degenerate with long-wavelength spin waves propagating normal to the dc field.
- 538.569.4:538.222 778
Paramagnetic Resonance—J. S. van Wieringen. (*Philips Tech. Rev.*, vol. 19, pp. 301–313; May 31, 1958.) The quantum-mechanical theory of the phenomenon is discussed with reference to results of experimental investigations.
- 538.569.4.029.6:539.2 779
Technical Applications of Microwave Physics—D. J. E. Ingram. (*Research, London*, vol. 11, pp. 401–407; October, 1958.) Particular reference is made to electron-resonance techniques.
- 538.569.4.029.64 780
Paramagnetic Resonance Spectrum of Gadolinium in Hydrated Lanthanum Trichloride—M. Weger and W. Low. (*Phys. Rev.*, vol. 111, pp. 1526–1528; September 15, 1958.) The paramagnetic resonance spectrum of Gd^{3+} in $LaCl_3 \cdot 7H_2O$ was measured and found to agree
- quite well with a spin Hamiltonian with dominant coefficients $b_2^0 = \pm 0.0131 \text{ cm}^{-1}$, $b_2^2 = \mp 0.0075 \text{ cm}^{-1}$ at room temperature, and $b_2^0 = \pm 0.0099 \text{ cm}^{-1}$, $b_2^2 = \mp 0.0115 \text{ cm}^{-1}$ at liquid air temperature."
- 539.2 781
Theory of Plasma Resonance in Solids—P. A. Wolff. (*Phys. Rev.*, vol. 112, pp. 66–69; October 1, 1958.) The modes of a confined plasma are studied for simple geometries. Modes are closely spaced in frequency and unresolvable unless the sample size is comparable to the Debye length. Observation in small samples is made difficult by line broadening due to surface scattering but might be possible in a suitably designed experiment.
- 539.2:548.0 782
Fourier Coefficients of Crystal Potentials—J. Callaway and M. L. Glasser. (*Phys. Rev.*, vol. 112, pp. 73–77; October 1, 1958.) A method is developed for the calculation of the Fourier coefficients of the electrostatic potential of a given distribution of valence electrons in a solid, taking full account of the nonspherical character of the atomic polyhedron.
- GEOPHYSICAL AND EXTRATERRESTRIAL PHENOMENA**
- 523.14:538.69:523.165 783
Interplanetary Magnetic Field and its Control of Cosmic-Ray Variations—J. H. Piddington. (*Phys. Rev.*, vol. 112, pp. 589–596; October 15, 1958.) A model interplanetary magnetic field is described which may explain some features of solar cosmic-ray increases and also fluctuations in the primary radiation. An attempt is made to show how localized solar fields may create the field, which should be largely radial in form.
- 523.15 784
A Theorem on Force-Free Magnetic Fields—L. Woltjer. (*Proc. Nat. Acad. Sci.*, vol. 44, pp. 489–491; June 15, 1958.) A variational principle is proved which provides a more direct and satisfactory approach than that given in 3788 of 1958 (Chandrasekhar and Woltjer).
- 523.164.32 785
Nonuniformity in the Brightness of the Sun's Disk Sunspot Minimum—J. C. Bhattacharyya. (*J. Atmos. Terr. Phys.*, vol. 13, pp. 43–44; December, 1958.) A comparison is made between the nonuniformity, as derived from ionospheric measurements during eclipses, observed in 1944 and 1954. The results suggest that there are significant differences for the two epochs.
- 523.164.32:523.75 786
Observation of a Solar Flare at 4.3-mm Wavelength—R. J. Coates. (*Nature, London*, vol. 182, p. 861; September 27, 1958.) Scans made across the sun on September 25–27, 1957, with a radio telescope ((1126i of 1958) are compared with corresponding scans for a quiet sun.
- 523.164.32:551.510.535 787
Solar Radiation on Decimetre Waves as an Index for Ionospheric Studies—M. R. Kundu and J. F. Denisse. (*J. Atmos. Terr. Phys.*, vol. 13, pp. 176–178; December, 1958.) The solar noise radiation flux at 10.7 cm λ is compared with other indexes of solar activity. It seems to be as good as any other index for ionospheric studies on a monthly time scale and better for shorter time intervals.
- 523.164.4 788
The Trapping of Cosmic Radio Waves beneath the Ionosphere—G. R. Ellis. (*J. Atmos. Terr. Phys.*, vol. 13, pp. 61–71; December, 1958.) When there is a horizontal gradient in

the critical frequency of a layer, incoming extraterrestrial radiation may be trapped between the layer and the ground and propagated over large distances. This would account for the reception of cosmic noise at frequencies lower than the local critical frequency.

523.164.4:523.74 789

Sudden Cosmic Noise Absorption Associated with the Solar Event of 23 March 1958—K. A. Sarada. (*J. Atmos. Terr. Phys.*, vol. 13, pp. 192–194; December, 1958.)

550.38 790

The Relationships between the Secular Change and the Non-dipole Fields—K. Whitham. (*Can. J. Phys.*, vol. 36, pp. 1372–1396; October, 1958.) The drift and decay contributions to the secular variation have been estimated from isomagnetic and isoporic charts for 1955 in Canada. The westward drift in recent years was found to be significantly smaller than the world-wide average. Relations are obtained between the Gaussian coefficients in the spherical harmonic analyses of the earth's main field and the secular variation. It is shown that one half of this variation is produced by westward drift and that the decay terms are unimportant.

550.389.2:551.510.535 791

Electron Density Profiles in the Ionosphere during the I.G.Y.—(*J. Atmos. Terr. Phys.*, vol. 13, pp. 195–197; December, 1958.) See 438 of February (Smith-Rose).

550.389.2:629.19 792

Use of Artificial Satellites to Explore the Earth's Gravitational Field: Results for Sputnik II (1957 β)—R. H. Merson and D. G. King-Hele. (*Nature, London*, vol. 182, pp. 640–641; September 6, 1958.)

550.389.2:629.19 793

Seasonal Illumination of a Circumpolar Earth Satellite at its Extreme-Latitude Orbit Point—W. N. Abbott. (*Nature, London*, vol. 182, pp. 651–652; September 6, 1958.)

550.389.2:629.19 794

Polyhedral Satellite for More Accurate Measurement of Orbit Data of Earth Satellites—D. R. Herriott. (*J. Opt. Soc. Amer.*, vol. 48, pp. 667–668; September, 1958.) A 270-face polyhedron would reflect to an observer a light pulse of intensity more than 3000 times that from a sphere.

550.389.2:629.19 795

Rotation of Artificial Earth Satellites—R. N. Bracewell and O. K. Garriot. (*Nature, London*, vol. 182, pp. 760–762; September 20, 1958.) Radio signals received from Sputnik I were subject to deep regular fading with a semiperiod of about 4s, probably due to free motion of the satellite about its centroid. These fluctuations were less noticeable in the field strength record of Sputnik III. The advantages of a disc-shaped satellite and methods of eliminating rotational effects are discussed.

550.389.2:629.19 796

The Faraday—Rotation Rate of a Satellite Radio Signal—S. A. Bowhill. (*J. Atmos. Terr. Phys.*, vol. 13, pp. 175–176; December, 1958.)

550.389.2:629.19 797

An Irregularity in the Atmospheric Drag Effects on Sputniks II and III (Satellites 1957 β , 1958 δ and 1958 δ_2)—D. G. King-Hele and D. M. C. Walker. (*Nature, London*, vol. 182, pp. 860–861; September 27, 1958.)

550.389.2:629.19 798

Satellite Tracking by H.F. Direction Finder—J. L. Wolfe. (*J. Atmos. Terr. Phys.*, vol. 13, pp. 155–164; December, 1958.) A twin-

channel cathode-ray DF with an Adcock aerial was used on the 20 mc signals from satellites 1957 α and β . The results obtained and their accuracy are discussed.

550.389.2:629.19:551.510.535 799

Comparison of Phase Difference and Doppler Shift Measurements for Studying Ionospheric Fine Structure using Earth Satellites—M. C. Thompson, Jr, and D. M. Waters. (*PROC. IRE*, vol. 46, p. 1960; December, 1958.)

551.510.535 800

On the Electron Production Rate in the F₂ Region of the Ionosphere—S. Datta. (*Indian J. Phys.*, vol. 32, pp. 483–491; October, 1958.) The F₂ region, between "bottom" and height of maximum density, is divided into four equal columns, the mean production rate in each being calculated. The results show a diurnal variation of the rate with a single peak at about half an hour before noon.

551.510.535 801

Drift Observations Evaluated by the Method of 'Similar Fades'—E. Harnischmacher and K. Rawer. (*J. Atmos. Terr. Phys.*, vol. 13, pp. 1–16; December, 1958.) A regular interference model is considered as opposed to the usual purely random model. Some of the observed features are well explained by a model which lies between these two views, provided a finite lifetime is assumed for the irregularities. Large changes of drift velocity can be explained by assuming small vertical velocities.

551.510.535 802

Bifurcations in the F Region at Baguio, 1952–1957—V. Marasigan. (*J. Atmos. Terr. Phys.*, vol. 13, pp. 26–31; December, 1958.) A five-year statistical survey of bifurcations at Baguio, Philippines is presented, and it is shown that the condition for bifurcation is mainly governed by the parameters h_m and y_m of the F₂ layer. h_m depends on latitude whilst y_m depends on solar activity.

551.510.535 803

The Diurnal Variation of f_0F_2 near the Auroral Zone during Magnetic Disturbances—B. Maehlum. (*J. Atmos. Terr. Phys.*, vol. 13, pp. 187–190; December, 1958.)

551.510.535 804

Horizontal Drifts and Temperature in the Lower Part of Region E—W. J. G. Beynon and G. L. Goodwin. (*J. Atmos. Terr. Phys.*, vol. 13, pp. 180–182; December, 1958.) Drift velocities deduced from the fading of CW signals at oblique incidence are related to results obtained using other techniques. A minimum velocity at 80–90 km is indicated and a possible connection with a temperature minimum at the same height is discussed.

551.510.535 805

Height Gradient of Electron Loss in the F Region—V. Marasigan. (*J. Atmos. Terr. Phys.*, vol. 13, pp. 107–112; December, 1958.) A theoretical expression is derived for an exponential height gradient of the electron loss coefficient in the F region on the assumption that this gradient completely accounts for F₁–F₂ bifurcation. Five models are investigated; they are second-power, linear, cosine, parabolic, and quasi-parabolic distributions of electron density with height.

551.510.535 806

The Electron Distribution in the Ionosphere over Slough: Part 2—Disturbed Days—J. O. Thomas and A. Robbins. (*J. Atmos. Terr. Phys.*, vol. 13, pp. 131–139; December, 1958.) The results are analysed of the distribution with height for three months in a year of low, and three months in a year of high sunspot number. It is shown that the variation in $h'F_2$

is not a quantitative guide to the changes in height of the F₂ layer during storms. The electron distributions for five individual storms are thoroughly investigated. Some important ionospheric changes have been noticed during a world-wide sudden impulse. Part 1: 1734 of 1958 (Thomas et al.).

551.510.535 807

On Instrument Effects in Ionosphere Data—H. J. Albrecht. (*J. Atmos. Terr. Phys.*, vol. 13, pp. 173–175; December, 1958.)

551.510.535:523.164.4 808

Abnormal Ionospheric Behaviour at 10 Metres Wavelength—M. Krishnamurthi, G. S. Sastry, and T. S. Rao. (*Curr. Sci.*, vol. 27, pp. 332–333; September, 1958.) During observations at Hyderabad, India, of cosmic radio noise total reflection of cosmic noise was observed on three occasions near sunrise. The effect is assumed to be caused by a locally high concentration of matter in the upper ionospheric layers.

551.510.535:621.396.11 809

On the Approximate Daytime Constancy of the Absorption of Radio Waves in the Lower Ionosphere—S. Chapman and K. Davies. (*J. Atmos. Terr. Phys.*, vol. 13, pp. 86–89; December, 1958.) The lower part of the D layer is due to photo-detachment of electrons from negative ions the concentration of which is large and nearly constant from day to night. The optical depth is small for the photo-detachment radiation but large for the radiation which can ionize neutral particles.

551.510.535:621.396.11 810

Ionospheric Absorption over Delhi—B. V. T. Rao and M. K. Rao. (*J. Instn Telecommun. Engrs, India*, vol. 4, pp. 205–208; September, 1958.) An analysis of further measurements made at 5 mc until October 1957. See also 3461 of 1958 (Mazumdar).

551.510.535:621.396.11:621.396.677.4 811

A New Antenna to Eliminate Ground-Wave Interference in Ionospheric Sounding Experiments—R. S. Macmillan, W. V. T. Rusch, and R. M. Golden. (*J. Atmos. Terr. Phys.*, vol. 13, pp. 183–186; December, 1958.)

551.594.5:621.396.11 812

Radio Reflections on Low Frequencies from 75–90 km Height during Intense Aurora Activity—W. Stoffregen. (*J. Atmos. Terr. Phys.*, vol. 13, pp. 167–169; December, 1958.)

551.594.6 813

Simultaneous Recording of Atmospherics on Four Different Frequency Bands in the Low-Frequency Region—M. W. Chiplonkar and V. N. Athavale. (*J. Atmos. Terr. Phys.*, vol. 13, pp. 32–37; December, 1958.) The number and intensity of atmospherics are recorded simultaneously on four narrow bands at 85, 125, 175, and 455 kc. Results show atmospherics with large field strengths to be less frequent than those with small field strengths on all bands, and the field strength of atmospherics to be a maximum in the 125 kc band.

551.594.6:551.594.221 814

The Relationship between Atmospheric Radio Noise and Lightning—F. Horner. (*J. Atmos. Terr. Phys.*, vol. 13, pp. 140–154; December, 1958.) In Europe atmospherics in a bandwidth of 300 c at 10 kc have median amplitude, amplitude range, and frequency occurrence in accordance with that expected from lightning discharges to the ground. In Australia atmospherics from tropical storms were found to consist of numerous pulses the largest of which probably originated in ground strokes. The origin of the smaller pulses is not clear. Some observations on atmospherics in the HF band are also described.

- 551.594.6:621.3.087.4/5 815
Waveforms of Atmospherics with Superimposed Pulses Recorded with an Automatic Atmospherics Recorder—B. A. P. Tantry and R. S. Srivastava. (*J. Atmos. Terr. Phys.*, vol. 13, pp. 38–42; December, 1958.) The recorder design is briefly outlined and observations are discussed in which “stepped” pulses from one lightning discharge are superimposed on the waveform from a second discharge. See also 3824 of 1958 (Tantry).
- LOCATION AND AIDS TO NAVIGATION**
- 621.396.932.1 816
A New Method of Component Determination in Radio Direction-Finding for Coherent Waves—H. Gabler and M. Wächtler. (*Elektrotech. Z.*, vol. 79, pp. 383–388; June 1, 1958.) The three ellipses produced by three suitably spaced crossed-loop antennas with a two-channel cathode-ray DF equipment are superimposed on the screen. Bearings free from night effect can be obtained even under unfavourable site conditions.
- 621.396.933.1 817
New V.H.F. Direction-Finding Equipment—(*Brit. Commun. Electronics*, vol. 5, p. 681; September, 1958.) A brief description is given of automatic equipment using a rotating Adcock antenna. The operational range is about 100 miles for aircraft flying at 10,000 ft and radiating 5W.
- 621.396.96 818
Radar Systems with Electronic Sector Scanning—D. E. N. Davies—(*J. Brit. IRE*, vol. 18, pp. 709–713; December, 1958.) The application to radar of a system previously described in relation to underwater acoustic echolocation [3676 of 1958 (Tucker et al.)] is discussed. Information rate is much higher than that of a conventional radar system.
- 621.396.96:551.51 819
Radar Echoes from Atmospheric Inhomogeneities—R. F. Jones. (*Quart. J. R. Met. Soc.*, vol. 84, pp. 437–442; October, 1958.) A quantitative examination of the possibility of radar echoes being caused by scattering or reflection from atmospheric inhomogeneities shows this to be theoretically possible but necessitating large changes in refractive index.
- 621.396.962.33 820
Decca Doppler and Airborne Navigation—T. Gray and M. J. Moran. (*Brit. Commun. Electronics*, vol. 5, pp. 764–771; October, 1958.) The techniques of transmission and reception used in Doppler systems are examined. The Decca Doppler sensor uses a self-coherent pulsed “Janus” system with a symmetrical four-beam aerial configuration. A qualitative description of the Decca Integrated Airborne Navigation system (DIAN) is given.
- 621.396.963 821
Accurate Method for Correction of Slant-Range Distortion in High-Altitude Radars and a Contribution to the Optics of Reflecting Conical Surfaces—I. Levi. (*J. Opt. Soc. Amer.*, vol. 48, pp. 680–686; October, 1958.)
- 621.396.967:621.396.65 822
Microwave Links for Radar Networks—Sutherland. (See 976.)
- 621.396.969.33:621.396.677.7 823
Slotted-Waveguide Array for Marine Radar—Byers and Katchky. (See 711.)
- MATERIALS AND SUBSIDIARY TECHNIQUES**
- 535.215 824
Internal Photoeffect and Exciton Diffusion in Cadmium and Zinc Sulphides—M. Bal-
- kanski and R. D. Waldron. (*Phys. Rev.*, vol. 112, pp. 123–135; October 1, 1958.) The absorption spectra of CdS and ZnS and the photoconductivity produced by illumination at a distance from the electrodes were studied to determine the mechanisms of photo-electron interaction and energy transport in these materials.
- 535.215 825
Photoemissive, Photoconductive, and Optical Absorption Studies of Alkali-Antimony Compounds—W. E. Spicer. (*Phys. Rev.*, vol. 112, pp. 114–122; October 1, 1958.) Experimental methods and results are given. Values for the band gaps and electron affinities are tabulated, and the conductivity types as indicated by photo-emission data are listed.
- 535.215:546.47:31 826
Photo-properties of Zinc Oxide with Ohmic and Blocking Contacts—H. J. Gerritsen, W. Ruppel, and A. Rose. (*Helv. Phys. Acta*, vol. 30, pp. 504–512; November 20, 1957.) Report of measurements of primary and secondary photocurrents in fine-grain ZnO layers.
- 535.215+535.37]:546.482.21 827
The Mechanism of Energy Transfer in Cadmium Sulphide Crystals—I. Broser and R. Broser-Warminsky. (*J. Phys. Chem. Solids*, vol. 6, pp. 386–400; In German.) The transfer of the energy of excitation from the point of absorption to non-irradiated regions over relatively large distances may be explained by the scattering and reabsorption of the incident light or the luminescent radiation generated in the crystal. The hypothesis of energy conduction by excitons is not confirmed.
- 535.215:546.482.21 828
Photoconductivity and Crystal Size in Evaporated Layers of Cadmium Sulphide—J. M. Gilles and J. Van Cakenberghe. (*Nature, London*, vol. 182, pp. 862–863; September 27, 1958.) The effect of heating a layer of CdS crystals in contact with a film of evaporated Ag to 500°–600°C in an inert atmosphere is discussed.
- 535.215:546.482.21 829
Progress in Cadmium Sulphide—L. L. Autes. (IRE TRANS. ON COMPONENT PARTS, vol. CP-4, pp. 129–132; December, 1957. Abstract, PROC. IRE, vol. 46, p. 801; April, 1958.)
- 535.215:546.817.231:539.23 830
Photoconductivity in Chemically Deposited Films of Lead Selenide—D. H. Roberts and J. E. Baines. (*J. Phys. Chem. Solids*, vol. 6, pp. 184–189; August, 1958.)
- 535.37 831
Electrophotoluminescent Amplification—R. E. Halsted. (*J. Appl. Phys.*, vol. 29, pp. 1706–1708; December, 1958.) An alternating electric field applied parallel to an excitation gradient in some sulphide phosphors can produce a pronounced characteristic modulation of the photoluminescent emission. Experimental results on this effect are discussed.
- 535.376:546.472.21 832
Electroluminescence of Zinc Sulphide Phosphors as an Equilibrium Process—W. Lehmann. (*J. Opt. Soc. Amer.*, vol. 48, pp. 647–653; September, 1958.) Predictions of phosphor characteristics based on the equilibrium condition relating monomolecular collision excitation and bimolecular recombination processes are compared with experimental results.
- 535.376:546.472.21 833
The Significance of Boundary Layers and Polarization Fields for Electroluminescence—D. Hahn and F. W. Seemann. (*Z. Phys.*, vol. 149, pp. 486–503; October 31, 1957.) Lumines-
- cence of ZnS-based phosphors was investigated using excitation by square pulses of alternating or single polarity. See also 2156 of 1957.
- 535.376:546.472.21 834
Cathodo-electroluminescence Phenomena in ZnS Phosphors—H. Gobrecht, H. E. Gumlisch, H. Nelkowski, and D. Langer. (*Z. Phys.*, vol. 149, pp. 504–510; October 31, 1957.) Two powder phosphors, one electroluminescent and the other nonelectroluminescent but with pronounced enhancement effect, are investigated.
- 535.376:546.472.21 835
Electroluminescence of ZnS Single Crystals with Cathode Barriers—D. R. Frankl. (*Phys. Rev.*, vol. 111, pp. 1540–1549; September 15, 1958.) Certain ZnS crystals show electroluminescence predominantly near the cathode. The major emission from Cu-activated crystals occurs as a burst of light when the exciting voltage is suddenly removed, the burst being quenched by a voltage in the initial direction or enhanced by a voltage in the opposite direction. These results, as well as the emission peaks obtained under sinusoidal voltage excitation, are explained in terms of ionization of luminescent centers in a barrier region.
- 537.226/227 836
Dielectric and Thermal Study of (NH₄)₂SO₄ and (NH₄)₂BeF₄ Transitions—S. Hoshino, K. Vedam, Y. Okaya, and R. Pepinsky. (*Phys. Rev.*, vol. 112, pp. 405–412; October 15, 1958.)
- 537.226 837
Electrical Dispersion Phenomena in Inhomogeneous Dielectrics—R. Parker and M. S. Smith. (*J. Electronics Control*, vol. 5, pp. 354–361; October, 1958.) The theory of Koops (162 of 1952) is generalized to include an arbitrary distribution of layer thicknesses and orientations. Observed deviations from the dispersion equations are ascribed to inhomogeneities in the current density vector. The evaluation of surface-layer parameters is discussed.
- 537.226 838
The Ternary Systems BaO-TiO₂-SnO₂ and BaO-TiO₂-ZrO₂—G. H. Jonker and W. Kwestroo. (*J. Amer. Ceram. Soc.*, vol. 41, pp. 390–394; October 1, 1958.)
- 537.226:621.315.612 839
Lightweight Ceramic Materials as High-Frequency Dielectrics—J. L. Pentecost and P. E. Ritt. (IRE TRANS. ON COMPONENT PARTS vol. CP-4, pp. 133–135; December, 1957. Abstract, PROC. IRE, vol. 46, p. 801; April, 1958.)
- 537.227 840
Room-Temperature Ferroelectricity in Lithium Hydrasium Sulphate, Li(N₂H₅)SO₄—R. Pepinsky, K. Vedam, Y. Okaya, and S. Hoshino. (*Phys. Rev.*, vol. 111, pp. 1467–1468; September 15, 1958.) A method of producing (and protecting) large crystals is described together with details of an investigation of the ferroelectric behaviour and crystallographic structure.
- 537.227 841
Ammonium Hydrogen Sulphate: A New Ferroelectric with Low Coercive Field—R. Pepinsky, K. Vedam, S. Hoshino, and Y. Okaya. (*Phys. Rev.*, vol. 111, pp. 1508–1510; September 15, 1958.) Details are given of the ferroelectric behaviour of (NH₄)HSO₄ in the range –3°C to –119°C, together with details of the crystallographic structure. A particular feature is the low coercive field which is about 150 v/cm at –13°C.
- 537.227:539.2 842
Polarization Fluctuations in a Ferroelectric Crystal—R. E. Burgess. (*Can. J. Phys.*, vol. 36,

pp. 1569-1581; November, 1958.) The theory of thermal fluctuations of electrical polarization in a ferroelectric crystal is considered, with special attention to temperatures in the neighborhood of the Curie point. By thermodynamical analysis of a dipole model, the fluctuations and their spectral density are related respectively to the real and imaginary parts of the susceptibility of the crystal.

537.227:546.431.824-31 **843**
Transition to the Ferroelectric State in Barium Titanate—D. Meyerhofer. (*Phys. Rev.*, vol. 112, pp. 413-423; October 15, 1958.) Besides raising the cubic-tetragonal transition about 15°C with an electric field along the cube-edge direction, an orthorhombic phase was induced above the Curie point by a field along a face-diagonal direction. Birefringence, polarization, and dielectric constant were measured above and below the Curie point as functions of field strength and field direction.

537.227:546.431.824-31 **844**
Polarization Changes during the Process of Ageing in Ferroelectrics of the BaTiO₃-Type—Z. Pajak and J. Stankowski. (*Proc. Phys. Soc.*, vol. 72, pp. 1144-1146; December 1, 1958.) The dielectric-hysteresis loops of barium metatitanate ceramics become constricted with age and eventually form a narrow double loop. The ageing process may be reversed by heating above the Curie point.

537.228.1 **845**
Some Piezoelectric Properties of Polycrystalline Solid Solutions (Ba, Sr)TiO₃, Ba(Ti, Sn)O₃ and Ba(Ti, Zr)O₃—V. A. Bokov. (*Akust. Z.*, vol. 3, pp. 104-108; April/June, 1957.) In certain solid solutions, the electro-mechanical response and effective piezoelectric modulus depend on the voltage of the polarizing field and temperature. This response and coefficient pass through a maximum, due to domain orientation, particularly in solid solutions of the type Ba(Ti, Sn)O₃ and Ba(Ti, Zr)O₃.

537.228.1:546.472.21 **846**
Theory of the Piezoelectric Effect in the Zinoblende Structure—J. L. Birman. (*Phys. Rev.*, vol. 111, pp. 1510-1514; September 15, 1958.) A theory is developed which leads to an equation relating the macroscopic piezoelectric constant to the static and dynamic effective charges, and a lattice parameter which relates the internal strain to the external strain. An order-of-magnitude check of the theory is made on ZnS.

537.311.33 **847**
The Prediction of Semiconducting Properties in Inorganic Compounds—C. H. L. Goodman. (*J. Phys. Chem. Solids*, vol. 6, pp. 305-314; September, 1958.) Various criteria are presented for predicting possible semiconductor behavior in inorganic compounds, based on the requirements of saturated ionic-covalent bonding. It is shown that new series of semiconducting compounds can be derived from known ones by replacing one element by pairs from other groups of the periodic table, while keeping the valence-electron:atom ratio constant. These concepts are illustrated with particular reference to diamond-type lattices.

537.311.33 **848**
Calculations on the Shape and Extent of Space-Charge Regions in Semiconductor Surfaces—G. C. Dousmanis and R. C. Duncan, Jr. (*J. Appl. Phys.*, vol. 29, pp. 1627-1629; December, 1958.) Curves showing the potential as a function of distance inside a semiconductor are obtained by numerical integration of the Poisson equation. The results apply to all semiconductors.

537.311.33 **849**
The Dependence of Minority-Carrier Lifetime on Majority-Carrier Density—D. M. Evans. (*Proc. IRE*, vol. 46, pp. 1962-1963; December, 1958.) The minority-carrier lifetime in Ge and Si is inversely proportional to the majority-carrier density only if the recombination levels lie near the appropriate band edge and/or the semiconductor is only weakly extrinsic.

537.311.33 **850**
Influence of Crystal Lattice Vibrations on the Production of Electron-Hole Pairs in a Strong Electric Field—L. V. Keldysh. (*Zh. Eksp. Teor. Fiz.*, vol. 34, pp. 962-968; April, 1958.) The probability for the production of an electron-hole pair in a semiconductor is calculated considering electron-phonon interaction. Other processes which may influence the diffusion of a valence electron into the conduction band are considered, in particular, the absorption of several phonons which may be decisive in relatively weak fields.

537.311.33 **851**
Semiconductor Surface Potential and Surface States from Field-Induced Changes in Surface Recombination—G. C. Dousmanis. (*Phys. Rev.*, vol. 112, pp. 369-380; October 15, 1958.) The variations in surface recombination are detected by changes in the reverse current of large-area "back-surface" diodes. Observation of a maximum of surface recombination in terms of applied field provides a reference point from which the zero-field value of the surface potential can be evaluated, and the dependence of the surface recombination velocity on the surface potential can be established.

537.311.33 **852**
Junction Capacitance and Related Characteristics using Graded Impurity Semiconductors—L. J. Giacoletto. (*IRE TRANS. ON ELECTRON DEVICES*, vol. ED-4, pp. 207-215; July, 1957. Abstract, *Proc. IRE*, vol. 45, p. 1760; December, 1957.)

537.311.33 **853**
The K-Edge Structures of the Elements of Various A_{III}B_V Compounds—W. Eberbeck. (*Z. Phys.*, vol. 149, pp. 412-424; October 31, 1957. The fine structure of the K X-ray absorption spectrum was investigated for Ga in GaP, GaAs, and GaSb, and for As in GaAs and InAs, for Zn in ZnS, and for pure Ge.

537.311.33:537.32 **854**
The Effect of Strain on the Thermoelectric Properties of a Many-Valley Semiconductor—J. R. Drabble. (*J. Electronics Control*, vol. 5, pp. 362-372; October, 1958.) A general treatment is given for non degenerate materials. It is shown that the absence of effects other than those due to carrier transfer between valleys can be checked by the condition that the trace of the conductivity tensor is unaltered by the strain. Under these conditions, the conductivity and thermoelectric power tensors can be combined to give an expression involving only the relative shifts in the minimum energies of the valleys.

537.311.33:538.632 **855**
Hall Effect in Semiconductor Compounds—M. J. O. Strutt. (*Electronic Radio Engr.*, vol. 36, pp. 2-10; January, 1959.) The effect in InAs and InSb, and the influence of probe shape and position are discussed. Applications to several types of wattmeter, to oscillators, to a flux-density meter, and to a receiver mixer stage are described.

537.311.33:538.632 **856**
Hall Mobility of Carriers in Impure Nondegenerate Semiconductors—M. S. Sodha and

P. C. Eastman. (*Phys. Rev.*, vol. 112, p. 44; October 1, 1958.) The case of low temperatures and high impurity concentrations is considered.

537.311.33:[546.28+546.289] **857**
Lattice Vibrational Spectra of Si and Ge—H. Cole and E. Kineke. (*Phys. Rev. Lett.*, vol. 1, pp. 360-361; November 15, 1958.)

537.311.33:[546.28+546.289] **858**
Theoretical Surface Conductivity Changes and Space Charge in Germanium and Silicon—V. O. Mowery. (*J. Appl. Phys.*, vol. 29, pp. 1753-1757; December, 1958.) Graphs are given showing the surface conductivity and space charge as functions of resistivity for various values of surface potential.

537.311.33:546.28 **859**
The Measurement of Surface Recombination Velocity on Silicon—A. H. Benny and F. D. Morten. (*Proc. Phys. Soc.*, vol. 72, pp. 1007-1012; December 1, 1958.) The surface recombination velocity on a Si filament can be determined by the measurement of the spectral distribution of the photoconductivity. On *n*-type Si the surface recombination velocity can be varied from less than 75 to greater than 7500 cm. sec⁻¹ by changing the ambient gas.

537.311.33:546.28 **860**
Microwave Spin Echoes from Donor Electrons in Silicon—J. P. Gordon and K. D. Bowers. (*Phys. Rev. Lett.*, vol. 1, pp. 368-370; November 15, 1958.) The relaxation time in Si containing Li and P has been measured at a frequency of 23 kmc using a heterodyne paramagnetic spectrometer. Results indicate that a spin-echo device could provide a storage system in which each element could store more than 10⁴ bits of information.

537.311.33:546.28 **861**
Neutron-Bombardment Damage in Silicon—G. K. Wertheim. (*Phys. Rev.*, vol. 111, pp. 1500-1505; September 15, 1958.) Neutron-bombardment damage in Si is compared to electron-bombardment effects which have been previously analysed (3515 of 1958). A discrete energy level 0.27 eV above the valence band is produced by both neutrons and electrons. A spectrum of energy levels running from 0.16 eV below the conduction band toward the middle of the gap is ascribed to a defect pair with variable spacing.

537.311.33:546.28 **862**
Recombination Properties of Gold in Silicon—G. Bemski. (*Phys. Rev.*, vol. 111, pp. 1515-1518; September 15, 1958.) The capture of electrons in *p*-type Si occurs through the Au donor level with a capture cross-section of 3.5 × 10⁻¹⁶ cm² at 300°K; this capture cross-section varies as T^{-2.5} between 200° and 500°K. In *n*-type Si the electron capture cross-section is 5 × 10⁻¹⁶ cm² and is of independent temperature; the hole capture cross-section is 1 × 10⁻¹⁶ cm² at 300°K and varies as T⁻⁴. The capture in this case occurs through the Au acceptor level.

537.311.33:546.28:535.215 **863**
Quantum Yield of Photoionization in Silicon—V. S. Vavilov and K. I. Britsyn. (*Zh. Eksp. Teor. Fiz.*, vol. 34, pp. 1354-1355; May, 1958.) Results of an investigation of the photo-effect in *p-n* junctions obtained by thermal diffusion of phosphorus indicate an increase in quantum yield and the presence of impact ionization by liberated carriers.

537.311.33:[546.28+546.289]:535.39-15 **864**
Antireflection Coatings for Germanium and Silicon in the Infrared—J. T. Cox and G. Hass. (*J. Opt. Soc. Amer.*, vol. 48, pp. 677-680; October, 1958.)

- 537.311.33:546.289 865
Production of Dislocations in Germanium by Thermal Shock—R. S. Wagner. (*J. Appl. Phys.*, vol. 29, pp. 1679-1682; December, 1958.) The results indicate that the imperfections are not generated during growth, but occur afterwards, as a result of thermal shock when the growth is terminated.
- 537.311.33:546.289 866
Effect of Monoenergetic Fast Neutrons on *n*-Type Germanium—S. L. Ruby, F. D. Schupp, and E. D. Wolley. (*Phys. Rev.*, vol. 111, pp. 1493-1496; September 15, 1958.) The density of vacancy-interstitial pairs produced unit of fast-neutron flux on *n*-type Ge has been measured experimentally using monoenergetic neutrons. The observed changes in resistivity and Hall coefficients indicate charge carrier removal rates per unit of neutron flux much lower than that calculated from current models.
- 537.311.33:546.289 867
Photoconductive Response of Single-Crystal Germanium Layers prepared by the Pyrolytic Decomposition of GeI₄—D. C. Crone-meyer. (*J. Appl. Phys.*, vol. 29, pp. 1730-1735; December, 1958.) The photo-response measured at 77°K was found to extend to about 6 μ , in agreement with the thermal activation energy. Doping of the Ge with Au and Ag was attempted, but no positive identification of the doping agents was obtained from the photoconductive response.
- 537.311.33:546.289 868
Radiation-Induced Recombination Centers in Germanium—O. L. Curtis, Jr, J. W. Cleland, and J. H. Crawford, Jr. (*J. Appl. Phys.*, vol. 29, pp. 1722-1729; December, 1958.) The effect of energetic particle bombardment on the minority carrier lifetime has been measured. It is concluded that a defect state located 0.20 eV below the conduction band dominates the recombination process.
- 537.311.33:546.289 869
Radiative Recombination in Germanium—P. H. Brill and R. F. Schwarz. (*Phys. Rev.*, vol. 112, pp. 330-333; October 15, 1958.) Dependence on excess-carrier density and on equilibrium-carrier density was studied by simultaneous measurements of output radiation and of photoconductivity as functions of incident light intensity. Results confirm the theory.
- 537.311.33:546.289 870
Magnetoresistance in *n*-Type Germanium at Low Temperatures—R. A. Laff and H. Y. Fan. (*Phys. Rev.*, vol. 112, pp. 317-321; October 15, 1958.) The effective anisotropy parameter *K* decreased from ~ 20 at 300°K to ~ 6 at 20°K, but values near 20 were again obtained at 7°K and 4.2°K. Introduction of compensating acceptors showed that the decrease of *K* was due to anisotropic scattering by ionized impurities. Below 7°K, scattering was controlled by neutral impurities with essentially isotropic relaxation time.
- 537.311.33:546.289 871
Infrared Absorption by Conduction Electrons in Germanium—H. J. G. Meyer. (*Phys. Rev.*, vol. 112, pp. 298-308; October 15, 1958.) A theory is developed taking into account the multivalley structure of the conduction band and present knowledge of the scattering mechanism. Explicit calculations are possible at all relevant wavelengths and temperatures.
- 537.311.33:546.289 872
Oscillation of the Electrical Resistance of *n*-Type Germanium in Strong Pulsed Magnetic Fields—I. G. Fakidov and E. A. Zavadskii. (*Zh. Eksp. Teor. Fiz.*, vol. 34, pp. 1036-1037; April, 1958.) Note on measurements of the resistance variation in single-crystal Ge in a transverse pulse magnetic field up to 120 kg at temperatures 300, 77 and 20°K.
- 537.311.33:546.289 873
Surface Effects in Electron-Irradiated Ge at 80°K—W. E. Spear. (*Phys. Rev.*, vol. 112, pp. 362-369; October 15, 1958.) Results are given of photoconductivity, surface-conductance, Hall-, and field-effect measurements made before and after electron irradiation. Use of both low- and high-energy irradiation distinguishes between volume and surface effects. Surface rather than volume effects are responsible for photoconductivity changes beyond the fundamental absorption edge.
- 537.311.33:546.289:535.215 874
Delayed Electron Emission and External Photoeffect of Germanium after Electron Bombardment—K. Seeger. (*Z. Phys.*, vol. 149, pp. 453-470; October 31, 1957.) Emission was investigated in the temperature range 103°-670°K. An interpretation of the effect as being due to slow surface states is discussed.
- 537.311.33:546.289:538.569 875
Experimental Evidence for Carriers with Negative Mass—G. C. Dousmanis, R. C. Duncan, Jr, J. J. Thomas, and R. C. Williams. (*Phys. Rev. Lett.*, vol. 1, pp. 404-407; December 1, 1958.) Cyclotron resonance experiments have been carried out on Ge crystals at 4°K. A spectrum of heavy hole has been revealed which may be assigned to carriers of negative mass.
- 537.311.33:546.289.231 876
The Crystal Structure of Germanium Selenide GeSe—A. Okazaki. (*J. Phys. Soc. Japan*, vol. 13, pp. 1151-1155; October, 1958.)
- 537.311.33:546.47-31 877
An Approach to Intrinsic Zinc Oxide—W. Ruppel, H. J. Gerritsen, and A. Rose. (*Helv. Phys. Acta*, vol. 30, pp. 495-503; November 20, 1957.) Measurements have been made on layers of finely divided ZnO powder the resistivity of which ($10^{17} \Omega \cdot \text{cm}$) is closer to that of intrinsic ZnO than that of single crystals. The formation of depletion layers and the rectifying action observed with ohmic and blocking contacts are discussed.
- 537.311.33:546.47-31 878
The Preparation of Zinc Oxide Single Crystals with Defined Impurity Content—G. Bogner and E. Mollwo. (*J. Phys. Chem. Solids*, vol. 6, pp. 136-143; August, 1958. In German.) A method is described by which ZnO crystals of a definite composition can be deposited from the gas phase. Measurements of the composition, conductivity, and infrared absorption of crystals doped with Cu or In are reported.
- 537.311.33:546.47-31 879
The Concentration and Mobility of Electrons in Zinc Oxide Single Crystals with Defined Impurity Content—H. Ruppel. (*J. Phys. Chem. Solids*, vol. 6, pp. 144-154; August, 1958. In German.) The conductivity and Hall effect in synthetic crystals of doped ZnO have been measured in the temperature range 65-700°K. Results are similar to those for other semiconductors such as Ge and Si.
- 537.311.33:546.47-31 880
Field Effect and Photoconductivity in ZnO Single Crystals—G. Heiland. (*J. Phys. Chem. Solids*, vol. 6, pp. 155-168; August, 1958.) Report and discussion of the results of measurements made on ZnO crystals with surface conductivity varying over a wide range.
- 537.311.33:546.681.19 881
The Preparation and Properties of Gallium Arsenide Single Crystals—J. M. Whelan and G. H. Wheatley. (*J. Phys. Chem. Solids*, vol. 6, pp. 169-172; August, 1958.) Apparatus is described for the preparation and purification of GaAs by horizontal zone refining, and for the production of single crystals by the floating-zone method. Resistivities up to $10^8 \Omega \cdot \text{cm}$ have been obtained. Hall coefficient and conductivity data for *n*-type samples are given. Electron mobility, the energy gap, and the position of an impurity level are deduced.
- 537.311.33:546.681.19 882
Diffusion, Solubility, and Electrical Behaviour of Copper in Gallium Arsenide—C. S. Fuller and J. M. Whelan. (*J. Phys. Chem. Solids*, vol. 6, pp. 173-177; August, 1958.)
- 537.311.33:546.682.18 883
Optical Properties of *n*-Type InP—R. Newman. (*Phys. Rev.*, vol. 111, pp. 1518-1521; September 15, 1958.)
- 537.311.33:546.682.19:537.312.9 884
Piezoresistance Constants of *n*-Type InAs—A. J. Tuzzolino. (*Phys. Rev.*, vol. 112, p. 30; October 1, 1958.) Results of measurements from 77°K to 300°K are consistent with a spherical conduction-band model.
- 537.311.33:546.72.23 885
FeSe₂, a Semiconductor containing Iron—G. Fischer. (*Can. J. Phys.*, vol. 36, pp. 1435-1438; October, 1958.) The preparation of this compound is described; the results of electrical-resistivity and Hall-coefficient measurements and X-ray examination are summarized.
- 537.311.33:546.812.221 886
The Semiconductor Properties of Synthetic Herzenbergite (SnS) Crystals—H. Gobrecht and A. Bartschat. (*Z. Phys.*, vol. 149, pp. 511-522; October 31, 1957.)
- 537.311.33:546.824-31:537.312.9 887
Piezoresistivity in Reduced Single-Crystal Rutile (TiO₂)—L. E. Hollander, Jr. (*Phys. Rev. Lett.*, vol. 1, pp. 370-371; November 15, 1958.) The effect of stress on resistivity has been measured at different temperatures.
- 537.311.33:621.314.63 888
Alloy Junctions in Semiconducting Devices—D. F. Taylor. (*Research. London*, vol. 11, pp. 335-338; September, 1958.) Outline of theory on which methods of preparing alloy junctions are based.
- 537.311.33:621.318.57 889
Current Build-Up in Semiconductor Devices—W. Shockley and J. Gibbons. (*Proc. IRE*, vol. 46, pp. 1947-1949; December, 1958.) Assuming that the minority-carrier densities and their associated currents have an exponential rise during the switching action, a solution to the partial differential equations can be found from which the efficiencies of various designs of switching devices may be derived.
- 538.22 890
An Interpretation of the Magnetic Properties of the Perovskite-Type Mixed Crystals La_{1-x}Sr_xCoO_{3- λ} —J. B. Goodenough. (*J. Phys. Chem. Solids*, vol. 6, pp. 287-297; August, 1958.)
- 538.221 891
Interatomic Distances in Ferromagnetics—F. M. Gal'perin. (*Zh. Eksp. Teor. Fiz.*, vol. 34, pp. 1000-1003; April, 1958.)
- 538.221 892
The Change of Spontaneous Magnetization with Hydrostatic Pressure—D. Guggan. (*Proc. Phys. Soc.*, vol. 72, pp. 1013-1026; December 1, 1958.)

- 538.221** **893**
Dipolar Energy. Application to the Magneto-static Energy of α -Fe₂O₃—F. Bertaut. (*Compt. Rend. Acad. Sci., Paris*, vol. 246, pp. 3335-3337; June 16, 1958.) The magnetic anisotropy and weak ferromagnetism of α -Fe₂O₃ cannot be explained in terms of dipolar energy.
- 538.221** **894**
Sendust Flake—a New Magnetic Material for Low-Frequency Application—W. M. Hubbard, E. Adams, and J. F. Haben. (*IRE TRANS. ON COMPONENT PARTS*, vol. CP-4, pp. 2-6; March, 1957. Abstract, *PROC. IRE*, vol. 45, p. 1035; July, 1957.)
- 538.221:539.231** **895**
Magnetic, Electrical and Electron-Optical Investigations of the Thermal Transformation of fathode-Sputtered Nickel films—L. Reimer. (*Z. Phys.*, vol. 149, pp. 425-431; October 31, 1957.)
- 538.221:621.3.042.2** **896**
Cube-Oriented Magnetic Sheet—(*J. Metals, N.Y.*, vol. 10, pp. 507-511; August, 1958.)
A Major Advance in Magnetic Materials—G. W. Wiener and K. Detert (pp. 507-508).
Magnetic Properties of Cube-Textured Transformer Sheet—J. L. Walter, W. R. Hibbard, Jr., H. C. Fiedler, H. E. Grenoble, R. H. Pry and P. G. Frischmann (pp. 509-511).
- 538.221:[621.318.124+621.318.134]** **897**
Data on Ferrite Core Materials—A. C. Hudson and E. J. Stevens. (*Electronic Eng.*, vol. 30, pp. 718-719; December, 1958.) Charts are presented which permit comparison of the permeability and loss at low levels for various ferrites over the frequency range 100 kc-100 mc.
- 538.221:[621.318.124+621.318.134]** **898**
Effect of Neutron Irradiation on the Curie Temperature of a Variety of Ferrites—E. I. Salkovitz, G. C. Bailey, and A. I. Schindler. (*J. Appl. Phys.*, vol. 29, pp. 1747-1748; December, 1958.) No significant change in Curie temperature after irradiation was found for either magnetically soft or hard ferrites.
- 538.221:621.318.124** **899**
Magnetization Studies and Possible Magnetic Structure of Barium Ferrate III—W. E. Henry. (*Phys. Rev.*, vol. 112, pp. 326-327; October 15, 1958.)
- 538.221:621.318.134** **900**
Modified Rotational Model of Flux Reversal—E. M. Gyorgy. (*J. Appl. Phys.*, vol. 29, pp. 1709-1712; December, 1958.) The mechanism of flux reversal in square-loop ferrites is analyzed showing that the flux in a toroid can be reversed by rotation without prohibitively large demagnetizing fields. This agrees with observations. See also 534 of 1958.
- 38.221:621.318.134** **901**
Magnetic Anisotropy Constant of Yttrium-Iron Garnet at 0°K—B. R. Cooper. (*Phys. Rev.*, vol. 112, pp. 395-396; October 15, 1958.)
- 538.221:621.318.134** **902**
Low-Temperature Transition of Magnetic Anisotropy in Nickel-Iron Ferrite—N. Menyuk and K. Dwight. (*Phys. Rev.*, vol. 112, pp. 397-405; October 15, 1958.) A study of the magnetic properties of single-crystal samples of Ni-Fe ferrite has revealed an abrupt transition in the magnetic anisotropy characteristics at 10°K. Predictions based on a proposed model are in accord with experimental findings.
- 538.221:621.318.134** **903**
An Investigation into the Magnesium and Magnesium-Manganese Ferrite System—L. C. F. Blackman. (*J. Electronics Control*, vol. 5, pp. 373-384; October, 1958.) "The influence of both manganese and firing conditions on certain physical and chemical properties of iron-deficient magnesium ferrite has been investigated. The results suggest that Fe²⁺ and Mn³⁺ can coexist, at least to a certain extent, in the solid state. It is also shown that the excess of magnesia, which is added to improve the microwave performance of the materials, plays an important role in the chemistry of the ferrite phase."
- 538.221:621.318.134** **904**
Ferrimagnetism in the System Na₂O-ZnO-Fe₂O₃—A. H. Mones and E. Banks. (*J. Phys. Chem. Solids*, vol. 6, pp. 267-270; August, 1958.)
- 538.221:621.318.134** **905**
Origin of Weak Ferromagnetism in Rare-Earth Orthoferrites—R. M. Bozorth. (*Phys. Rev. Lett.*, vol. 1, pp. 362-363; November 15, 1958.)
- 538.221:621.318.134:538.569.4** **906**
Ferromagnetic Resonance in Polycrystalline Ferrites with Large Anisotropy: Part I—General Theory and Application to Cubic Materials with a Negative Anisotropy Constant—E. Schlömann. (*J. Phys. Chem. Solids*, vol. 6, pp. 257-266; August, 1958.)
- 538.221:621.318.134:538.569.4** **907**
Ferrimagnetic Resonance in Yttrium-Iron Garnet at Liquid Helium Temperatures—J. F. Dillon, Jr. (*Phys. Rev.*, vol. 111, pp. 1476-1478; September 15, 1958.) Experiments performed on single crystal spheres at 24 kmc are described. The paper gives in some detail the low-temperature results on line width and the variation of the resonance field with crystal direction and temperature.
- 538.221:621.318.134:538.569.4** **908**
Magnetostatic Modes in Ferrimagnetic Spheres—J. F. Dillon, Jr. (*Phys. Rev.*, vol. 112, pp. 59-63; October 1, 1958.) Experiments on Y-Fe garnet show that the positions of the modes are not functions of crystal direction as previously reported. Specimens produced by tumbling procedures may deviate slightly from sphericity and in these experiments truly spherical samples were used. Evidence has been given of the effect of dielectric inhomogeneities in the neighborhood of the sample in a ferrimagnetic-resonance experiment.
- 538.222:538.569.4** **909**
Paramagnetic-Resonance Spectrum of Gadolinium in Single Crystals of Thorium Oxide—W. Low and D. Shaltiel. (*J. Phys. Chem. Solids*, vol. 6, pp. 315-323; September, 1958.) Measurements at 290° and 90°K at 3 cm λ give line positions and intensities which can be explained by a crystalline field of cubic symmetry. It is suggested that oxygen vacancies are randomly distributed throughout the crystal.
- 539.2:537.311.31** **910**
Electronic Band Structures of the Alkali Metals and of the Noble Metals and their α -Phase Alloys—M. H. Cohen and V. Heine. (*Advances Phys.*, vol. 7, pp. 395-434; October, 1958.)
- 621.315.616.96** **911**
Electrical Properties of Epoxy Resins—C. F. Pitt, B. P. Barth, and B. E. Godard. (*IRE TRANS. ON COMPONENT PARTS*, vol. CP-4, pp. 110-113; December, 1957. Abstract, *PROC. IRE*, vol. 46, p. 801; April, 1958.)
- MATHEMATICS**
- 517.942:538.566** **912**
Method of Liouville Applied to Weber's Equation—R. Meynieux. (*Compt. Rend. Acad. Sci., Paris*, vol. 246, pp. 3208-3210; June 9, 1958.) Applications include the propagation of a plane em wave across an ionospheric layer.
- 517.942:538.66** **913**
Gamma-Function Approximations Applied to Solutions of Weber's Equation—R. Meynieux. (*Compt. Rend. Acad. Sci., Paris*, vol. 246, pp. 3312-3314; June 16, 1958.)
- MEASUREMENTS AND TEST GEAR**
- 621.3.018.41(083.74):529.786:525.35** **914**
Comparison of Astronomical Time Measurements with Atomic Frequency Standards—J. P. Blaser and J. De Prins. (*Nature, London*, vol. 182, pp. 859-860; September 27, 1958.) Comparisons have been made in Neuchâtel between "atomic" time determined by integration of the frequency of a quartz clock calibrated against an NH₃ maser, and astronomical time determined by means of photographic zenith tube and astrolabe. Plotting UT1 against atomic time shows the variation in the rate of rotation of the earth, which is in agreement with the measurements of Essen *et al.* (3195 of 1958).
- 621.3.018.41(083.74):621.396.11** **915**
Comparison of an Ammonia Maser with a Caesium Atomic Frequency Standard—J. P. Blaser and J. Bonanomi. (*Nature, London*, vol. 182, p. 859; September 27, 1958.) Note of a comparison made in Neuchâtel by means of MSF standard-frequency transmissions during 1957 and 1958 of the frequencies of an NH₃ maser and the Cs resonator of the National Physical Laboratory. Two different methods were used: a) differentiation of the phase of MSF time signals at 5 and 10 mc; b) direct frequency comparison using the 60-kc transmission. See also 1208 of 1958 (Essen *et al.*).
- 621.3.018.41(083.74):621.396.11:551.535** **916**
Frequency Variations in Short-Wave Propagation—T. Ogawa. (*Proc. IRE*, vol. 46, pp. 1934-1939; December, 1958.) Frequency measuring equipment, with an accuracy written 1×10^{-8} is described. Observations were made on 5- and 10-mc standard-frequency transmissions from station JJY and the results are discussed in relation ionospheric conditions.
- 621.317.1.029.6** **917**
Reciprocity in Radio-Frequency Measurements—G. D. Monteath. (*Electronic Radio Eng.*, vol. 36, pp. 18-20; January, 1959.) A discussion of the advantages of interchangeability of source and detector in measurements of radiation patterns and impedance.
- 621.317.3:538.632** **918**
Alternate Current Apparatus for Measuring the Ordinary Hall Coefficient of Ferromagnetic Metals and Semiconductors—J. M. Lavine. (*Rev. Sci. Instr.*, vol. 29, pp. 970-976; November, 1958.) Apparatus for measurements at 1000 c is described having a sensitivity of 10^{-16} w, a noise level of 10^{-9} v and a voltage resolution of 1 in 10^6 for use with sample impedances ranging from less than 1 Ω to several thousand ohms.
- 621.317.3.018.7:534.78** **919**
A Sampling Comparator—A. Fischmann-Arbel. (*Electronic Eng.*, vol. 30, pp. 685-689; December, 1958.) The instrument described compares the instantaneous values of two waveforms at constant intervals of time. Applications of the comparator circuit in a delta modulator and a binary quantizer are detailed.

- 621.317.326 920
Measurement of the Peak Value of a High-Voltage Pulse—G. Giralt. (*Compt. Rend. Acad. Sci., Paris*, vol. 246, pp. 3227-3229; June 9, 1958.) Two methods involving the use of a ballistic galvanometer are described: one in which the rectified current through a standard capacitor is measured [see 1851 of 1957 (Lagasse and Giralt)], the other a blocking method, using a single half-wave rectifier and a circuit-breaking device, applicable for pulses of any waveform.
- 621.317.335.3.029.6:621.317.733 921
Bridge Method for Microwave Dielectric Measurements—S. H. Glarum. (*Rev. Sci. Instr.*, vol. 29, pp. 1016-1019; November, 1958.) The length of a short-circuited section of liquid-dielectric-filled coaxial line, is adjusted until its input admittance, measured using a microwave bridge, is purely resistive. The dielectric constant, between 1 and 3 kmc obtained by this method, compares well with published values.
- 621.317.335.3.029.64 922
The Measurement of the Dielectric Properties of Liquids in an H_{01} Resonator—J. S. Dryden. (*J. Sci. Instr.*, vol. 35, pp. 439-440; December, 1958.) A thin-walled silica cup with a flat metal disc at the bottom has proved suitable as a sample container. A method of correction for the meniscus is described.
- 621.317.34 + 621.317.38].029.62 923
Triple V.H.F. Reflectometer—G. H. Millard. (*Electronic Radio Eng.*, vol. 36, pp. 11-13; January, 1959.) The instrument is designed for use in the frequency bands 41-68 mc and 88-95 mc for powers of 1 kW or less.
- 621.317.39:531.76 924
A Catapult End-Speed Recorder—J. R. Pollard. (*Brit. Commun. Electronics*, vol. 5, pp. 676-680; September, 1958.) A description is given of electronic equipment for indicating and recording in printed form the launch speed attained by a steam catapult.
- 621.317.733:621.314.7 925
A Wide-Band Bridge Yielding Directly the Device Parameters of Junction Transistors—J. Zawels. (IRE TRANS. ON ELECTRON DEVICES, vol. ED-5, pp. 21-25; January, 1958. Abstract, PROC. IRE, vol. 46, Part 1, p. 932; May, 1958.)
- 621.317.75:621.372.413 926
Microwave Double-Sweep Method for Analysis of Time-Dependent Cavity Characteristics—S. Ruthberg. (*Rev. Sci. Instr.*, vol. 29, pp. 999-1003; November, 1958.) A frequency-sweep FM search signal and a frequency-sweep receiver are used to obtain a pulse whose shape is sensitive to cavity resonance. Frequency shift is determined from pulse shape and position along the received signal trace.
- 621.317.755:621.385.832 927
Oscilloscope Tube with Travelling-Wave Deflection System and Large Field of View—W. F. Niklas and J. Wimpffen. (*J. Brit. IRE*, vol. 18, pp. 653-660; November, 1958.) A tube is described having a balanced helix system as deflection plates and with a large viewing field ($1\frac{1}{2}$ in. \times 4 in.). Typical operating conditions and performance are described and the relative merits of magnetic and electrostatic focusing in a high-speed oscilloscope are discussed in detail.
- 621.317.799:621.314.7 928
Sweep Equipment Displays Transistor Beta R. Zuleg and J. Lindmayer. (*Electronics*, vol. 31, pp. 100-101; December 5, 1958.)
- OTHER APPLICATIONS OF RADIO AND ELECTRONICS
- 612.1:621.396.62-519 929
Radio Control of Ventricular Contraction in Experimental Heart Block—M. Verzeano, R. C. Webb, Jr., and M. Kelly. (*Science*, vol. 128, pp. 1003-1005; October 24, 1958.) A method is described for the stimulation of the ventricular myocardium by transmitting a pulse-modulated 2.5-mc carrier which is detected by a receiver enclosed in the chest of the animal under test.
- 612.84:621.397.5 930
Eye Fixations Recorded on Changing Visual Scenes by the Television Eye-Marker—J. F. Mackworth and N. H. Mackworth. (*J. Opt. Soc. Amer.*, vol. 48, pp. 439-445; July, 1958.) The corneal reflection of a light is picked up by a television camera and is superimposed upon a television monitor displaying the scene which the subject views on a separate screen. The resulting light spot can be made to lie accurately, within one or two degrees, on the part of the scene being regarded by the subject.
- 621.3.087.5 931
High-Fidelity Video Recording Using Ultrasonic Light Modulation—L. Levi. (*J. Soc. Mot. Pict. Telev. Eng.*, vol. 67, pp. 657-661; October, 1958. Discussion.) A method is described for recording video information with bandwidths up to 20 mc on photographic film, using a piezoelectric ultrasonic transducer.
- 621.3.087.9:621.395.625.3 932
Tones find Data in High-Speed Tape Systems—R. Wasserman and P. Hurney. (*Electronics*, vol. 31, pp. 92-95; November 21, 1958.) A digital timing generator, operating during recording, and an associated search unit enable selected data to be extracted from multi-channel magnetic-tape systems.
- 621.365.5:621.316.726.078.3 933
Frequency Stability of R.F. Heating Generators—J. Verstraten. (*Electronic Applic.*, vol. 18, pp. 122-128; August, 1958.) A cavity resonator of large dimensions is used as a tank circuit. Details are given of a 2-kw generator whose frequency remains constant to within 0.5 per cent of 27.12 mc.
- 621.384.62 934
New Design makes 10-MeV Particle Accelerator Possible—J. L. Danforth. (*Can. Electronics Eng.*, vol. 2, pp. 18-21; July, 1958.) See 935 below.
- 621.384.62 935
10-MeV Particle Accelerator will Aid Nuclear Research at Chalk River—H. E. Gove. (*Can. Electronics Eng.*, vol. 2, pp. 14-17; July, 1958.) A general description of the tandem Van de Graaff accelerator and associated equipment.
- 621.385.833 936
Investigations of the Remote-Focus Cathode of Steigerwald—F. W. Braucks. (*Optik, Stuttgart*, vol. 15, pp. 242-260; April, 1958.) Control voltage, and aperture, intensity, position and diameter of the smallest cross section of the beam are discussed in relation to the design parameters of the system.
- 621.385.833 937
System Design of Asymmetric Unipotential Electron Lenses—K. J. Hanssen. (*Optik, Stuttgart*, vol. 15, pp. 304-317; May, 1958.) See also 1558 of 1957 (Everitt and Hanssen).
- 621.385.833 938
Shadow-Casting Carbon Films used in Electron Microscopy—A. Oberlin and C. Tchoubar. (*Compt. Rend. Acad. Sci., Paris*, vol. 246, pp. 3329-3332; June 16, 1958.) Carbon films are shown to be preferable to metal for shadow techniques as they have less granulation.

PROPAGATION OF WAVES

621.396.11 + 621.372.2 939

Transmission and Reflection of Electromagnetic Waves in the Presence of Stratified Media—J. R. Wait. (*J. Res. Nat. Bur. Stand.*, vol. 61, pp. 205-232; September, 1958.) "A general analysis is presented for the electromagnetic response of a plane stratified medium consisting of any number of parallel homogeneous layers. The solution is first developed for plane-wave incidence and then generalized to both cylindrical and spherical-wave incidence. Numerical results for interesting special cases are presented and discussed. The application of the results to surface-wave propagation over a stratified ground is considered in some detail."

621.396.11 940

An Example of Guided Propagation in the Mediterranean—L. Boitlias and P. Misue. (*Ann. Télécommun.*, vol. 12, pp. 126-132; April, 1957.) Results are analyzed of field-strength measurements at 10 cm λ made on board ship, at distances up to 180 nautical miles from the transmitter, together with meteorological data provided by a tethered radiosonde. Three types of ducting are suggested.

621.396.11:551.510.535 941

Variations in the Direction of Arrival of High-Frequency Radio Waves—J. E. Titheridge. (*J. Atmos. Terr. Phys.*, vol. 13, pp. 17-25; December, 1958.) The effect of propagation in a non-horizontally uniform ionosphere is investigated. The equations are solved for linear and parabolic layers and used to calculate layer tilts necessary to produce the large diurnal bearing changes in the arrival of short waves at Auckland, New Zealand.

621.396.11:551.510.535 942

Very-Long-Distance Ionospheric Propagation—N. C. Gerson. (*J. Atmos. Terr. Phys.*, vol. 13, pp. 169-172; December, 1958.) A brief discussion on the effectiveness of propagation in the spherical shell between the earth and the ionosphere, and also magnetic (whistler-mode) propagation.

621.396.11:551.510.535 943

Long-Distance Single-F-Hop Transmission—W. Dieninger, H. G. Möller and G. Rose. (*J. Atmos. Terr. Phys.*, vol. 13, pp. 191-192; December, 1958.)

621.396.11:551.510.535 944

Magneto-ionic Fading in Pulsed Radio Waves Reflected at Vertical Incidence from the Ionosphere—C. A. Reddy, B. R. Rao, and M. S. Rao. (*J. Brit. IRE*, vol. 18, pp. 669-675; November, 1958.) The difference in phase paths of the two interfering magneto-ionic components is calculated on the basis of ray theory assuming a parabolic electron-density distribution for the F_2 region. The calculated fading frequencies agree fairly well with the observed values. A method of deducing the semi-thickness of the F_2 region from these fading frequencies is described, and some results are given.

621.396.11:551.510.535 945

A New Type of Fading Observable on High-Frequency Radio Transmissions Propagated over Paths Crossing the Magnetic Equator—K. C. Yeh and O. G. Villard, Jr. (*Proc. IRE*, vol. 46, pp. 1968-1970; December, 1958.) The received energy is split into two independently fading components of comparable strength, separated in frequency by some tens of c. It is

suggested that the phenomenon is caused by a combination of conventional and tilt-supported propagation across the evening equatorial height bulge in the F layer of the ionosphere.

621.396.11:551.510.535:621.3.018.41(083.74) 946
Frequency Variations in Short-Wave Propagation—Ogawa. (See 916.)

621.396.11:621.396.812 947
Some Relations between the Bearing and Amplitude of a Fading Radio Wave—H. A. Whale and L. M. Delves. (*J. Atmos. Terr. Phys.*, vol. 13, pp. 72-85; December, 1958.) A correlation ratio connecting the changes in amplitude and bearing of a fading wave made up of several randomly phased components is derived. Experimental and theoretical conclusions have been compared.

621.396.11.029.45 948
Propagation of Very-Low-Frequency Pulses to Great Distances—J. R. Wait. (*J. Res. Nat. Bur. Stand.*, vol. 61, pp. 187-203; September, 1958.) The space between the earth and the ionosphere is represented as a sharply bounded waveguide with concentric spherical boundaries. The concept of phase and group velocity is discussed and applied to determine the influence of the propagation medium on the shape of the envelope of a quasi-monochromatic pulse. An alternative method is described that is applicable to wide-band sources containing many spectral components.

RECEPTION

621.372.632.029.6 949
Design Considerations in a Wide-Band Microwave Mixer and I. F. Preamplifier—J. C. Rennie. (*IRE TRANS. ON COMMUNICATIONS SYSTEMS* vol. CS-5, pp. 21-25; September, 1957.)

621.396.621.22:621.375.121.2 950
An Electronic Multicoupler and Antenna Amplifier for the V.H.F. Range—K. Fischer. (*IRE TRANS. ON COMMUNICATIONS SYSTEMS*, vol. CS-5, pp. 43-48; December, 1957. Abstract, *PROC. IRE*, vol. 46, p. 515; February, 1958.)

621.396.66:621.316.726.078.3 951
A.F.C. in Band-II F.M. Receivers: using a Junction Diode—G. D. Browne. (*Mullard Tech. Commun.*, vol. 4, pp. 152-157; November, 1958.) The reactance variation obtained by varying the Ge-diode reverse voltage provides a frequency control operating successfully above 10 mc.

621.396.666 952
Laboratory Tests on Kahn's Theory of Anti-fading Reception—G. Bronzi. (*Alla Frequenza*, vol. 27, pp. 17-43; February, 1958.) Analysis of an experimental comparison of methods of double-diversity reception using strongest-signal selection or the ratio-squarer combining system [(541 of 1955) Kahn] shows the advantages of the latter method.

621.396.81 953
Correlation Measurements in the Short-Wave Range—J. Grosskopf, M. Scholz, and K. Vogt. (*Nachrichtentech. Z.*, vol. 11, pp. 91-95; February, 1958.) Report on measurements of the correlation coefficient in diversity reception using rhombic and dipole antennas.

621.396.82 954
Radio Interference: Part 5—Industrial, Scientific and Medical Apparatus and Radiating Receivers—C. W. Sowton and A. C. R. Britton. (*P.O. Elect. Engr. J.*, vol. 51, Part 3, pp. 202-205; October, 1958.) International frequency allocations for industrial, scientific, and medical apparatus are discussed and exam-

ples of the field strength of radiation at fundamental and harmonic frequencies are tabulated. The free-radiation frequency of 27.12 mc with harmonic attenuation has been adopted for medical apparatus. Methods for measuring the radiation field receivers are outlined. These methods have been accepted by most countries. Part 4: 3964 of 1958 (Macpherson).

621.396.822:621.397.62 955
Design Considerations in the Reduction of Sweep Interference from Television Receivers—A. M. Intrator. (*IRE TRANS. ON BROADCAST AND TELEVISION RECEIVERS*, vol. BTR-2, pp. 1-5; April, 1956.)

STATIONS AND COMMUNICATION SYSTEMS

621.376.5 956
Using Markerless Pulse Trains to Communicate—M. Davidson, H. Joseph, and N. Zucker. (*Electronics*, vol. 31, pp. 89-91; November 21, 1958.) Three types of markerless pulse-train modulation are compared, and demodulating circuits for pulse-interval modulation are described.

621.376.5:621.391 957
Statistics of Regenerative Digital Transmission—W. R. Bennett. (*Bell Syst. Tech. J.*, vol. 37, pp. 1501-1542; November, 1958.) Specific problems considered include the properties of a digital message pulse train as a random noise source, the effect of time jitter in a received pulse train on the recovered analogue signal, and the derivation of the pulse repetition frequency from a pulse train by shock excitation of a tuned circuit.

621.391 958
The Central Concepts of Communication Theory for Infinite Alphabets—I. Fleischer. (*J. Math. Phys.*, vol. 37, pp. 223-228; October, 1958.)

621.391:621.376 959
Demodulation and Detection—D. A. Bell. (*Electronic Radio Eng.*, vol. 36, pp. 21-24; January, 1959.) A discussion of the basic processes, particularly in relation to information theory.

621.394.3:621.396.65 960
Teleprinting over Long-Distance Radio Links—A. C. Croisdale. (*P.O. Elec. Eng. J.*, vol. 51, Parts 2 and 3, pp. 88-93 and 219-225; July and October, 1958.) Methods for the transmission of 5-unit telegraphy signals and techniques for reducing the mutilation of signals on radio links are described. Automatic error correction and the resulting improvement in performance are discussed with reference to CCITT recommendations.

621396(667) 961
Radio Communications in Ghana—R. G. Sharpe and D. R. Gamlen. (*Brit. Commun. Electronics*, vol. 5, pp. 750-756; October, 1958.)

621.396.2 962
The Bandwidth Occupied by a Class A1 Transmission and its Determination—J. Marique. (*Rev. HF, Brussels*, vol. 3, no. 10, pp. 359-368; 1957.)

621.396.2 963
Performance of Some Radio Systems in the Presence of Thermal and Atmospheric Noise—A. D. Watt, R. M. Coon, E. L. Maxwell, and R. W. Plush. (*PROC. IRE*, vol. 46, pp. 1914-1923; December, 1958.) "The performance of several basic types of communication systems are determined experimentally, and in some cases theoretically, under typical conditions with steady or fading carriers, and in the presence of thermal or atmospheric noise. The relative efficiency of various carriers and the

interference factor of various types of noise are found to be dependent upon the characteristics of the particular communication system as well as the characteristics of the carrier and noise themselves. Methods are considered for calculating errors expected from a given system, based upon the amplitude distribution of the noise envelope."

621.396.2:[629.19+523.3 964
Long-Distance Telecommunications by means of Satellites—F. Vilbig. (*Elektrotech. Z.*, vol. 79, pp. 375-382; June 1, 1958.) Propagation conditions and operational problems relating to the use of the moon and of artificial satellites as reflectors or relay stations are discussed.

621.396.25:621.394 965
High-Speed Frequency-Shift Keying of L.F. and V.L.F. Radio Circuits—H. G. Wolff. (*IRE TRANS. ON COMMUNICATIONS SYSTEMS*, vol. CS-5, pp. 29-42; December, 1957. Abstract, *PROC. IRE*, vol. 46, p. 515; February, 1958.)

621.396.3 966
Automatic Error Correction—P. R. Keller and L. K. Wheeler. (*Wireless World*, vol. 65, pp. 28-33; January, 1959.) A description, with block diagrams, of the "Autoplex" two-channel time-division electronic equipment, and of the improvement in the error rate with automatic repetition. See also 2224 of 1958 (Keller) and 960 above.

621.396.4:621.376.5 967
The Timing of High-Speed Regenerative Repeaters—O. E. De Lange. (*Bell Syst. Tech. J.*, vol. 37, pp. 1455-1486; November, 1958.) A simplified method for determining the performance of the timing portion of chains of regenerative repeaters in multi-channel PCM systems. Two types are considered, those in which a repetitive timing signal is sent on one channel, and those in which timing is obtained from the coded pulse trains. The effect of random noise is calculated and other transmission defects are discussed.

621.396.4:621.376.5 968
Experiments on the Timing of Regenerative Repeaters—O. E. De Lange and M. Pustelnyk. (*Bell Syst. Tech. J.*, vol. 37, pp. 1487-1500; November, 1958.) Experiments performed with self-timed binary regenerative repeaters to determine the behavior of the timing portion of a chain of such repeaters are described. The number of errors produced by the action of noise on the timing system was negligible compared with those produced by other effects of noise.

621.396.4:621.376.5 969
Timing in a Long Chain of Regenerative Binary Repeaters—H. E. Rowe. (*Bell Syst. Tech. J.*, vol. 37, pp. 1543-1598; November, 1958.) The power spectra and the total powers of the timing noise, spacing noise, and alignment noise, caused by the input noise at each repeater are determined for a long chain of regenerative repeaters using either tuned-circuit or locked-oscillator timing filters. Tuning error effects are studied for a repeater chain using locked-oscillator timing circuits.

621.396.41 970
The 'Third Method'—J. F. H. Aspinwall. (*Wireless World*, vol. 65, pp. 39-43; January, 1959.) The method described by D. K. Weaver, Jr. (*PROC. IRE*, vol. 44, pp. 1703-1705; December, 1956.) is compared with filter and phasing methods of generating sss signals, and its application to radio telephony is briefly described.

621.396.41 971

A Compatible Single-Sideband Modulation System—L. R. Kalin. (*Proc. Radio Club Amer.*, vol. 34, pp. 3-9; March, 1958.) A system is described which is compatible with the existing dsb am system. It also compares favorably in signal/noise ratio, spectrum economy and reduction of selective fading distortion with the conventional ssb system, and it is suitable for aeronautical communications. Operational tests show that the greatest improvement in audio fidelity and signal/noise ratio occurs in narrow-bandwidth domestic receivers. See 3247 of 1958 (Costas) for mathematical analysis of the system.

621.396.41:551.510.52 972

Quadruple-Diversity Tropospheric Scatter Systems—W. G. Long and R. R. Weeks. (*IRE TRANS. ON COMMUNICATIONS SYSTEMS*, vol. CS-5, pp. 8-19; December, 1957.)

621.396.41:621.396.65 973

Microwave Network now Spans Canada—M. James. (*Can. Electronics Eng.*, vol. 2, pp. 28-31; September, 1958.) A general description of the TD-2 multiplex FM system. See also 3638 of 1958 (Curtis et al.).

621.396.5 974

Practical and Theoretical Design Considerations for Bridge Negative-Feedback Amplifiers in Carrier Telephony—M. J. Cotteill and J. W. Halina. (*IRE TRANS. ON COMMUNICATIONS SYSTEMS*, vol. CS-5, pp. 26-31; September, 1957.)

621.396.65 975

Scatter Equipment Built for Canadian Use—J. A. Grant. (*Can. Electronics Eng.*, vol. 2, pp. 30-33; July, 1958.) Terminal and repeater FM equipment covering the range 755-980 mc is described, with particular reference to the "serrasoid" sawtooth modulator.

621.396.65:621.396.967 976

Microwave Links for Radar Networks—J. W. Sutherland. (*Brit. Commun. Electronics*, vol. 5, pp. 688-695; September, 1958.) The operational advantages of remote presentation of radar information and the parameters of practical transmission systems are discussed in detail. The use of travelling-wave tubes in IF and nondemodulating types of repeater is described.

621.396.7:621.396.11 977

Radio Propagation Transmitting Station WWI at Havana, Illinois—(*Tech. News Bull. Nat. Bur. Stand.*, vol. 42, pp. 154-155; August, 1958.) The station, which is centered at 40° 13.27' N, 90° 1.39' W, is intended mainly for research in VHF transmission. Its twelve transmitters operate on 30-108 mc at 3-50 kw. Details of the antenna system are given.

SUBSIDIARY APPARATUS

621.311.62:621.314.7 978

Boosting Power-Transistor Efficiency—J. W. Caldwell and T. C. G. Wagner. (*Fletronics*, vol. 31, pp. 86-88; November 21, 1958.) High efficiency is obtained by carefully controlling the instantaneous voltage and current through the transistor.

621.316.721:621.318.3:621.314.7 979

Precision Current Regulator using Transistors—S. D. Johnson and J. R. Singer. (*Rev. Sci. Instr.*, vol. 29, pp. 1026-1028; November, 1958.) A regulator for electromagnets of field strength between 1000 and 5000 G is described which is accurate to within two parts in 10⁵.

621.316.722:621.314.7 980

Transistor Voltage Regulators—G. W. Meszaros. (*Bell Lab. Rec.*, vol. 36, pp. 442-445;

December, 1958.) Design considerations are discussed for series-type regulators and the magnetic-amplifier type designed for the TRIDAC computer is described.

TELEVISION AND PHOTOTELEGRAPHY

621.397.24:621.3.018.782.4 981

Demonstration of Delay Distortion Correction by Time-Reversal Techniques—B. P. Bogert. (*IRE TRANS. ON COMMUNICATIONS SYSTEMS* vol. CS-5, pp. 2-7; December, 1957. Abstract, *Proc. IRE*, vol. 46, p. 515; February, 1958.)

621.397.5 982

The Possibilities of Reduced Television Bandwidth—S. Deutsch. (*IRE TRANS. ON BROADCAST AND TELEVISION RECEIVERS*, vol. BTR-2, pp. 69-82; October, 1956. Abstract, *Proc. IRE*, vol. 45, p. 253; February, 1957.)

621.397.5:621.396.4 983

Study of Multichannel Sound Transmission from a Single Transmitter: Application to Bilingual Television—L. Bourassin. (*Électronique, Paris*, pp. 45-50 and 37-44; May and July/August, 1957.) Continuation of 3312 of 1957.

621.397.611.001.4 984

Two New B.B.C. Transparencies for Testing Television Camera Channels—(*BBC Eng. Div. Monographs*, n.p. pp. 5-17; November, 1958.) [Part 1—Requirements, Design and Use of the Colour Response, and the Gradation and Resolution Transparencies—G. Hersee (pp. 5-13). [Part 2—The Manufacture of the B.B.C. Test Transparency No. 51—J. R. T. Royle (pp. 14-17).

621.397.611.2 985

The Problem of Inertia Effects in Television Camera Tubes of the Vidicon Type—C. Kunze. (*Hochfreq. und Elektroak.*, vol. 66, pp. 84-89; November, 1957.) Measurements show that inertia effects are mainly due to incomplete recharging of the picture elements [see also 252 of 1956 (Heimann)]. The dependence of these effects on operating parameters, and methods of eliminating inertia effects, such as roughening the target surface, are discussed.

621.397.62:535.623 986

Tentative Methods of Measurement of Colour Television Receiver Performance—S. P. Ronzheimer and R. J. Farber. (*IRE TRANS. ON BROADCAST AND TELEVISION RECEIVERS*, vol. BTR-2, pp. 10-30; April, 1956.)

621.397.62:621.314.7 987

Transistors in Television Receivers—B. R. Overton. (*J. Telev. Soc.*, vol. 8, pp. 444-468; July-September, 1958.) "A complete receiver, operating from a 12-v battery (consumption 12 w approximately), and employing transistors throughout is described. Special attention is given to the three major technical problems of incorporating transistors in television receivers, namely, RF and IF amplification, video drive and line scanning. The paper discusses some new techniques for dealing with these problems, in particular a system of scan magnification, hitherto undisclosed. Some attempt is made to forecast future trends."

621.397.62:621.372.54 988

Trap Improves TV Picture—G. C. Field. (*Electronics*, vol. 31, pp. 100, 102; November 21, 1958.) The use of a bifilar-T trap to suppress adjacent-channel interference in 40-mc IF amplifiers is described.

621.397.621.2 989

Improvements in Television Receivers: Part 4—Stabilization of the Line Deflection Circuit by means of a V.D.R. Resistor—B. G.

Dammers, A. G. W. Uitjens, A. Boekhorst, and H. Heyligers. (*Electronic Applic.*, vol. 18, pp. 118-121; August, 1958.) A simplified version of the circuit proposed in 3316 of 1957 makes the protection device proposed in 282 of January (Dammers et al.) unnecessary. A voltage-dependent resistor is used to control the line output valve. The scanning current is stabilized to about ± 2 per cent for line voltage variations of ± 13 per cent.

621.397.2:535.623:621.385.832 990

Error Correction in Mask-Type Colour Television Tubes—S. H. Kaplan. (*J. Telev. Soc.*, vol. 8, pp. 470-480; July-September, 1958.) Corrections for the errors which increase as a function of scan angle, and optical exposure methods for correcting triad size and location errors, are described. A proposal to eliminate triad shape errors by means of a radially distorted aperture mask pattern is given in detail.

621.397.7 991

B.B.C. Install 'Translator' for Improved TV Reception—(*Brit. Commun. Electronics*, vol. 5, p. 757; October, 1958.) Signals transmitted on one channel are converted, without demodulation, to another and automatically reradiated at low power over line-of-sight paths to the area to be served. Equipment at Folkestone is briefly described.

621.397.7:621.315.212 992

Interconnection of Television Cable Links at the Carrier-Frequency State according to the C.C.I.F.—R. Hoffmann. (*Nachrichtentech. Z.*, vol. 11, pp. 96-99; February, 1958.) Summary of the CCIF recommendations of December, 1956, concerning the transmission of television signals over international cable routes.

621.397.8:535.623 993

The Origin and Measurement of Level-Dependent Phase and Amplitude Fluctuations in the Transmission of the Subcarrier in Colour Television—J. Piening. (*Nachrichtentech. Z.*, vol. 11, pp. 70-77; February, 1958.) Causes of amplitude and phase distortion are investigated quantitatively.

TUBES AND THERMIONICS

621.314.63:546.289 994

New Types of Germanium Diodes and their Circuit Applications—G. Grimsdell. (*Electronic Eng.*, vol. 30, pp. 709-710; December, 1958.) The properties of gold-bonded diodes and small-area junction diodes are compared with those of point-contact types and the relative advantages and disadvantages are outlined.

621.314.7 995

On the Variation of Transistor Small-Signal Parameters with Emitter Current and Collector Voltage—N. J. Meyer. (*J. Electronics Control*, vol. 5, pp. 329-337; October, 1958.) Addendum to 3285 of 1958.

621.314.7 996

The Characteristic Frequencies of a Junction Transistor—J. M. Rollett. (*J. Electronics Control*, vol. 5, pp. 344-347; October, 1958.) The relations between characteristic frequencies and intrinsic parameters are considered using the model which assumes one-dimensional flow of carriers across the base region. The frequencies discussed are the cut-off frequencies in the common-base and common-emitter connections, and the frequency at which the common-emitter current gain is unity.

621.314.7 997

Structure-Determined Gain-Band Product of Junction-Triode Transistors—J. M. Early. (*Proc. IRE*, vol. 46, pp. 1924-1927; December, 1958.) The fundamental frequency limitations

are discussed, and it is shown that mesa-type transistors for use in the microwave region are theoretically possible. The gain-bandwidth product is an order of magnitude better than that of field-effect or analogue transistors.

- 621.314.7 998
Theory of the *P-N* Junction Device using Avalanche Multiplication—T. Misawa. (PROC. IRE, vol. 46, p. 1954; December, 1958.)
- 621.314.7 999
The Internal Current Gain of Drift Transistors—F. J. Hyde. (PROC. IRE, vol. 46, pp. 1963–1964; December, 1958.)
- 621.314.7:546.289 1000
High-Frequency Germanium Transistors—J. S. Lamming. (*Research, London*, vol. 11, pp. 425–431; November, 1958.) Design theory and production techniques are reviewed.
- 621.314.7:546.289 1001
Very-High-Power Transistors with Evaporated Aluminium Electrodes—H. W. Henkels and G. Strull. (IRE TRANS. ON ELECTRON DEVICES, vol. ED-4, pp. 291–294; October, 1957. Abstract, PROC. IRE, vol. 46, p. 515; February, 1958.)
- 621.314.7:621.317.733 1002
A Wide-Band Bridge Yielding Directly the Device Parameters of Junction Transistors—J. Zawels. (IRE TRANS. ON ELECTRON DEVICES, vol. ED-5, pp. 21–25; January, 1958. Abstract, PROC. IRE, vol. 46, Part 1, p. 932; May, 1958.)
- 621.314.7:621.317.799 1003
Sweep Equipment Displays Transistor Beta—R. Zuleeg and J. Lindmayer. (*Electronics*, vol. 31, pp. 100–101; December 5, 1958.)
- 621.314.7:621.318.57 1004
A New High-Current Mode of Transistor Operation—C. G. Thornton, and C. D. Simons. (IRE TRANS. ON ELECTRON DEVICES, vol. ED-5, pp. 6–10; January, 1958. Abstract, PROC. IRE, vol. 46, Part 1, p. 932; May, 1958.)
- 611.314.7:621.318.57 1005
The 'Thyristor'—a New High-Speed Switching Transistor—C. W. Mueller and J. Hilibrand. (IRE TRANS. ON ELECTRON DEVICES, vol. ED-5, pp. 2–5; January, 1958. Abstract, PROC. IRE, vol. 46, Part 1, pp. 931–932; May, 1958.)
- 621.314.7:621.318.57 1006
A Transistor with Thyatron Characteristics and Related Devices—W. von Münch. (*J. Brit. IRE*, vol. 18, pp. 645–652; November, 1958.) Details of production and electrical performance are given for a device produced by immersing a tungsten whisker in the collector of an *n-p-n*-junction transistor, of high base resistivity, during the alloy process. Devices with more than one output electrode are developed from this design. A special structure for triggering by radiation and a symmetrical switching transistor are also studied.
- 621.314.7.002.2:546.28 1007
Silicon Transistors—J. T. Kendall. (*Research, London*, vol. 11, pp. 381–386; October, 1958.) Industrial manufacturing techniques are described.
- 621.314.7.01 1008
On the Need for Revision in Transistor Terminology and Notation—H. L. Armstrong. (PROC. IRE vol. 46, pp. 1949–1950; December, 1958.)
- 621.314.7.012.8 1009
Transistor Equivalent Circuits—C. Moerder. (*Elektrotech. Z.*, vol. 79, pp. 469–472;

July 1, 1958.) Derivation of equivalent circuits from fundamental considerations.

- 621.383.4 1010
Properties of Cadmium Sulphide Photoconductive Cells—R. L. Williams. (*Can. J. Phys.*, vol. 36, pp. 1536–1550; November, 1958.)
- 621.383.49 1011
The Characteristics of Evaporated CdS and CdSe Photistors—D. A. Anderson. (*Can. Electronics Eng.*, vol. 2, pp. 23–29; July, 1958.) The performance of various types of photoconductive cell is discussed.
- 621.383.8:535.215–15 1012
High-Sensitivity Crystal Infrared Detectors—M. E. Lasser, P. Cholet, and E. C. Wurst, Jr. (*J. Opt. Soc. Amer.*, vol. 48, pp. 468–473; July, 1958.) The characteristics of *n*-type Au-doped Ge photoconductive cells are tabulated, and comparisons are made with the photo-voltaic *p-n*-junction InSb cell. A multiple-contact cell is described which can locate a target as well as detect it without a moving optical system [see also 3691 of 1957 (Wallmark)].
- 621.385:534.39 1013
Analysis of Microphony in Electron Tubes—A. Stecker. (*Electronic Applic.*, vol. 18, pp. 99–117; August, 1958.)
- 621.385.029.6 1014
On the Coupling Coefficients in the 'Coupled-Mode' Theory—A. Yariv. (PROC. IRE, vol. 46, pp. 1956–1957; December, 1958.) Perturbation theory is used to evaluate the coupling coefficients for the case of small coupling, taking the field and current values as those applicable to the no-coupling case.
- 621.385.029.6 1015
Effect of Beam Coupling Coefficient on Broad-Band Operation of Multicavity Klystrons—S. V. Yadavalli. (PROC. IRE, vol. 46, pp. 1957–1958; December, 1958.) Wide-band multicavity klystrons are more efficient in the L band of frequencies than in the S band, and are better operated at higher voltages than synchronously tuned klystrons.
- 621.385.029.6 1016
Pulse-Modulated Beam Current Improves Operation of Mixer-Series Klystrons—A. K. Scrivens. (*Can. Electronics Eng.*, vol. 2, pp. 32–34; October, 1958.)
- 621.385.029.6 1017
On the Design of the Transition Region of Axisymmetric, Magnetically Focused Beam Valves—V. Bevc, J. L. Palmer, and C. Süskind. (*J. Brit. IRE*, vol. 18, pp. 696–708; December, 1958.) A method is described for using an analogue computer to trace out electron trajectories. It is applied to the presentation of beam envelopes for Brillouin flow, periodic magnetic focusing and space-charge-balanced flow. By matching these with envelopes derived from the theory of the Pierce gun, it is possible to specify the dimensions of a gun for producing a required beam.
- 621.385.029.6 1018
A Relativistic Treatment of Space-Charge-Limited Current in a Planar Diode Magnetron before Cut-Off—J. A. Bradshaw. (*J. Electronics Control*, vol. 5, pp. 300–306; October, 1958.) "Relativistic expressions, correct to first order in a current density parameter, are obtained from two cross-coupled integral equations for the potential functions in a planar diode magnetron. These expressions are evaluated and plotted in two figures, and compared with expressions given by Gold [3695 of 1957]."
- 621.385.029.6 1019
Travelling-Wave Valves—J. Voge. (*Ann. Télécommun.*, vol. 12, pp. 92–104 and 105–119; March and April, 1957.) A general survey of the development of the device. Carcinotrons and amplifiers are described and comparative tables of French and American types are given. Amplifier noise and methods for reducing it, and the characteristics of several linear accelerators are discussed. 28 references.
- 621.385.029.6 1020
Wave Matrices Applied to a Periodically Loaded Travelling-Wave Tube—D. E. T. F. Ashby. (*J. Electronics Control*, vol. 5, pp. 338–343; October, 1958.) The derivation of the matrices is shown, and they are used to determine the conditions necessary for oscillation due to feedback caused by reflections from the periodic discontinuities. Oscillations may be produced unintentionally, and be mistaken for backward-wave oscillations.
- 621.385.029.6:621.318.2 1021
The Design of Periodic Magnetic Focusing Structures—J. E. Sterrett and H. Heffner. (IRE TRANS. ON ELECTRON DEVICES, vol. ED-5, pp. 35–42; January, 1958. Abstract, PROC. IRE, vol. 46, Part 1, p. 932; May, 1958.)
- 621.385.029.6:621.372.2 1022
A Note on the Dispersion of Interdigital Delay Lines—F. Paschke. (*RCA Rev.*, vol. 19, pp. 418–422; September, 1958.) "It is shown that the effect of the backwall on the dispersion of an interdigital delay line can be taken into account by a lumped susceptance which periodically loads the 'ideal' line. Experimental results are in good agreement with the theory." See also 629 of 1957.
- 621.385.029.6:621.396.822 1023
Noise Wave Excitation at the Cathode of a Microwave Beam Amplifier—W. R. Beam. (IRE TRANS. ON ELECTRON DEVICES, vol. ED-4, pp. 226–234; July, 1957. Abstract, PROC. IRE, vol. 45, p. 1760; See also 4067 of 1957 (Knechtli and Beam).)
- 621.385.029.621.63 1024
Travelling-Wave Amplifiers and Backward-Wave Oscillators for V.H.F.—D. A. Dunn. (IRE TRANS. ON ELECTRON DEVICES, vol. ED-4, pp. 246–264; July, 1957. Abstract, PROC. IRE, vol. 45, pp. 1760–1761; December, 1957.)
- 621.385.029.64:537.533:621.375.9 1025
Parametric Amplification of Space-Charge Waves—A. Ashkin. (*J. Appl. Phys.*, vol. 29, pp. 1646–1651; December, 1958.) An experimental investigation of the theory of Louisell and Quate (2273 of 1958), which shows that a signal imposed on a beam as a "fast" or "slow" space-charge wave can be exponentially amplified by strongly modulating the beam with a RF wave of twice the signal frequency. Over a 10-inch length of beam a 41-db increase has been observed. With the high-level signal frequency lower than the signal frequency, an increase of 30 db over a 9.2-inch length was observed.
- 621.385.032.213.13 1026
On the Conduction Mechanism of Oxide-Coated Cathode—H. Mizuno. (*J. Phys. Soc. Japan*, vol. 13, pp. 1234–1235; October, 1958.)
- 621.385.032.213.13:621.396.822 1027
Noise in Oxide Cathode Coatings—H. J. Hannam and A. van der Ziel. (*J. Appl. Phys.*, vol. 29, pp. 1702–1705; December, 1958.) A discussion of noise measurements at 8 mc and 30 c. The HF measurements show thermal noise at high and low cathode temperatures with a pronounced noise peak caused by shot noise where pore conduction changes to grain conduction. At LF the results show that the pores are inherently noisier than the grains.

621.385.032.213.13:621.396.822 1028

New Mechanism for the Generation of Flicker Noise—F. Fisher and I. P. Valkó. (*J. Appl. Phys.*, vol. 29, p. 1772; December, 1958.) The effect of cathode porosity on flicker noise in valves has been investigated, and results confirm the theoretical predictions of Lindemann and van der Ziel (1284 of 1957).

621.385.032.213.63 1029

The Breakdown of Cathode Coatings—B. Wolk. (*Sylvania Technologist*, vol. 10, pp. 106–110; October, 1957.) A report is given of an experimental study of the processing of cathode coatings under a set of controlled temperature and time conditions. Results indicate that thermal decomposition characteristics and particle size are related. Factors accounting for poor processing reliability are also considered.

621.385.032.24 1030

The Grid Emitting Properties of Titanium—J. A. Champion. (*Brit. J. Appl. Phys.*, J. A. Champion. (*Brit. J. Appl. Phys.*, vol. 9, pp. 491–495; December, 1958.) Experiments show that titanium is suitable as a screen-grid winding wire and for other electrode applications when used in the temperature range 700–900°C; above this cathode poisoning occurs.

621.385.032.26 1031

Dynamics of Electron Beams from Magnetically Shielded Guns—A. Ashkin. (*J. Appl. Phys.*, vol. 29, pp. 1594–1604; November, 1958.) Theoretical and experimental investiga-

tion of electron orbits and beam shapes. Current density variations and transverse velocity are measured with a beam analyser. In the limit of negligible space charge the observations are explained on the basis of simple energy considerations, taking account of the effect of transverse thermal velocities. In the presence of space charge the beam behavior is qualitatively unchanged, provided that the magnetic field is higher than about three times the Brillouin field.

621.385.3 1032

New Electron Tubes for Wide-Band Amplifiers—S. Edsman. (*Ericsson Rev.*, vol. 35, no. 3, pp. 98–102; 1958.) A note on the characteristics and operation of a pentode Type 5847/404A, triode Type 5842/417A, and tetrode Type 7150.

621.385.3:621.365.5 1033

Two Methods of Calculation for the Class-C Operation of Transmitter Valves—N. Weyss. (*Elektrotech. u. Maschinenb.*, vol. 75, pp. 633–638; December 1, 1958.) Oscillators for RF heating are considered.

621.385.832:621.317.755 1034

Oscilloscope Tube with Travelling-Wave Deflection System and Large Field of View—Niklas and Wimpffen. (See 927.)

621.385.832:621.397.621.2:666.1 1035

A Method of Sealing the Window and Cone of Television Picture Tubes—A. H. Edens.

(*Philips Tech. Rev.*, vol. 19, pp. 318–323; May 31, 1958. *Glass Ind.*, vol. 39, pp. 534–538; October, 1958.)

MISCELLANEOUS

621.6:621.396 1036

International Radio Organizations—some Aspects of their Work—R. L. Smith-Rose. (*J. Brit. IRE*, vol. 18, pp. 631–639; November, 1958.) An historical outline is given of the growth of communications and the resulting organizations set up to control international affairs. Details of the present work of the International Radio Consultative Committee (CCIR) are given and the activities of the International Scientific Radio Union (URSI) are reviewed.

621.3.002.5 1037

Production Machinery for the Electronics Industry—G. Sideris. (*Electronics*, vol. 31, pp. 73–84; October 24, 1958.) A review dealing with the modernization of machinery, tools, and plant layout, and with advances in component production and equipment assembly techniques.

621.37/.38].004.1 1038

The Influence of Interaction Reliabilities—M. A. Acheson. (*Sylvania Technologist*, vol. 11, pp. 91–95; July, 1958.) Examples are given of simple electronic systems in which interaction between two or more reliabilities of parts influences the total reliability.